

**Modelling and dynamic optimisation of quality  
indicator profiles during drying**

**Elisabeth Johanna Quirijns**

**Promotor**

**Prof. Dr. Ir. G. van Straten**

Hoogleraar Meet-, Regel- en Systeemtechniek  
Wageningen Universiteit

**Co-promotor**

**Dr. Ir. W. K. P. van Loon**

Universitair docent, leerstoelgroep Meet-, Regel- en  
Systeemtechniek, Wageningen Universiteit

**Promotiecommissie**

**Prof. Dr. Ir. M.A.J.S. van Boekel**

Wageningen Universiteit

**Prof. Ir. O.H. Bosgra**

Technische Universiteit Delft

**Prof. Dr. Ir. P.J.A.M. Kerkhof**

Technische Universiteit Eindhoven

**Prof. B. Nicolai**

Katholieke Universiteit Leuven, België

# **Modelling and dynamic optimisation of quality indicator profiles during drying**

**Elisabeth Johanna Quirijns**

**Proefschrift**

Ter verkrijging van de graad van doctor  
op gezag van de rector magnificus  
van Wageningen Universiteit,  
Prof. Dr. M. J. Kropff  
in het openbaar te verdedigen op  
maandag 24 april 2006  
des namiddags 13.30 in de Aula

E.J. Quirijns - Modelling and dynamic optimisation of quality indicator profiles during drying  
- 2006

Thesis Wageningen University, Wageningen, The Netherlands – with summary in Dutch –  
254 p.

Keywords: drying, dynamic optimisation, quality indicator profile, optimal quality control,  
diffusion-sorption drying model, sorption isotherm, GAB parameters, bound and free water,  
enzyme inactivation, fractional conversion model, calibration, validation

ISBN 90-8504-428-6

*voor ons pa en ma*

*“We zijn geroepen-  
niet om succes te hebben  
maar om vol vertrouwen te geloven”*

Mother Theresa



## Abstract

Food properties change during processing, causing an altered quality experience by the consumer. Apart from quality considerations, also economic and environmental aspects are important in industry. They are conflicting, leading to the wish to find the optimal operation. Since quality is a subjective quantity, quality indicators are used that can be objectively measured. Those quality indicators are linked to the relevant quality attributes. In many processes a spatial distribution of the quality indicator will arise, the so-called quality indicator profile (QIP). In this thesis, it is investigated whether the consideration of QIPs is necessary in quality optimisation. Drying of the enzyme catalase, immobilised in starch cylinders is used as case study, where the residual catalase activity formed the quality indicator.

Simulation and optimisation studies demonstrate that average values for the quality indicator do not uniquely represent QIPs inside the material. Safety of the product can only be guaranteed by using QIPs in optimisation procedures. By optimisation, the spatial distribution of the quality indicator can be influenced, creating advanced possibilities to control product quality.

Based on these findings a new microscopic drying model is developed, to obtain a proper description of QIPs. In this model a distinction is made between different classes of water present in the material. The conversion between them is described by a sorption process. Since the model consists of both a diffusion and a sorption part, it is called the diffusion-sorption model. In this model all parameters have a physical meaning. The assumptions made in the model are supported by independent sorption experiments, that also provide the essential parameters. The diffusion-sorption model is compared with four other diffusion models known from literature. It performs best in both calibration and validation, confirming the confidence in this model.

Experimental verification establishes the central role of QIPs in quality description and optimisation. The experiments show that QIPs exist during and after drying and that they are significantly influenced by varying the air conditions. Based on independent enzyme inactivation experiments a fractional conversion model is developed that can predict the residual enzyme activity as function of moisture content and temperature.

Both the diffusion-sorption model and the quality model lead to reliable predictions. The two models are combined to predict QIPs during drying. The drying curve agrees with the moisture content measurements. The predicted QIPs are qualitatively comparable with the experimental ones, though higher in enzyme activity.

The diffusion-sorption model is successfully applied in optimal control computations. They lead to improved control of product properties in an efficient way.

The major contribution of this thesis is that it has been demonstrated in theory, simulation and experiments that quality indicator *profiles* are required for optimisation of quality. This thesis illustrates that optimal process control based on QIPs is potentially of great economic value in biotechnology, agricultural and food engineering.

# Contents

Abstract		
<i>Chapter 1</i>	<b>Introduction</b>	11
<i>Chapter 2</i>	<b>Definition of quality during drying</b>	27
	The use of moisture and temperature profiles in predicting product quality for optimal control of drying processes	
<i>Chapter 3</i>	<b>Optimisation of quality during drying</b>	41
	The significance of modelling spatial distributions of quality in optimal control of drying processes	
<i>Chapter 4</i>	<b>Development and validation of the diffusion-sorption drying model</b>	69
4.1	Diffusion-sorption drying model for optimal quality control	70
4.2	An improved experimental and regression methodology for sorption isotherms	107
4.3	Sorption isotherms, GAB parameters and isosteric heat of sorption	134
4.4	Mathematical description and parameter values of the diffusion-sorption drying model	160
<i>Chapter 5</i>	<b>Development and validation of the quality model</b>	177
	Quality indicator profiles inside food during drying	
<i>Chapter 6</i>	<b>Optimisation of quality during drying with the diffusion-sorption drying model</b>	205
	New perspectives for optimal control of drying processes	
<i>Chapter 7</i>	<b>General discussion</b>	225
Summary		237
Samenvatting		241
Dankwoord		247
List of publications		251
Curriculum Vitae		253



## **Chapter 1**

### **Introduction**

## Quality of food during processing

### Quality in processing

The processing of raw materials to food products consists of a whole chain of production steps. Examples are pre-treatments, concentration, heating, cooling, drying, storage and packaging (Bimbenet and Lebert, 1992; Oliveira *et al.*, 1994). Each step in the processing chain leads to changes in product properties, caused by (bio)chemical, biological or physical changes (McMinn and Magee, 1997; Chua *et al.*, 2000). These changes might be either wanted or unwanted. In both cases quality, as experienced by the consumers, is affected. For example in baking processes, it is the browning reaction that is responsible for the desired colour and flavour (Martins *et al.*, 2001; Bimbenet and Lebert, 1992). Similar changes in colour and flavour are, however, undesirable in drying processes, leading to quality loss if they occur. Table 1.1 shows a large variety of phenomena that play a role in quality modifications (Bimbenet and Lebert, 1992).

### Description of quality

Quality is the extent to which a product meets the needs of the consumer. It includes sensory properties, psychological factors as well as other factors such as contributions to health and compatibility with life-style conditions (Bruhn, 1994; Bimbenet and Lebert, 1992; Bonazzi *et al.*, 1996). In general, the quality experience of the consumer can be linked to product properties, so-called quality attributes.

Quality attributes can be divided into three major categories: sensory, hidden and quantitative (Salunkhe *et al.*, 1991). The sensory characteristics of quality include colour, gloss, size, shape, texture, consistency, flavour and aroma, which the consumer can evaluate with his senses (Salunkhe *et al.*, 1991; Bruhn, 1994; Holdsworth, 1985; Ávila and Silva, 1999). One of the most important sensory quality attributes is colour, because it measures the first impact of the product on the consumer's perception (Ávila *et al.*, 1999; Bonazzi *et al.*, 1996). Other important attributes in the initial acceptance of a food are appearance, flavour and texture (Ávila and Silva, 1999). Quality attributes that the consumer cannot evaluate with his senses are the hidden characteristics, such as nutritive value, presence of harmful or toxic substances (Salunkhe *et al.*, 1991). Quantity is also considered an attribute of quality, since it forms a part of the total quality evaluation of a product, e.g. the finished product yield of fruits or vegetables (Salunkhe *et al.*, 1991).

**Table 1.1.** Several types of quality modifications (Bimbenet and Lebert, 1992).

Types of phenomena involved in quality modification	
<ul style="list-style-type: none"> <li>• <b>biochemical reactions</b> <ul style="list-style-type: none"> <li>enzymatic reactions</li> <li>protein denaturation</li> <li>maillard reaction</li> <li>lipid oxidation</li> <li>vitamin oxidation/inactivation</li> </ul> </li> <li>• <b>microbiological reactions</b> <ul style="list-style-type: none"> <li>product modification by microbiological reactions</li> <li>development of micro organisms</li> <li>destruction of micro organisms</li> </ul> </li> <li>• <b>aroma loss</b> <ul style="list-style-type: none"> <li>mainly by evaporation</li> <li>occasionally by oxidation or other reaction</li> </ul> </li> <li>• <b>mechanical phenomena and phase changes</b> <ul style="list-style-type: none"> <li>crystallisation, glass transition, collapse, due to water elimination and to thermo/hydric effects</li> <li>shrinkage</li> <li>formation of cracks, holes, folds</li> </ul> </li> <li>• <b>migration (other than water)</b> <ul style="list-style-type: none"> <li>solutes</li> <li>fats</li> </ul> </li> </ul>	

Quality attributes are usually a consequence of subjective evaluation. Therefore, they are linked to quality indicators which can be reliably measured with objective instrumentation (Van Loey *et al.*, 1994). For example the quality attribute colour can be caused by pigments like  $\beta$ -carotene (Mishkin *et al.*, 1982). The quality attribute colour can therefore be measured by its indicator: carotenoid content. Another example is texture, which can be measured by tenderometers.

During processing of the food product, spatial distribution of the quality indicator can arise inside the product: the so-called quality indicator profile (QIP). Many examples can be found. During heating of lasagne (Stigter *et al.*, 2001), the temperature distribution causes positions with different cook value inside the food. During drying, the surface of the product can

change leading to stickiness and caking, crust formation and case hardening (Karel, 1992; Abid *et al.*, 1990; Karel and Flink, 1983). In pasteurisation and sterilisation processes the location with the least-lethality is of major importance (Banga *et al.*, 1991; Ávila *et al.*, 1999; Lund, 1977). Besides, when sterilised by conduction-heating, there is the danger of loss of colour or excessive softening of product at the periphery of the container (Lund, 1982; Ávila *et al.*, 1999). The formation of cracks during pasta drying originates from mechanical stresses due to internal moisture distributions (Andrieu *et al.*, 1988; Bonazzi *et al.*, 1996). In the fermentation process of olives, a sodium or potassium hydroxide solution is allowed to penetrate about two thirds, but not completely, towards the pits of the fruit. A small amount of bitter flesh remains and imparts a pleasing flavour to the pickled olives (Salunkhe *et al.*, 1991). In food preservation operations, like drying, cooling and heating, the growth of food poisoning micro organisms need to be prevented and food deteriorating enzymes need to be inactivated. This can only be achieved when the position with the worst condition of the quality indicator is taken into account.

Clearly, in the description of quality, the distribution of the quality indicator is often more relevant than its average value. Therefore the quality indicator profile or QIP needs focus.

### **Optimisation of quality**

The increased consumer awareness of food quality emphasises the need for product and process design optimisation. In industry not just quality considerations are important, but also economic and environmental aspects. The increase in energy costs as well as the adoption of more strict safety and environmental regulations and legislation are relevant (Kiranoudis *et al.*, 1994; Ávila and Silva, 1999; Holdsworth, 1985; Chou and Chua, 2001). In many cases product quality and productivity are conflicting criteria. Quality optimisation strategy favours mild processing conditions. This leads to higher processing times and hence lower productivity. Increasing the efficiency of the process will generally result in lower product quality.

The conflicting and opposing influences of the productivity of industrial operations and the final product quality can be balanced out to give the optimum operation (Holdsworth, 1985). Dynamic optimisation allows the explicit formulation of quality and other objectives as energy, productivity and resource consumption goals in a so-called objective function. This function expresses economic considerations including product price as a function of its

quality and processing costs as a function of the control variables. The optimal process control is concerned with the selection of a time-varying trajectory of control variables that either maximises or minimises the objective function (Olmos *et al.*, 2002; Ho *et al.*, 2001). With the variation of control variables the periods in which the product is more sensitive to quality reduction can be passed faster or in a more moderate way.

Five elements make up a dynamic optimisation problem (Evans, 1982; Ávila and Silva, 1999):

- 1) objective function: a mathematical expression reflecting the control objectives when maximised or minimised.
- 2) mathematical model: a model that describes mathematically the behaviour of the dynamic system and its outputs as determined by the inputs and the initial conditions.
- 3) initial conditions: initial values of the state-variables of the mathematical model.
- 4) control and state constraints: constraints on the state and control variables such as upper and lower bounds.
- 5) optimisation technique: a methodology to find the time depending trajectory of control variables that minimises or maximises the objective function.

The optimal operating conditions are usually computed off-line and then applied to the process without change. Thus, control could be successfully accomplished by a very simple controller like PID (Olmos *et al.*, 2002).

In the majority of reported studies, average values of the quality indicator are applied in the objective function or the optimisation procedure (e.g. Banga and Singh, 1994; Banga *et al.*, 1991; Van Boxtel and Knol, 1996; Ho *et al.*, 2001). In view of the earlier description of quality, it is not the average value of the quality indicator, but its spatial distribution inside the material that should be considered for an adequate optimisation of quality. This leads to the core hypothesis of present thesis:

*Core Hypothesis*

The consideration of quality indicator profiles (QIPs) inside the material is necessary to optimise quality.

## Quality optimisation during drying

To investigate the core hypothesis, a process or production step needs to be selected. It should be a step with high relevance, with an impact on quality, with the presence of QIPs, with conflicting criteria that need optimisation. This section explains the choice of drying as model process, because it fulfils all these requirements.

### Relevance

Drying of fruits and vegetables was practice in ancient times by Chinese, Hindus, Persians, Greeks and Egyptians. The ancient Hindus and Chinese dried herbs, fruits and vegetables by the sun and wind five thousand years ago (Salunkhe *et al.*, 1991). And until now, drying is one of the most important ways to preserve perishable food products throughout the world.

In tropical countries fresh food materials are dried to prevent wastage of surplus of seasonal crops. In India, a characteristic product is the mangobar, prepared by dehydration of fruit pulp (Chauhan *et al.*, 1993; Harigopal and Tonap, 1980). In Africa, kale, a green leafy vegetable with high amounts of vitamins and other micronutrients is dried. Since less than 4% of its population have access to refrigerators, drying is the ideal way to preserve kale (Mwithiga and Olwal, 2005). Waste of crops occurs due to the low level of processing in most of these countries. Furthermore, the tropical climate provides ideal conditions for rapid growth of micro organisms and for chemical reactions. The fruits or vegetables are dried in the open sun. This technique is extremely weather dependent, and has the problems of contamination with dust, soil, sand particles and insects. Also, the required drying time can be quite long (Doymaz, 2004).

In western countries drying of products takes place not only to improve shelf-life but also to improve the handling of products, to lower weight, packaging costs, transportation costs and storage space. It also enhances appearance, encapsulates original flavour and maintains nutritional value (Chou and Chua, 2001; Mwithiga and Olwal, 2005). Drying is a major operation in a wide range of industries. Insulin or other hormones are dried for inhalers in pharmaceuticals (Ståhl *et al.*, 2002). Baby foods are dried to preserve a high nutritional quality (Ávila and Silva, 1999). Drying of vegetables is also applied for military purposes, because of its space and weight-saving possibilities (Salunkhe *et al.*, 1991). Since the drying processes are not only applied for preservation, they are characterised by an increased level of

requirements, expressed in functional properties (foaming, emulsifying power of proteins), microbiological contamination, particle size distribution (e.g. low content of fines in powders), constancy of apparent density, powder flow ability, ability to quick rehydration, composition, colour, aroma, etc. (Bonazzi *et al.*, 1996; Kompany *et al.*, 1993).

Many fresh foods contain moisture levels of about 20-30% by weight and possess a water activity of about 0.95-1.00. Water activity is defined as the ratio of the vapour pressure of water in the food and the vapour pressure of pure water at the same temperature. It characterises the state of the water in foods (Van den Berg, 1981). At high water activity, the water in the food has similar properties as pure water. It can serve as medium for chemical, enzymatic and microbial reactions, many of which lead to ultimate loss of quality and nutritional value (Askar and Treptow, 1993; Labuza, 1980). So, in the fresh state of foods, deterioration and spoilage occur under ambient conditions (Robson, 1976). At lower water activity, the water is more bound to the material, and cannot take part in the deteriorative reactions. Consequently, it is not so much the water content, but its state, nature or availability in the food, expressed by the water activity that plays a role in the deteriorative processes. Changing the availability of water, by reducing the water activity, can result in an effective prevention of food from spoilage. On this idea the first preservation techniques were based that were deliberately used by man: the removal of water from foodstuffs by drying or the altering of the water status by addition of salts or sugars (Gould, 1989).

### **Impact on quality**

So the first objective of drying is to remove water and hence to stabilise the food product. However, during food drying, many other changes occur simultaneously resulting in a modified overall quality (Kompany *et al.*, 1993; Lund, 1977). In general, drying leads to reduction of visual, organoleptic and nutritional quality (Mudahar *et al.*, 1990). Reactions as illustrated in Table 1.1 lead to well-known changes in the fresh products during drying: colouring, loss of aroma, textural changes, reduction of nutritive value, cracking, altering of shape (e.g. Abid *et al.*, 1990; Madamba, 1997; Luyben *et al.*, 1982). These reactions are caused by both the increase in product temperature and the removal of moisture (Abid *et al.*, 1990). For example: vitamin C is destructed at high temperatures, whereas at lower moisture contents vitamin C is less sensitive to temperature inactivation (Mishkin *et al.*, 1982).

## **Presence of QIPs**

Among many factors affecting the quality attributes during drying, the most important are moisture content and temperature (Strumiłło *et al.*, 1991; Adamiec *et al.*, 1995). Hence, irrespective of the food, the prediction of the quality indicator during drying can be simplified to the prediction of moisture and temperature (Rossen and Hayakawa, 1977; Karel, 1992). Quality indicator profiles (QIPs) can thus be expected when spatial distributions of moisture and temperature arise.

Drying is a process of simultaneous heat and mass transfer (Parti, 1993; Langrish *et al.*, 1997). Energy from the air stream is transferred to the food material. The energy is used to evaporate the water and to heat the material. The water is removed from the material by the air stream. In both mass and heat transfer, two resistances towards transfer play a role. The two relevant mass transfer phenomena are diffusion and convection. Diffusion controls the transfer of moisture inside the material. Convection controls the transfer of moisture from the surface of the material to the air. For heat transfer, conduction controls the heat transfer within the material and convection the transfer from the air to the food's surface. The ratio between the intensities to internal and external transfer determines whether distributions of either mass or energy arise in the food. For example: when the controlling resistance for drying is the internal mass transfer resistance, the transfer from water from the inside of the food to the surface is much slower than the transport from the surface to the air. Therefore, the moisture content at the surface will be much lower than its concentration in the centre. Clearly, a distribution of water arises inside the food. The ratio between the internal and external resistances is evaluated with the corresponding Biot numbers. They depend on drying parameters as well as material properties (Parti, 1993). This indicates that distributions of moisture and/or temperature can arise in the food. And consequently, QIPs will occur in the food during and after drying.

## **Conflicting criteria**

Drying forms an important part in the final cost of most industrial products (Ouhab and le Pourhiet, 1985). This is due to the high energy costs and the costly investment of a drying unit (Ouhab and le Pourhiet, 1985). Drying accounts for up to 15% of all industrial energy usage, making it a notoriously energy intensive operation (Chua *et al.*, 2000; Chua *et al.*, 2001). Energy management is thus an essential part in food drying processes (Ho *et al.*, 2001). Most

energy-saving measures are harmful for quality aspects and visa versa. This indicates that drying is a process with conflicting criteria. And therefore, it is attractive to optimise the design and operation of these processes. By elucidating the interaction of product quality with energy efficiency the operating conditions of the drying process can be optimised (Ho *et al.*, 2001). Drying conditions will then be selected based on economic considerations including product price as a function of its quality and processing costs as a function of total drying time and the drying air parameters (Olmos *et al.*, 2002).

## **Research questions**

Drying fulfils all requirements to investigate the core hypothesis: the consideration of quality indicator profiles (QIPs) inside the material is necessary to optimise quality during drying. The research questions can be worked out for drying as follows:

- 1) do QIPs in simulation positively contribute to the prediction of quality?
- 2) do QIPs in simulation really make a difference in optimisation of quality?
- 3) can existing drying models describe QIPs adequately or does a new model need to be developed?
- 4) can it be demonstrated experimentally that QIPs makes a difference in prediction and optimisation of quality?
- 5) can an adequate drying model predict the experimental QIPs?
- 6) can this adequate model be used in the optimisation routine?

## **Outline of the thesis**

The general aim of this thesis is to confirm the core hypothesis by studying the optimisation of quality during drying. As quality indicator residual activity of enzymes or micro organisms is chosen. The optimisation is composed of several components: a mathematical model that describes the drying process and the material during drying; a model that describes the quality indicator during drying; an objective function that needs to be maximised; criteria and constraints of the process. These components and their mutual relations are presented in Figure 1.1.

The research questions, required to study the core hypothesis, form the basis of the arrangement of the chapters. The relation to the optimisation scheme is depicted in Figure 1.1 in the grey boxes. *Chapter 2* treats the definition of quality during drying, based on simulation studies. It shows whether the consideration of QIPs really makes a difference in the prediction of quality. In *Chapter 3*, optimisation studies demonstrate whether the QIPs should be considered in the whole optimisation procedure. Does the consideration of QIPs lead to different optimal trajectories or to higher quality or higher efficiency? *Chapter 4* investigates existing drying models for the material and the need to develop a new one. The models as well as the required sorption isotherms are validated with experimental data. In *Chapter 5* the existence of QIPs and the influence of drying conditions are investigated experimentally. In this chapter, the possibility to predict the QIPs with the most adequate drying model is investigated as well. It forms the central chapter of this thesis, by combining all preceding theoretical and modelling considerations with practice. *Chapter 6* investigates whether this most adequate drying model can be applied in the optimisation of quality during drying. The question whether the core hypothesis will be rejected or confirmed will be concluded in *Chapter 7*. In this chapter, the final conclusions and some recommendations for further research will be presented.

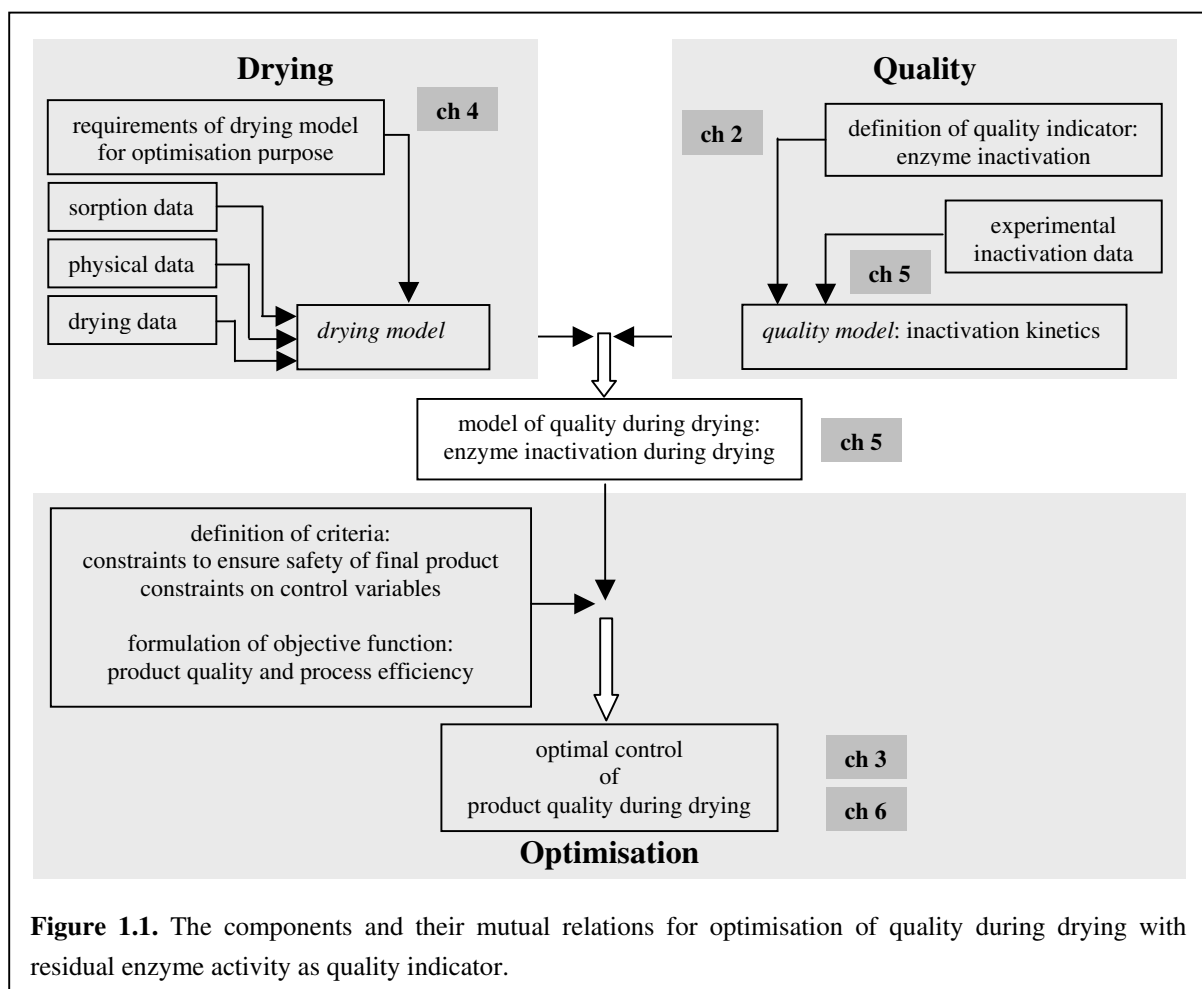


**Figure 1.1.** The components and their mutual relations for optimisation of quality during drying with residual enzyme activity as quality indicator.

## References

Abid, M., R. Gibert and C. Laguerie. An experimental and theoretical analysis of the mechanisms of heat and mass transfer during the drying of corn grains in a fluidized bed. *International Chemical Engineering*, vol. 30, 1990, no. 4, p. 632-642.

Adamiec, J., W. Kamiński, A.S. Markowski and C. Strumiłło. Drying of biotechnological products. p. 775-808. In: Mujumdar, A.S. (Ed.). *Handbook of industrial drying. Volume II*. New York, etc.: Marcel Dekker, Inc., 1995. 743-1423 p.

Andrieu, J., M. Bouvin and A. Stamatopoulos. Heat and mass transfer modelling during pasta drying. Application to crack formation risk reduction. p. 183-192. In: Bruin, S. (Ed.). *Preconcentration and drying of food materials*. Amsterdam, etc.: Elsevier Science Publishers B.V., 1988. 353 p.

Askar, A. and H. Treptow. *Quality assurance in tropical fruit processing*. Berlin, etc.: Springer-Verlag, 1993. 238 p.

Ávila, I.M.L.B. and C.L.M. Silva. Methodologies to optimize thermal processing conditions: an overview. p. 67-82. In: Oliveira, F.A.R. and J.C. Oliveira (Eds.). *Processing Foods. Quality optimization and process assessment*. Boca Raton, etc.: CRC Press Inc., 1999. 415 p.

Ávila, I.M.L.B., C. Smout, C.L.M. Silva and M. Hendrickx. Development of a novel methodology to validate optimal sterilization conditions for maximizing the texture quality of white beans in glass jars. *Biotechnology Progress*, vol. 15, 1999, no. 3, p. 565-572.

Banga, J.R., R.I. Perez-Martin, J.M. Gallardo and J.J. Casares. Optimization of the thermal processing of conduction-heated canned foods: study of several objective functions. *Journal of Food Engineering*, vol. 14, 1991, p. 25-51.

Banga, J.R. and R.P. Singh. Optimization of air drying of foods. *Journal of Food Engineering*, vol. 23, 1994, p. 189-211.

Bimbenet, J.J. and A. Lebert. Food drying and quality interactions. p. 42-57. In: Mujumdar, A.S. (Ed.). *Drying '92. Vol. I*. Amsterdam, etc.: Elsevier Science Publishers B.V., 1992. 1953 p.

Bonazzi, C., E. Dumoulin, A.-L. Raoult-Wack, Z. Berk, J.J. Bimbenet, F. Courtois, G. Trystram and J. Vasseur. Food drying and dewatering. *Drying Technology*, vol. 14, 1996, no. 9, p. 2135-2170.

Bruhn, C.M. Consumer perception of quality. p. 493-504. In: Singh, R.P. and F.A.R. Oliveira (Eds.). *Minimal processing of foods and process optimization. An interface*. Boca Raton, etc.: CRC Press, Inc., 1994. 529 p.

Chauhan, S.K., V.K. Joshi and B.B. Lal. Apricot-soy fruitbar – a new protein-enriched product. *Journal of Food Science and Technology*, vol. 30, 1993, no. 6, p. 457-458.

Chou, S.K. and K.J. Chua. New hybrid drying technologies for heat sensitive foodstuffs. *Trends in Food Science and Technology*, vol. 12, 2001, no. 10, p. 359-369.

Chua, K.J., J.C. Ho, A.S. Mujumdar, M.N.A. Hawlader and S.K. Chou. Convective drying of agricultural products - effect of continuous and stepwise change in drying air temperature. Paper No.29. In: Kerkhof, P.J.A.M., W.J. Coumans and G.D. Mooiweer. *Proceedings of the 12th International Drying Symposium IDS2000*. Amsterdam: Elsevier Science, 2000.

Chua, K.J., A.S. Mujumdar, M.N.A. Hawlader, S.K. Chou and J.C. Ho. Batch drying of banana pieces - effect of stepwise change in drying air temperature on drying kinetics and product colour. *Food Research International*, vol. 34, 2001, no. 8, p. 721-731.

Doymaz, İ. Convective air drying characteristics of thin layer carrots. *Journal of Food Engineering*, vol. 61, 2004, no. 3, p. 359-364.

Evans, L.B. Optimization theory and its application in food processing. *Food Technology*, vol. 36, 1982, no. 7, p. 88-93.

Gould, G.W. Drying, raised osmotic pressure and low water activity. p. 97-117. In: Gould, G.W. (Ed.). *Mechanisms of action of food preservation procedures*. London and New York: Elsevier Applied Science, 1989. 441 p.

Harigopal, U. and K.V. Tonapi. Technology for villages – solar drier. *Indian Food Packer*, vol. 34, 1980, no. 2, p. 48-49.

Ho, J.C., S.K. Chou, A.S. Mujumdar, M.N.A. Hawlader and K.J. Chua. An optimisation framework for drying of heat-sensitive products. *Applied Thermal Engineering*, vol. 21, 2001, no. 17, p. 1779-1798.

Holdsworth, S.D. Optimisation of thermal processing – a review. *Journal of Food Engineering*, vol. 4, 1985, p. 89-116.

Karel, M. Optimization of quality of dehydrated foods and biomaterials. p. 3-16. In: Mujumdar, A.S. (Ed.). *Drying '92. Vol. I*. Amsterdam, etc.: Elsevier Science Publishers B.V., 1992. 1953 p.

Karel, M. and J.M. Flink. Some recent developments in food dehydration research. p. 103-153. In: Mujumdar, A.S. (Ed.). *Advances in drying. Volume II*. Washington, etc.: Hemisphere Publishing Corporation in cooperation with McGraw-Hill International Book Company, 1983. 301 p.

Kiranoudis, C.T., Z.B. Maroulis and D. Marinos-Kouris. Dynamic simulation and control of conveyor-belt dryers. *Drying Technology*, vol. 12, 1994, no. 7, p. 1575-1603.

Kompany, E., J. Benchimol, K. Allaf, B. Ainseba and J.M. Bouvier. Carrot dehydration for instant rehydration: dehydration kinetics and modelling. *Drying Technology*, vol. 11, 1993, no. 3, p. 451-470.

Labuza, T.P. Water activity: physical and chemical properties. p. 320-325. In: Linko, P., Y. Mälkki, J. Olkku and J. Larinkari (Eds). *Food process engineering. Volume I. Food processing systems*. London: Applied Science Publishers LTD, 1980. 967 p.

Langrish, T.A.G., A.S. Brooke, C.L. Davis, H.E. Musch and G.W. Barton. An improved drying schedule for Australian ironbark timber: optimisation and experimental validation. *Drying Technology*, vol. 15, 1997, no. 1, p. 47-70.

Lund, D.B. Applications of optimization in heat processing. *Food Technology*, vol. 36, 1982, no. 7, p. 97-100.

Lund, D.B. Design of thermal processes for ... maximizing nutrient retention. *Food Technology*, vol. 31, 1977, no. 2, p. 71-78.

Luyben, K.Ch.A.M., J.K. Liou and S. Bruin. Enzyme degradation during drying. *Biotechnology and Bioengineering*, vol. 24, 1982, p. 533-552.

Madamba, P.S. Optimization of the drying process: an application to the drying of garlic. *Drying Technology*, vol. 15, 1997, no. 1, p. 117-136.

Martins, S.I.F.S., W.M.F. Jongen and M.A.J.S. van Boekel. A review of Maillard reaction in food and implications to kinetic modelling. *Trends in Food Science and Technology*, vol. 11, 2001, p. 364-373.

McMinn, W.A.M. and T.R.A. Magee. Quality and physical structure of a dehydrated starch-based system. *Drying Technology*, vol. 15, 1997, no. 6-8, p. 1961-1971.

Mishkin, M., M. Karel and I Saguy. Applications of optimization in food dehydration. *Food Technology*, vol. 36, 1982, no. 7, p. 101-109.

Mudahar, G.S., R.T. Toledo and J.J. Jen. A response surface methodology approach to optimize potato dehydration process. *Journal of Food Processing and Preservation*, vol. 14, 1990, no. 2, 93-106.

Mwithiga, G. and J.O. Olwal. The drying kinetics of kale (*Brassica oleracea*). *Journal of Food Engineering*, vol. 71, 2005, no. 4, p. 373-378.

Oliveira, J.C., P.M. Pereira and F.A.R. Oliveira. The role of transport phenomena. p. 253-280. In: Singh, R.P. and F.A.R. Oliveira (Eds.). *Minimal processing of foods and process optimization. An interface*. Boca Raton, etc.: CRC Press, Inc., 1994. 529 p.

Olmos, A., I.C. Trelea, F. Courtois, C. Bonazzi and G. Trystram. Dynamic optimal control of batch rice drying process. *Drying Technology*, vol. 20, 2002, no. 7, p. 1319-1345.

Ouhab, R. and A. le Pourhiet. Optimal drying conditions of grains. p. 428-433. In: Toei, R. and A.S. Mujumdar (Eds.). *Drying '85*. Washington, etc.: Hemisphere Publishing Corporation, 1985. 547 p.

Parti, M. Selection of mathematical models for drying grain in thin-layers. *Journal of Agricultural Engineering Research*, vol. 54, 1993, p. 339-352.

Robson, J.N. Some introductory thoughts on intermediate moisture foods. p. 32-42. In: Davies, R., G.G. Birch and K.J. Parker (Eds.). *Intermediate moisture foods*. London: Applied Science Publishers LTD, 1976. 306 p.

Rossen, J.L. and K.-I. Hayakawa. Simultaneous heat and moisture transfer in dehydrated food: A review of theoretical models. *AIChE Symposium series*, vol. 73, 1977, no. 163, p. 71-81.

Salunkhe, D.K., H.R. Bolin and N.R. Reddy (Eds.). *Storage, processing and nutritional quality of fruits and vegetables. Volume II. Processed fruits and vegetables*. Boca Raton, etc.: CRC Press, Inc., 1991. 195 p.

Ståhl, K., M. Claesson, P. Lilliehorn, H. Lindén and K. Bäckström. The effect of process variables on the degradation and physical properties of spray dried insulin intended for inhalation. *International Journal of Pharmaceutics*, vol. 233, 2002, no. 1-2, p. 227-237.

Stigter, J.D., N. Scheerlinck, B.M. Nicolai and J.F. van Impe. Optimal heating strategies for a convection oven. *Journal of Food Engineering*, vol. 48, 2001, no. 4, p. 335-344.

Strumiłło, C., A.S. Markowski and J. Adamiec. Selected aspects of drying of biotechnological products. p. 36-55. In: Mujumdar, A.S. and I. Filková (Eds.). *Drying '91*. Amsterdam, etc.: Elsevier Science Publishers B.V., 1991. 632 p.

Van Boxtel, A.J.B. and L. Knol. A preliminary study on strategies for optimal fluid-bed drying. *Drying Technology*, vol. 14, 1996, no. 3&4, p. 481-500.

Van den Berg, C. *Vapour sorption equilibria and other water-starch interactions; a physico-chemical approach*. Wageningen: Wageningen Agricultural University, Section Process Engineering, Department of Food Science, 1981. 186 p. PhD thesis.

Van Loey, A., A. Fransis, M. Hendrickx, J. Noronha, G. Maesmans and P. Tobback. The optimisation of product quality during thermal processing: a case study on white beans in brine. p. 369-390. In: Singh, R.P. and F.A.R. Oliveira (Eds.). *Minimal processing of foods and process optimization. An interface*. Boca Raton, etc.: CRC Press, Inc., 1994. 529 p.



### **Definition of quality during drying**

The use of moisture and temperature profiles in predicting product quality for optimal control of drying processes

This chapter has been published with minor modifications as:

Quirijns, E.J., A.J.B. van Boxtel and G. van Straten. The use of moisture and temperature profiles in predicting product quality for optimal control of drying processes. p. 485-490. In: Skjöldebrand, C. and G. Trystam (Eds.). *Proceedings on Automatic Control of Food and Biological Processes IV*. Göteborg, Sweden, 1998.

## **Abstract**

Drying of food, agricultural and biological active materials is highly energy consuming and can lead to decrease or destruction of product quality. Simulation of fluid bed drying of enzymes, immobilised in starch cylinders elucidates that the internal moisture distribution and local temperature of the material characterise the quality indicator of the material, expressed as residual enzyme activity. It is also shown that optimisation procedures should be based on quality indicator profiles inside the material instead of the common practice of the average value of this indicator or the indicator obtained from average conditions.

## Nomenclature

$A_f$	cross section area of fluid bed	$[m^2]$
$A_m$	exchange area of material	$[m^2]$
$a$	exponent in relation for diffusion coefficient (equation 2.3)	
$c_p$	heat capacity	$[J.kg^{-1}.K^{-1}]$
$D$	internal diffusion coefficient of moisture in material	$[m^2.s^{-1}]$
$D_0$	parameter in relation for diffusion coefficient (equation 2.3)	$[m^2.s^{-1}]$
$E_a$	activation energy for moisture diffusion	$[J.mol^{-1}]$
$E_{a,e}$	activation energy for enzyme inactivation	$[J.mol^{-1}]$
$E_{a,0}, E_{a,\infty}$	activation energy at $X = 0$ $[kg.kg^{-1}]$ and $X = \infty$ $[kg.kg^{-1}]$ , resp.	$[J.mol^{-1}]$
$G_a$	air flow rate	$[m^3.s^{-1}]$
$h$	external convective heat transfer coefficient	$[J.s^{-1}.m^{-2}.K^{-1}]$
$h_a$	specific enthalpy of air	$[J.kg^{-1}]$
$h_m$	material specific enthalpy	$[J.kg^{-1}]$
$J_T$	heat flux	$[J.s^{-1}.m^{-2}]$
$J_{Xs}$	mass flux, on surface of material	$[kg.m^{-2}.s^{-1}]$
$k$	external convective mass transfer coefficient	$[m.s^{-1}]$
$k_e$	inactivation rate constant of the enzyme	$[s^{-1}]$
$k_\infty$	frequency factor	$[s^{-1}]$
$k_{\infty,0}, k_{\infty,\infty}$	frequency factor at $X = 0$ $[kg.kg^{-1}]$ and $X = \infty$ $[kg.kg^{-1}]$ , resp.	$[s^{-1}]$
$L_f$	bed height	$[m]$
$L_m$	length of cylinder	$[m]$
$N_m$	number of material particles	
$p, q$	parameter for enzyme inactivation	$[kg_{ds}.kg^{-1}]$
$Q_e$	concentration of enzyme, quality indicator of the material	$[kg_{enzyme}.kg_{ds}^{-1}]$
QIP	Quality Indicator Profile	
$\mathcal{R}$	gas constant	$[J.mol^{-1}.K^{-1}]$
$R$	maximum radius of material	$[m]$
$RH$	relative humidity of drying air	$[\%]$
$r$	radius of material	$[m]$
$T$	temperature	$[^{\circ}C]$
$T_K$	absolute temperature	$[K]$
$t$	time	$[s]$
$X$	moisture content	$[kg.kg^{-1}]$

$Y_a$	absolute humidity of air	$[\text{kg.kg}^{-1}]$
$\Delta h_{vo}$	heat of evaporation at 0 °C	$[\text{J.kg}^{-1}]$
$\varepsilon$	bed porosity	$[\text{m}^3_{\text{air}}.\text{m}^{-3}_{\text{bed}}]$
$\lambda_m$	thermal conductivity of material	$[\text{J.s}^{-1}.\text{m}^{-1}.\text{K}^{-1}]$
$\rho$	density	$[\text{kg.m}^{-3}]$

*Subscripts*

a	air	ref	reference
av	average	s	surface
i	ingoing	v	vapour
m	material	w	water
o	outgoing	0	initial
pr	profiles		

## Introduction

Drying food, agricultural and biological active materials is a major operation in agro-food industries to improve the preservation properties of the product, to reduce transportation costs and to facilitate the utilisation of the products. The reduction of water content and the increase of the temperature of the solid during drying can lead to destruction or decrease of product quality. Structural and physical modifications can take place, as for example colouring, crust formation, decrease of organoleptic quality, inactivation of bacteria and enzymes, loss of nutrients and aroma (Liou *et al.*, 1985; Mishkin *et al.*, 1984).

Additionally, drying processes are highly energy consuming. The objectives of an energy efficient process and the highest possible product quality are conflicting in many cases. Optimisation allows the explicit formulation of energy and quality objectives, and will therefore have a large potential in enhancing the operation of drying processes (Madamba, 1997; Banga and Singh, 1994).

In the optimal control of drying of biological material, the quality of the material is the most important aspect. Since dried products are used in various situations and in various forms, it is obvious that the corresponding quality attributes are different. The quality attributes are linked to measurable quality indicators. Among many factors affecting the quality indicators, the most important are temperature and moisture content. As during the drying process, gradients of moisture content and temperature arise inside the material, the temperature and moisture distributions characterise the quality indicator rather than the average moisture content and average material temperature. For instance, in the case of food preservation, prevention of microbiological deterioration or the growth of organisms that could give rise to food poisoning is achieved by not exceeding a safe moisture content which is based on the local moisture concentration (Mishkin *et al.*, 1984; Wang and Brennan, 1995; Lievense, 1991; Villota and Karel, 1980). Consequently, the quality of biological material is based on the local evolution of moisture and temperature profiles in the materials, irrespective of the defined quality indicator.

Models used for dynamic optimal control approaches reported in literature differ. Differences can be found in the use of average moisture content and temperature for the prediction of the quality indicator (Van Boxtel and Knol, 1996; Sun *et al.*, 1995), the application of moisture concentration profiles for defining an average value of the quality indicator, while the external resistance to mass transfer is neglected (Mishkin *et al.*, 1984; Banga and Singh, 1994) or the

prediction of a quality indicator at every position in the material (Langrish *et al.*, 1997). The latter only take into account the model on material level, while the influence of the dryer itself and the energy consumption are not considered.

In the approach described in this chapter, the dynamical model on the contrary contains both internal and external resistances towards mass and heat transfer on the level of the material and is embedded in an overall process model. The attention is mainly focussed on the evolution of the quality indicator during drying. The inactivation of enzymes immobilised in starch cylinders, which are being dried in a fluid bed will be discussed as a case study. For the simulations gPROMS has been employed.

## Modelling

### Model on micro-scale: material level

The drying of material can be described as coupled heat and mass transport both to and from the surface and within the material. The general process model consists of two nonlinear partial differential equations, one for moisture diffusion and the other for conductive heat transfer in the material. The equations for the transfer of moisture and heat at the surface of the material form boundary conditions for the partial differential equations.

$$\frac{\partial(\rho_m \cdot X)}{\partial t} = \frac{1}{r} \cdot \frac{\partial}{\partial r} \left( r \cdot \rho_m \cdot D \cdot \frac{\partial X}{\partial r} \right) \quad (2.1)$$

$$\frac{\partial(\rho_m \cdot h_m)}{\partial t} = \frac{1}{r} \cdot \frac{\partial}{\partial r} \left( r \cdot \lambda_m \cdot \frac{\partial T_m}{\partial r} \right) \quad \text{with} \quad h_m = c_{p,m} \cdot T_m + X \cdot c_{p,w} \cdot T_m \quad (2.2)$$

The internal diffusion is governed by the effective diffusion coefficient, which is a function of both material temperature ( $T_m$ ) and moisture content ( $X$ ) (Lievens, 1991):

$$D = D_0 \cdot \exp \left( - \frac{E_a}{\mathfrak{R}} \cdot \left( \frac{1}{T_{m,K}} - \frac{1}{T_{ref,K}} \right) \right) \cdot (X)^a \quad (2.3)$$

### Initial and boundary conditions

At the beginning of the drying process, moisture concentration and temperature profiles in the material are uniform:

$$t = 0 \quad 0 \leq r \leq R \quad X = X_0 \quad t = 0 \quad 0 \leq r \leq R \quad T_m = T_{m0} \quad (2.4)$$

Moisture and temperature distribution in the material are symmetrical during drying:

$$r = 0 \quad t > 0 \quad \left. \frac{\partial X}{\partial r} \right|_{r=0} = 0 \quad r = 0 \quad t > 0 \quad \left. \frac{\partial T_m}{\partial r} \right|_{r=0} = 0 \quad (2.5)$$

The solid surface and the air are assumed to be at equilibrium:

$$r = R \quad t > 0 \quad J_{Xs} = -D \cdot \rho_m \cdot \left. \frac{\partial X}{\partial r} \right|_{r=R} = k \cdot (\rho_{w,s} - \rho_{w,a}) \quad (2.6)$$

where  $k \cdot (\rho_{w,s} - \rho_{w,a})$  is the waterflux from the surface to the air due to convection.  $\rho_{w,s}$  is determined by the GAB sorption isotherm (Lievens, 1991) and the saturated vapour pressure.

$$r = R \quad t > 0 \quad J_T = \lambda_m \cdot \left. \frac{\partial T_m}{\partial r} \right|_{r=R} = h \cdot (T_a - T_m|_{r=R}) - J_{Xs} \cdot (\Delta h_{vo} - (c_{p,w} - c_{p,v}) \cdot T_m|_{r=R}) \quad (2.7)$$

where  $J_T$  is the residue of the convective heat transport,  $h \cdot (T_a - T_m|_{r=R})$  and the heat required for the evaporation of moisture.

### Model of quality: enzyme inactivation

Quality ( $Q_e$ ) degradation of enzymes can usually be described by first-order reaction kinetics (Mishkin *et al.*, 1984; Villota and Karel, 1980; Luyben *et al.*, 1982):

$$\frac{dQ_e}{dt} = -k_e \cdot Q_e \quad \text{with} \quad k_e = k_\infty \cdot \exp\left(-\frac{E_{a,e}}{\mathfrak{R} \cdot T_{m,K}}\right) \quad (2.8)$$

The activation energy,  $E_{a,e}$  as well as the frequency factor,  $k_\infty$  depend on the moisture content:

$$E_{a,e} = E_{a,\infty} + (E_{a,0} - E_{a,\infty}) \cdot \exp(-p \cdot X) \quad (2.9)$$

$$\ln k_{\infty} = \ln k_{\infty,\infty} + (\ln k_{\infty,0} - \ln k_{\infty,\infty}) \cdot \exp(-q \cdot X) \quad (2.10)$$

The kinetic parameters for the degradation of the enzyme catalase are obtained from literature (Luyben *et al.*, 1982).

### Model on macro-scale: process level

The batch fluidised bed is assumed to be an ideally mixed bed, with uniform temperature and humidity of the air which equal the outgoing air conditions (i.e.  $Y_{a,o} = Y_a$  and  $T_{a,o} = T_a$ ). Due to this hypothesis, the material particles are all at the same stage of drying at any instant of the batch operation. Moreover, there is no interaction between the particles, as far as drying is concerned (Kerkhof, 1994; Mourad *et al.*, 1995).

#### Air humidity

Due to the properties of an ideally mixed bed, the mass flux to the air is the same for all particles ( $J_{Xs}$ ). The accumulation of water in air is described by:

$$\frac{dY_a}{dt} = \frac{\rho_a \cdot G_a \cdot (Y_{a,i} - Y_a) + J_{Xs} \cdot A_m \cdot N_m}{\varepsilon \cdot \rho_a \cdot L_f \cdot A_f} \quad (2.11)$$

#### Air temperature

The enthalpy of the air decreases due to the transfer of energy from the air to the particle and increases by the enthalpy content of the flux of evaporated water, resulting in the enthalpy balance:

$$\varepsilon \cdot \rho_a \cdot V \cdot \frac{dh_a}{dt} = \rho_a \cdot G_a \cdot (h_{a,i} - h_{a,o}) - A_m \cdot N_m \cdot h \cdot (T_a - T_m|_{r=R}) + A_m \cdot N_m \cdot J_{Xs} \cdot [\Delta h_{vo} + c_{p,v} \cdot T_m|_{r=R}] \quad (2.12)$$

with  $T_{a,o} = T_a$ ,  $Y_{a,o} = Y_a$  and the enthalpy of air  $h_a = c_{p,a} \cdot T_a + Y_a \cdot (\Delta h_{vo} + c_{p,v} \cdot T_a)$ , the temperature change in time can finally be described by:

$$\frac{dT_a}{dt} = \frac{\rho_a \cdot G_a \cdot (T_{a,i} - T_a) \cdot (c_{p,a} + Y_{a,i} \cdot c_{p,v}) - A_m \cdot N_m \cdot ((h + J_{Xs} \cdot c_{p,v}) \cdot (T_a - T_m|_{r=R}))}{\varepsilon \cdot \rho_a \cdot V \cdot (c_{p,a} + c_{p,v} \cdot Y_a)} \quad (2.13)$$

## Results and discussion

### Enzyme inactivation

Enzymes are sensitive to both temperature and moisture content (Figure 2.1). The inactivation rate constant,  $k_e$  increases due to an increase in temperature as well as an increase in moisture content. Moreover, the enzymes are less sensitive to thermal inactivation at lower moisture contents. The enzyme activity stabilises as the material becomes dry.

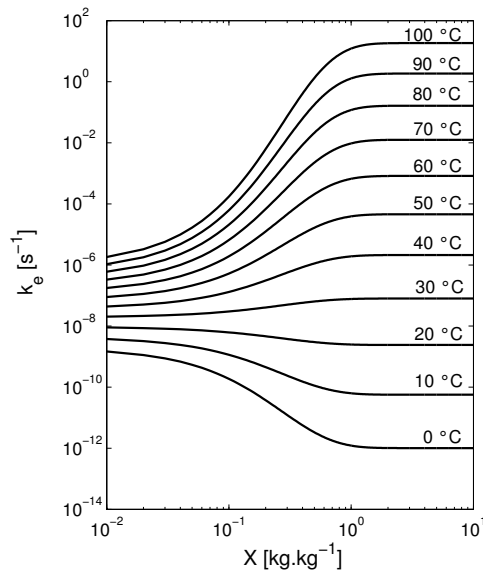


**Figure 2.1.** Inactivation constant of catalase as function of moisture content and temperature.

### Importance of distributions of $X$ , $T_m$ and $Q_e$ inside the material

The value of a quality indicator can be expressed in three different ways:

- the quality indicator corresponds to the spatial enzyme activity distribution inside the material, based on the local moisture content and temperature,  $Q_e$  (Figures 2.2c and 2.3a).
- the quality indicator is defined as the mean enzyme activity, by averaging the spatial activity distribution,  $Q_{e,pr}$  (equation AI, solid lines in Figures 2.2d and 2.3b).
- the average enzyme activity, obtained from average moisture content and average temperature of the material, can be applied as quality indicator,  $Q_{e,av}$  (dashed lines in Figure 2.2d and 2.3b).  $Q_{e,av}$  is achieved by applying  $\bar{X}$  and  $\bar{T}_m$  (from equation AI) in the relations for enzyme inactivation (equation 2.8, 2.9 and 2.10).

The drying behaviour of the starch cylinders is affected by the control variables,  $T_{a,i}$ ,  $Y_{a,i}$  and  $v_a$  as well as by the initial moisture content and dimensions of the cylinders. Due to the influence of these variables on the local moisture content and temperature distributions, the distribution of the residual activity of the enzyme inside the material will also be affected.

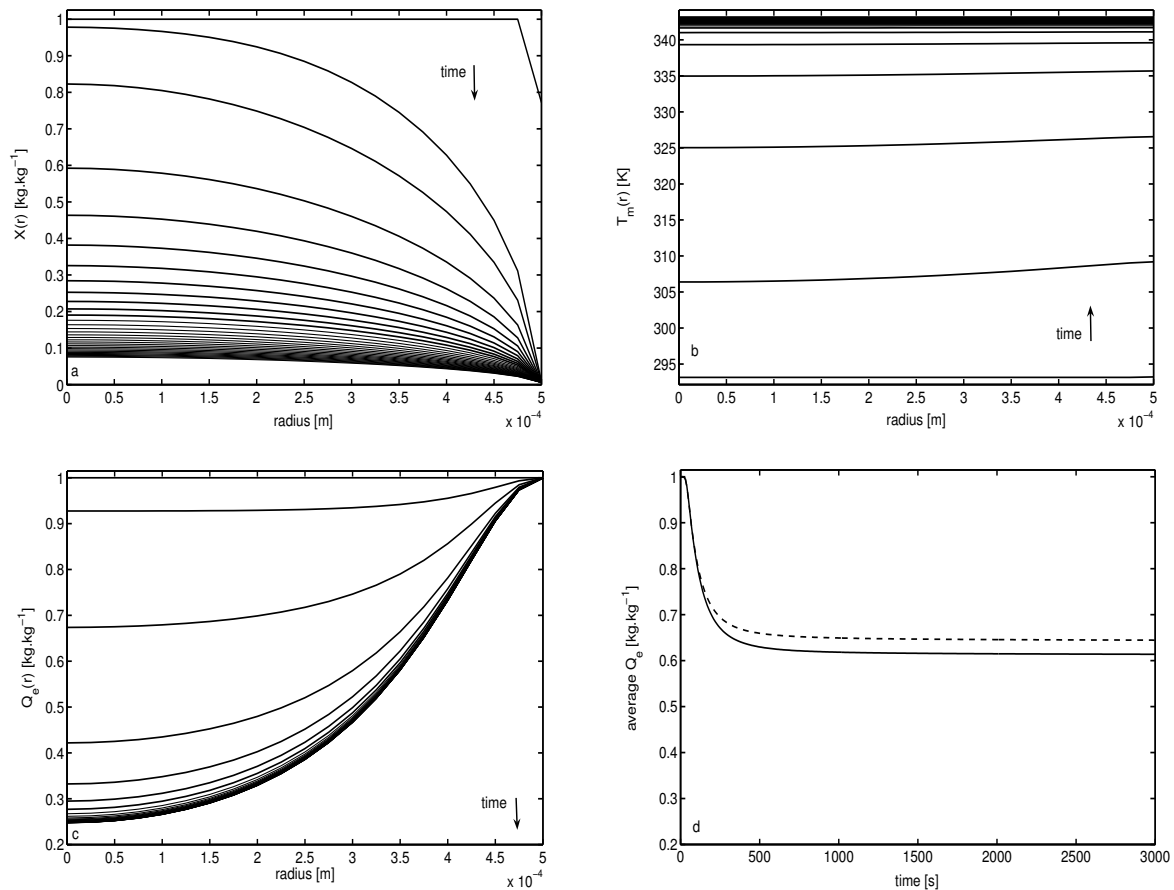


**Figure 2.2.** Moisture concentration (a), enzyme activity (c) (at  $t = 0, 50, 100$ , after that every 100 [s]), temperature (b) profiles (every 10 [s]) inside the material and average enzyme activities (d), drying time 3000 [s],  $T_{a,i} = 70^\circ\text{C}$ ,  $Y_{a,i} = 0.002$  [kg.kg<sup>-1</sup>],  $v_a = 2$  [m.s<sup>-1</sup>],  $r = 0.5$  mm.

From the spatial distribution of enzyme activity, it appears clearly that the local moisture content and temperature characterise the quality indicator of the material (Figure 2.2). Due to diffusion limitation of the drying process, the surface moisture content reaches almost immediately the equilibrium value. Since catalase is less sensitive to temperature at low moisture contents, the activity is retained at the surface. Consequently, the enzyme activity is preserved in a thin layer near the surface of the material, while inside the particle, the enzyme is almost completely inactivated. By changing external air conditions, the resistance to

external mass transfer can be enlarged. For example, by increasing the air humidity or decreasing the air flow, the drying process is initially controlled by convection. The surface moisture content decreases more gradually, resulting in more inactivation at the surface. However, during this period the moisture profiles are flat leading to less steep quality indicator profiles (QIPs) inside the material (Figure 2.3a).

The quality indicator should, therefore, at least be obtained from moisture content and temperature distributions inside the material. The quality indicator assuming an average uniform moisture content and temperature,  $Q_{e,av}$  does not describe the enzyme activity in a proper way. Moreover,  $Q_{e,av}$  deviates from the quality indicator characterised by the profiles,  $Q_{e,pr}$  (Figure 2.2d).

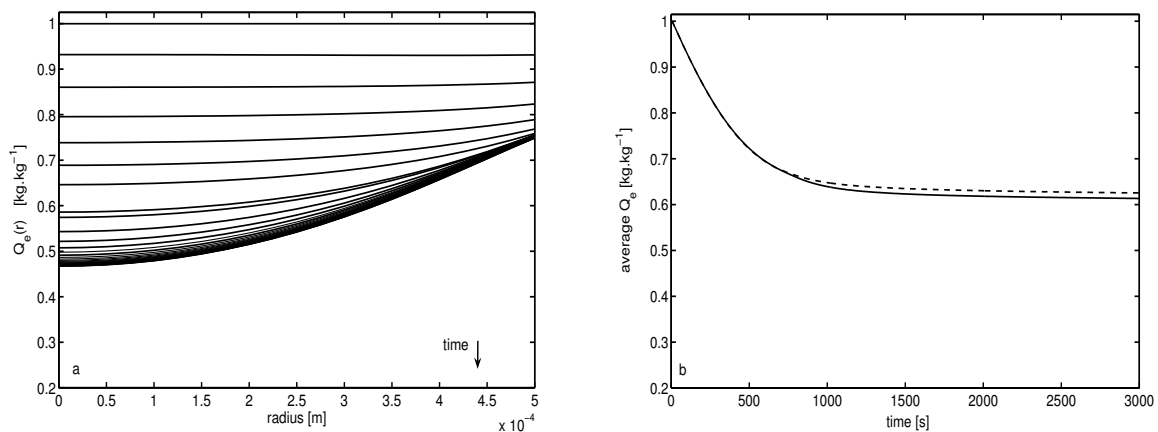


**Figure 2.3.** Enzyme activity profiles (a) inside the material (every 100 [s]) and average enzyme activities (b), drying time 3000 [s],  $T_{a,i} = 70^{\circ}\text{C}$ ,  $\text{RH} = 70\%$ ,  $v_a = 2$  [m.s<sup>-1</sup>],  $r = 0.5$  mm.

Besides, comparison of the Figures 2.2 and 2.3 elucidates, that the average quality indicator based on the local moisture content and temperature,  $Q_{e,pr}$  does not give an unambiguous description of the quality indicator distribution inside the material. After all, the same average value for the quality indicator of 0.61 [kg.kg<sup>-1</sup>] after a drying time of 3000 [s], corresponds with different spatial distribution of the enzyme activity. Moreover, due to the steep QIPs in Figure 2.2c, much higher (0.99 [kg.kg<sup>-1</sup>]) as well as lower activities (0.25 [kg.kg<sup>-1</sup>]) than indicated by the average value of the quality indicator are present in the material. In the case that enzyme activity retention is desired, the QIPs can be averaged out, since the final total activity is of importance. However, when deteriorative enzymes or bacteria, organoleptic

quality attributes, e.g. colouring are considered, the spatial distribution of the quality indicator has to be taken into account.

## Conclusions

For the optimal drying control of heat and moisture sensitive products, the model has to consider external and internal limitations to mass and heat transfer on material level. Moreover, a model describing the drying on macro-level is required to link the changes in the product to operation conditions.

Control variables,  $T_{a,i}$ ,  $Y_{a,i}$  and  $v_a$  and also material properties as initial moisture content and particle dimensions influence the quality indicator profiles inside the material. The QIPs demonstrate that the quality indicator has to be achieved from the distribution of moisture content and temperature inside the material.

To optimise the quality of material after drying, an objective function has to be formulated. Two possibilities exist: an objective function based on the average value of the quality indicator, based on moisture and temperature distributions, or an objective function which takes the distribution of the quality indicator inside the material into consideration. The simulation results establish that the spatial distribution of the quality indicator inside the material has to be employed in the objective function.

This is in contrast with the dynamic optimal control approaches reported in literature. In the objective functions only average values of the quality indicator are applied, while the use of moisture concentration and temperature profiles in the prediction of quality is recognised by other researchers (Mishkin *et al.*, 1984; Banga and Singh, 1994; Wang and Brennan, 1995; Villota and Karel, 1980).

## References

- Banga, J.R. and R.P. Singh. Optimization of air drying of foods. *Journal of Food Engineering*, vol. 23, 1994, p. 189-211.
- Kerkhof, P.J.A.M. Relations between local and effective air-side mass and heat transfer coefficients in fluidized bed drying. *Drying Technology*, vol. 12, 1994, no. 5, p. 1191-1210.
- Langrish, T.A.G., A.S. Brooke, C.L. Davis, H.E. Musch and G.W. Barton. An improved drying schedule for Australian ironbark timber: optimisation and experimental validation. *Drying Technology*, vol. 15, 1997, no. 1, p. 47-70.
- Lievens, L.C. *The inactivation of Lactobacillus plantarum during drying*. Wageningen: Wageningen Agricultural University, Department of Food Processing, 1991. 118 p. PhD thesis.
- Liou, J.K., K.Ch.A.M. Luyben and S. Bruin. A simplified calculation method applied to enzyme inactivation during drying. *Biotechnology and Bioengineering*, vol. 27, 1985, p. 109-116.
- Luyben, K.Ch.A.M, J.K. Liou and S. Bruin. Enzyme degradation during drying. *Biotechnology and Bioengineering*, vol. 24, 1982, p. 533-552.
- Madamba, P.S. Optimization of the drying process: an application to the drying of garlic. *Drying Technology*, vol. 15, 1997, no. 1, p. 117-136.
- Mishkin, M., I. Saguy and M. Karel. Optimization of nutrient retention during processing: ascorbic acid in potato dehydration. *Journal of Food Science*, vol. 49, 1984, p. 1262-1266.
- Mourad, M., M. Hémati and C. Laguérie. Séchage de maïs en lit fluidisé à flottation II: modélisation de la cinétique de séchage (Drying of corn in a flotation fluidized bed. II: modelling of the kinetics of drying). *Chemical Engineering Journal*, vol. 60, 1995, no. 103, p. 39-47.
- Sun, Y., C.C. Pantelides and Z.S. Chalabi. Mathematical modelling and simulation of near-ambient grain drying. *Computers and Electronics in Agriculture*, vol. 13, 1995, p. 243-271.

Van Boxtel, A.J.B. and L. Knol. A preliminary study on strategies for optimal fluid-bed drying. *Drying Technology*, vol. 14, 1996, no. 3&4, p. 481-500.

Villota, R. and M. Karel. Prediction of ascorbic acid retention during drying. *Journal of Food Processing and Preservation*, vol. 4, 1980, p. 111-159.

Wang, N. and J.G. Brennan. A mathematical model of simultaneous heat and moisture transfer during drying of potato. *Journal of Food Engineering*, vol. 24, 1995, no.1, p. 47-60.

## Appendix 2.I. Linked relations

Average values for  $X$ ,  $T_m$  and  $Q_e$  in the material are determined by an integral over the starch cylinder:

$$\bar{X} = \frac{1}{\pi \cdot (R)^2 \cdot L_m} \cdot \int_0^R 2 \cdot \pi \cdot r \cdot L_m \cdot X(r) dr \quad (\text{AI})$$

The average values  $\bar{T}_m$  and  $\bar{Q}_{e,pr}$  can be described in a similar way.

# Optimisation of quality during drying

The significance of modelling spatial distributions of quality in optimal control of drying processes

This chapter has been published with minor modifications as:

Quirijns, E.J., L.G. van Willigenburg, A.J.B. van Boxtel and G. van Straten. The significance of modelling spatial distributions of quality in optimal control of drying processes. *Journal A. Benelux Quarterly Journal on Automatic Control*, vol. 41, 2000, no. 3, p. 56-64.

## **Abstract**

Drying processes are highly energy consuming and can lead to degradation of product quality. Optimisation of a drying process is studied based on an extensive model, which combines a model on macro-scale with a distributed, nonlinear and stiff model on micro-scale. Using a multi objective function, optimal control trajectories are computed for different drying times and for two cases: a biotechnological and a food industry application of enzyme drying. The optimisation results indicate the existence of an optimal drying time, an increase in the profit and an improvement of the performance of the operation. Particularly, the optimisations reveal that the spatial distribution of the quality indicator needs to be integrated in the optimisation procedure, either in the objective function or as a constraint, instead of the common practice of average conditions of the quality indicator. It even appears that the quality indicator profiles inside the material can be influenced by the trajectory of control variables.

## Nomenclature

$A_f$	cross section area of fluid bed	$[m^2]$
$A_m$	exchange area of material	$[m^2]$
$a$	exponent in relation for diffusion coefficient (equation 3.2)	
$c_1, c_2$	weighing factors in the penalty functions $J_X$ and $J_Q$ resp.	
$c_p$	heat capacity	$[J.kg^{-1}.K^{-1}]$
$D$	internal diffusion coefficient of moisture in material	$[m^2.s^{-1}]$
$D_0$	parameter in relation for diffusion coefficient (equation 3.2)	$[m^2.s^{-1}]$
$d_f$	diameter of fluidised bed	$[m]$
$E_a$	activation energy for moisture diffusion	$[J.mol^{-1}]$
$E_{a,e}$	activation energy for enzyme inactivation	$[J.mol^{-1}]$
$E_{a,0}, E_{a,\infty}$	activation energy at $X = 0$ $[kg.kg^{-1}]$ and $X = \infty$ $[kg.kg^{-1}]$ , resp.	$[J.mol^{-1}]$
$G_a$	air flow rate	$[m^3.s^{-1}]$
$h$	external convective heat transfer coefficient	$[J.s^{-1}.m^{-2}.K^{-1}]$
$h_m$	material specific enthalpy	$[J.kg^{-1}]$
$J$	total value of objective function/cash flow	$[fl.kg^{-1}.s^{-1}]$
$J_D$	objective function with quality and energy aspects	$[fl.kg^{-1}.s^{-1}]$
$J_{energy}$	absolute value of energy part in $J_D$	$[fl.kg^{-1}]$
$J_Q$	value of penalty function on final surface quality indicator	$[fl.kg^{-1}.s^{-1}]$
$J_{qual}$	absolute value of quality part in $J_D$	$[fl.kg^{-1}]$
$J_T$	heat flux	$[J.s^{-1}.m^{-2}]$
$J_X$	value of penalty function on final moisture content	$[fl.kg^{-1}.s^{-1}]$
$J_{Xs}$	mass flux, on surface of material	$[kg.m^{-2}.s^{-1}]$
$k$	external convective mass transfer coefficient	$[m.s^{-1}]$
$k_e$	inactivation rate constant of the enzyme	$[s^{-1}]$
$k_\infty$	frequency factor	$[s^{-1}]$
$k_{\infty,0}, k_{\infty,\infty}$	frequency factor at $X = 0$ $[kg.kg^{-1}]$ and $X = \infty$ $[kg.kg^{-1}]$ , resp.	$[s^{-1}]$
$L_f$	bed height	$[m]$
$L_m$	length of cylinder	$[m]$
$N$	number of discretisation points	
$N_m$	number of material particles	
$N_u$	number of control intervals	
$p, q$	parameter for enzyme inactivation	$[kg_{ds}.kg^{-1}]$
$Q_d$	desired final surface quality indicator	$[kg_{enzyme}.kg_{ds}^{-1}]$

$Q_e$	concentration of enzyme, quality indicator of the material	$[\text{kg}_{\text{enzyme}} \cdot \text{kg}_{\text{ds}}^{-1}]$
QIP	Quality Indicator Profile	
$\mathcal{R}$	gas constant	$[\text{J} \cdot \text{mol}^{-1} \cdot \text{K}^{-1}]$
$R$	maximum radius of material	$[\text{m}]$
$r$	radius of material	$[\text{m}]$
$T$	temperature	$[^{\circ}\text{C}]$
$T_{,K}$	absolute temperature	$[\text{K}]$
$t$	time	$[\text{s}]$
$t_f$	final drying time	$[\text{s}]$
$t_r$	reloading time	$[\text{s}]$
$X$	moisture content	$[\text{kg}_{\text{H}_2\text{O}} \cdot \text{kg}_{\text{ds}}^{-1}]$
$X_d$	desired final moisture content	$[\text{kg}_{\text{H}_2\text{O}} \cdot \text{kg}_{\text{ds}}^{-1}]$
$X_e$	equilibrium moisture content	$[\text{kg}_{\text{H}_2\text{O}} \cdot \text{kg}_{\text{ds}}^{-1}]$
$Y_a$	absolute humidity of air	$[\text{kg}_{\text{H}_2\text{O}} \cdot \text{kg}_{\text{da}}^{-1}]$
$\Delta h_{vo}$	heat of evaporation at 0 °C	$[\text{J} \cdot \text{kg}^{-1}]$
$\varepsilon$	bed porosity	$[\text{m}^3_{\text{air}} \cdot \text{m}^{-3}_{\text{bed}}]$
$\gamma$	constant in objective function related to energy costs	$[\text{fl} \cdot \text{J}^{-1} \cdot \text{kg}^{-1}]$
$\eta$	constant in objective function related to quality profit	$[\text{fl} \cdot \text{kg}^{-1}]$
$\lambda_m$	thermal conductivity of material	$[\text{J} \cdot \text{s}^{-1} \cdot \text{m}^{-1} \cdot \text{K}^{-1}]$
$\rho$	density	$[\text{kg} \cdot \text{m}^{-3}]$

*Subscripts*

a	air	ref	reference
dm	dry matter	s	surface
env	environment	v	vapour
i	ingoing	w	water
m	material	0	initial
o	outgoing		

## Introduction

Drying is an important unit operation in food processing and in the chemical and pharmaceutical industry. The main purpose of drying is the removal of water to preserve the material and guarantee safety during storage. Furthermore, drying reduces the transportation costs and facilitates the utilisation of the products.

One of the major side effects during drying of biological materials is the degradation of product quality. The fall in moisture content and the higher temperature of the material during drying leads to several irreversible biological or chemical reactions as well as structural, physical and mechanical modifications. Examples of this are colouring, crust formation, decrease of organoleptic quality, inactivation of bacteria and enzymes, loss of nutrients and aroma, development of stresses, and changes of shape and texture (Abid *et al.*, 1990; Madamba, 1997; Luyben *et al.*, 1982).

Drying processes are highly energy consuming. Rapid drying employing high temperatures may reduce the cost of processing but adverse reactions causing quality degradation of the product may increase. Hence, the objectives of an efficient process and the highest possible product quality are conflicting in many cases.

Provided that suitable models are available, dynamic optimisation is a powerful technique to resolve these conflicts. In this chapter dynamic optimisation is used to compute optimal time trajectories of the control variables on the basis of the explicit formulation of energy and quality objectives, thus showing the large potential of optimal control in enhancing the operation of drying processes (Madamba, 1997; Banga and Singh, 1994). Moreover, by varying the control variables in time, the periods in which the product is more sensitive to quality destruction can be passed faster or in a more moderate way. Consequently, higher product quality can be expected in comparison with the conventional control with constant air conditions.

Before proceeding it is useful to outline briefly the components necessary to achieve the optimal operation of drying processes of biological materials. In contrast to other approaches, the spatial distribution within the particles will be taken into account because of its marked effect upon the quality.

Simulation studies demonstrated that the quality of the material can be expressed by the quality indicator profiles (QIPs) inside the material, which is characterised by the internal

moisture distribution and local temperature, and not by average material moisture content and temperature (*Chapter 2*). Consequently, an accurate description of the kinetics of the drying process on the level of the material is essential. Since the control variables, i.e. the drying air conditions, will vary due to the optimisation, the model should describe the mass and heat transfer for a range of experimental conditions. Therefore, the mathematical model has to consider external as well as internal resistances to mass and heat transfer on material level.

From the energy perspective, a model of the overall dryer is necessary. Not only the total drying time as in Langrish *et al.* (1997), Mishkin *et al.* (1982; 1984; 1983) is of concern, but also the energy consumption for achieving and maintaining the desired air conditions.

So, in order to solve the dynamic optimal control problem the following elements are needed:

1. a mathematical model of the spatial distribution of moisture and temperature as a function of the external air conditions (micro-level),
2. a model describing the kinetics of quality degradation as a function of local moisture and temperature within the particles,
3. a model relating the air conditions around the particles to the controlled air conditions entering the drying equipment (macro-level),
4. an objective function which expresses the relevant aspects of product quality and process efficiency,
5. a computational method to compute the trajectories of the control variables in time that optimise the objective function.

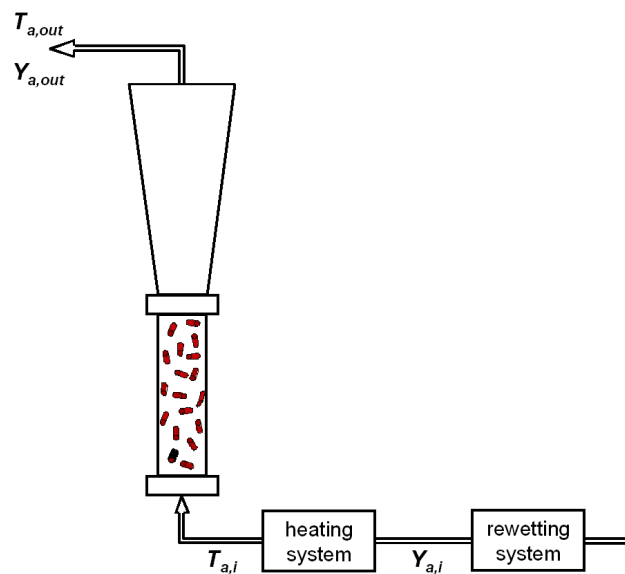


**Figure 3.1.** Schematic presentation of the pilot-plant fluidised bed dryer.

To illustrate the methodology, fluidised bed drying of enzyme, immobilised in starch cylinders, is taken as a case study. The residual activity of enzymes after drying is an important issue in biotechnological and food industries. In biotechnology, the objective of drying optimisation will be to maximise the retention of enzyme activity for the production of dry enzyme preparations, which can for example be used in detergents and in enzyme powders for pharmaceutical industries. In food processing, the goal may be opposite. In order to preserve the food quality during storage, enzymes which would catalyse undesired deteriorative conversions need to be inactivated (Liou *et al.*, 1985; Banga and Singh, 1994; Luyben *et al.*, 1982). Since enzyme inactivation strongly depends upon moisture and temperature, the drying of enzymes is an attractive subject for optimisation studies.

## Case description

The enzyme catalase is immobilised in starch cylinders with an average radius of 0.5 mm. The properties of starch and catalase are derived from literature. The starch cylinders are dried in a batch fluidised bed according to a pilot-plant dryer in our department (Figure 3.1). The fluidised bed has a diameter  $d_f$  of  $5 \cdot 10^{-2}$  [m] and a bed height  $L_f$  of  $20 \cdot 10^{-2}$  [m]. The control variables employed in this study are the ingoing air temperature,  $T_{a,i}$ , and humidity,  $Y_{a,i}$ , while the flow rate ( $G_a$ ) of the ingoing drying air as well as the shape, the size and the load of the material are kept constant.

Between the minimum value required for fluidisation and the maximum value to prevent entrainment, the flow rate does not significantly influence the drying behaviour at the relatively low load applied here. Therefore, the flow rate of the drying air is not considered as control variable.

## Elements of optimisation

### Model

#### *Model on micro-scale: material level*

##### *Drying model for cylindrical particles*

The mathematically simplest model, which can describe the heat and mass transport across the surface as well as within the particles needed for quality control is the distributed diffusional model. This model expresses the internal resistance to mass transfer by moisture diffusion, which can be described inside an infinite cylindrical particle by a nonlinear partial differential equation:

$$\frac{\partial (\rho_m \cdot X)}{\partial t} = \frac{1}{r} \cdot \frac{\partial}{\partial r} \left( r \cdot \rho_m \cdot \mathcal{D}(X, T_m) \cdot \frac{\partial X}{\partial r} \right) \quad (3.1)$$

where the internal diffusion is governed by an effective diffusion coefficient, which is a function of both material temperature ( $T_m$ ) and moisture content ( $X$ ) (Lievens, 1991):

$$\mathcal{D}(X, T_m) = \mathcal{D}_0 \cdot \left( \frac{X - X_e}{X_0 - X_e} \right)^a \cdot \exp \left( -\frac{E_a}{\mathcal{R}} \cdot \left( \frac{1}{T_{m,K}} - \frac{1}{T_{ref,K}} \right) \right) \quad (3.2)$$

At the beginning of the drying process, the moisture concentration profile inside the material is assumed to be uniform:

$$t = 0 \quad 0 \leq r \leq R \quad X = X_0 \quad (3.3)$$

During drying, the moisture distribution in the centre of the material is symmetrical:

$$r = 0 \quad t > 0 \quad \left. \frac{\partial X}{\partial r} \right|_{r=0} = 0 \quad (3.4)$$

The moisture content at the surface of the material is assumed to be in equilibrium with the air. The corresponding water concentration  $\rho_{w,s}$  is determined by the GAB sorption isotherm (Lievens, 1991) and the psychrometric relation for the saturated vapour pressure. The mass

flux of water from the surface to the air ( $J_{Xs}$ ) is proportional to the difference between the water concentration at the surface of the material ( $\rho_{w,s}$ ) and in the bulk air stream ( $\rho_{w,a}$ ):

$$r = R \quad t > 0 \quad J_{Xs} = -D \cdot \rho_m \cdot \left. \frac{\partial X}{\partial r} \right|_{r=R} = k \cdot (\rho_{w,s} - \rho_{w,a}) \quad (3.5)$$

The equations for the mass transfer in the centre and at the surface of the material (equation 3.4 and 3.5 respectively) form the boundary conditions for the partial differential equation (equation 3.1).

The internal resistance to heat transfer is expressed by heat conduction, which describes the change of the specific enthalpy of the material,  $h_m$  by:

$$\frac{\partial (\rho_m \cdot h_m)}{\partial t} = \frac{1}{r} \cdot \frac{\partial}{\partial r} \left( r \cdot \lambda_m \cdot \frac{\partial T_m}{\partial r} \right) \quad \text{with} \quad h_m = c_{p,dm}(T_m) \cdot T_m + X \cdot c_{p,w} \cdot T_m \quad (3.6)$$

The initial condition and boundary conditions for this nonlinear partial differential equation are equivalent to the ones for the equation describing the moisture diffusion:

$$t = 0 \quad 0 \leq r \leq R \quad T = T_{m0} \quad (3.7)$$

$$r = 0 \quad t > 0 \quad \left. \frac{\partial T_m}{\partial r} \right|_{r=0} = 0 \quad (3.8)$$

$$r = R \quad t > 0 \quad J_T = \lambda_m \cdot \left. \frac{\partial T_m}{\partial r} \right|_{r=R} = h \cdot (T_a - T_m|_{r=R}) - J_{Xs} \cdot (\Delta h_{vo} - (c_{p,w} - c_{p,v}) \cdot T_m|_{r=R}) \quad (3.9)$$

The latter describes the energy flux ( $J_T$ ), determined by the residue of the convective heat transport, which is proportional to the difference between the temperature of the drying air ( $T_a$ ) and the surface temperature ( $T_m|_{r=R}$ ), and the heat transfer required for the evaporation of moisture, under the assumption that evaporation of moisture only takes place at the surface of the material.

The external heat and mass transfer coefficients,  $h$  and  $k$  respectively, are characterised by dimensionless numbers and coupled by the Chilton-Colburn relation.

Although the distributed diffusional model is one of the simplest models describing spatial distributions, it still consists of two nonlinear partial differential equations, which cannot be solved analytically. Moreover, the dynamics of the boundary conditions and of the partial differential equation describing internal heat conduction are generally fast compared to the internal diffusion of moisture. This means that the system is stiff. The model could be simplified by neglecting these fast dynamics, leading to a constant boundary condition for the diffusion and to an ordinary differential equation describing the temperature changes. However, mentioned dynamics cannot be neglected since the varying control variables, which can alter the ratio of internal and external resistances, appear in the boundary conditions through  $Y_a$  and  $T_a$ .

#### *Quality model: enzyme inactivation*

The inactivation of enzymes, as well as other degradation reactions of bioproducts, is usually described by first-order reaction kinetics:

$$\frac{dQ_e}{dt} = -k_e \cdot Q_e \quad (3.10)$$

in which  $Q_e$  is the concentration of active enzyme, characterising the quality indicator of the material (Luyben *et al.*, 1982; Villota and Karel, 1980; Wijnhuizen *et al.*, 1979; Daemen and van der Stege, 1982; Strumiłło *et al.*, 1991; Mishkin *et al.*, 1984).

The temperature dependence of the inactivation rate of the enzyme,  $k_e$  can be described according to the Arrhenius equation:

$$k_e = k_\infty \cdot \exp\left(-\frac{E_{a,e}}{\mathfrak{R} \cdot T_{m,K}}\right) \quad (3.11)$$

where both the activation energy,  $E_{a,e}$  and the frequency factor,  $k_\infty$  depend on moisture content:

$$E_{a,e} = E_{a,\infty} + (E_{a,0} - E_{a,\infty}) \cdot \exp(-p \cdot X) \quad (3.12)$$

$$\ln k_\infty = \ln k_{\infty,\infty} + (\ln k_{\infty,0} - \ln k_{\infty,\infty}) \cdot \exp(-q \cdot X) \quad (3.13)$$

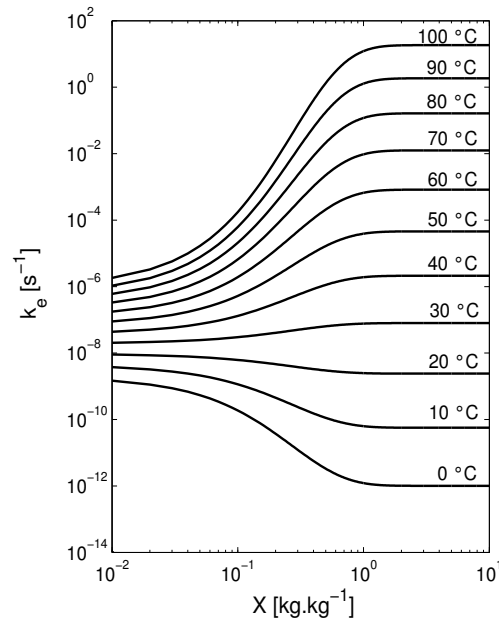


**Figure 3.2.** Inactivation constant of catalase as function of moisture content and temperature.

The enzyme considered is catalase, for which appropriate degradation rate models are available in literature (Luyben *et al.*, 1982). The inactivation rate of the enzyme,  $k_e$  is a function of both temperature and moisture content (Figure 3.2). It appears clearly that the enzyme is less sensitive to thermal inactivation at lower moisture contents. The enzyme activity stabilises as the material becomes dry.

#### *Model of enzyme inactivation during drying of cylindrical particles*

The mathematical models for the drying behaviour of the starch cylinders and for the kinetics of enzyme degradation are combined to obtain the retention of the enzyme as function of drying conditions and time. It is assumed that other products and reactants diffuse at a much slower rate than water, which makes the enzyme immobile with respect to the solids (Mishkin *et al.*, 1983). The moisture concentration and temperature at each position in the starch cylinder are substituted in the equations 3.10 to 3.13, which yields the catalase enzyme activity at the concerned position. Since during the drying of starch cylinders gradients of moisture content and temperature arise inside the material, a spatial distribution of the quality indicator can now be predicted.

**Model on macro-scale: process level**

In the batch fluidised bed dryer (Figure 3.1), the starch cylinders are completely dispersed in the vertically flowing air stream, as a consequence of the buoyancy effect of the air. The drying behaviour of the starch cylinders is governed by the evolution of the temperature and absolute humidity of the air. Each cylinder meets the local temperature and humidity of the surrounding air, while the air stream encounters all cylinders. Accordingly, micro and macro scale interact with each other (Taprantzis *et al.*, 1997; Mourad *et al.*, 1995; Kerkhof, 1994b). Since a small dryer with a low loading is considered, the following assumptions can be formulated (Taprantzis *et al.*, 1997; Soponronnarit and Prachayawarakorn, 1994; Kerkhof, 1994a; Van 't Land, 1991):

- no profiles in air temperature and air humidity exist along the height of the bed. This means that the dryer is assumed to be ideally mixed, causing the outgoing air conditions to be equal to the uniform temperature and humidity of the air (i.e.  $Y_{a,o} = Y_a$  and  $T_{a,o} = T_a$ ).
- the starch cylinders are all at the same stage of drying at any instance of the batch operation, arising from the well-mixed bed hypothesis.
- there is no interaction between the particles, due to the high ratio of air to mass of product.

The derivation of the total balances of mass and energy over the dryer is based on these assumptions, leading to differential equations, which express the dynamical behaviour of the absolute humidity,  $Y_a$  and temperature,  $T_a$  of the air.

The absolute humidity of the air changes as a consequence of the mass flux of moisture ( $J_{Xs}$ ) from the cylinders to the air, which is the same for all cylinders:

$$\frac{dY_a}{dt} = \frac{\rho_a \cdot G_a \cdot (Y_{a,i} - Y_a) + J_{Xs} \cdot A_m \cdot N_m}{\varepsilon \cdot \rho_a \cdot L_f \cdot A_f} \quad (3.14)$$

The enthalpy content of this mass flux of evaporated water causes an increase in the enthalpy of the air. Besides, the air enthalpy decreases due to the transfer of energy to all cylinders. The enthalpy residue determines the change in air enthalpy, which leads to a corresponding alteration in air temperature:

$$\frac{dT_a}{dt} = \frac{\rho_a \cdot G_a \cdot (T_{a,i} - T_a) \cdot (c_{p,a} + Y_{a,i} \cdot c_{p,v}) - A_m \cdot N_m \cdot ((h + J_{Xs} \cdot c_{p,v}) \cdot (T_a - T_m|_{r=R}))}{\varepsilon \cdot \rho_a \cdot V \cdot (c_{p,a} + c_{p,v} \cdot Y_a)} \quad (3.15)$$

Obviously, the control variables,  $T_{a,i}$  and  $Y_{a,i}$  come into view in these total balances over the dryer. Furthermore, they will become visible in the relation expressing the energy costs to

obtain and maintain the desired control. Instead of the control variables, the resulting state variables,  $T_a$  and  $Y_a$ , are encountered by the cylinders and appear in the boundary conditions 3.5 and 3.9. This indirect influence of the control variables, and the fact that they appear in the cost function rather than the states, stresses the need for an overall process model.

## Objective function

The objective function expresses the desired aims of the process explicitly. In contrast with the model, which is fixed by the physical characteristics of the system, the objective function can be chosen freely to accomplish a desired behaviour of the system. It represents the wishes with regard to the final product and the performance of the process.

Among the many possibilities, in this chapter a multi objective criterion function is used, expressing quality retention and energy efficiency in economic terms (Kamiński *et al.*, 1989; Van Boxtel and Knol, 1996; McFarlane and Bruce, 1996). The income of the drying process is indicated by the profit of the amount of dried end product, which increases linearly with its quality indicator:  $\eta \cdot Q_e(t_f)$ . This end product is achieved at the expense of energy to realise and maintain the trajectory of control variables,  $T_{a,i}$  and  $Y_{a,i}$ . The corresponding charges are expressed as the integrated energy costs for heating the air from the environmental temperature ( $T_{env}$ ) to the desired course of ingoing air temperature  $T_{a,i}$  with a certain humidity  $Y_{a,i}$ . Since a batch process is considered, the cash flow is divided by the sum of drying time  $t_f$  and time for reloading  $t_r$ , in order to express the efficiency of the equipment:

$$J_D = \frac{\eta \cdot \overline{Q_e(t_f)} - \int_0^{t_f} \gamma \cdot \rho_a \cdot G_a \cdot (c_{p,a} + c_{p,v} \cdot Y_{a,i}) \cdot (T_{a,i} - T_{env}) dt}{t_f + t_r} \quad (3.16)$$

in which the average value for  $Q_e$ , as well as the averages for  $X$  and  $T_m$ , is determined by an integral over the starch cylinder:

$$\overline{Q_e} = \frac{1}{\pi \cdot (R)^2 \cdot L_m} \cdot \int_0^R 2 \cdot \pi \cdot r \cdot L_m \cdot Q_e(r) dr \quad (3.17)$$

The weighting factors  $\eta$  and  $\gamma$  are expressed in currency units, and can be used to modify the compromise between the quality retention after the drying process and the efficient use of the

equipment during drying. However, these aspects are subordinate to the main purpose of drying, which is to reduce the moisture content of the product below a certain level in order to guarantee safety of the dried product during storage. Therefore, a constraint is defined on the final moisture content, by penalising the objective function with  $J_X$ , when the final average moisture content is higher than the safe moisture content,  $X_d$  of 0.05 [ $\text{kg}_{\text{H}_2\text{O}} \cdot \text{kg}_{\text{ds}}^{-1}$ ]:

$$J_X = c_1 \cdot (\overline{X(t_f)} - X_d) \quad \overline{X(t_f)} > X_d$$

$$J_X = 0 \quad \overline{X(t_f)} \leq X_d$$

By selecting  $c_1$  sufficiently large, the constraint on  $X(t_f)$  has priority with respect to the optimisation of the multi objective function  $J_D$ . Since the optimisation is achieved by minimisation, the overall objective function  $J$  can ultimately be described by:

$$J = J_X - J_D \quad (3.18)$$

### Optimisation procedure

The aim of the optimisation procedure is to find the schedule of control variables,  $T_{a,i}$  and/or  $Y_{a,i}$  that yields the minimal value for  $J$ , for a system whose dynamics are described by the equations 3.1 to 3.15. The optimisation problem is to solve:

$$\min_{T_{a,i}, Y_{a,i}} J(T_{a,i}, Y_{a,i}) \quad (3.19)$$

subject to the system equations (3.1 to 3.15) and the control input constraints:

$$298 \text{ [K]} < T_{a,i} < 373 \text{ [K]} \quad 0 < Y_{a,i} < 0.6 \text{ [kg}_{\text{H}_2\text{O}} \cdot \text{kg}_{\text{da}}^{-1}] \quad (3.20)$$

#### *Method to simulate system equations: centred finite differences*

For the numerical simulation of the system (equation 3.1 to 3.9), the infinite dimensional model is discretised with respect to the spatial coordinate by applying the implicit centred finite difference approximation. The discretisation leads to a stiff system of ordinary differential equations. By approximating the spatial integral in equation 3.17 with the

trapezoidal numerical integration rule, the remaining system can be integrated with respect to time together with the other (differential) equations. The time integration is performed by using an integrator suitable for stiff systems, provided by Matlab/Simulink.

*Method to derive a trajectory of control variables that minimises  $J$ : control parameterisation*

Among the various methods to solve dynamic optimisation problems, control parameterisation was selected because it is relatively simple and robust, and does not set restrictions to the form of the model. The control interval  $[0, t_f]$  is divided into  $N_u$  equidistant time intervals, in which the control variables remain constant. This is done for different fixed values of the final time  $t_f$ . The optimisation problem is then reduced to the estimation of the value of the control variables in each interval. The optimal control trajectory of  $N_u$  values for the control variables which minimises  $J$  (equation 3.18), can be determined with a constrained optimisation routine, where upper and lower bounds are defined for the control variables according to equation 3.20. The constrained optimisation routine is available in the Optimisation Toolbox of Matlab and based on the Sequential Quadratic Programming method, which is a very efficient, but rather complicated second-order technique (Trelea *et al.*, 1997). Since control parameterisation cannot guarantee a global minimum of  $J$ , several initial guesses for the control variables are applied to insure that the optimisation does not end up in a local minimum. From these calculations the temperature and humidity of the air at the dryer inlet are obtained as a function of time. The results are compared with the results of static optimisation, where  $J$  is minimised while the control variables are kept constant during the whole operation (Figure 3.3).

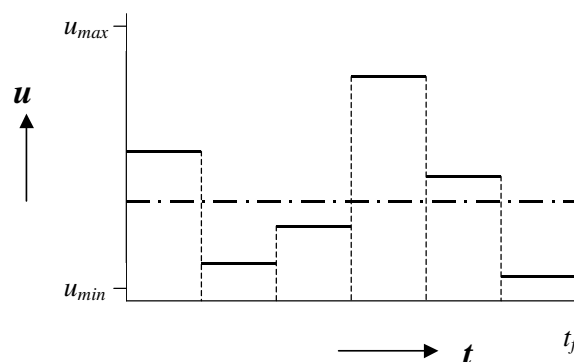


**Figure 3.3.** Trajectory of control variable ( $u$ ) during dynamic (solid) and static optimisation (-.-).

## Results and discussion

### Biotechnology application: retention of enzyme activity

The drying process where enzyme activity retention is desired, as in biotechnological industries, is optimised by applying only one control variable,  $T_{a,i}$  initially. The air humidity,  $Y_{a,i}$  is 3 [g<sub>H2O</sub>.kg<sup>-1</sup><sub>da</sub>]. The objective function  $J$  (equation 3.18) is minimised for different  $t_f$  and  $N_u$  (respectively 1, 3, 6 and 9) with a desired final moisture content of  $X_d = 0.05$  [kg.kg<sup>-1</sup>].  $N_u$  equal to 1 corresponds with static optimisation.

An optimal drying time can be observed at 1000 [s] for the dynamic optimisations (Figure 3.4). Moreover, in contrast with the expectations an increasing number of intervals does not significantly improve the performance. This agrees with Trelea *et al.* (1997), where three or more intervals only gave rise to minor decrease in the cost function. The optimal drying time is the most advantageous compromise between quality retention and energy consumption. Longer drying times do not save the enzyme anymore against inactivation. After 2000 [s] the quality indicator, expressed as the enzyme activity at  $t_f$ , remains the same, while the energy consumption increases due to the longer drying times.

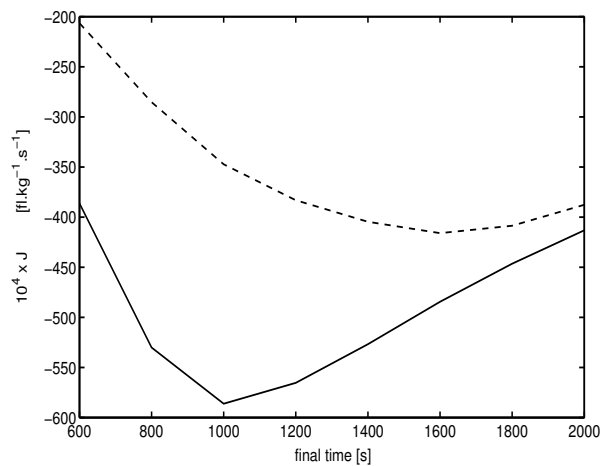


**Figure 3.4.** The value of  $J$  as function of final time for  $N_u = 1$  (---) and 6 (solid).

The static optimisation reaches its optimal drying time later, after 1600 [s] and at a smaller absolute value of the minimised objective function. The explanation for these phenomena follows from the comparison of the trajectories of the control variable and the resulting average moisture content and quality indicator for dynamic and static optimisation for a final

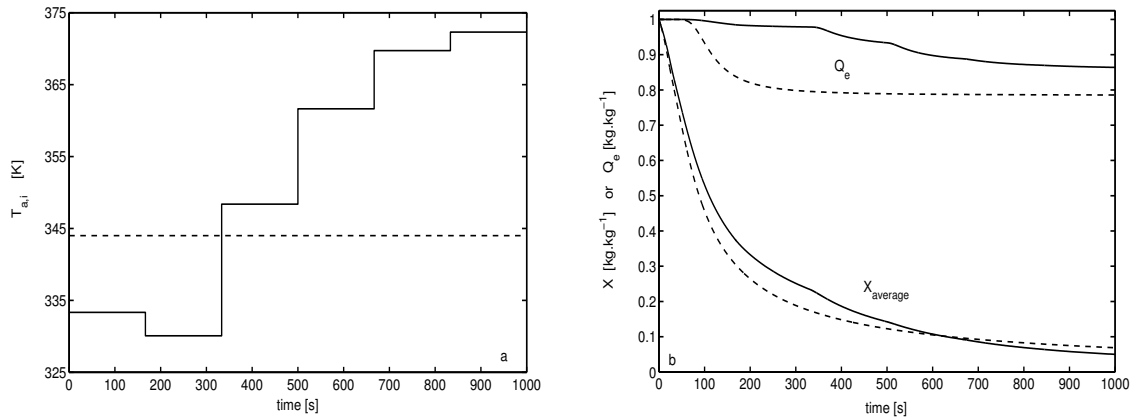


**Figure 3.5.** Trajectory of control variable  $T_{a,i}$  (a) and resulting average moisture content and average value for quality indicator (b) for static (---) and dynamic optimisation (solid), retention of enzyme ( $N_u=6$ ,  $t_f=1000$  [s]).

time of 1000 [s] (Figure 3.5). Evidently, the static optimisation is not able to attain the desired final moisture content within 1000 [s], leading to a penalty on the objective function. This causes a shift in time for the optimal value of  $J$  to the drying time, which at least is required to be able to achieve  $X(t_f)$  with a constant value for the control variable. Moreover, the final enzyme activity is much lower in the case of static optimisation, causing a lower absolute value for  $J$  as well. Due to the possible variation of the temperature in time, the dynamic optimisation can pass the temperature-sensitive phases of the enzyme catalase more moderately, i.e. at lower temperatures. When during drying the moisture content is reduced, catalase is rendered less sensitive to inactivation (Figure 3.2) and the temperature may be increased, in order to fulfil the constraint on  $X(t_f)$ .

Consequently, the benefits of the dynamic optimisation are distinct, since the safe moisture content is reached earlier and at elevated enzyme activity, owing to the possibility of changing  $T_{a,i}$  in time. Comparable tendencies in the trajectory of the control variable are obtained for optimisations of drying of other enzymes, vitamins, nutrients and wood (Mishkin *et al.*, 1982; Villota and Karel, 1980; Langrish *et al.*, 1997).

By omitting the  $X(t_f)$  penalty, the components of the objective function,  $J_D$  (equation 3.16), regarding quality and energy aspects respectively, can be compared for static and dynamic optimisation ( $N_u = 6$ ) at the optimal drying time of 1000 [s] (Table 3.1). Absolute values for  $J_{qual}$  and  $J_{energy}$  are considered, while the total profit is relative, divided by the sum of drying time and reloading time ( $t_f + t_r$ ). The dynamic optimisation leads to a higher retention of the enzyme activity, which is also revealed in  $J_{qual}$ . However, the increase of the quality objective

**Table 3.1.** Values of the (components of the) objective function  $J$  for static and dynamic optimisation, in case of enzyme retention ( $t_f = 1000$  [s],  $N_u = 6$ ,  $X_d = 0.05$  [kg.kg<sup>-1</sup>]).

Component of $J$		Static optimisation	Dynamic optimisation	Relative difference
$J_{qual}$	[fl.kg <sup>-1</sup> ]	86.242	95.039	+9.97%
$J_{energy}$	[fl.kg <sup>-1</sup> ]	-1.060	-1.238	-16.8%
$J_D \times 10^4$	[fl.kg <sup>-1</sup> .s <sup>-1</sup> ]	533.526	586.259	+9.85%
$-J_X$	[fl.kg <sup>-1</sup> .s <sup>-1</sup> ]	-186.205	-	+100%
$-J \times 10^4$	[fl.kg <sup>-1</sup> .s <sup>-1</sup> ]	347.321	586.259	+68.8%

with 10% is at the expense of higher energy costs (17%), due to the elevated temperatures at the final stage of drying to reach the constraint on  $X(t_f)$ . Nevertheless, the total profit  $J_D$  is enhanced with 10%, under the employed weighing factors. By including the penalty  $J_X$ , the overall performance is improved with 69%. Changing the ratio of the weighing factors,  $\eta$  and  $\gamma$ , will lead to different optimisation results. When longer drying times are considered, the dynamic optimisation enhances also the energy efficiency compared to the static optimisation, yet at lower value for  $J_D$  than for  $t_f = 1000$  [s].

Consequently, in case of enzyme retention, dynamic optimisation can reduce the optimal drying time with 37.5%, while improving the performance of the drying process, in comparison with static optimisation where a constant setpoint of  $T_{a,i}$  is maintained.

### Food industry application: inactivation of undesirable enzymes

#### *Optimisation considering average quality indicator only*

In food industry, material is dried to inactivate undesirable enzymes, which can catalyse deteriorative conversions during storage. In order to optimise this application, the quality term in the objective function  $J_D$  (equation 3.16) is changed into  $\eta \cdot (1 - \overline{Q_e(t_f)})$ , so that the maximisation of the destruction of the enzyme is expressed. The weighing factors in  $J_D$  are the same as in the case of enzyme activity retention, assuming that 1 kg of completely inactivated enzyme renders the same income as 1 kg of active enzyme. Initially, only one control variable  $T_{a,i}$  is used in the optimisations. Again, the air humidity,  $Y_{a,i}$  is 3 [g<sub>H2O</sub>.kg<sup>-1</sup><sub>da</sub>].

It is quite obvious that the minimisation of  $J$  in this case results in short-time-high-temperature drying, in order to save energy and to damage the thermal sensitive enzyme. The

**Table 3.2.** Values of the (components of the) objective function  $J$  for static and dynamic optimisation, in case of enzyme inactivation ( $t_f = 1000$  [s],  $N_u = 6$ ,  $X_d = 0.05$  [kg.kg<sup>-1</sup>]).

Component of $J$	Static optimisation	Dynamic optimisation	Relative difference
$J_{qual}$ [fl.kg <sup>-1</sup> ]	80.344	80.314	-0.04%
$J_{energy}$ [fl.kg <sup>-1</sup> ]	-1.662	-1.315	+ 20.9%
$J_D \times 10^4$ [fl.kg <sup>-1</sup> .s <sup>-1</sup> ]	491.763	493.746	+0.40%
$-J_X$ [fl.kg <sup>-1</sup> .s <sup>-1</sup> ]	-	-	-
$-J \times 10^4$ [fl.kg <sup>-1</sup> .s <sup>-1</sup> ]	491.763	493.746	+0.40%

only restriction on the drying time is the achievement of the safe final moisture content,  $X_d$ . The minimal drying time is 600 [s]. When inactivation of the enzyme is intended, the variation in  $T_{a,i}$  is mainly focussed on the minimisation of energy costs (Table 3.2).

With dynamic optimisation the same final enzyme activity is achieved as for the static one, while it improves the performance of the drying process, by preventing the material to be overdried (Figure 3.6). However, still approximately 30% of the initial enzyme activity is maintained. Initially, the enzyme is inactivated very fast, due to the high temperature. After this decrease of enzyme activity, no further reduction of the activity occurs, despite the persistent high temperature. The quality indicator profiles (QIPs) inside the cylinder demonstrate that near the surface the enzyme is not destructed at all (Figure 3.7). Due to the initial high temperature, the drying process is directly diffusion limited. The moisture content at the surface instantaneously reaches the moisture content, which is in equilibrium with the drying air. At this low moisture content, the enzyme is hardly sensitive to thermal inactivation

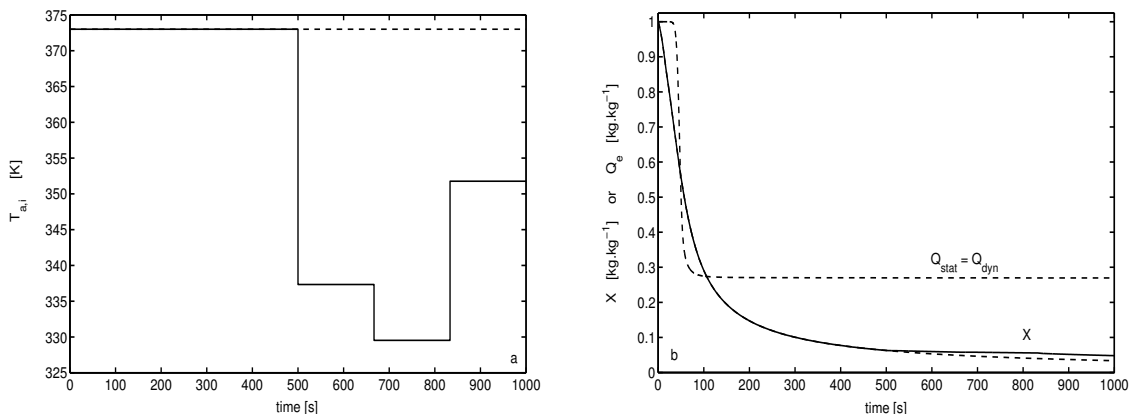


**Figure 3.6.** Trajectory of control variable  $T_{a,i}$  (a) and resulting average moisture content and average value for quality indicator (b) for static (--) and dynamic optimisation (solid), inactivation of enzyme ( $N_u = 6$ ,  $t_f = 1000$  [s],  $X_d = 0.05$  [kg.kg<sup>-1</sup>]).

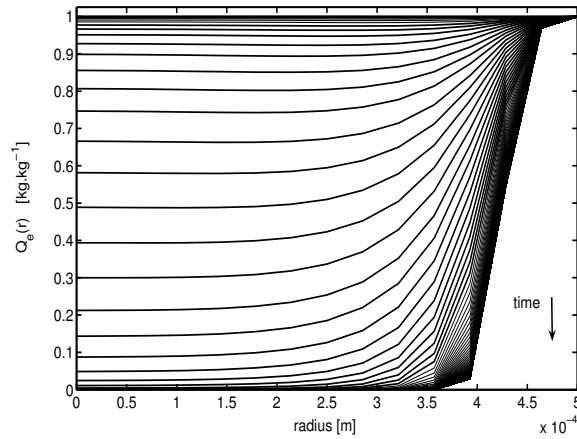


**Figure 3.7.** Spatial distribution of quality indicator inside material (every 1 [s]), dynamic optimisation of enzyme inactivation with control variable  $T_{a,i}$  ( $N_u = 6$ ,  $t_f = 1000$  [s]).

(Figure 3.2), leading to the retention of enzyme activity near the surface of the cylinder. Consequently, the enzyme can still cause spoilage and therefore safety is not guaranteed during storage, even if the average enzyme activity would indicate so.

#### *Optimisation considering spatial distribution of the quality indicator*

The dynamic optimisation considering only the average value of the quality indicator appeared not to be able to guarantee safety, since the activity of the undesirable enzyme is retained near the surface. To remedy this, the spatial distribution of the quality indicator should be considered in the optimisation procedure, in order to ensure stability of the material after drying. For this purpose, a constraint is defined on the residual enzyme activity at the surface of the cylinder by penalising the objective function  $J$ :

$$J = J_X + J_Q - J_D \quad (3.21)$$

where

$$\begin{aligned} J_Q &= c_2 \cdot (Q_e|_{r=R} - Q_d) & Q_e|_{r=R} > Q_d \\ J_Q &= 0 & Q_e|_{r=R} \leq Q_d \end{aligned}$$

To achieve this constraint, which is assumed to be  $Q_d = 0.3$  [-], an extra control variable has to be applied,  $Y_{a,i}$ . It is not possible to force the decline of the surface enzyme activity by only varying  $T_{a,i}$  under the present air humidity. From Figure 3.2, it appears that the enzyme is mainly sensitive for inactivation at higher moisture contents. Therefore, in order to inactivate

the enzyme at the surface of the material, a high moisture content is required at the boundary, which means that the drying process needs to be limited by external resistances. By varying the temperature, under the applied humidity  $Y_{a,i} = 3 \cdot 10^{-3}$  [kg.kg<sup>-1</sup>], the drying process will always be internally limited, leading to low moisture contents at the surface of the material. By using a higher constant air humidity, the drying can be externally limited. However, this will be accompanied by the need for high temperatures and very long drying times to achieve the final moisture content. At lower temperatures the final safe moisture content cannot be achieved at all. This reveals that in case of achieving the two constraints and optimal process efficiency, both temperature and air humidity should be varied in time, which means that the application of two control variables is essential. The employment of both control variables involves the risk of convergence problems of the optimisation routine.

By means of the extra constraint on the surface enzyme activity and the application of two

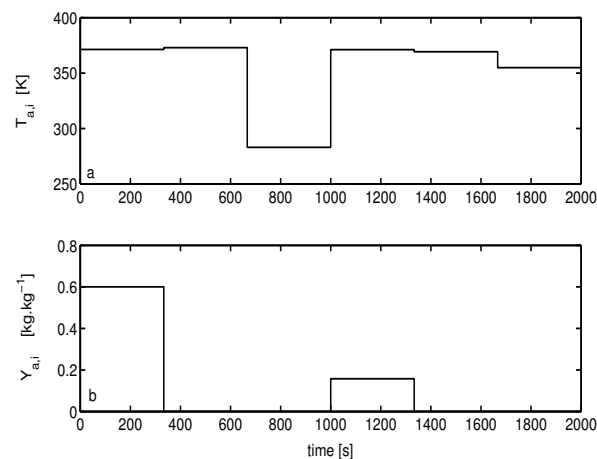


**Figure 3.8.** Trajectory of control variables,  $T_{a,i}$  (a) and  $Y_{a,i}$  (b), for dynamic optimisation of enzyme inactivation with constraint on  $Q_e|_{r=R}$  ( $N_u = 6$ ,  $t_f = 2000$  [s]).

control variables, the safety of the material after drying can be guaranteed, since the enzyme is completely inactivated, even at the surface of the material (Figure 3.8). The trajectory of control variables, corresponding to this optimisation, exhibits a combination of a high temperature and an elevated humidity of the drying air at the beginning of the drying process (Figure 3.9). As a consequence, the moisture content at the surface remains high, while the temperature of the material increases, causing inactivation of the enzyme at the surface. It is elucidated that the consideration of the QIPs inside the material in the optimisation procedure enhances the performance of the drying process. This is consistent with the increase of the

absolute value of the objective function, compared with the application of one control variable without the constraint on  $Q_e|_{r=R}$ , though at the expense of augmented energy costs (Table 3.3).

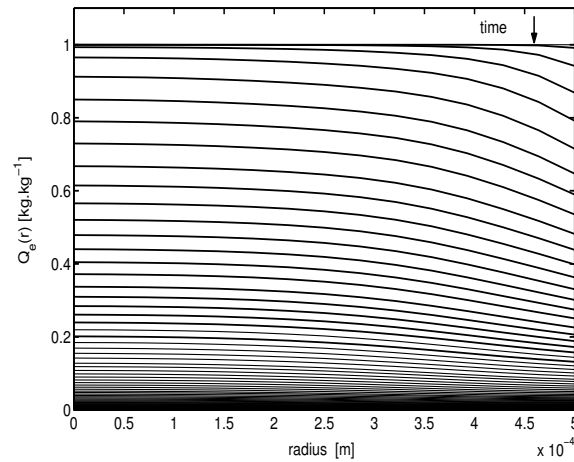


**Figure 3.9.** Spatial distribution of quality indicator inside material (every 1 [s]), dynamic optimisation of enzyme inactivation with control variables  $T_{a,i}$  and  $Y_{a,i}$  and constraint on  $Q_e|_{r=R}$  ( $N_u = 6$ ,  $t_f = 2000$  [s]).

**Table 3.3.** Values of the (components of the) objective function  $J$  for dynamic optimisation of the inactivation of enzyme with one or two control variables ( $t_f = 2000$  [s],  $N_u = 6$ ,  $X_d = 0.05$  [kg.kg<sup>-1</sup>],  $Q_d = 0.3$  [-]).

Component of $J$		one control variable, $T_{a,i}$ (without constraint on $Q_e _{r=R}$ )	two control variables, $T_{a,i}$ and $Y_{a,i}$ (with constraint on $Q_e _{r=R}$ )	Relative difference
$J_{qual}$	[fl.kg <sup>-1</sup> ]	80.294	110.00	+37.0%
$J_{energy}$	[fl.kg <sup>-1</sup> ]	-1.807	-3.268	-80.9%
$J_D \times 10^4$	[fl.kg <sup>-1</sup> .s <sup>-1</sup> ]	301.873	410.508	+36.0%
$-J_X$	[fl.kg <sup>-1</sup> .s <sup>-1</sup> ]	-	-	-
$-J \times 10^4$	[fl.kg <sup>-1</sup> .s <sup>-1</sup> ]	301.873	410.508	+36.0%

## Conclusions

The operation of drying processes can be enhanced by dynamic optimisation, based on a comprehensive model and a multi objective function, defined as an economic criterion involving quality and energy aspects. Such an extensive model, combining a model on macro-level with a distributed, highly nonlinear and stiff model on micro-level, has not been contemplated before in optimisation studies.

The improved operation is revealed in a higher absolute value of the objective function, expressed in [ $\text{fl.kg}^{-1}.\text{s}^{-1}$ ], due to either improving the quality indicator (e.g. case of retention of enzyme activity) or saving energy (e.g. case of inactivation of enzyme), by varying the control variable during the drying process. Moreover, the performance of the drying process is improved, since the dried material reaches the constraint on the final moisture content, preventing it from under- or over-drying, as can occur during the conventional drying with constant control variables. As a consequence, the dynamic optimisation reduces the optimal drying time with 37.5% in the optimisation for enzyme activity retention.

In the application for food industry, where undesired and deteriorative enzymes need to be inactivated, the dynamic optimisation results elucidate a very important item. In case that in the optimisation procedure only average values of the quality indicator are considered, it is possible that the optimisation leads to a dried product that still can spoil during storage, since the deteriorative enzyme has retained its activity near the surface of the material. This reveals that the distribution of the quality indicator inside the material must be taken into account in the optimisation procedure. Stability of the dried product can be ensured, when the enzyme at the surface of the material is inactivated. The surface enzyme activity can only be forced to reduce by applying two control variables, i.e. the temperature and humidity of the drying air. Consequently, the optimisations establish that spatial distribution of the quality indicator should be considered in the optimisation procedure, either in the objective function  $J$  or as a constraint. Apparently, the QIPs do not only characterise the quality of material during the simulation of the evolution of quality during drying, but is of relevance in optimisation procedures as well, in order to guarantee safety of the dried material and to increase the performance of the process. Furthermore, the trajectory of control variables can alter the QIPs inside the material. The integration of the spatial quality indicator in the optimisation procedure creates new possibilities for the food industry, where usually only average conditions of the quality indicator are applied. It is mainly important in drying processes, where deteriorative enzymes or bacteria need to be inactivated and where organoleptic quality aspects, e.g. colour need to be preserved.

Mishkin *et al.* (1983) concluded the opposite. They demonstrated that in case the objective function is based on an average quality indicator, the optimal trajectories of the control variables agree irrespective whether the quality indicator is obtained from average moisture content or from local moisture content. Since the consideration of moisture content distribution to find the local quality indicator kinetics increases the complexity of the optimisation procedure, they concluded that it is not necessary to take the quality indicator distribution into account during the optimisation. However, the optimisation results of the present study clearly illustrate that quality indicator distributions should be considered in the optimisation procedure, either in the objective function  $J$  or as a constraint.

It has to be remarked that in flat regions of the objective function surface (Figure 3.10), the numerical simulation inaccuracies sometimes stalled the search. The numerical efficiency could be improved in the simulation if the trajectory of control variables was not interrupted by the discontinuities inherent to control parameterisation. Another reason to remove the discontinuities is that they cause long calculation times due to the stiff character of the system, requiring very small time steps after each change in control variables.

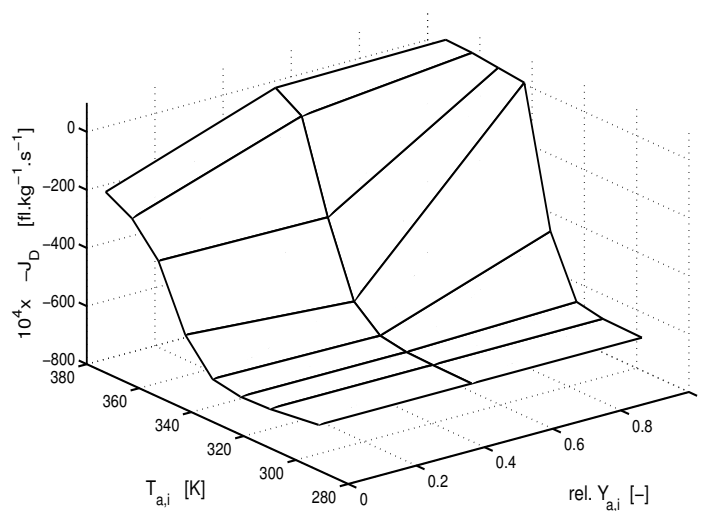


**Figure 3.10.** Sensitivity of the objective function  $J$  for the control variables  $T_{a,i}$  and  $Y_{a,i}$  ( $N_u = 1$ ).

## References

- Abid, M., R. Gibert and C. Laguerie. An experimental and theoretical analysis of the mechanisms of heat and mass transfer during the drying of corn grains in a fluidized bed. *International Chemical Engineering*, vol. 30, 1990, no. 4, p. 632-642.
- Banga, J.R. and R.P. Singh. Optimization of air drying of foods. *Journal of Food Engineering*, vol. 23, 1994, p. 189-211.
- Daemen, A.L.H. and H.J. van der Stege. The destruction of enzymes and bacteria during the spray-drying of milk and whey. 2. The effect of the drying condition. *Netherlands Milk and Dairy Journal*, vol. 36, 1982, p. 211-229.
- Kamiński, W., I. Zbiciński, S. Grabowski and C. Strumiłło. Multiobjective optimization of drying process. *Drying Technology*, vol. 7, 1989, no. 1, p. 1-16.
- Kerkhof, P.J.A.M. Relations between local and effective air-side mass and heat transfer coefficients in fluidized bed drying. *Drying Technology*, vol. 12, 1994a, no. 5, p. 1191-1210.
- Kerkhof, P.J.A.M. The role of theoretical and mathematical modelling in scale-up. *Drying Technology*, vol. 12, 1994b, no. 1&2, p. 1-46.
- Langrish, T.A.G., A.S. Brooke, C.L. Davis, H.E. Musch and G.W. Barton. An improved drying schedule for Australian ironbark timber: optimisation and experimental validation. *Drying Technology*, vol. 15, 1997, no. 1, p. 47-70.
- Lievens, L.C. *The inactivation of Lactobacillus plantarum during drying*. Wageningen: Wageningen Agricultural University, Department of Food Processing, 1991. 118 p. PhD thesis.
- Liou, J.K., K.Ch.A.M. Luyben and S. Bruin. A simplified calculation method applied to enzyme inactivation during drying. *Biotechnology and Bioengineering*, vol. 27, 1985, p. 109-116.
- Luyben, K.Ch.A.M, J.K. Liou and S. Bruin. Enzyme degradation during drying. *Biotechnology and Bioengineering*, vol. 24, 1982, p. 533-552.

Madamba, P.S. Optimization of the drying process: an application to the drying of garlic. *Drying Technology*, vol. 15, 1997, no. 1, p. 117-136.

McFarlane, N.J.B. and D.M. Bruce. A cost function for continuous-flow grain drying and its use in control. *Journal of Agricultural Engineering Research*, vol. 65, 1996, p. 63-75.

Mishkin, M., M. Karel and I Saguy. Applications of optimization in food dehydration. *Food Technology*, vol. 36, 1982, no. 7, p. 101-109.

Mishkin, M., I. Saguy and M. Karel. Dynamic optimization of dehydration processes: minimizing browning in dehydration of potatoes. *Journal of Food Science*, vol. 48, 1983, p. 1617-1621.

Mishkin, M., I. Saguy and M. Karel. Minimizing ascorbic acid loss during air drying with a constraint on enzyme inactivation for a hypothetical foodstuff. *Journal of Food Processing and Preservation*, vol. 7, 1983, p. 193-210.

Mishkin, M., I. Saguy and M. Karel. Optimization of nutrient retention during processing: ascorbic acid in potato dehydration. *Journal of Food Science*, vol. 49, 1984, p. 1262-1266.

Mourad, M., M. Hémati and C. Laguérie. Séchage de maïs en lit fluidisé à flottation II: modélisation de la cinétique de séchage (Drying of corn in a flotation fluidized bed. II. modelling of the kinetics of drying). *Chemical Engineering Journal*, vol. 60, 1995, no. 103, p. 39-47.

Soponronnarit, S. and S. Prachayawarakorn. Optimum strategy for fluidized bed paddy drying. *Drying Technology*, vol. 12, 1994, no. 7, p. 1667-1686.

Strumiłło, C., A.S. Markowski and J. Adamiec. Selected aspects of drying of biotechnological products. p. 36-55. In: Mujumdar, A.S. and I. Filková (Eds.). *Drying '91*. Amsterdam, etc.: Elsevier Science Publishers B.V., 1991. 632 p.

Taprantzis, A.V., C.I. Siettos and G.V. Bafas. Fuzzy control of a fluidized bed dryer. *Drying Technology*, vol. 15, 1997, no. 2, p. 511-537.

Trelea, I.C., G. Trystram and F. Courtois. Optimal constrained non-linear control of batch processes: application to corn drying. *Journal of Food Engineering*, vol. 31, 1997, p. 403-421.

Van Boxtel, A.J.B. and L. Knol. A preliminary study on strategies for optimal fluid-bed drying. *Drying Technology*, vol. 14, 1996, no. 3&4, p. 481-500.

Van 't Land, C.M. *Industrial drying equipment. Selection and application*. New York, etc.: Marcel Dekker, Inc., 1991. 362 p.

Villota, R. and M. Karel. Prediction of ascorbic acid retention during drying. II. Simulation of retention in a model system. *Journal of Food Processing and Preservation*, vol. 4, 1980, p. 139-159.

Wijlhuizen, A.E., P.J.A.M. Kerkhof and S. Bruin. Theoretical study of the inactivation of phosphatase during spray drying of skim-milk. *Chemical Engineering Science*, vol. 34, 1979, p. 651-660.



## Chapter 4

# Development and validation of diffusion-sorption drying model

### Chapter 4.1

Diffusion-sorption drying model for optimal quality control

### Chapter 4.2

An improved experimental and regression methodology for sorption isotherms

### Chapter 4.3

Sorption isotherms, GAB parameters and isosteric heat of sorption

### Chapter 4.4

Mathematical description and parameter values of the diffusion-sorption drying model

## **Chapter 4.1**

### **Diffusion-sorption drying model for optimal quality control**

This chapter is submitted for publication as:

Quirijns, E.J., A.J.B. van Boxtel, W.K.P. van Loon, and G. van Straten. Diffusion-sorption drying model for optimal quality control.

## **Abstract**

To optimise product quality during drying, the prediction of spatial distributions of moisture content and temperature is essential. For this purpose a new microscopic drying model is developed in this chapter: the diffusion-sorption drying model. This model is based on the existence of different classes of water in food products and the conversion between them. All parameters in this model have a physical meaning. Moreover, the value of some parameters can be directly obtained from the sorption isotherm, which always has to be determined experimentally. The model is calibrated with a selection of experiments from drying experiments, where a continuous weighing procedure is applied. The diffusion-sorption model is compared with four other diffusion models known from literature. The results show that the new model performs best in both calibration and validation. It has the lowest number of parameters and it is the best identifiable model, leading to unique parameter values. The accuracy of those is more than two times higher than in the other diffusion models. The diffusion-sorption model yields the most reliable prediction of drying curves at different experimental conditions, enlarging the confidence in this model.

## Nomenclature

$A_{bed}$	cross area of dryer	$[m^2]$
$a$	parameter in the moisture dependence of the diffusion coefficient	
$a_{Sh}$	parameter in relation for Sherwood number	
$a_w$	water activity of material	$[-]$
$b$	parameter in the moisture dependence of the diffusion coefficient	
$b_{Sh}$	parameter in relation for Sherwood number	
$C_g$	Guggenheim constant in GAB sorption equation	$[-]$
$c_w$	friction factor	
$D_p$	characteristic diameter of particle (appendix 4.1.I)	$[m]$
$D$	internal diffusion coefficient of moisture in material	$[m^2.s^{-1}]$
$D_0$	parameter in Arrhenius-type relation for diffusion coefficient	$[m^2.s^{-1}]$
$D_{OT}$	temperature dependent diffusion coefficient	$[m^2.s^{-1}]$
$D_{w,a}$	diffusion coefficient of moisture in air (appendix 4.1.I)	$[m^2.s^{-1}]$
$E_a$	activation energy for moisture diffusion	$[J.mol^{-1}]$
$g$	gravitational acceleration	$[m.s^{-2}]$
$J_{xs}$	mass flux, on surface of material	$[kg.m^{-2}.s^{-1}]$
$K$	constant in GAB sorption equation	$[-]$
$K_{eq}$	equilibrium constant in sorption process	
$k$	external convective mass transfer coefficient	$[m.s^{-1}]$
$k_a$	adsorption rate constant	$[s^{-1}]$
$k_d$	desorption rate constant	$[s^{-1}]$
$L_m$	length of the cylinder	$[m]$
$m_b$	mass reading on balance	$[kg]$
$m_{empty}$	empty mass of dryer	$[kg]$
$m_m$	mass of material in dryer	$[kg]$
$\mathcal{R}$	gas constant, 8.314	$[J.mol^{-1}.K^{-1}]$
$\mathcal{R}^*$	gas constant, 0.462	$[kJ.kg^{-1}.K^{-1}]$
$R$	maximum radius of material	$[m]$
Re	Reynolds number	
RH	relative air humidity	$[\%]$
$r$	radius of material	$[m]$
$r_a$	rate of adsorption	$[s^{-1}]$
$r_B$	conversion rate between bound and free water	$[s^{-1}]$

$r_d$	rate of desorption	[s <sup>-1</sup> ]
rSSQ	relative difference in SSQ	[%]
Sc	Schmidt number (appendix 4.1.I equation I.4)	
Sh	Sherwood number (appendix 4.1.I equation I.2)	
SSQ	residual sum of squares	
SSQ <sub>nom</sub>	residual sum of squares at nominal parameter values	
$T$	air temperature	[°C]
$T_m$	immediate temperature of material	[K]
$t$	time	[s]
$t_0$	starting time/start of drying process	[s]
$t_f$	final time/end of drying process	[s]
$v_a$	velocity of air	[m.s <sup>-1</sup> ]
$X$	moisture content	[kg.kg <sup>-1</sup> <sub>dm</sub> ]
$X_B$	concentration of bound water	[kg.kg <sup>-1</sup> <sub>dm</sub> ]
$X_{B,e}$	equilibrium concentration of bound water	[kg.kg <sup>-1</sup> <sub>dm</sub> ]
$X_e$	equilibrium moisture content	[kg.kg <sup>-1</sup> <sub>dm</sub> ]
$\overline{X}_{exp}$	experimental average moisture content	[kg.kg <sup>-1</sup> <sub>dm</sub> ]
$X_F$	concentration of free water	[kg.kg <sup>-1</sup> <sub>dm</sub> ]
$X_{F,e}$	equilibrium concentration of free water	[kg.kg <sup>-1</sup> <sub>dm</sub> ]
$X_m$	monolayer moisture content or GAB monolayer value	[kg.kg <sup>-1</sup> <sub>dm</sub> ]
$X_p$	moisture content predicted by the model	[kg.kg <sup>-1</sup> <sub>dm</sub> ]
$\overline{X}_p$	average moisture content predicted by the model	[kg.kg <sup>-1</sup> <sub>dm</sub> ]
$X_{part}$	partition moisture content	[kg.kg <sup>-1</sup> <sub>dm</sub> ]
$\Delta G^s$	difference in Gibbs free energy due to water sorption per kg of solid	[kJ.kg <sub>dm</sub> <sup>-1</sup> ]
$\Delta G_{X_{part}}^s$	Gibbs free energy of sorption at the transition between bound and free water, the partition moisture content	[J.mol <sup>-1</sup> ]
$\Delta G_a^s$	difference in Gibbs free energy between solid/solute in solution and of pure solid	[kJ.kg <sub>dm</sub> <sup>-1</sup> ]
$\Delta G_w^s$	difference in Gibbs free energy between water in solution and in pure water	[kJ.kg <sub>water</sub> <sup>-1</sup> ]
$\epsilon_{bed}$	bed porosity (appendix 4.1.I equation I.2 and I.3)	[m <sup>3</sup> <sub>air</sub> .m <sup>-3</sup> <sub>bed</sub> ]
$\phi$	sphericity particle (appendix 4.1.I equation I.2 and I.3)	[-]
$\phi_a$	airflow rate	[m <sup>3</sup> .h <sup>-1</sup> ]

$\eta$	dynamic viscosity (appendix 4.1.I equation I.4)	[Pa.s]
$\nu$	kinematic viscosity (appendix 4.1.I equation I.3)	[m <sup>2</sup> .s <sup>-1</sup> ]
$\rho_a$	density of air	[kg.m <sup>-3</sup> ]
$\rho_m$	density of material	[kg.m <sup>-3</sup> ]
$\rho_{w,a}$	water concentration in the air stream	[kg.m <sup>-3</sup> ]
$\rho_{w,s}$	water concentration at the surface of the material	[kg.m <sup>-3</sup> ]

## Introduction

Drying of agricultural products, foods, and other biologically active products is widely applied in agro-food and biotechnological industries. After the drying process the moisture content of the products is low enough to preserve them for a long time. Due to the reduced water activity, the products are stabilised against microbiological and chemical spoilage. Moreover, transportation and utilisation of the products are facilitated (McMinn and Magee, 1999).

Conventional drying processes are characterised by high energy costs. Moreover, in the products several irreversible biological or chemical degradations take place, resulting in for example colouring or loss of aroma. Changes of shape and texture, the formation of crusts and cracks are consequences of structural, physical and mechanical modifications (Abid *et al.*, 1990; Madamba, 1997; Luyben *et al.*, 1982). These conflicting problems can be handled and resolved by applying dynamic optimisation. Simulation studies have demonstrated that an improved quality of the dried products and a more efficient drying process were achieved by optimising the process (*Chapter 3*).

In optimisation procedures an objective function has to be formulated that expresses a specific goal, incorporating the relevant aspects of product quality and energy efficiency. It calculates time trajectories of air temperature, humidity and flow rate to achieve the formulated goal. The solution of the optimisation is founded on a mathematical drying model that describes the system. Drying models can be built on different levels to describe either the macroscopic level behaviour or the microscopic particle. When optimising the drying process with product quality in mind, it is not sufficient to use a macro-scale model only. This is because quality is largely determined by what happens on or within the drying particle. So, a microscopic model is needed. This forms the core of the optimal quality control philosophy advocated by us.

The goal of this chapter is to develop a microscopic drying model which is appropriate for optimal quality control of drying processes.

This chapter is organised as follows:

- 1) existing drying models are reviewed and evaluated in terms of optimal quality control.
- 2) a novel microscopic drying model is presented: the diffusion-sorption drying model.
- 3) the diffusion-sorption drying model is compared with existing diffusion models.

## Motivation for the development of a new microscopic drying model

### Requirements for product quality prediction

Among many factors affecting quality indicators during drying, the most important are temperature and moisture content (Strumiłło and Markowski, 1991; Rossen and Hayakawa, 1977). To achieve optimal quality control, prediction of the quality indicator is needed for each trajectory of air temperature and humidity. During the drying process, gradients of moisture content and temperature arise inside the material. So not the average temperature and moisture content, but their distributions characterise the quality indicator. For instance, in the case of food preservation, the growth of micro organisms that can give rise to food poisoning need to be prevented. This can only be achieved by not exceeding a safe moisture content on every location in the material. After all, if the average moisture content was taken as quality indicator, it is possible that in some places of the material still spoilage occurs (Mishkin *et al.*, 1984; Wang and Brennan, 1995; Villota and Karel, 1980; Fyhr and Kemp, 1998). Consequently, the quality of biological material is based on the local evolution of moisture and temperature. This means that for the use in the optimisation of drying processes, the micro-scale drying model should be able to:

- 1) describe moisture content and temperature distributions in the material. The model should be independent of material properties as shape, size and initial moisture content.
- 2) describe these distributions for a large range of experimental conditions.
- 3) describe the mass and heat transfer independent of the drying process and the type of dryer.

### Existing micro-scale drying models in relation to the description of quality

The micro-scale models found in literature can be divided into three groups:

1. *comprehensive models* associating energy, mass and momentum transport equations with all the thermodynamically interactive fluxes (Abid *et al.*, 1990; Fyhr and Kemp, 1998; Ketelaar, 1992; Hayakawa and Furuta, 1989).
2. coupled heat and mass *diffusion models* with or without thermodynamically interactive fluxes (Abid *et al.*, 1990; Rossen and Hayakawa, 1977; Waananen *et al.*, 1993).

Neglecting cross-effects, they can be classified into three subdivisions, dependent on the Biot numbers:

- (a) distributed models, which take into account internal and external resistances of a single particle to heat and mass transfer (Wang and Brennan, 1995; Maroulis *et al.*, 1995; Parti, 1993; Langrish *et al.*, 1997; Mourad *et al.*, 1995).
  - (b) ‘lumped’ models, describing the mass and heat transfer for the whole particle, while ignoring the internal resistances against energy and/or mass transfer (Parti, 1993; Mourad *et al.*, 1995; Rovedo *et al.*, 1995).
  - (c) equilibrium models, which assume equilibrium of the particle surface temperature and/or moisture content with the drying air, ignoring the external resistances (Parti, 1993; Mourad *et al.*, 1995; Patil, 1988; Elbert *et al.*, 2001; Simal *et al.*, 2005; Karathanos *et al.*, 1990).
3. *empirical* drying rate models (Fyhr and Kemp, 1998 ; Simal *et al.*, 2005; Vasseur *et al.*, 1991; Langrish *et al.*, 1991).

In view of the presented prerequisites of the microscopic drying model, the models of class 1 are theoretically most valid. However, they are difficult to solve mathematically and it is very complicated to achieve all relevant parameters (Rossen and Hayakawa, 1977; Fyhr and Kemp, 1998). The empirical models of class 3 are mathematically most simple, but they only consider average conditions of moisture content and temperature, which makes them unsuitable (requirement 1). Moreover, these models are system specific (requirement 1, 2 and 3) (McMinn and Magee, 1999; Fyhr and Kemp, 1998; Patil, 1988; Simal *et al.*, 2005). The models in class 2, which are able to describe the concerning gradients inside the material, are left over. In most biological material, thermodiffusion is negligible (Abid *et al.*, 1990; Waananen *et al.*, 1993; Mourad *et al.*, 1995; Vagenas *et al.*, 1990). The driving force for diffusion thus is the moisture gradient (McMinn and Magee, 1999; Wang and Brennan, 1992). In order to satisfy requirements 2 and 3, the internal mass transfer resistance, which is generally the controlling resistance during drying, as well as the external resistance, which can be rate limiting due to the variable drying conditions resulting from the optimisations, both need to be considered. This eliminates model types 2b and 2c. This means that the distributed diffusion model in class 2a is the mathematically simplest model that still complies with all requirements.

### **Motivation for the development of a more physical based drying model**

In the distributed diffusion models in literature, the internal mass transfer resistance is governed by the effective diffusion coefficient. It is a so-called lumped parameter, which represents all internal physical phenomena (McMinn and Magee, 1999; Langrish *et al.*, 1997; Xiong *et al.*, 1991). Due to this lumped character, the value of the effective diffusion coefficient is linked to the specific model of the drying process (Mourad *et al.*, 1995; Patil, 1988; Zogzas *et al.*, 1996; Mulet, 1994). This means that the diffusion coefficient compensates for phenomena that are neglected by the model, e.g. external convection. The same can be said about the thermal conductivity, although this parameter plays a minor role in the model, due to the external energy limitation (Waananen *et al.*, 1993). Other parameters present in the drying model are usually not linked to a specific model of the drying process, but to broadly accepted concepts (McMinn and Magee, 1999; Hayakawa and Furuta, 1989; Maroulis *et al.*, 1995; Ben-Mabrouk and Belghith, 1995). Parameters as the heat capacity and water activity can be derived from independent experiments. In short, the main difficulty in the distributed drying model is the lumped character of the effective diffusion coefficient.

No theoretically based relationship is available to predict the values of the effective diffusion coefficient in distributed drying models, (McMinn and Magee, 1999; Waananen *et al.*, 1993; Zogzas *et al.*, 1996). Its variability throughout the drying process is very complex. It not only depends on temperature and moisture content of the material but also on the structure and composition of the material, material heterogeneity and interactions of material components with water (McMinn and Magee, 1999).

The dependence of the diffusion coefficient on structure and composition can be considered as a given material property. The dependence on temperature, secondly, can be cast in the form of the generally accepted Arrhenius-type relation, based on the principle that molecular kinetic energy increases with temperature (Maroulis *et al.*, 1995; Zogzas *et al.*, 1996; Kiranoudis *et al.*, 1995). The dependency on moisture content on the contrary is complex and system specific (McMinn and Magee, 1999). In models for foods and biological materials, the effective diffusion coefficient reduces with decreasing moisture content, to account for the characteristic falling drying rate at low moisture contents (Maroulis *et al.*, 1995; Rovedo *et al.*, 1995, Xiong *et al.*, 1991; Zogzas *et al.*, 1996). However, the choice of this relationship is not based on any theoretical ground (Zogzas *et al.*, 1996). It is an arbitrary choice (Ketelaar, 1992). As a consequence, a range of expressions from simple algebraic to complex exponentials exists to describe the dependency on moisture content,  $X$  (Patil, 1988; Ben-Mabrouk and Belghith, 1995; Kiranoudis *et al.*, 1993; Liou and Bruin, 1982). For convenience, this type of models are called  $ID(X)$ -model in the remaining of this chapter. In

**Table 4.1.1.** The estimated parameters in the various microscopic drying models, with the resulting SSQ of the direct fit on the three diffusion limited experiments

microscopic drying model	parameters in relation for diffusion coefficient				SSQ of fit	references
	$ID_0$ [m <sup>2</sup> .s <sup>-1</sup> ]	$E_a$ [J.mol <sup>-1</sup> ]	$a$	$b$		
diffusion-sorption model	$3.75 \cdot 10^{-8}$	$1.06 \cdot 10^4$			0.243	this chapter
<i>ID(X)</i> -model						
$ID = ID_{0T} *$	$1.71 \cdot 10^{-8}$	$9.16 \cdot 10^3$			0.302	Wang and Brennan, 1995, Fyhr and Kemp, 1998, Langrish <i>et al.</i> , 1997, Rovedo <i>et al.</i> , 1995, Vagenas <i>et al.</i> , 1990, Mulet, 1994, Crank, 1975
$ID = ID_{0T} \cdot \exp(a \cdot X)$	$5.47 \cdot 10^{-8}$	$1.31 \cdot 10^4$	1.33		0.254	Fyhr and Kemp, 1998, Ketelaar, 1992, Karathanos <i>et al.</i> , 1990, Zogzas <i>et al.</i> , 1996, Mulet, 1994, Crank, 1975
$ID = ID_{0T} \cdot \exp\left(\frac{a \cdot X}{b + X}\right)$	$3.55 \cdot 10^{-8}$	$1.40 \cdot 10^4$	1.63	$9.25 \cdot 10^{-2}$	0.250	Ketelaar, 1992, Crank, 1975
$ID = ID_{0T} \cdot X^a$	$8.34 \cdot 10^{-10}$	$2.68 \cdot 10^3$	-0.12		0.370	Fyhr and Kemp, 1998, Karathanos <i>et al.</i> , 1990, Liou and Bruin, 1982, Crank, 1975

ad \*: In the *ID(X)*-model,  $ID_0$  and  $E_a$  appear in  $ID_{0T}$ , which corresponds with  $ID(T_m)$  in equation 4.1.3.

Table 4.1.1, examples of reported  $ID(X)$ -models are given, which will be compared with our new model.

Due to the absence of a theoretical relation, experimental data are required to obtain the parameters in the empirical  $ID(X)$ -model. The experimental determination of the moisture content dependence is usually very difficult. Actually measurements of the internal moisture profiles are needed (Fyhr and Kemp, 1998; Waananen *et al.*, 1993). Commonly and also in this project, only drying curves are available, representing the course of the average moisture content during drying. They can be used for the derivation of the diffusion coefficient, by comparing the numerical solution of the diffusion equation including the  $ID(X)$ -model with the experimental data (Rovedo *et al.*, 1995; Vagenas *et al.*, 1990; Ben-Mabrouk and Belghith, 1995). This method has a major drawback in view of the required quality prediction during drying. It appears that the drying curve is not sensitive to the exact value of the diffusion coefficient (Ketelaar, 1992). Various  $ID(X)$ -models, obtained with this method, can lead to comparable drying curves but different moisture profiles (Ketelaar, 1992; Mourad *et al.*, 1995; Viollaz and Suarez, 1985) and hence to potentially different predictions of quality. Consequently, it is not possible to judge the different  $ID(X)$ -models in their prediction of the gradients inside the material and therefore in the prediction of material quality, based on the drying curves solely.

Therefore, the new microscopic model is designed in such a way that the parameters have a physical meaning and can be derived from independent experiments.

## **The new diffusion-sorption model**

### **Basis of the diffusion-sorption model**

Many researchers have tried to explain the reason for the reduced diffusion at low moisture contents. They assume that this is due to the increase of energy requirement as drying progresses. As moisture content drops the water molecules are more firmly bound to the material and more energy is required to remove the sorbed water molecules (e.g. Rossen and Hayakawa, 1977; Elbert *et al.*, 2001; Mulet, 1994; Bramhall, 1997; Vagenas and Karathanos, 1991). This is illustrated for example by McMinn and Magee (1999), Wang and Brennan (1992), Xiong *et al.* (1991) and Van den Berg (1981) where the effective diffusion coefficient

remains constant with moisture until a critical moisture content is reached. Below this moisture concentration the diffusion coefficient shows a sharp decrease with decreasing water concentration.

Towards this background, three assumptions are made for the development of the new microscopic drying model. The first assumption is that different classes of water exist in biological material: bound and free water. This existence is clearly demonstrated in various materials (e.g. Elbert *et al.*, 2001; Karathanos *et al.*, 1990; Wang and Brennan, 1992; Mulet, 1994; Bramhall, 1997; Lewicki, 2000; Kamagai *et al.*, 1994). Experimental sorption data, obtained with an improved methodology in our laboratory, illustrated that three classes of water could be distinguished: water strongly bound to the material in a monolayer, water structured in a multilayer and free water (*Chapter 4.3*). The multilayer formed a continuous transition between the bound and free water. The moisture content where a maximum in isosteric heat of sorption is reached, coincided with  $X_m$  from the GAB sorption isotherm. At this moisture content water behaves strictly different from multilayer and free water. Therefore, this moisture content was taken as model boundary between bound and (thus more or less) free water (*Chapter 4.2 and 4.3*).

Secondly, it is assumed that only free water molecules are diffusing (Wang and Brennan, 1992; Mulet, 1994; Bramhall, 1997). The driving force for diffusion thus is the gradient in free moisture content. In this setting it is no longer necessary to assume that the diffusion coefficient itself depends upon the moisture content.

The last assumption is that the decrease of the drying rate at low moisture content is caused by the decreasing availability of free water molecules (Xiong *et al.*, 1991; Kiranoudis *et al.*, 1995). Hence, the reducing drying rate results from a decreasing driving force, rather than from a decreasing diffusion coefficient as generally assumed (Table 4.1.1).

Following the model, the portion of free moisture content is initially very large. The free moisture molecules diffuse through the bulk and evaporate at the boundary of the material. As drying continues, the bound moisture molecules form the majority. Then the conversion between the bound and free water controls the overall mass transfer phenomenon, leading to the decrease in drying rate.

The distinction between bound and free water lies at the heart of this new drying model. It is therefore interesting to discuss this in view of three prevailing views in the drying community:

1. it is sometimes argued that bound water cannot be removed. The conversion between bound and free water would therefore not be realistic. However, our sorption as well as drying data showed that moisture can still be removed below the defined model boundary moisture content,  $X_m$  (*Chapter 4.2 and 4.3*).

2. another view is that it is impossible to define a boundary between the bound and free water, since the transition between them is gradual. The experimental sorption data demonstrated this gradual transition indeed. On the other hand, the isosteric heat of sorption also showed a point of extreme heat of sorption (*Chapter 4.3*). This extreme can certainly be used instrumentally in the definition of a model boundary.

3. some people (e.g. Wang and Brennan, 1992; Kiranoudis *et al.*, 1993) chose the moisture content where the heat of sorption approaches the heat of vaporisation of water as indicative for the amount of bound water. This chosen moisture content is the boundary between more or less bound multilayer water and free water. Part of this weakly bound water can still take part in certain biochemical reactions (Van den Berg, 1981) and thus behaves in a similar fashion as the free water. In our choice, nevertheless, the bound water behaves *strictly* different from bulk or free water, indicated by an extremum in both enthalpy and entropy (*Chapter 4.3*).

Consequently, the experimental sorption data reported in this thesis strongly support the assumptions of this microscopic drying model.

Although these phenomena are also described by Elbert *et al.* (2001), Xiong *et al.* (1991) and Kiranoudis *et al.* (1995), the presented modelling is new. The originality of this new model lies in the way of modelling the conversion between bound and free water by a sorption process. This corresponds with the theory of localised sorption. Moreover, its parameters can be retrieved from independently performed sorption experiments. Since the new model consists of a diffusion part and a sorption part, it is called the diffusion-sorption drying model.

### **Development of the diffusion-sorption model**

In this section the new diffusion-sorption drying model is developed. Standard components, as the microscopic heat model, macroscopic balances, the boundary and initial conditions are described in *Chapter 4.4*.

The microscopic moisture transfer during the drying process is described by three basic mechanisms: external convection at the boundary of the material, the diffusion of free water and conversion between bound and free water inside the material.

### ***Modelling the external convection***

At the surface of the material, external convection takes place, represented by the external mass transfer coefficient,  $k$ . The mass flux of free water from the surface to the air ( $J_{X_S}$ ) is proportional to the difference in water concentration at the surface of the material,  $\rho_{w,s}$  and the water concentration in the air stream,  $\rho_{w,a}$ :

$$J_{X_S} = -ID(T_m|_{r=R}) \cdot \rho_m \cdot \left. \frac{\partial X_F}{\partial r} \right|_{r=R} = k \cdot (\rho_{w,s} - \rho_{w,a}) \quad (4.1.1)$$

The parameter to be estimated from experimental drying data is:  $k$  (see appendix 4.1.I).

### ***Modelling the diffusion of free water***

The total moisture content,  $X$ , is composed of two components: free and bound moisture content,  $X_F$  and  $X_B$ . The concentration of free water changes due to diffusion, represented by its corresponding diffusion coefficient,  $ID$  and due to the conversion between the bound and free water, with rate  $r_B$ :

$$\frac{\partial (\rho_m \cdot X_F(r, t))}{\partial t} = \nabla(\rho_m \cdot ID(T_m(r, t)) \cdot \nabla X_F(r, t)) + \rho_m \cdot r_B(r, t) \quad (4.1.2)$$

The relation for the diffusion coefficient is restricted to the dependence on temperature, for which the Arrhenius relation is accepted:

$$ID(T_m) = ID_0 \cdot e^{\frac{-E_a}{R \cdot T_m}} \quad (4.1.3)$$

The concentration of bound water is only changing due to the conversion between free and bound water,  $r_B$ , which is derived in the next section:

$$-\frac{\partial X_B(r,t)}{\partial t} = r_B(r,t) \quad (4.1.4)$$

The parameters to be estimated from experimental drying data are:  $ID_0$  and  $E_a$ .

### ***Modelling the conversion between bound and free water***

#### *Model for the sorptive conversion between bound and free water*

The interaction between water and the material is modelled through the adsorption of free water to become bound water and vice versa. It is assumed that the solid surface of the material is covered with a number of sites at which the water may be held. At low moisture contents, the water is tightly bound to the material. At increasing moisture content, the active sites become occupied and the water molecules become less bound or not bound at all, behaving like free water. Experimental evidence is given in *Chapter 4.3*. The number of active sites corresponds with the partition moisture content between bound and free water. At this moisture content,  $X_{part}$  the bound water behaves strictly different from free or bulk water. The equilibrium between bound and free water is a dynamic one, in which the number of molecules being adsorbed at active sites is balanced by the number that desorbs.

The rate of adsorption of free water  $r_a$  is proportional to the product of the concentration of those sites not yet occupied ( $X_{part} - X_B$ ) and the concentration of free water,  $X_F$ :

$$r_a = k_a \cdot X_F \cdot (X_{part} - X_B) \quad (4.1.5)$$

The rate of desorption of bound water,  $r_d$  is proportional to the concentration of sites already occupied:

$$r_d = k_d \cdot X_B \quad (4.1.6)$$

The difference between the two rates equals the decrease of bound water and the increase of free water inside the particle:

$$r_B = k_d \cdot X_B - k_a \cdot (X_{part} - X_B) \cdot X_F \quad (4.1.7)$$

with equilibrium constant,  $K_{eq}$ :

$$K_{eq} = \frac{k_a}{k_d} = \frac{X_{B,e}}{X_{F,e} \cdot (X_{part} - X_{B,e})} \quad (4.1.8)$$

The equilibrium constant is related to the Gibbs free energy (Van 't Riet and Tramper, 1991). In the current model  $K_{eq}$  refers to the transition between bound and free water,  $\Delta G_{X_{part}}^s$  :

$$\ln K_{eq} = -\frac{\Delta G_{X_{part}}^s}{\mathfrak{R} \cdot T_m} \quad (4.1.9)$$

#### *Determination of the parameters in the conversion between bound and free water*

The partition moisture content,  $X_{part}$  which is the model boundary between bound and free water, can be obtained directly from the GAB sorption isotherm, since it appeared to correspond with the GAB monolayer value as is shown in *Chapter 4.3*:

$$X_{part} = X_m \quad (4.1.10)$$

with the GAB sorption isotherm given as:

$$\frac{X}{X_m} = \frac{C_g \cdot K \cdot a_w}{(1 - K \cdot a_w) \cdot (1 - K \cdot a_w + C_g \cdot K \cdot a_w)} \quad (4.1.11)$$

The Gibbs free energy of sorption at the partition moisture content,  $\Delta G_{X_{part}}^s$  can be derived from the GAB sorption isotherm by applying solution thermodynamics. With the derived  $\Delta G_{X_{part}}^s$ , the equilibrium constant  $K_{eq}$  can subsequently be determined (equation 4.1.9). Solution thermodynamics can be considered to be the most suitable way to evaluate the affinity of a material for water, since it reflects the interaction between water and solid and the change of the solid during sorption. The application of solution thermodynamics to the water sorption isotherms of food materials is explained and derived by Kumagai *et al.* (1994, 1997). Their derivation is used in the current model.

The change in Gibbs free energy due to water sorption,  $\Delta G^s$  in [kJ.kg<sub>dm</sub><sup>-1</sup>] consists of two components: the difference between the chemical potential of water in solution and that of pure water,  $\Delta G_w^s$  and the difference between the chemical potential of solid in solution and that of pure solid,  $\Delta G_a^s$ :

$$\Delta G^s = X \cdot \Delta G_w^s + \Delta G_a^s \quad (4.1.12)$$

in which:

$$\Delta G_w^s = \mathfrak{R}' \cdot T_m \cdot \ln(a_w) \quad (4.1.13)$$

$\Delta G_w^s$  can be calculated directly from the water sorption isotherm, applied in the transformed GAB equation form  $a_w=f(X)$  (Maroulis *et al.*, 1995):

$$a_w = \frac{\left[ 2 + \left( \frac{X_m}{X} - 1 \right) \cdot C_g - \left\{ \left( 2 + \left( \frac{X_m}{X} - 1 \right) \cdot C_g \right)^2 - 4 \cdot (1 - C_g) \right\}^{\frac{1}{2}} \right]}{[2 \cdot K \cdot (1 - C_g)]} \quad (4.1.14)$$

If the volume change of the material by water sorption is small,  $\Delta G_a^s$  can be approximated by:

$$\Delta G_a^s \approx -\mathfrak{R}' \cdot T_m \cdot \int_0^{a_w} \frac{X}{a_w} da_w = -\mathfrak{R}' \cdot T_m \cdot X_m \cdot \ln \frac{1 + (C_g - 1) \cdot K \cdot a_w}{1 - K \cdot a_w} \quad (4.1.15)$$

The presented thermodynamic functions are expressed by mass units, while the Gibbs free energy in the relation for  $K_{eq}$  is expressed in [J.mol<sup>-1</sup>]. Conversion into the right units finally leads to:

$$\ln K_{eq} = -\frac{\Delta G^s}{\mathfrak{R}' \cdot T_m \cdot X} \quad (4.1.16)$$

Since  $K_{eq}$  refers to the transition from bound to free water, all relations contributing to the Gibbs free energy need to be evaluated at  $X_{part}$ .

From the presented models, it appears clearly that not only the diffusion of free water (equation 4.1.3) but also the conversion between bound and free water, describing the moisture dependence of diffusion, are temperature dependent. This subscribes to the mechanisms described in *Chapter 4.3* and Van Loon *et al.* (1995), that an increase in temperature induces increased mobility of the water molecules as well as a reduced amount of hydrated water.

The remaining parameters are  $k_a$  and  $k_d$ . The ratio of their values is given by  $K_{eq}$ . Since  $K_{eq}$  is derived from the sorption isotherm, only one parameter needs to be determined from the experimental drying data. The only parameter to be estimated from experimental drying data is chosen to be:  $k_d$ .

## Material and methods

### *Material*

The experimental verification of the drying models was performed on starch cylinders with a diameter of 3 mm and length > 30 mm. The starch cylinders with immobilised catalase were prepared, by manually mixing native potato starch (Perfectamyl D6, AVEBE) with 0.05 M phosphate buffer (pH=7) containing catalase (EC 1.11.1.6, Sigma C-40) in a mass ratio 1.5:1 to a homogeneous paste. The paste was extruded to cylinders with the desired diameter and length. During preparation the starch cylinders were kept on ice. Until use they were stored in a sealed glass in a refrigerator (4°C). Just before use equilibration with the environment took place. The average initial moisture content was 0.97 kg per kg dry basis.

### Experimental methods

#### *Drying method: apparatus and weighing procedure*

The starch cylinders were dried in a thin layer in a pilot-plant tray dryer with a diameter of 14 cm developed by the Systems and Control Group of Wageningen University. The dryer was equipped with a conditioner unit consisting of an electrical heater, a moistener and a valve, to

control the conditions of the ingoing air stream: temperature (30-70°C), relative humidity (5-70%), airflow rate (20-30 m<sup>3</sup>.h<sup>-1</sup>). The actual ingoing air conditions were logged with a sampling time of 0.3 [s]. The corresponding absolute accuracy of the sensors was  $T \pm 0.1^\circ\text{C}$ ,  $RH \pm 2\%$  and relative accuracy  $\phi_a \pm 0.75\% \cdot \phi_a$  respectively.

The mass of the starch cylinders were obtained by continuous weighing in a closed chamber with a balance (Mettler,  $\Delta m \pm 5\text{mg}$ , every 0.3 [s]) placed on the top of the dryer. In contrast to periodic weighing, as usually applied in drying research, the air stream was not diverted from the dryer during weighing. Therefore, a correction was required for the dynamic pressure caused by the airflow. Based on the forces acting on the balance a relation was derived, in which the parameter  $c_w$  was estimated from a large number of experiments on an empty dryer under a wide range of varying air conditions:

$$m_m = m_b + \frac{\frac{1}{2} \cdot \rho_a \cdot v_a^2 \cdot c_w \cdot A_{bed}}{g} - m_{empty} \quad (4.1.17)$$

with

$$c_w = -0.0016 \cdot \text{Re} + 19.41 \text{ for } 2500 < \text{Re} < 5500 \quad (4.1.18)$$

$m_m$  = mass of material [kg]

$m_b$  = mass reading on balance [kg]

$m_{empty}$  = empty mass of dryer [kg]

Testing the continuous weighing procedure on solid bodies during a wide range of varying air conditions yielded an average absolute deviation of 0.36% at an airflow rate of 20 m<sup>3</sup>.h<sup>-1</sup> and 0.72% at 30 m<sup>3</sup>.h<sup>-1</sup>. Compared to the periodic weighing, the weighing was 6 to 10 times less accurate. This was highly compensated by an increase of the sampling frequency by a factor 800 and by the fact that there were no inadvertent interruptions in air flow (which would have complicated the outcome of the diffusion-sorption process).

### ***Drying experiments***

The starch cylinders were dried under a wide range of air conditions in 18 experimental runs. Before the start of each drying experiment, the drying air was conditioned to the desired setpoints. The tray was filled with a thin layer of starch cylinders, with an average initial total weight of 48 g, while the conditioned air stream was diverted. The drying experiment started at the moment that the air stream was led into the dryer ( $t_0$ ). The experiment was stopped

when equilibrium was reached ( $t_f$ ). After each drying experiment, the final equilibrium moisture content was determined gravimetrically, by drying the remains in a conventional oven at 103°C and atmospheric pressure, until equilibrium was reached ( $\pm 1$  mg/successive weighings). The moisture content of all samples was measured in triplicate.

With the equilibrium moisture content, the drying curve was calculated from the collected mass of the cylinders:

$$\overline{X}_{\text{exp}}(t) = \frac{m_m(t)}{m_m(t_f)} \cdot (1 + X_e) - 1 \quad (4.1.19)$$

$X_e$  = equilibrium moisture content [kg.kg<sup>-1</sup>]

### Numerical methods

To numerically simulate the microscopic drying models, the nonlinear partial differential equations were discretised with respect to the spatial coordinate by applying the implicit centred finite difference approximation. The spatial coordinate was divided into non-equidistant intervals. Together with macroscopic balances, in which the microscopic models are embedded, the discretisation resulted in a stiff system of ordinary differential equations.

The average moisture content in the cylinder was obtained by integrating the predicted moisture profiles:

$$\overline{X}_p(t) = \frac{1}{\pi \cdot (R)^2 \cdot L_m} \cdot \int_0^R 2 \cdot \pi \cdot r \cdot L_m \cdot X_p(r,t) dr \quad (4.1.20)$$

This integral was approximated with the trapezoidal numerical integration rule.

The total system of equations was integrated with respect to time by using an integrator suitable for stiff systems, provided by Matlab/Simulink (The Mathworks). The true ingoing air conditions were applied as inputs to the simulation.

## Methodology of regression

### *Selection of experiments*

For each drying curve, the drying rate along the curve,  $dX/dt$  was determined and plotted as function of moisture content. The presence of a constant flux period (CFP) was characterised by a constant drying rate at high moisture contents and established by the method presented by Mulet (1994). Seven drying experiments were selected for calibration of the various microscopic drying models: 4 experiments with a CFP and 3 experiments without a CFP. The remaining 11 drying experiments were used for validation of the models.

### *Methodology of regression: criterion*

The calibration was done by comparing the average moisture content predicted by the various microscopic models, under the measured ingoing air conditions, with the average moisture content derived from the weighing of the material during the experiments. The unknown parameters in the various microscopic drying models were estimated by minimising the residual sum of squares (SSQ) defined as:

$$SSQ = \sum_{t_0}^{t_f} (\overline{X_{\text{exp}}(t)} - \overline{X_p(t)})^2 \quad (4.1.21)$$

A standard subroutine in Matlab (fminsearch) was applied for this purpose (The Mathworks).

## Results and discussion

### Calibration results

#### *Calibration of parameters in the convective part*

The external mass transfer coefficient  $k$  controls the external transfer of moisture from the surface of the material to the drying air (equation 4.1.1). In common drying experiments, it only plays a role at the beginning of the drying process.

In the first step of the calibration procedure,  $k$  is estimated in the 4 experiments with a CFP, since the presence of a CFP indicates that the external resistance prevails. Subsequently, the estimated values for  $k$  are substituted in:

$$Sh = a_{Sh} + b_{Sh} \cdot Re^{1/2} \cdot Sc^{1/3} \quad (4.1.22)$$

to estimate the Sherwood coefficients,  $a_{Sh}$  and  $b_{Sh}$  (appendix 4.1.I).

With the specific experimental set-up, it was found that  $a_{Sh} = -15$  [ $\pm 43\%$ ] and  $b_{Sh} = 2.1$  [ $\pm 28\%$ ]. Despite the relatively large confidence intervals of these parameters, the resulting values for  $k$  approach the estimated  $k$  in the CFP experiments very well, leading to a deviation of less than 5%.

The obtained relation for  $k$  indicates that the mass transfer coefficient increases mainly with the airflow rate.

Moreover, in the beginning of each drying curve the prediction of all models falls within the experimental error, indicating that the value of the convective transfer coefficient is satisfying (see for example Figure 4.1.4).

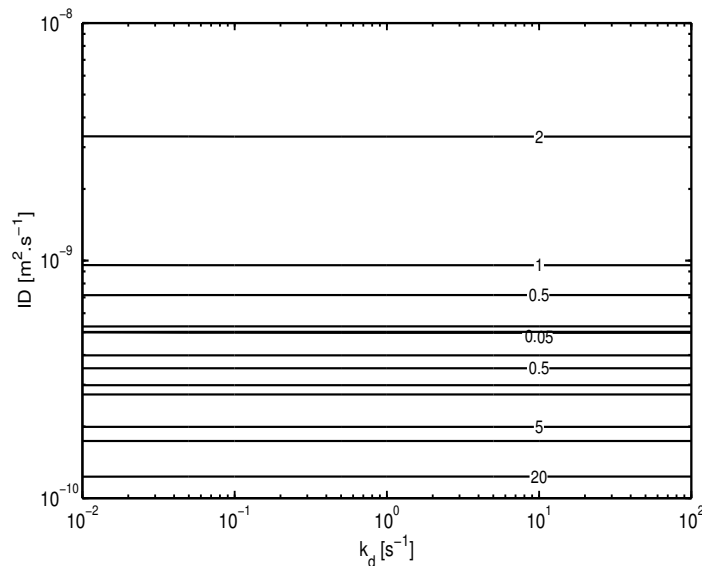


**Figure 4.1.1.** Contourplot showing the sensitivity of SSQ for the parameters in the diffusion-sorption model:  $ID$  and  $k_d$ .

### ***Calibration of the parameters in the conversion between bound and free water***

In the equations describing the conversion between bound and free water, only  $k_d$  needs to be derived from experimental drying data. The sensitivity of the diffusion-sorption model for  $k_d$  is determined. In each fit experiment, the SSQ (equation 4.1.21) is calculated for a range of  $k_d$  values between  $10^{-2} - 10^2$  [ $s^{-1}$ ] and for various values for  $ID$  in the range of  $1 \cdot 10^{-10} - 5 \cdot 10^{-9}$  [ $m^2 \cdot s^{-1}$ ]. The contourplot for one experiment is given in Figure 4.1.1, which is representative for all experiments.

Figure 4.1.1 shows that the results are independent for the value of  $k_d$  for  $10^{-2} - 10^2$  [ $s^{-1}$ ]. Apparently, the ratio between  $k_d$  and  $k_a$  is the most important factor, instead of the distinct values. Therefore, the value of  $k_d$  can be fixed to one value. This means that for the mechanism describing the conversion between bound and free water no additional parameter need to be estimated from the drying curve. This reduces the number of parameters to be estimated from the drying curve in the diffusion-sorption model to three ( $k$ ,  $ID_0$  and  $E_a$ ), which is the same as what is needed for the simplest diffusion model with constant diffusion coefficient.

### ***Calibration of free moisture diffusion in the diffusion-sorption model: $ID_0$ and $E_a$***

The final step in the calibration procedure is the estimation of the parameters in the relation for the diffusion coefficient ( $ID_0$ ,  $E_a$ ). For this step, the 3 remaining drying experiments without a CFP are used, since in those experiments diffusion prevails. The estimated parameters yielding the lowest value of SSQ are given in Table 4.1.1. The sensitivity of SSQ for  $ID_0$  and  $E_a$  is investigated by varying the parameters around their nominal value presented in Table 4.1.1 (Figure 4.1.2). The contourplot shows that  $E_a$  can be estimated with highest accuracy: SSQ increases with 5% when  $E_a$  increases with 1.5% or  $ID_0$  with 7%.

### ***Calibration of the $ID(X)$ -models: $ID_0$ , $E_a$ and $a$ and $b$***

In the same way, the parameters in the  $ID(X)$ -models are estimated with the three diffusion limited drying experiments. The resulting parameters are also presented in Table 4.1.1. The sensitivity of SSQ for the parameters in the different  $ID(X)$ -models is determined in similar way. As an illustrative example, the results for the  $ID(X)$ -model with one parameter  $a$  in the

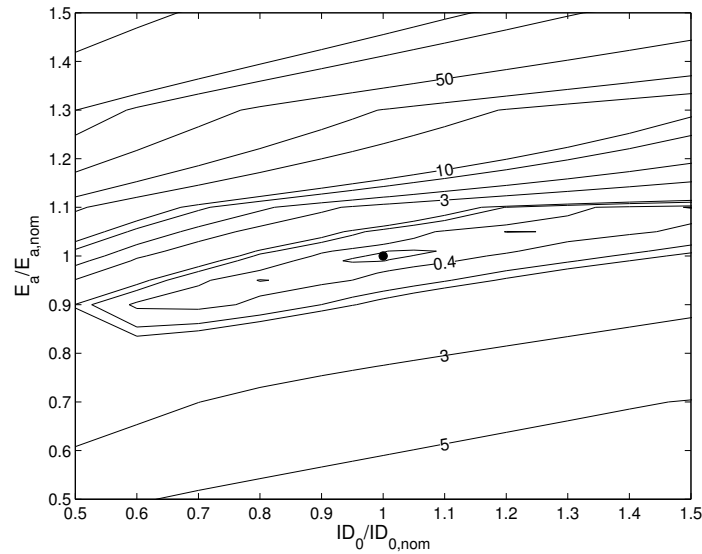


**Figure 4.1.2.** Contourplot showing the sensitivity of SSQ for the parameters  $ID_0$  and  $E_a$  in the diffusion-sorption model (with • the nominal parameter values and the first contourline =  $SSQ_{nom} + 5\%$ ).

exponential relation are shown in Figure 4.1.3a for  $ID_0$  and  $a$  at nominal  $E_a$  and in Figure 4.1.3b for  $E_a$  and  $a$  at nominal  $ID_0$ . The sensitivity of SSQ for  $ID_0$  and  $E_a$  at nominal  $a$  is comparable with the sensitivity found for the diffusion-sorption model (Figure 4.1.2). The contourplots clearly demonstrate that parameter  $a$ , expressing the moisture dependence of the diffusion coefficient cannot be estimated accurately. SSQ increases with 5% as  $a$  increases with 32% at nominal  $E_a$  (Figure 4.1.3a) and with 22% at nominal  $ID_0$  (Figure 4.1.3b).

#### ***Comparison of the diffusion-sorption model and the $ID(X)$ -models during calibration***

The calibration results show that the diffusion-sorption model with only two parameters to be estimated, leads to the lowest SSQ (Table 4.1.1). The only other model with two fit parameters is the diffusion model with constant diffusion coefficient. However, its SSQ is considerably higher. All other models need 3 or 4 fit parameters, while their SSQ is higher. Especially the power law relation, which is applied very often by other researchers (Table 4.1.1), yields very bad calibration results. Moreover, it is the only relation in which the tendency of the diffusion coefficient with moisture content is not in accordance to the physical relevance:  $a$  should be positive, since at higher moisture contents the diffusion should be easier.

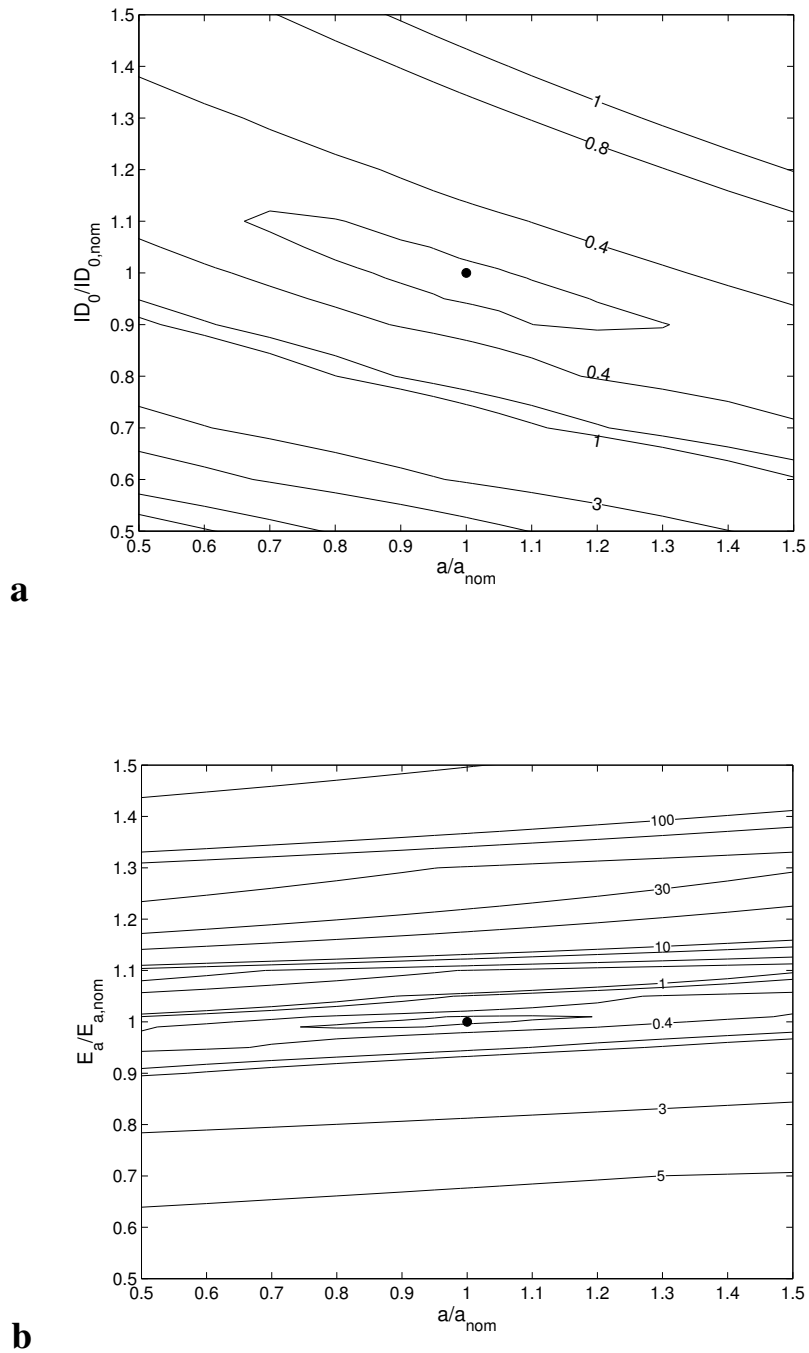


**Figure 4.1.3.** Contourplot showing the sensitivity of SSQ for the parameters: **(a)**  $ID_0$  and  $a$  in  $ID(X)$ -model with one parameter in the exponential relation (with  $\bullet$  the nominal parameter values and the first contourline =  $SSQ_{\text{nom}} + 5\%$ ); **(b)**  $E_a$  and  $a$  in  $ID(X)$ -model with one parameter in the exponential relation (with  $\bullet$  the nominal parameter values and the first contourline =  $SSQ_{\text{nom}} + 5\%$ ).

Although the application of literature values should be done with the utmost precaution, they can give an indication of the range of values for  $ID_0$  and  $E_a$ . The authors state that in 92% of the cases  $ID_0$  was between  $1 \cdot 10^{-8}$  and  $10^{-12}$  [ $m^2 \cdot s^{-1}$ ].  $E_a$  was around 13 to 110 [ $kJ \cdot mol^{-1}$ ]. The estimated values of  $ID_0$  and  $E_a$  are in the same range.

Sensitivity studies illustrate that together with the constant diffusion coefficient model, the diffusion-sorption model is the best identifiable having three drying curves with diffusion limitation. The calibration procedure leads to unique values for the parameters  $ID_0$  and  $E_a$ . The additional parameters expressing the moisture dependence of the diffusion coefficient make the other  $ID(X)$ -models more difficult to identify. Large changes in the parameter values barely influence the SSQ of the fit on diffusion limited experiments. This illustrates that the drying curve is not sensitive to the exact value of the diffusion coefficient. Moreover, it confirms the statement of Brandão and Oliveira (1997), that a good fit between experimental results and model predictions does not necessarily indicate that the parameters estimated are accurate.

The tendency in sensitivity of SSQ for the different parameters is typical for all models:

- $E_a$  can be estimated with the highest accuracy. An average change of only 1.3% in  $E_a$  leads to an increase in SSQ of 5%.
- $ID_0$  is the second most accurate. A change in  $ID_0$  of approximately 7-10% leads to an increase in SSQ of 5%.
- $a$  in the moisture dependent relations for the diffusion coefficient is least accurate. A change in  $a$  of more than 25% leads to an increase of 5% in SSQ.

In the diffusion-sorption model, an additional parameter is derived from the independently measured water activity at the monolayer value,  $K_{eq}$  (equation 4.1.12 to 4.1.16). The water activity can be predicted with the GAB sorption isotherm (*Chapter 4.2*). With the presented GAB parameters, the accuracy of the prediction of the water activity at this moisture content is around 8%. At higher temperature, the prediction is less accurate (19%). It is obvious that the prediction of this parameter is much more accurate than the parameters in the  $ID(X)$ -models expressing the moisture dependence of the diffusion coefficient.

In Zogzas *et al.* (1996) and Kiranoudis *et al.* (1995), it is mentioned that it is not possible to estimate  $ID_0$  and  $E_a$  separately. The Arrhenius factor  $ID_0$  and the energy of activation for moisture diffusion  $E_a$  are strongly related properties. They state that the estimation accuracy of the final value of the diffusion coefficient is affected only by the combination of  $ID_0$  and  $E_a$

and not by each one separately. However, Figure 4.1.2 and 4.1.3 clearly show that  $E_a$  can be estimated with great accuracy for all microscopic models. Although expected that the combination of  $ID_0$  and  $E_a$  would be accurate, and not the separate values of the parameters, it is illustrated that  $E_a$  is very accurate for all cases. This is also shown in Vagenas *et al.* (1990).

### ***Evaluation of calibration procedure***

In drying processes, two mass transfer resistances control the removal of moisture from the material: diffusion, controlling the transfer of moisture inside the material and convection, controlling the transfer of moisture from the surface of the material to the air, represented by  $ID$  and  $k$  respectively. Joint estimation of  $ID$  and  $k$  should be avoided. Therefore, in common calibration procedures, the external mass transfer is neglected (Mulet, 1994; Azevedo *et al.*, 1998). Although seemingly good fits can be obtained by only estimating  $ID$ , ignoring  $k$ , the values for  $ID$  are inaccurate and unreliable, because of the inherent compensation for neglected external transport phenomena (Mulet, 1994; Brandão and Oliveira, 1997; Azevedo *et al.*, 1998).

In this study, the experiments are designed in such a way that the respective effects are distinguished. Experiments with external limitations, that are experiments with a constant flux period, are used for the estimation of  $k$ . Experiments with diffusion limitation are used for the estimation of parameters characterising the transfer of moisture inside the material,  $ID_0$ ,  $E_a$  and  $k_d$  or  $a$  and  $b$  respectively. As a consequence of this calibration procedure, the value of  $k$  is independent of the type of microscopic drying model as it should be. In contrast to the common procedure, this procedure thus yields accurate and reliable values of the parameters.

### **Validation results**

The capability of the various microscopic models including the diffusion-sorption model, to predict the drying curve with the relations for  $k$  and  $ID$  in a wide range of experimental conditions is investigated in the validation procedure. The predicted drying curves are compared to the experimental ones under the same experimental conditions for 11 drying experiments, not used in the calibration, varying for  $T = 30-70^\circ\text{C}$ ,  $RH = 5-70\%$  and  $\phi_a = 20-30$  [ $\text{m}^3 \cdot \text{h}^{-1}$ ]. An example of the prediction of a drying curve by the diffusion-sorption model is

presented in Figure 4.1.4. The performance of the various models are compared to that of the diffusion-sorption model by evaluating the relative difference in SSQ, defined by:

$$rSSQ = \frac{SSQ_{\text{model}} - SSQ_{DS \text{ model}}}{SSQ_{DS \text{ model}}} \quad (4.1.23)$$

Table 4.1.2 presents the average rSSQ and the minimum and maximum over all validation experiments for each model.

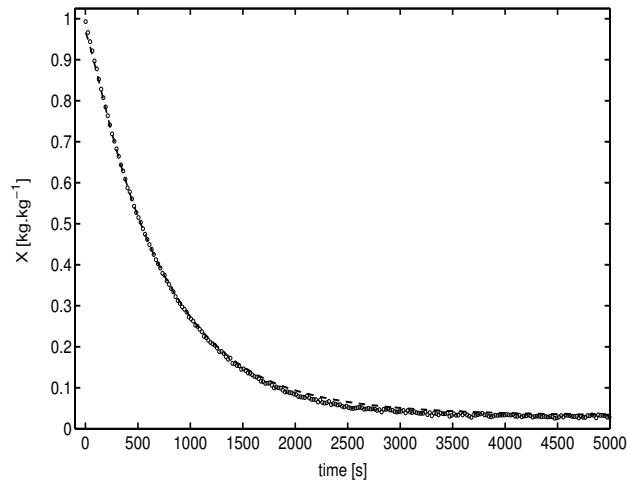


**Figure 4.1.4.** Validation of the diffusion-sorption drying model at  $T = 70^{\circ}\text{C}$ ,  $RH = 5\%$ ,  $\phi_a = 20 \text{ [m}^3 \cdot \text{h}^{-1}\text{]}$  (o experimental and -- predicted drying curve).

The average values of rSSQ demonstrate that the diffusion-sorption model is on average better than all other diffusion models. The minimum and maximum values reveal, that for some individual drying experiments, the DS model might be worse in predicting the drying curve. However, for the majority of the experiments, 64-73%, the DS model has a better prediction of the drying curve than the other models.

The validation results emphasise the results achieved during the calibration procedure. Towards the model with the same amount of fit parameters, the diffusion model with constant diffusion coefficient, the diffusion-sorption model exhibits significant improvements, with an average of 15%. The improvement of the diffusion-sorption model compared to the models with 3 or 4 fit parameters, amounts to 1-113%. Once more, the power law relation for the diffusion coefficient has the worst prediction of the drying curve for almost all experiments. Clearly, additional physical knowledge contributes more to improvement of the prediction of

**Table 4.1.2.** The SSQ of the different microscopic models compared to the SSQ of the diffusion-sorption model at each fresh experiment during validation, expressed as rSSQ .

$ID(X)$ model	validation results			
	average	rSSQ <sup>a</sup> [%]		ratio of experiments that DS <sup>b</sup> model is better [%]
		min	max	
$ID = ID_{0T}$	15	-21	91	73
$ID = ID_{0T} \cdot \exp(a \cdot X)$	1	-6	8	64
$ID = ID_{0T} \cdot \exp\left(\frac{a \cdot X}{b + X}\right)$	2	-1	18	73
$ID = ID_{0T} \cdot X^a$	113	-45	995	73

ad a: a positive rSSQ means that the prediction of the drying curve by the diffusion-sorption model is better than the prediction by the  $ID(X)$ -model.

ad b: DS stands for diffusion-sorption model

the drying curves than additional parameters in the empirical relations for the diffusion coefficient.

The continuous weighing applied in both calibration and validation eventuates in valuable information about drying and the modelling of drying. Because of the larger amount of experimental data points (Figure 4.1.4) and because the airflow is not diverted, continuous weighing allows a much better scrutiny than discontinuous or periodic weighing.

## Conclusions

The strategy for optimal control is founded on a new microscopic drying model that is able to describe spatial distributions of a quality indicator inside the material for a large range of experimental conditions and is independent of the type of dryer. The reduced diffusion at lower moisture contents is a consequence of the decreasing driving force, rather than the decreasing diffusion coefficient as generally assumed. The moisture content has two components: the bound moisture content which corresponds to water molecules connected strongly to the material molecules and the free moisture content which corresponds to the water molecules connected loosely to the material molecules. The conversion between bound and free water is physically described as a sorption process. The existence of the bound and

free water as well as the parameters describing the sorption process are derived from the sorption isotherm, obtained from independent experiments.

The diffusion-sorption model is compared in both calibration and validation with four diffusion models from literature. The simplest model with a constant diffusion coefficient has the same amount of parameters to be estimated from the drying curve. In the other three models, 1 or 2 additional fit parameters are needed to model the diffusion coefficient.

Compared to the other diffusion models, the diffusion-sorption model has the following advantages demonstrated in calibration and validation:

- 1) all parameters in the diffusion-sorption model have a physical meaning with relevant values. The diffusion coefficient in this model is not moisture dependent. The found empirical relations for apparent moisture dependency of the diffusion coefficient in the other models do not always coincide with the physically expected tendency.
- 2) in the diffusion-sorption model, the parameters describing the decreasing falling rate at low moisture contents can be fully derived from independent experiments. The model has the lowest amount of parameters to be estimated from the drying curve,  $ID_0$  and  $E_a$ . The other models, except the constant diffusion coefficient model, have 1 or 2 fit parameters more.
- 3) having the diffusion-sorption model and the constant diffusion coefficient model are the best identifiable of all. The calibration procedure leads to unique parameter values. The other models are more difficult to identify, due to additional parameters needed to express the apparent moisture dependency of the diffusion coefficient.
- 4) the accuracy of the parameter estimates in the diffusion-sorption model is much higher than in the other models: 8-19% against more than 25%.
- 5) the diffusion-sorption model leads to the best fit during calibration. It outcompetes the constant diffusion coefficient model with more than 20%, while having the same amount of fit parameters. Moreover, it has a lower SSQ compared to models with moisture dependent diffusion coefficients.
- 6) on average, the diffusion-sorption model yields the best prediction of independent drying curves not used in calibration.

Altogether it can be concluded that the new diffusion-sorption model leads to a reliable prediction of drying curves over a wide range of experimental conditions. All presented results are in agreement with the theoretical background of the diffusion-sorption model. Moreover, due to the physical meaning and interpretation of all parameters, the model can be

adjusted relatively easy to other materials. This means that the diffusion-sorption drying model can be seen as a generic model.

The motivation for the development of the model was not just the prediction of the drying curve over a wide range of experimental conditions, but more specifically the prediction of the gradients of moisture content and temperature to describe the quality of the material. Due to the uniqueness of the parameters in the diffusion-sorption model, and the fact that the parameters are derived from independent experiments, and have the highest accuracy, the predicted gradients inside the material are more reliable. The fact that the diffusion-sorption model in addition yields the most reliable prediction of the drying curves at different experimental conditions, enhances the confidence in this model. The new diffusion-sorption model is therefore expected to have the best and most reliable prediction of the gradients of moisture content and temperature.

## **Acknowledgement**

We would like to thank AVEBE, Veendam The Netherlands for their free supply of native potato starch, perfectamyl D6.

## References

Abid, M., R. Gibert and C. Laguerie. An experimental and theoretical analysis of the mechanisms of heat and mass transfer during the drying of corn grains in a fluidized bed. *International Chemical Engineering*, vol. 30, 1990, no. 4, p. 632-642.

Azevedo, I.C.A., F.A.R. Oliveira and M.C. Drumond. A study on the accuracy and precision of external mass transfer and diffusion coefficients jointly estimated from pseudo-experimental simulated data. *Mathematics and Computers in Simulation*, vol. 48, 1998, p. 11-22.

Ben-Mabrouk, S. and A. Belghith. Numerical simulation of the drying of a deformable material: evaluation of the diffusion coefficient. *Drying Technology*, vol. 13, 1995, no. 8&9, p. 1789-1805.

Bird, R.B., W.E. Stewart and E.N. Lightfoot. *Transport Phenomena*. 2<sup>nd</sup> edition. New York, etc.: John Wiley & Sons, Inc., 2002. 895 p.

Bramhall, G. Sorption diffusion in wood. *Wood Science*, vol. 12, 1979, no. 1, p. 3-13.

Brandão, T.R.S. and F.A.R. Oliveira. The influence of the temperature increase rate on the accuracy of diffusion parameters estimated under non-isothermal conditions. *International Journal of Food Science and Technology*, vol. 32, 1997, no. 1, p. 63-72.

Crank, J. *The mathematics of diffusion*. Oxford: Oxford University Press, 1975. 414 p.

Elbert, G., M.P. Tolaba, R.J. Aguerre and C. Suárez. A diffusion model with a moisture dependent diffusion coefficient for parboiled rice. *Drying Technology*, vol. 19, 2001, no. 1, p. 155-166.

Fyhr, C. and I.C. Kemp. Comparison of different drying kinetics models for single particles. *Drying Technology*, vol. 16, 1998, no. 7, p. 1339-1369.

Hayakawa, K.-I. and T. Furuta. Thermodynamically interactive heat and mass transfer coupled with shrinkage and chemical reactions. p. 201-221. In: Singh, R.P. and A.G. Medina

(Eds.). *Food properties and computer-aided engineering of food processing systems*. Dordrecht, etc.: Kluwer Academic Publishers, 1989. 593 p.

Karathanos, V.T., G. Villalobos and G.D. Saravacos. Comparison of two methods of estimation of the effective moisture diffusivity from drying data. *Journal of Food Science*, vol. 55, 1990, no. 1, p. 218-223.

Kemp, I.C. and D.E. Oakley. Modelling of particulate drying in theory and practice. *Drying Technology*, vol. 20, 2002, no. 9, p. 1699-1750.

Ketelaars, A.A.J. *Drying deformable media. Kinetics, shrinkage and stresses*. Eindhoven: Technische Universiteit Eindhoven, 1992. 105 p. PhD thesis.

Kiranoudis, C.T., Z.B. Maroulis and D. Marinos-Kouris. Heat and mass transfer model building in drying with multiresponse data. *International Journal of Heat and Mass Transfer*, vol. 38, 1995, no. 3, p. 463-480

Kiranoudis, C.T., Z.B. Maroulis and D. Marinos-Kouris. Mass transfer model building in drying. *Drying Technology*, vol. 11, 1993, no. 6, p. 1251-1270

Krokida, M.K., Z.B. Maroulis and D. Marinos-Kouris. Heat and mass transfer coefficients in drying: compilation of literature data. *Drying Technology*, vol. 20, 2002, no. 1, p. 1-18.

Kumagai, H., M. Iwase, H. Kumagai, A. Mizuno and T. Yano. Application of solution thermodynamics to the water sorption isotherms of food materials. *Bioscience, Biotechnology and Biochemistry*, vol. 58, 1994, no. 3, p. 475-481.

Kumagai, H., H. Seto, H. Sakurai, K. Ishii and H. Kumagai. Analysis of water sorption behaviour of native and denatured proteins by solution thermodynamics. *Bioscience, Biotechnology and Biochemistry*, vol. 61, 1997, no. 8, p. 1307-1311.

Langrish, T.A.G., R.E. Bahu and D. Reay. Drying kinetics of particles from thin layer drying experiments. p. 196-206. In: Mujumdar, A.S. and I. Filková (Eds.). *Drying '91*. Amsterdam, etc.: Elsevier Science Publishers B.V., 1991. 632 p.

Langrish, T.A.G., A.S. Brooke, C.L. Davis, H.E. Musch and G.W. Barton. An improved drying schedule for Australian ironbark timber: optimisation and experimental validation. *Drying Technology*, vol. 15, 1997, no. 1, p. 47-70.

Lewicki, P.P. Raoult's law based food water sorption isotherm. *Journal of Food Engineering*, vol. 43, 2000, no. 1, p. 31-40.

Liou, J.K. and S. Bruin. An approximate method for the nonlinear diffusion problem with a power relation between diffusion coefficient and concentration-II. Computation of concentration profiles. *International Journal of Heat and Mass Transfer*, vol. 25, 1982, no. 8, p. 1221-1229.

Luyben, K.Ch.A.M., J.K. Liou and S. Bruin. Enzyme degradation during drying. *Biotechnology and Bioengineering*, vol. 24, 1982, p. 533-552.

Madamba, P.S. Optimization of the drying process: an application to the drying of garlic. *Drying Technology*, vol. 15, 1997, no. 1, p. 117-136.

Maroulis, Z.B., C.T. Kiranoudis and D. Marinou-Kouris. Heat and mass transfer modeling in air drying of foods. *Journal of Food Engineering*, vol. 26, 1995, p. 113-130.

McMinn, W.A.M. and T.R.A. Magee. Principles, methods and applications of the convective drying of foodstuffs. *Food and Bioproducts Processing: Transactions of the Institution of Chemical Engineers*, vol. 77, 1999, part C, p. 175-193.

Mishkin, M., I. Saguy and M. Karel. Optimization of nutrient retention during processing: ascorbic acid in potato dehydration. *Journal of Food Science*, vol. 49, 1984, p. 1262-1266.

Mourad, M., M. Hémati and C. Laguérie. Séchage de maïs en lit fluidisé à flottation II: modélisation de la cinétique de séchage (Drying of corn in a flotation fluidized bed. II. modelling of the kinetics of drying). *Chemical Engineering Journal*, vol. 60, 1995, no. 103, p. 39-47.

Mulet, A. Drying modelling and water diffusivity in carrots and potatoes. *Journal of Food Engineering*, vol. 22, 1994, no. 1-4, p. 329-348.

Parti, M. Selection of mathematical models for drying grain in thin-layers. *Journal of Agricultural Engineering Research*, vol. 54, 1993, p. 339-352.

Patil, N.D. Evaluation of diffusion equation for simulating moisture movement within an individual grain kernel. *Drying Technology*, vol. 6, 1988, no. 1, p. 21-42.

Rossen, J.L. and K.-I. Hayakawa. Simultaneous heat and moisture transfer in dehydrated food: A review of theoretical models. *AIChE Symposium series*, vol. 73, 1977, no. 163, p. 71-81.

Rovedo, C.O., C. Suarez and P.E. Viollaz. Drying of foods: evaluation of a drying model. *Journal of Food Engineering*, vol. 26, 1995, no. 1, p. 1-12.

Simal, S., A. Femenia, M.C. Garau and C. Rosselló. Use of exponential, Page's and diffusional models to simulate the drying kinetics of kiwi fruits. *Journal of Food Engineering*, vol. 66, 2005, no. 3, p. 323-328.

Strumiłło, C., A.S. Markowski and J. Adamiec. Selected aspects of drying of biotechnological products. p. 36-55. In: Mujumdar, A.S. and I. Filková (Eds.). *Drying '91*. Amsterdam, etc.: Elsevier Science Publishers B.V., 1991. 632 p.

Vagenas, G.K., D. Marinou-Kouris and G.D. Saravacos. An analysis of mass transfer in air-drying of foods. *Drying Technology*, vol. 8, 1990, no. 2, p. 323-342.

Vagenas, G.K. and V.T. Karathanos. Prediction of moisture diffusivity in granular materials, with special applications to foods. *Biotechnology Progress*, vol. 7, 1991, p. 419-426.

Van den Berg, C. *Vapour sorption equilibria and other water-starch interactions; a physico-chemical approach*. Wageningen: Wageningen Agricultural University, Section Process Engineering, Department of Food Science, 1981. 186 p. PhD thesis.

Van Loon, W.K.P., P.E.A. Smulders, C. van den Berg and I.A. van Haneghem. Time-domain reflectometry in carbohydrate solutions. *Journal of Food Engineering*, vol. 26, 1995, p. 319-328.

Van 't Riet, K. and J. Tramper. *Basic bioreactor design*. New York, etc.: Marcel Dekker, inc., 1991. 465 p.

Vasseur, J., R. Kabbert and A. Lebert. Kinetics of drying in drum-drying. p. 352-360. In: Mujumdar, A.S. and I. Filková (Eds.). *Drying '91*. Amsterdam, etc.: Elsevier Science Publishers B.V., 1991. 632 p.

Villota, R. and M. Karel. Prediction of ascorbic acid retention during drying. II. Simulation of retention in a model system. *Journal of Food Processing and Preservation*, vol. 4, 1980, p. 139-159.

Viollaz, P. and C. Suarez. Drying of shrinking bodies. *AIChE Journal*, vol. 31, 1985, no. 9, p. 1566-1568.

Waananen, K.M., J.B. Litchfield and M.R. Okos. Classification of drying models for porous solids. *Drying Technology*, vol. 11, 1993, no. 1, p. 1-40.

Wang, N. and J.G. Brennan. A mathematical model of simultaneous heat and moisture transfer during drying of potato. *Journal of Food Engineering*, vol. 24, 1995, no.1, p. 47-60.

Wang, N. and J.G. Brennan. Effect of water binding on the drying behaviour of potato. p. 1350-1359. In: Mujumdar, A.S. (ed.). *Drying '92. Vol. I*. Amsterdam, etc.: Elsevier Science Publishers B.V., 1992. 1953 p.

Xiong, X., G. Narsimhan and M.R. Okos. Effect of composition and pore structure on binding energy and effective diffusivity of moisture in porous food. *Journal of Food Engineering*, vol. 15, 1991, p. 187-208.

Youcef-Ali, S., H. Messaoudi, J.Y. Desmons, A. Abene and M. Le Ray. Determination of the average coefficient of internal moisture transfer during the drying of a thin bed of potato slices. *Journal of Food Engineering*, vol. 48, 2001, no. 2, p. 95-101.

Zogzas, N.P., Z.B. Maroulis and D. Marinou-Kouris. Moisture diffusivity data compilation in foodstuffs. *Drying Technology*, vol. 14, 1996, no. 10, p. 2225-2253.

### Appendix 4.1.I. Relations for external mass transfer coefficient

The external mass transfer coefficient  $k$  depends on many factors such as velocity of the drying air, rheological and thermophysical properties of the drying air in contact with the material surface, structure of the material surface, orientation of the surface with regard to the direction of the air as well as on the geometry of the system (Ketelaar, 1992; Krokida *et al.*, 2002). These influences are included in semi-empirical relations of dimensionless numbers, which need to be adjusted experimentally to the specific experimental set-up under consideration. The relation for forced convection through a fixed bed of solid particles is (Kemp and Oakley, 2002; Youcef-Ali *et al.*, 2001; Bird *et al.*, 2002):

$$Sh = a_{Sh} + b_{Sh} \cdot Re^{1/2} \cdot Sc^{1/3} \quad (I.1)$$

in which  $a_{Sh}$  and  $b_{Sh}$  need to be estimated for the experimental set-up.

Bed porosity is included according to Bird *et al.* (2002):

$$Sh = \frac{k \cdot D_p}{D_{w,a} \cdot (1 - \varepsilon_{bed}) \cdot \phi} \quad (I.2)$$

and

$$Re = \frac{v_a \cdot D_p}{v \cdot (1 - \varepsilon_{bed}) \cdot \phi} \quad (I.3)$$

with  $D_p$  the characteristic dimension of the particle and  $\phi$  its sphericity;

and

$$Sc = \frac{\eta_a}{\rho_a \cdot D_{w,a}} \quad (I.4)$$

## Chapter 4.2

### An improved experimental and regression methodology for sorption isotherms

This chapter has been published as:

Quirijns, E.J., A.J.B. van Boxtel, W.K.P. van Loon and G. van Straten. An improved experimental and regression methodology for sorption isotherms. *Journal of the Science of Food and Agriculture*, vol. 85, 2005, no. 2, p. 175-185.

## Abstract

Sorption isotherms of corn and starch cylinders with immobilised catalase are experimentally determined at different temperatures for use in drying models in optimal control studies. This application of the sorption isotherm requires an accurate prediction of the sorption data at different temperatures for the low water activity range. The GAB equation is used for the prediction of the sorption isotherms. Two major problems are encountered by employing standard procedures, i.e. prediction of sorption at  $a_w < 0.11$  and sensitivity of the GAB parameters to the applied data range. An improved methodology is developed, consisting of extending the standard experimental procedure with additional data points in the low water activity range and changing the criterion in the regression procedure in the sum of squares, which is weighed by the variance of the experimental data. The new methodology leads to accurate, consistent and physically relevant parameters of the GAB equation, which are independent of the applied data range in the regression analysis and which result in accurate predictions of the sorption behaviour at low water activity. The sorption data at different temperatures at low water activity can be predicted in the best way with parameters obtained after direct regression based on weighed SSQ.

## Nomenclature

$a_w$	water activity of material	[-]
$C_g$	Guggenheim constant in GAB sorption equation	[-]
$C_{g0}$	Arrhenius type constant to express temperature dependence of $C_g$	[-]
$E$	mean relative percentage deviation modulus	[%]
$H_1$	molar enthalpy of sorption of molecules sorbed in the first layer	[J.mol <sup>-1</sup> ]
$H_\ell$	molar enthalpy for condensation of bulk liquid	[J.mol <sup>-1</sup> ]
$H_m$	molar enthalpy of sorption of molecules sorbed in the multilayer	[J.mol <sup>-1</sup> ]
$K$	constant in GAB sorption equation, factor correcting properties of the multilayer molecules relative to the bulk liquid	[-]
$K_0$	Arrhenius type constant to express temperature dependence of $K$	[-]
$N$	total number of experiments	[-]
$n_i$	the number of replicates in the $i$ th experiment	[-]
$\mathcal{R}$	gas constant	[J.mol <sup>-1</sup> .K <sup>-1</sup> ]
$RH$	relative humidity	[%]
SSQ	residual sum of squares	[-]
$T$	temperature	[K]
$w_i$	weighing factor in the wSSQ criterion	[-]
wSSQ	residual sum of squares, weighed by the variance of the experimental data	[-]
$X$	moisture content (dry basis)	[kg.kg <sup>-1</sup> <sub>dm</sub> ]
$X_{\text{exp}}$	experimental data for moisture content	[kg.kg <sup>-1</sup> <sub>dm</sub> ]
$X_m$	monolayer moisture content	[kg.kg <sup>-1</sup> <sub>dm</sub> ]
$X_{m0}$	constant to express temperature dependence of $X_m$	[kg.kg <sup>-1</sup> <sub>dm</sub> ]
$X_p$	predicted moisture content	[kg.kg <sup>-1</sup> <sub>dm</sub> ]
$Y_a$	absolute humidity of air	[kg.kg <sup>-1</sup> <sub>da</sub> ]
$Y_{as}$	absolute humidity of air on surface of material	[kg.kg <sup>-1</sup> <sub>da</sub> ]
$\Delta H_{Cg}$	difference in enthalpy between monolayer and multilayer $H_1 - H_m$	[J.mol <sup>-1</sup> ]
$\Delta H_{is}$	isosteric enthalpy of sorption	[J.mol <sup>-1</sup> ]
$\Delta H_K$	difference in enthalpy between bulk liquid and multilayer $H_\ell - H_m$	[J.mol <sup>-1</sup> ]
$\Delta H_v$	evaporation enthalpy of water	[J.mol <sup>-1</sup> ]
$\Delta H_X$	constant to express temperature dependence of $X_m$	[J.mol <sup>-1</sup> ]

## Introduction

Water is the most dominant component in food systems. It has a considerable influence on process variables, product characteristics and stability features. All these are influenced by the concentration and state of the water. The state of water is established by the complex interaction existing between the water present and the material components such as proteins, carbohydrates and lipids (Van den Berg, 1981; McMinn and Magee, 1997; Diab *et al.*, 2001). The most fundamental relation which describes this interaction between water and a food material, is the relation between the *water activity* and the *water content* of the mixture of water and material, at a certain temperature and pressure. This relation is called the water sorption isotherm. It is an essential means for prediction and evaluation of physical, chemical and microbiological stability and quality changes of foods during processing, as well as during storage (Van den Berg, 1981; McMinn and Magee, 1997; Pezzutti and Crapiste, 1997; Acker, 1969; Wang and Brennan, 1991; Iglesias and Chirife, 1982).

Many expressions have been postulated to relate the amount of water in material to the water activity. The most versatile sorption model available in literature is the three-parameter GAB equation, which has been recommended by the European COST 90 project (Van den Berg, 1981; McMinn and Magee, 1997; Wolf *et al.*, 1984). In comparison with other sorption isotherm models, the best prediction of sorption data was usually achieved using the GAB equation (Wang and Brennan, 1991; Tsami *et al.*, 1999; Lomauro *et al.*, 1985a/b; Menkov and Dinkov, 1999; Sanni *et al.*, 1997; Veltchev and Menkov, 2000).

The GAB sorption isotherm is based on localised sorption theory. It describes the material moisture content,  $X$ , which is in equilibrium with a certain water activity,  $a_w$  (Van den Berg, 1981):

$$\frac{X}{X_m} = \frac{C_g \cdot K \cdot a_w}{(1 - K \cdot a_w) \cdot (1 - K \cdot a_w + C_g \cdot K \cdot a_w)} \quad (4.2.1)$$

where  $C_g$  and  $K$  are material characteristics, representing the nature of the interaction between water and the material. Both parameters are a function of temperature, expressed as:

$$C_g = C_{g0} \cdot \exp\left(\frac{\Delta H_{C_g}}{\mathfrak{R} \cdot T}\right) \quad (4.2.2)$$

$$K = K_0 \cdot \exp\left(\frac{\Delta H_K}{\mathfrak{R} \cdot T}\right) \quad (4.2.3)$$

$X_m$  is the monolayer value, which is considered to be a function of temperature:

$$X_m = X_{m0} \cdot \exp\left(\frac{\Delta H_X}{\mathfrak{R} \cdot T}\right) \quad (4.2.4)$$

Due to their physical meaning, the value of these parameters is restricted (Table 4.2.1). In the temperature relations for  $C_g$  and  $K$ , all parameters have a physical meaning. They describe the influence of temperature on the thermodynamic changes in the interaction between water and the material. Therefore, the value of each parameter,  $C_{g0}$ ,  $\Delta H_{Cg}$ ,  $K_0$  and  $\Delta H_K$ , has to independently support its physical relevance. In the relation for the monolayer value, on the other hand, only  $X_m$  has a physical meaning. Equation 4.2.4 is merely a descriptive model to postulate the possible temperature dependence of  $X_m$ . The combination of  $X_{m0}$  and  $\Delta H_X$  needs to describe its decreasing tendency with temperature.

**Table 4.2.1.** Sets of the GAB parameter values corresponding with their physical meaning.

$C_g$	$K$	$X_m$ [kg.kg <sup>-1</sup> ]
$C_g \geq 1$	$0 < K < 1$	$X_m > 0$
$0 < C_{g0} < 1$	$K_0 > 1$	$X_{m0} > 0$
$\Delta H_{Cg} > 0$	$\Delta H_K < 0$	$\Delta H_X > 0$

This study is motivated by the role of the GAB sorption isotherm in the optimal control design of drying processes. Drying processes are characterised by high energy costs and deterioration of product quality. Improved quality of the dried products, as well as a more efficient drying process, can be achieved by optimising the process. The purpose of optimal control design is to compute trajectories of temperature and humidity of the drying air in time such that a specific goal is reached. A typical example of such a goal is to reach a specific final moisture content with maximum preservation of quality (*Chapter 3 and 6*). The role of the sorption isotherm during this application is twofold.

Firstly, it determines the driving force for externally controlled moisture transfer. This driving force is the difference between the humidity of the air,  $Y_a$ , and the humidity  $Y_{as}$  of the air near the material surface. It is assumed that  $Y_{as}$  is in equilibrium with the dried material and hence

can be determined on the basis of the sorption isotherm. Since a trajectory of drying air conditions will result from the optimisation, the model should describe the sorption isotherm of the material at different temperatures. Secondly, it predicts the final moisture content of the material, which eventually is in equilibrium with the drying air. It can thus be used to evaluate the optimum residual moisture content of the dried material, in order to increase its stability and safety, or to make a proper choice of the endpoint of the drying process (Pezzutti and Crapiste, 1997; Wang and Brennan, 1991; Kiranoudis *et al.*, 1993). Hence, prediction of the equilibrium moisture content should be very accurate at low water activities.

Since the GAB sorption isotherm needs to be able to fulfil these requirements, the goal of this study is to develop a method, consisting of an experimental as well as a regression methodology, which yields objective and accurate GAB parameters that lead to a good description of the sorption data, at low water activity and at different temperatures during drying.

## Material and methods

### Experimental procedures

#### *Materials*

Corn was purchased in cans (Dutch supermarket C1000). The corn was drained and equilibrated with the environment just before use. The average initial moisture content was 2.6 [kg.kg<sup>-1</sup><sub>dm</sub>].

Starch cylinders with immobilised catalase were prepared, by manually mixing native potato starch (Perfectamyl D6, AVEBE) with 0.05 M phosphate buffer (pH=7) containing catalase (EC 1.11.1.6, Sigma C-40) in a mass ratio 1.5:1 to a homogeneous paste. The paste was extruded into cylinders of diameter 3 mm and length > 30 mm. During preparation the starch cylinders were kept on ice, and then stored in a sealed glass container in a refrigerator (4°C) until use. Just before use equilibration with the environment took place. The average initial moisture content was 0.97 [kg.kg<sup>-1</sup><sub>dm</sub>].

### Sorption isotherm

The sorption isotherms of corn and starch cylinders were determined gravimetrically, using the static gravimetric method, standardised in the European COST 90 project (Wolf *et al.*, 1984). The method is based on the use of saturated salt solutions to maintain a fixed relative humidity, which corresponds with water activity. The over-saturated salt slurries were prepared following the recommendations of Labuza *et al.* (1976). The water activity of the solutions at different temperatures were determined from Greenspan (1977) (Table 4.2.2). Missing data were supplemented from other literature sources (Maroulis *et al.*, 1988; Bilali *et al.*, 2000; Young, 1967) and by extrapolation. No reliable data were available for NH<sub>4</sub>Cl and KNO<sub>3</sub> for temperatures higher than 30°C and 50°C, respectively.

**Table 4.2.2.** Relative humidity above saturated salt solutions at different temperatures (Greenspan, 1977).

Saturated Salt	Temperature				
	4°C	30°C	45°C	60°C	70°C
NaOH	-	7.6	5.6	3.6	2.3
LiCl	11.2	11.3	11.2	10.9	10.8
KCH <sub>3</sub> COO	-	21.6	19.5 <sup>a</sup>	16.0 <sup>a</sup>	13.4 <sup>a, b</sup>
MgCl <sub>2</sub>	33.6	32.4	31.1	29.3	27.8
K <sub>2</sub> CO <sub>3</sub>	-	43.2	42.3 <sup>c</sup>	39.2 <sup>c</sup>	37.4 <sup>c</sup>
Mg(NO <sub>3</sub> ) <sub>2</sub>	58.9	54.4	46.9	44.0 <sup>a</sup>	38.8 <sup>b, d</sup>
KI	-	67.9	65.3	63.1	61.9
NaCl	75.7	75.1	74.5	74.5	75.1
NH <sub>4</sub> Cl	-	77.9	-	-	-
KCl	-	83.6	81.7	80.3	79.5
KNO <sub>3</sub>	96.3	92.3	87.0	-	-
K <sub>2</sub> SO <sub>4</sub>	-	97.0	96.1	95.0 <sup>d</sup>	94.5 <sup>d</sup>

(a) from Maroulis *et al.* (1988); (b) obtained after extrapolation; (c) from Bilali *et al.* (2000); (d) from Young (1967)

The sorbostats were placed in a well-insulated thermostatically controlled ( $\pm 0.5^\circ\text{C}$ ) water bath (Figure 4.2.1). To ensure that the solution was completely saturated, an excess of analytical grade, crystalline salt was always present on the bottom of the sorbostat. The samples were placed in nets, after equilibration for 1-2 hours at environmental room temperature. The nets were filled with sufficient material to ensure accurate mass determination after desorption. The nets were placed on tripods in the jars. Each experiment

was performed in duplicate. To prevent microbial spoilage, a little glass bottle with crystalline thymol was placed near the samples in each sorbostat (Wolf *et al.*, 1985; Tsami *et al.*, 1990).

The samples were equilibrated for a few weeks at fixed temperatures at the specified relative humidity. Weighing, to establish equilibrium, started after two or three weeks (dependent on the temperature), and at an interval of 3 days initially. When the mass remained almost constant, the samples were weighed every day. Equilibrium was reached when three consecutive daily weighings were constant ( $\pm 1-10$  mg/day). The total time required for removal, weighing and replacing the samples in the sorbostats was minimised to about one minute to prevent, as much as possible, atmospheric moisture sorption, or desorption, during weighing (McMinn and Magee, 1997; Tsami *et al.*, 1990).

For corn, sorption isotherms were determined at 30, 45, 60 and 70°C ( $\pm 0.5^\circ\text{C}$ ) using the salt solutions in Table 4.2.2, except NaOH and KCH<sub>3</sub>COO.

The sorption isotherm for the starch cylinders was measured at 30, 45 and 60°C ( $\pm 0.5^\circ\text{C}$ ) using all the salt solutions in Table 4.2.2. For the starch cylinders an additional sorption isotherm was measured at 4°C, by placing sorbostats in a cold room at 4°C ( $\pm 2^\circ\text{C}$ ).

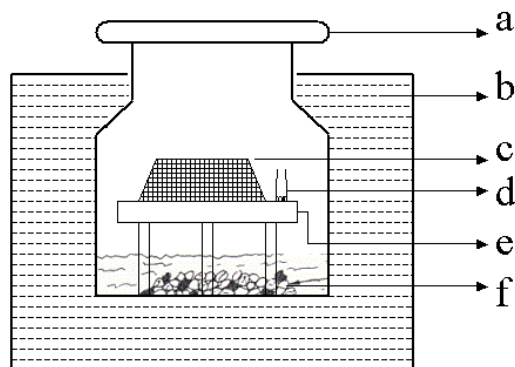


**Figure 4.2.1.** Experimental setup for the determination of sorption isotherms: a. closed lid, b. temperature controlled water bath, c. net containing material, d. glass bottle with thymol, e. tripod, f. saturated salt solution.

### ***Equilibrium moisture content***

The moisture content of the equilibrated samples was determined gravimetrically, by drying in a conventional oven at 103°C ( $\pm 1^\circ\text{C}$ ) and atmospheric pressure, until equilibrium was reached ( $\pm 1$  mg/successive weighings). The moisture content of all samples was measured in triplicate.

### **Methodology of regression**

The parameters in the GAB equation, and in the equations expressing the temperature dependence of the parameters, were estimated by fitting the mathematical model to the experimental data. Two criteria were applied:

- 1) minimisation of the residual sum of squares (SSQ), defined as

$$\text{SSQ} = \sum_{i=1}^N \sum_{j=1}^{n_i} (X_{\text{exp},ij} - X_{\text{p},i})^2 \quad (4.2.5)$$

- 2) minimisation of a weighed residual sum of squares (wSSQ), defined as:

$$\text{wSSQ} = \sum_{i=1}^N \sum_{j=1}^{n_i} w_i \cdot (X_{\text{exp},ij} - X_{\text{p},i})^2 \quad w_i = \frac{1}{\sqrt{\text{var}(X_{\text{exp},ij})}} \quad (4.2.6)$$

in which

$X_{\text{exp},ij}$	= experimental moisture content of the $j$ th replicate of the $i$ th experiment
$X_{\text{p},i}$	= moisture content of the $i$ th experiment according to the GAB model
$\text{var}(X_{\text{exp},ij})$	= variance of the $j$ replicates of the moisture content in the $i$ th experiment
$n_i$	= number of replicates in the $i$ th experiment
$N$	= total number of experiments

The GAB sorption isotherm equation is nonlinear, therefore, a standard subroutine in Matlab (lsqnonlin) for nonlinear regression was applied (The Mathworks, 2000). The Jacobian matrix and residuals were evaluated to obtain an approximation of the reliability of the parameter estimates (Ljung, 1987).

Two different regression procedures were employed:

a) indirect successive nonlinear regression

The GAB relation (equation 4.2.1) was fitted to the experimental data for each temperature. The value and reliability of each parameter,  $C_g$ ,  $K$  and  $X_m$  was determined.

The parameter estimates were subsequently used in regression analysis of the relations expressing the temperature dependence (equation 4.2.2, 4.2.3 or 4.2.4), to obtain the constants  $C_{g0}$ ,  $\Delta H_{Cg}$ ,  $K_0$ ,  $\Delta H_K$ ,  $X_{m0}$ ,  $\Delta H_X$ .

b) direct nonlinear regression

The constants  $C_{g0}$ ,  $\Delta H_{Cg}$ ,  $K_0$ ,  $\Delta H_K$ ,  $X_{m0}$ ,  $\Delta H_X$  were estimated by substituting the relations for the temperature dependence (equation 4.2.2, 4.2.3 and 4.2.4) into the GAB equation (equation 4.2.1), which was then fit on all the experimental data.

Both criteria (SSQ and wSSQ) were used in the regression procedures for estimation of the parameters in the GAB sorption isotherm. The various procedures, as well as application of the two criteria, were compared and evaluated. The standard evaluation criterion in the sorption isotherm literature is the mean relative percentage deviation modulus,  $E$ :

$$E = \frac{100}{n_{ij}} \cdot \sum_{i=1}^N \sum_{j=1}^{n_i} \frac{|X_{\text{exp},ij} - X_{p,i}|}{X_{\text{exp},ij}} \quad (4.2.7)$$

where  $n_{ij}$  is the total number of experimental data.

This parameter is widely adopted throughout the literature to evaluate the goodness-of-fit of the equation with the estimated parameters to the experimental data. In general, moduli below 10% are indicative of a reasonably good fit for practical purposes (McMinn and Magee, 1997; Lomauro *et al.*, 1985a/b).

In addition to the modulus,  $E$ , the methods were compared based on the reliability of the parameters, expressed by their confidence intervals and consistency.

To keep the results comparable with standard regression procedures, experimental data for  $a_w \leq 0.9$  were used in the regression. However, in some cases, data for  $a_w$  up to 0.95 were applied, in order to evaluate the robustness of the regression method.

## Results and discussion

### Experimental sorption isotherms

The experimental sorption isotherms for corn at 30, 45, 60 and 70°C and for starch cylinders at 4, 30, 45 and 60°C are presented in Figure 4.2.2 and 4.2.3, respectively.

For both materials, the sorption isotherms have a sigmoid shape, classifying them as type II isotherms (Van den Berg, 1981; Brunauer *et al.*, 1940). This shape of isotherm is characteristic for many materials of biological origin (McMinn and Magee, 1997; Wang and Brennan, 1991). It is characteristic for localised sorption, which justifies the application of the

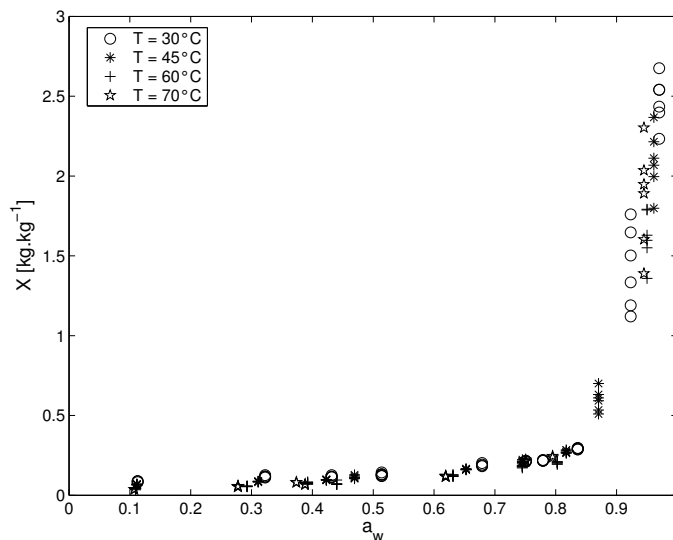


**Figure 4.2.2.** Experimental sorption data of corn at different temperatures (30, 45, 60 and 70°C).

GAB equation (Van den Berg, 1981; McMinn and Magee, 1997; Acker, 1969). At a fixed temperature, the equilibrium moisture content increases as water activity increases. The equilibrium moisture content, at a specific water activity, decreases at increasing temperature, as expected from a thermodynamical point of view (Van den Berg, 1981; McMinn and Magee, 1997; Tsami *et al.*, 1990; Samaniego-Esguerra *et al.*, 1991).

Furthermore, the figures show large variance in experimental data at high water activity. This is very common in experimental sorption data (Van den Berg, 1981; Wang and Brennan, 1991; Wolf *et al.*, 1984/1985; Menkov and Dinkov, 1999; Maroulis *et al.*, 1988; Samaniego-

Esguerra *et al.*, 1991). The first reason for the large variation is the difficulty to reach equilibrium conditions at high water activity (Wolf *et al.*, 1984; Samaniego-Esguerra *et al.*, 1991). In addition, at this steep part of the sorption isotherm, the data are more sensitive to experimental spreadings.

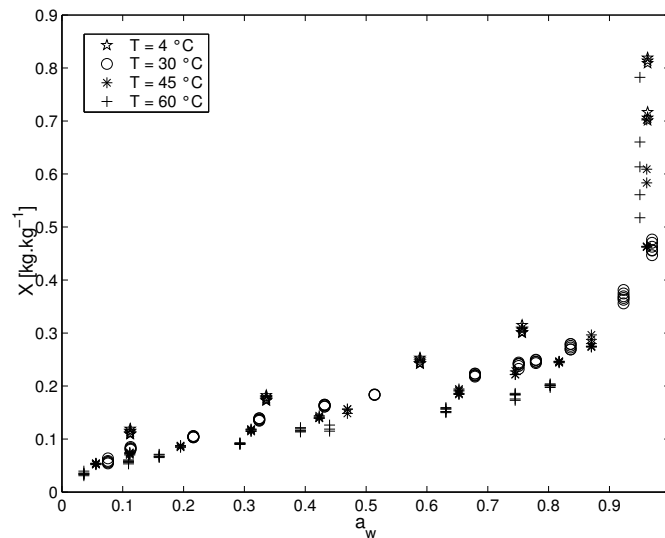


**Figure 4.2.3.** Experimental sorption data of starch at different temperatures (4, 30, 45 and 60°C).

The initial moisture content of the materials (2.6 and 0.97 [kg.kg<sup>-1</sup>], resp.) is higher than the equilibrium moisture content corresponding to the highest water activity, demonstrating that the sorption isotherms are always related to desorption. Therefore, hysteresis does not need to be considered.

## GAB parameters at each temperature

### *GAB parameters at each temperature for corn*

The parameters  $C_g$ ,  $K$  and  $X_m$  of the GAB equation for corn are given in Table 4.2.3. The parameters were obtained after regression of the experimental data at each individual temperature. The parameters, as well as their confidence intervals and modulus, are presented for each regression method (SSQ or wSSQ) and data range ( $a_w \leq 0.9$  or  $a_w \leq 0.95$ ).

The calculated GAB parameters give a very good description of the sorption data at 60 and 70°C, as indicated by values of the modulus,  $E$ , less than 10%. At 30 and 45°C some fitted sorption isotherms are also adequate, except for cases using SSQ as the criterion, or where the data at the high end of  $a_w$  are incorporated ( $E > 10\%$ ).

**Table 4.2.3.** Corn: GAB parameters and confidence intervals for sorption isotherms at 30°C, 45°C, 60°C and 70°C obtained after various regression procedures (two different criteria, SSQ and wSSQ and two data ranges,  $0.11 \leq a_w \leq 0.9$  and  $0.11 \leq a_w \leq 0.95$ ).

Regression procedure: Criterion and data range	Temperature [°C]	GAB parameters			$E$ [%]
		$C_g$	$K$	$X_m$ [kg.kg <sup>-1</sup> ]	
SSQ and $a_w \leq 0.9$	30	8·10 <sup>3</sup> *	0.88 (±4%)	0.074 (±11%)	5.8
	45	1·10 <sup>4</sup> *	1.06 (±1%)	0.043 (±12%)	17.7
	60	15 (±70%)	0.94 (±4%)	0.052 (±11%)	8.3
	70	16 (±97%)	1.02 (±3%)	0.048 (±13%)	6.1
SSQ and $a_w \leq 0.95$	30	1·10 <sup>4</sup> *	1.05 (±1%)	0.042 (±34%)	24.5
	45	1·10 <sup>4</sup> *	1.06 (±1%)	0.043 (±12%)	17.7
	60	3·10 <sup>3</sup> *	1.03 (±0%)	0.039 (±18%)	8.3
	70	2·10 <sup>1</sup> *	1.03 (±2%)	0.046 (±62%)	7.2
wSSQ and $a_w \leq 0.9$	30	9·10 <sup>3</sup> *	0.89 (±7%)	0.072 (±16%)	6.0
	45	9·10 <sup>3</sup> *	0.97 (±2%)	0.059 (±3%)	7.5
	60	16 (±59%)	0.97 (±3%)	0.048 (±10%)	7.9
	70	19 (±36%)	1.03 (±3%)	0.046 (±9%)	5.7
wSSQ and $a_w \leq 0.95$	30	1·10 <sup>4</sup> *	0.89 (±6%)	0.071 (±14%)	16.7
	45	9·10 <sup>3</sup> *	0.97 (±2%)	0.059 (±3%)	7.5
	60	2·10 <sup>2</sup> *	1.03 (±1%)	0.040 (±4%)	8.4
	70	19 (±25%)	1.03 (±1%)	0.046 (±5%)	7.3

ad\*: confidence interval larger than 100%.

The confidence intervals of the GAB parameters of corn clearly demonstrate a difference in accuracy of the estimated  $C_g$ ,  $K$  and  $X_m$ .

$K$  is always very accurate. Its value increases with temperature when wSSQ is applied in the regression, while no trend with temperature is found in  $K$  obtained with SSQ.

$X_m$  is always significant and is in most cases accurate.  $X_m$  acquired with wSSQ as the criterion decreases with temperature. Regression with SSQ results in  $X_m$  values, which do not exhibit a trend with temperature.

$C_g$  is never significant at 30 and 45°C, irrespective of which criteria is used or which data range is applied in the regression. At higher temperatures a significant value for  $C_g$  can be achieved, but this value is still very inaccurate.

The regression method influences the value of the parameters, their accuracy, their tendency with temperature and the dependence of the parameter values on the applied data range.

In general, the parameter estimates have values that are consistent with their physical bounds (Table 4.2.1), with the exception of  $K$ , which is often slightly larger than 1.

Regressions based on minimisation of wSSQ result in GAB parameters with the expected temperature tendency;  $C_g$  and  $X_m$  decrease with temperature and  $K$  increases. SSQ in contrast leads to parameters without this temperature tendency. Moreover, with wSSQ the confidence intervals of the parameters are smaller than the intervals obtained using SSQ as the criterion. The modulus is smaller as well, indicating a better overall fit of the sorption isotherm to the experimental data of corn when wSSQ is used in the regression. Finally, the magnitude of the parameters remains the same when a larger  $a_w$  range is applied during regression. In contrast, the GAB parameters achieved with SSQ as the criterion are sensitive to the data range used. The findings clearly reveal that wSSQ is the preferred criterion in the regression method.

#### ***Sensitivity of the sorption isotherm to GAB parameter $C_g$ in the standard experimental setup: improvement of the experimental setup***

In the standard experimental setup, as was applied for corn, a significant value for  $C_g$  could not be achieved. The sorption isotherm is apparently not sensitive to the parameter  $C_g$  when based on experimental data for  $a_w > 0.11$ . This is clearly demonstrated in Figure 4.2.4, where sorption isotherms of corn at 30°C are shown for different values of  $C_g$  (-1000, -100, 1 to  $10^5$ ), at the estimated values for  $K$  and  $X_m$ . Above  $C_g \approx 20$  and  $a_w > 0.11$ , the sorption isotherm is insensitive to  $C_g$ . Even the physically impossible negative values render a good description of the sorption isotherm at  $a_w > 0.11$ . This makes clear, that this insensitivity of the sorption data to  $C_g$  would not only be applicable to corn data, but also to other materials with  $C_g > 20$ . According to the physical meaning of  $C_g$ , the water in those materials is strongly bound in a monolayer (Van den Berg, 1981). So, at the high  $C_g$  that can be expected for food materials (Lomauro *et al.*, 1985a/b),  $C_g$  can only be estimated from the experimental sorption data, when experiments are performed in the low  $a_w$  range ( $a_w < 0.1$ ).

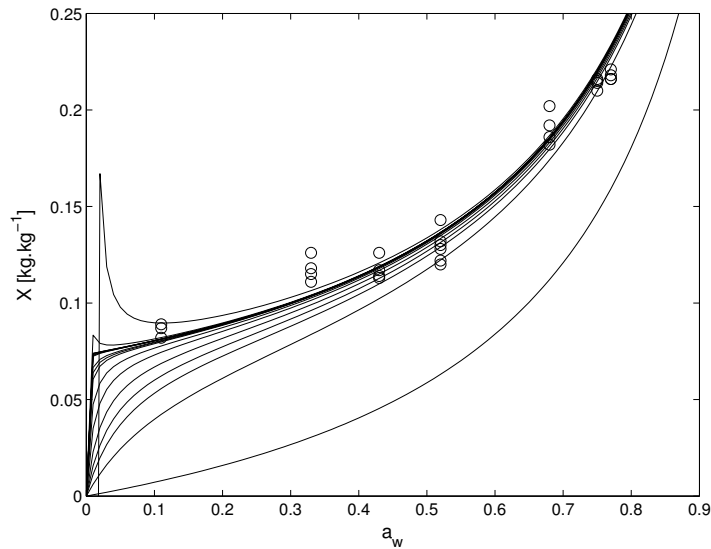


**Figure 4.2.4.** Predicted sorption isotherms of corn at 30°C for different  $C_g$  values (from bottom to top  $C_g = 1, 10, 20, 30, 50, 1 \cdot 10^2, 2 \cdot 10^2, 5 \cdot 10^2, 7 \cdot 10^2, 1 \cdot 10^3, 5 \cdot 10^3, 7 \cdot 10^3, 1 \cdot 10^4, 3 \cdot 10^4, 5 \cdot 10^4, 1 \cdot 10^5, -1000, -100$ ).

The demonstrated sensitivity of the sorption isotherm to  $C_g$  in the low  $a_w$  range follows directly from the physical meaning of  $C_g$ .  $C_g$ , mainly represents the thermodynamic difference

in enthalpy between water in the monolayer and multilayer. Monolayer water is only present at low  $a_w$ . When no data are available in this region,  $C_g$  cannot be estimated in an accurate way. Since higher temperatures reduce  $C_g$ , the accuracy in  $C_g$  can be increased by the experimental determination of sorption isotherms at higher temperatures, as is observed in Table 4.2.3.

Examples of an inaccurate estimation of  $C_g$  with the standard experimental setup can be found, although they are difficult to discover, since only a few papers (< 3%) present a measure for the reliability of the parameters (Maroulis *et al.*, 1988; Samaniego-Esguerra *et al.*, 1991; Timmermann *et al.*, 2001; Cadden, 1988). In some cases investigated by Timmermann *et al.* (2001), the confidence interval of  $C_g$  was approximately 100% of the estimated value or more, demonstrating the low sensitivity of the sorption isotherm for  $C_g$ .

A negative value for  $C_g$  illustrates the observation that the sorption isotherm can have any form for  $a_w < 0.11$ , without influencing the criterion. Negative values, which do not correspond to the theoretical meaning of  $C_g$  (Table 4.2.1), were found by Menkov (1999) for

tobacco seed and by Bassal and Vasseur (1992) for microcrystalline cellulose, starch and cake.

Very large values of  $C_g$  indicate that no convergence for the value of  $C_g$  could be obtained for experimental data in the region  $a_w > 0.11$ . Chen and Jayas (1998) found  $C_g$  values approaching infinity for rapeseed. Yoshida and Menegalli (2000) also achieved a very large value for  $C_g$  of 2000 for corn, as did Hossain *et al.* (2001) for pineapple.

Since the sorption isotherm is only sensitive to  $C_g$  in the low  $a_w$  range ( $a_w < 0.1$ ), an improved experimental setup is proposed with additional salts for obtaining measurements at  $a_w < 0.1$ . Salts that can be used for this purpose are CsF (RH=3.0% at 30°C), LiBr (6.2%), KOH (7.4%), ZnBr<sub>2</sub> (7.6%) and NaOH (7.6%) (Greenspan, 1977).

#### ***GAB parameters at each temperature for starch cylinders***

The parameters  $C_g$ ,  $K$  and  $X_m$  of the GAB equation for starch cylinders are given in Table 4.2.4. These parameters are obtained after regression of the experimental data with two additional salts, i.e. NaOH and KCH<sub>3</sub>COO at each temperature separately. The parameters, as well as their confidence interval and the modulus, are presented for each regression method (SSQ or wSSQ) and data range ( $a_w < 0.9$  or  $a_w < 0.95$ ).

The GAB parameters for starch cylinders lead to very good descriptions of the sorption data at most temperatures, indicated by values of the modulus  $E$  smaller than 10%. In general the modulus for starch cylinders is approximately a factor of 2 smaller than the  $E$  for corn, which can be explained by the more homogeneous character of the model material.

The confidence intervals of the GAB parameters of starch cylinders show good estimates of  $X_m$  and  $K$ , independent of the applied regression method. As with corn,  $K$  can be estimated with the highest precision. Even  $C_g$  can be estimated accurately when wSSQ is used as criterion, although it is still less accurate than  $K$  and  $X_m$ . The estimation of  $C_g$  is worse, or even impossible when SSQ is used.

In all cases, both regression methods give GAB parameter values that are consistent with their physical meaning (Table 4.2.1). Regressions based on wSSQ as the criterion show the same advantages over SSQ as for corn. The resulting parameters display the expected tendency with temperature. The confidence interval of  $C_g$  has improved slightly, as compared to the

interval obtained with SSQ. Most importantly, incorporating the data at the high end of  $a_w$  does not change the magnitude of the parameters.

**Table 4.2.4.** Starch cylinders: GAB parameters and confidence intervals for sorption isotherms at 4°C, 30°C, 45°C and 60°C obtained after various regression procedures (two different criteria: SSQ and wSSQ and different data ranges).

Regression procedure: Criterion and data range	Temperature [°C]	GAB parameters			E [%]
		$C_g$	$K$	$X_m$ [kg.kg <sup>-1</sup> ]	
SSQ and $0.05 \leq a_w \leq 0.9$	4	24 (±17%)	0.67 (±5%)	0.16 (±5%)	1.9
	30	14 (±10%)	0.61 (±4%)	0.14 (±5%)	2.9
	45	19 (±16%)	0.72 (±3%)	0.11 (±5%)	3.6
	60	17 (±16%)	0.69 (±5%)	0.094 (±6%)	4.9
SSQ and $0.05 \leq a_w \leq 0.95$	4 <sup>(b)</sup>	2.10 <sup>3</sup> (a)	0.89 (±2%)	0.11 (±10%)	8.4
	30	21 (±29%)	0.75 (±3%)	0.11 (±6%)	5.3
	45	19 (±16%)	0.72 (±3%)	0.11 (±5%)	3.6
	60	1.10 <sup>2</sup> (a)	0.96 (±1%)	0.055 (±11%)	15.9
wSSQ and $0.05 \leq a_w \leq 0.9$	4	24 (±15%)	0.67 (±5%)	0.16 (±5%)	1.9
	30	11 (±9%)	0.54 (±7%)	0.16 (±6%)	3.2
	45	21 (±10%)	0.73 (±3%)	0.10 (±4%)	3.5
	60	18 (±17%)	0.72 (±3%)	0.088 (±5%)	4.6
wSSQ and $0.11 \leq a_w \leq 0.9$ <sup>(c)</sup>	60	14 (±21%)	0.69 (±5%)	0.088 (±7%)	3.2
wSSQ and $0.05 \leq a_w \leq 0.95$	4 <sup>(b)</sup>	25 (±17%)	0.68 (±5%)	0.15 (±6%)	10.0
	30	12 (±12%)	0.59 (±6%)	0.15 (±6%)	4.4
	45	22 (±10%)	0.73 (±3%)	0.10 (±4%)	3.5
	60	18 (±19%)	0.73 (±4%)	0.088 (±6%)	9.1
wSSQ and $0.11 \leq a_w \leq 0.95$ <sup>(c)</sup>	60	15 (±26%)	0.66 (±6%)	0.085 (±9%)	9.2

a: confidence interval larger than 100%; b:  $a_w \leq 0.963$ ; c: old experimental setup

### *Evaluation of the improved experimental setup*

In standard experimental procedures, sorption isotherms are usually determined for the range of water activity greater than 0.11 (Wolf *et al.*, 1984/1985; Labuza *et al.*, 1976). As a result of

the sensitivity analysis for corn, the experiments for starch cylinders were designed such that  $a_w < 0.11$  were also included.

To elucidate that  $C_g$  can be estimated more accurately as a consequence of the additional experimental data points at low water activity, the parameters that would be obtained from the old experimental setup are also presented in Table 4.2.4 for the sorption isotherm at 60°C. It appears clearly that the additional data points improve the confidence interval of  $C_g$ .

### ***Comparison of regression methods: wSSQ as criterion is best method***

The results of the regressions at each temperature illustrate clearly the importance of using the weighed sum of squares (wSSQ) rather than the standard SSQ as criterion (Van den Berg, 1981; Weisser, 1985) for the estimations of the GAB parameters:

First of all, the regression method based on wSSQ leads to better estimations of the sorption data at lower water activity, indicated by the lower value of  $E$ . In the general regression procedure, applying SSQ as the criterion, the high moisture contents at high water activity, associated with a large experimental error evidenced by large standard deviations, dominate the fitting. This causes a bad estimation of the sorption data at lower water activity values, as can also be found in many regressions based on SSQ (Van den Berg, 1981; Tsami *et al.*, 1999; Sanni *et al.*, 1997; Maroulis *et al.*, 1988).

Secondly, with wSSQ, the confidence of the estimated GAB parameters, mainly  $C_g$ , has increased.

Thirdly, the regression method based on wSSQ leads to GAB parameters with a temperature dependence that is consistent with their theoretical background. Deviation of the expected temperature tendency occurs very often in literature when SSQ is used as the criterion in the regression of sorption isotherms at each temperature separately (Cadden, 1988; Chen and Jayas, 1998; Yoshida and Menegalli, 2000; McLaughlin and Magee, 1998; Serris and Biliaderis, 2001).

Finally, the regressions with wSSQ as the criterion lead to consistent parameters. Additional experimental data at high water activity do not induce changes in the magnitude of the parameters. This is in contrast with the resulting parameters from the regression based on SSQ which, with no exception, change considerably when the data range is expanded. When the regression is based on wSSQ, the parameters are not dependent on an arbitrary chosen boundary. The same value is obtained, despite a larger  $a_w$  range applied.

**Table 4.2.5.** Corn: temperature dependence and confidence intervals of GAB parameters for sorption isotherms ( $0.11 < a_w < 0.9$ ) obtained after various regression procedures (indirect successive regression and direct regression based on wSSQ) accompanied with  $E$  at 30, 45, 60, 70°C and all temperatures.

Regression method	GAB parameters						$E_T$ at different temperatures				
	$C_{g0}$	$\Delta H_{Cg}$	$K_0$	$\Delta H_K$	$X_{m0}$	$\Delta H_{Xm}$	$E_{30}$ [%]	$E_{45}$ [%]	$E_{60}$ [%]	$E_{70}$ [%]	$E_{all T}$ [%]
		[J.mol <sup>-1</sup> ]		[J.mol <sup>-1</sup> ]	[kg.kg <sup>-1</sup> ]	[J.mol <sup>-1</sup> ]					
Indirect successive regression	$2 \cdot 10^{-3} *$	$4 \cdot 10^4 *$	3 *	$-3 \cdot 10^3 *$	$1 \cdot 10^{-3} *$	$1.0 \cdot 10^4$ (±33%)	5.8	9.5	17.7	11.7	11.3
Direct regression	$4 \cdot 10^{-5} *$	$4 \cdot 10^4$ (±94%)	3.6 (±41%)	$-3.6 \cdot 10^3$ (±31%)	$8 \cdot 10^{-4}$ (±98%)	$1.2 \cdot 10^4$ (±23%)	6.4	11.1	12.2	4.8	9.2

ad\*: confidence interval larger than 100%.

**Table 4.2.6.** Starch cylinders: temperature dependence and confidence intervals of GAB parameters for sorption isotherms ( $0.02 < a_w < 0.9$ ) obtained after various regression procedures (indirect successive regression and direct regression based on wSSQ) accompanied with  $E$  at 4, 30, 45, 60°C and all temperatures.

Regression method	GAB parameters						$E_T$ at different temperatures				
	$C_{g0}$	$\Delta H_{Cg}$	$K_0$	$\Delta H_K$	$X_{m0}$	$\Delta H_{Xm}$	$E_4$ [%]	$E_{30}$ [%]	$E_{45}$ [%]	$E_{60}$ [%]	$E_{all T}$ [%]
		[J.mol <sup>-1</sup> ]		[J.mol <sup>-1</sup> ]	[kg.kg <sup>-1</sup> ]	[J.mol <sup>-1</sup> ]					
Indirect successive regression	5 *	$3 \cdot 10^3 *$	1 *	$-2 \cdot 10^3 *$	$8 \cdot 10^{-3} *$	$7 \cdot 10^3 *$	2.1	4.2	3.9	9.2	5.2
Direct regression	$1 \cdot 10^3 *$	$-1.1 \cdot 10^4$ (±36%)	3.5 (±60%)	$-4.3 \cdot 10^3$ (±36%)	$9.5 \cdot 10^{-4}$ (±68%)	$1.3 \cdot 10^4$ (±14%)	9.0	3.4	6.2	5.1	5.4

ad\*: confidence interval larger than 100%.

### Temperature dependence of GAB parameters

For determination of the temperature dependence of the GAB parameters only wSSQ is employed, based on the discussion of regression methods in the former section.

#### *Estimates of the temperature relation of the GAB parameters of corn*

The temperature dependence of the GAB parameters for corn is shown in Table 4.2.5. The corresponding predicted sorption isotherms for the direct regression method is shown, with the experimental data, in Figure 4.2.5.

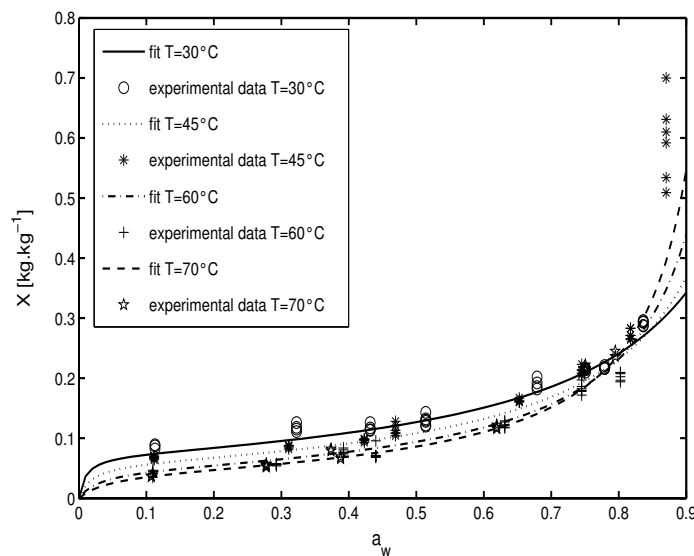


**Figure 4.2.5.** Predicted sorption isotherms of corn at different temperatures (30, 45, 60 and 70°C) with GAB parameters obtained using direct regression based on wSSQ ( $a_w \leq 0.9$ ).

The direct regression method results in the best fit for most temperatures and all temperatures together. Moreover, only this regression method leads to significant parameters (Table 4.2.5). The temperature dependence of the GAB parameters achieved with direct regression, as well as with indirect successive regression, exhibit the required physical dependence as presented in Table 4.2.1.

#### *Estimates of the temperature relation of the GAB parameters of starch cylinders*

The temperature dependence of the GAB parameters for starch cylinders is shown in Table 4.2.6. The corresponding predicted sorption isotherms for the direct regression method is shown, with the experimental data, in Figure 4.2.6.

For starch cylinders, the different regression methods do not differ significantly in the description of the sorption isotherms at different temperatures, indicated by comparable values for the modulus,  $E$ .

As for corn, the confidence intervals of the parameters are best for the direct regression method.  $C_{g0}$  is the only parameter that cannot be determined with confidence. This implies that it is not possible to reliably determine the temperature dependence of  $C_g$  as well, as inferred from the negative value for  $\Delta H_{Cg}$ .

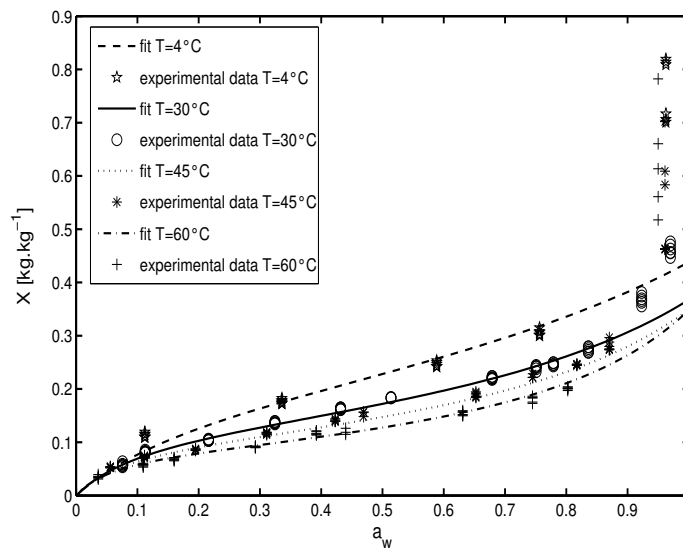


**Figure 4.2.6.** Predicted sorption isotherms of starch cylinders at different temperatures (4, 30, 45 and 60°C) with GAB parameters obtained using direct regression based on wSSQ ( $a_w \leq 0.9$ ).

### ***Comparison of regression methods for the estimates of the temperature relation of GAB parameters***

The results obtained for the temperature dependence of the GAB parameters illustrate that the direct regression, based on wSSQ, is the preferred method.

The first reason is that this method results in a better or comparable, prediction of sorption data at different temperatures. However, the temperature dependent GAB equation does not result in better predictions of the sorption data at one temperature compared to the GAB equation obtained at each temperature separately (Table 4.2.3 and 4.2.4). If a prediction has to be made at a specific temperature, then the use of the nonlinear regression at that temperature is adequate and more simple.

Secondly, the direct regression based on wSSQ leads to the most accurate parameter predictions. The indirect successive regression method results in a lower accuracy; as successive regressions are involved, the first estimation may introduce significant uncertainties into the second regression (Maroulis *et al.*, 1988; Samaniego-Esguerra *et al.*, 1991).

Finally, the direct regression based on wSSQ yields a temperature dependence of most GAB parameters, which is consistent with theory. Only one misfit is found:  $\Delta H_{C_g}$  is negative for starch cylinders. The large values for  $C_{g0}$  are not in agreement with theory either, but these are very inaccurate and can thus be left out of this evaluation.

The question arises as to whether the physical meaning of the parameters is preserved during use of the nonlinear regression methods to obtain the temperature dependence of the parameters. It is known that nonlinear regression applied to models with Arrhenius-type relationships generates very highly correlated parameter estimates (Samaniego-Esguerra *et al.*, 1991). Specifically,  $C_{g0}$  and  $\Delta H_{C_g}$ ,  $K_0$  and  $\Delta H_K$ , and  $X_{m0}$  and  $\Delta H_{X_m}$  are highly correlated, as demonstrated by correlation coefficients approaching 1 (not shown). Therefore, the physical interpretation of these parameters should be executed with the utmost of care.

These statements are supported by results presented in literature. In many cases the value for the parameters expressing the temperature dependence,  $C_{g0}$  and  $\Delta H_{C_g}$ ,  $K_0$  and  $\Delta H_K$  does not agree with the theoretical background. In almost all these cases, a positive  $\Delta H_K$  is associated with  $K_0 < 1$ , indicating internal compensation as a consequence of the high correlation (McMinn and Magee, 1997; Tsami *et al.*, 1999; Menkov and Dinkov, 1999; Sanni *et al.*, 1997; Veltchev and Menkov, 2000; Kiranoudis *et al.*, 1993; Bassal and Vasseur, 1992). Sometimes, the  $C_g$  resulting from the combination  $C_{g0}$  and  $\Delta H_{C_g}$ , and  $K$  from  $K_0$  and  $\Delta H_K$  do not correspond with the values for these parameters obtained from regression at each temperature separately (Chen and Jayas, 1998; Sanni *et al.*, 1999).

## Conclusions

Drying of foods is a highly energy consumptive process, leading to deterioration of product quality. Optimal control design of the process can improve both the quality of the dried products and the efficiency of the drying process. For application of the GAB sorption isotherm in optimal control design, the isotherm should yield objective and accurate GAB parameters that lead to a good prediction of the sorption data at low water activity and at

different temperatures. This objective has been achieved by improving the standard procedures for sorption isotherms:

1) improvement of the experimental setup

With the standard experimental procedure ( $a_w > 0.11$ ), it is not always possible to predict sorption at low  $a_w$ . The improvement of the standard experimental procedure consists of an extension of the data range to low water activity values. The additional data increase the sensitivity of the sorption isotherm for  $C_g$  and improve the confidence intervals of the GAB parameters, mainly of  $C_g$ .

2) improvement of the regression method

The GAB parameters achieved with SSQ as the criterion are sensitive to the data range used. The standard regression analysis is improved by adjusting the criterion SSQ: the sum of squares is weighed by the variance of the experimental data (wSSQ). The major advantages of applying wSSQ are:

- better predictions at low water activity are obtained.
- the confidence of the GAB parameters, mainly of  $C_g$ , increase.
- the temperature dependence of the GAB parameters is consistent with the theoretical background.
- the obtained GAB parameters are not dependent on the applied data range, indicating that it is not required to fix an arbitrary boundary in the  $a_w$  range. Moreover, it illustrates the robustness of the improved regression method.

For the temperature dependence of the sorption isotherms, the direct regression based on the same criterion, wSSQ, results in parameters with the narrowest confidence band and the best estimation of the sorption isotherms at the different temperatures. However, occasionally the magnitude of the parameters expressing the temperature dependence of the GAB parameters does not correspond with their physical meaning. This indicates that the physical relevance of the parameters may get lost during the direct regression.

## **Acknowledgement**

We would like to thank AVEBE, Veendam The Netherlands for their free supply of native potato starch, perfectamyl D6.

## References

- Acker, L.W. Water activity and enzyme activity. *Food Technology*, vol. 23, 1969, p. 1257-1270.
- Bassal, A. and J. Vasseur. Measurement of water activity at high temperature. p. 312-321. In: Mujumdar, A.S. (ed.). *Drying '92. Vol. I*. Amsterdam, etc.: Elsevier Science Publishers B.V., 1992. 1953 p.
- Bilali, L., M. Kouhila, M. Benchanaa, A. Mokhlisse and A. Belghit. Application of the Henderson and the BET model to the moisture sorption isotherms of humid natural phosphate. Paper No.13. In: Kerkhof, P.J.A.M., W.J. Coumans and G.D. Mooiweer. *Proceedings of the 12th International Drying Symposium IDS2000*. Amsterdam: Elsevier Science, 2000.
- Brunauer, S., L.S. Deming, W.E. Deming and E. Teller. On a theory of the van der Waals adsorption of gases. *Journal of the American Chemical Society*, vol. 62, 1940, no. 7, p. 1723-1732.
- Cadden, A. Moisture sorption characteristics of several food fibers. *Journal of Food Science*, vol. 53, 1988, no. 4, p. 1150-1155.
- Chen, C. and D.S. Jayas. Evaluation of the GAB equation for the isotherms of agricultural products. *Transactions of the ASAE (American Society of Agricultural Engineers)*, vol. 41, 1998, no. 6, p. 1755-1760.
- Diab, T., C.G. Biliaderis, D. Gerasopoulos and E. Sfakiotakis. Physicochemical properties and application of pullulan edible films and coatings in fruit preservation. *Journal of the Science of Food and Agriculture*, vol. 81, 2001, p. 988-1000.
- Greenspan, L. Humidity fixed points of binary saturated aqueous solutions. *Journal of Research of the National Bureau of Standards – A. Physics and Chemistry*, vol. 81A, 1977, no. 1, p. 89-96.
- Hossain, M.D., B.K. Bala, M.A. Hossain and M.R.A. Mondol. Sorption isotherms and heat of sorption of pineapple. *Journal of Food Engineering*, vol. 48, 2001, no. 2, p. 103-107.

Iglesias, H.A. and J. Chirife. *Handbook of food isotherms: water sorption parameters for food and food components*. New York, etc.: Academic Press, INC., 1982. 347 p.

Kiranoudis, C.T., Z.B. Maroulis, E. Tsami and D. Marinos-Kouris. Equilibrium moisture content and heat of desorption of some vegetables. *Journal of Food Engineering*, vol. 20, 1993, p. 55-74.

Labuza, T.P., K. Acott, S.R. Tatini, R.Y. Lee, J. Flink and W. McCall. Water activity determination: a collaborative study of different methods. *Journal of Food Science*, vol. 41, 1976, no. 4, p. 910-917.

Ljung, L. *System Identification. Theory for the user*. New Jersey: Prentice Hall PTR, 1987. 519 p.

Lomauro, C.J., A.S. Bakshi and T.P. Labuza. Evaluation of food moisture sorption isotherm equations. Part I: fruit, vegetables and meat products. *Lebensmittel-Wissenschaft und -Technologie*, vol. 18, 1985a, no. 2, p. 111-117.

Lomauro, C.J., A.S. Bakshi and T.P. Labuza. Evaluation of food moisture sorption isotherm equations. Part II: milk, coffee, tea, nuts, oilseeds, spices and starchy products. *Lebensmittel-Wissenschaft und -Technologie*, vol. 18, 1985b, no. 2, p. 118-124.

Maroulis, Z.B., E. Tsami, D. Marinos-Kouris and G.D. Saravacos. Application of the GAB model to the moisture sorption isotherms of dried fruits. *Journal of Food Engineering*, vol. 7, 1988, p. 63-78.

McLaughlin, C.P. and T.R.A. Magee. The determination of sorption isotherm and the isosteric heats of sorption for potatoes. *Journal of Food Engineering*, vol. 35, 1998, no. 3, p. 267-280.

McMinn, W.A.M. and T.R.A. Magee. Moisture sorption characteristics of starch materials. *Drying Technology*, vol. 15, 1997, no. 5, p. 1527-1551.

Menkov, N.D. Sorption equilibrium moisture content of the seeds of several tobacco varieties. *Journal of Agricultural Engineering Research*, vol. 72, 1999, p. 347-353.

Menkov, N.D. and K.T. Dinkov. Moisture sorption isotherms of tobacco seeds at three temperatures. *Journal of Agricultural Engineering Research*, vol. 74, 1999, no. 3, p. 261-266.

Pezzutti, A. and G.H. Crapiste. Sorption equilibrium and drying characteristics of garlic. *Journal of Food Engineering*, vol. 31, 1997, p. 113-123.

Samaniego-Esguerra, C.M., I.F. Boag and G.L. Robertson. Comparison of regression methods for fitting the GAB model to the moisture isotherms of some dried fruit and vegetables. *Journal of Food Engineering*, vol. 13, 1991, p. 115-133.

Sanni, L.O., C. Atere and A. Kuye. Moisture sorption isotherms of fufu and tapioca at different temperatures. *Journal of Food Engineering*, vol. 34, 1997, p. 203-212.

Sanni, L.O., A.G. Kolawole, J.O. Akingbala and A. Kuye. Effect of drying methods on moisture sorption isotherms of fufu at three temperatures. *Drying Technology*, vol. 17, 1999, no. 1-2, p. 285-297.

Serris, G.S. and C.G. Biliaderis. Degradation kinetics of beetroot pigment encapsulated in polymeric matrices. *Journal of the Science of Food and Agriculture*, vol. 81, 2001, p. 691-700.

The Mathworks, *Optimization Toolbox. For use with Matlab®*. Natick: The Mathworks Inc., 2000.

Timmermann, E.O., J. Chirife and H.A. Iglesias. Water sorption isotherms of foods and foodstuffs: BET or GAB parameters? *Journal of Food Engineering*, vol. 48, 2001, no. 1, p. 19-31.

Tsami, E., M.K. Krokida and A.E. Drouzas. Effect of drying method on the sorption characteristics of model fruit powders. *Journal of Food Engineering*, vol. 38, 1999, no. 4, p. 381-392.

Tsami, E., D. Marinos-Kouris and Z.B. Maroulis. Water sorption isotherms of raisins, currants, figs, prunes and apricots. *Journal of Food Science*, vol. 55, 1990, no. 6, p. 1594-1597, 1625.

Van den Berg, C. *Vapour sorption equilibria and other water-starch interactions; a physico-chemical approach*. Wageningen: Wageningen Agricultural University, Section Process Engineering, Department of Food Science, 1981. 186 p. PhD thesis.

Veltchev, Z.N. and N.D. Menkov. Desorption isotherms of apples at several temperatures. *Drying Technology*, vol. 18, 2000, no. 4&5, p. 1127-1137.

Wang, N. and J.G. Brennan. Moisture sorption isotherm characteristics of potatoes at four temperatures. *Journal of Food Engineering*, vol. 14, 1991, p. 269-287.

Weisser, H. Influence of temperature on sorption equilibria. p. 95-118. In: Simatos, D. and J.L. Multon (Eds.). *Properties of water in foods in relations to quality and stability*. Dordrecht, The Netherlands: Martinus Nijhoff Publishers, 1985. 693 p.

Wolf, W., W.E.L. Spiess and G. Jung. Standardisation of isotherm measurements (cost-project 90 and 90 bis). p. 661-679. In: Simatos, D. and J.L. Multon (Eds.). *Properties of water in foods*. Dordrecht, The Netherlands: Martinus Nijhoff Publishers, 1985. 693 p.

Wolf, W., W.E.L. Spiess, G. Jung, H. Weisser, H. Bizot and R.B. Duckworth. The water-vapour sorption isotherms of microcrystalline cellulose (MCC) and of purified potato starch. Results of a collaborative study. *Journal of Food Engineering*, vol. 3, 1984, p. 51-73.

Yoshida, C.M.P. and F.C. Menegalli. Drying of supersweet corn. Paper No.95. In: Kerkhof, P.J.A.M., W.J. Coumans and G.D. Mooiweer. *Proceedings of the 12th International Drying Symposium IDS2000*. Amsterdam: Elsevier Science, 2000.

Young, J.F. Humidity control in the laboratory using salt solutions – a review. *Journal of Applied Chemistry*, vol. 17, 1967, p. 241-245.

## Chapter 4.3

### Sorption isotherms, GAB parameters and isosteric heat of sorption

This chapter has been published as:

Quirijns, E.J., A.J.B. van Boxtel, W.K.P. van Loon and G. van Straten. Sorption isotherms, GAB parameters and isosteric heat of sorption. *Journal of the Science of Food and Agriculture*, vol. 85, 2005, no. 11, p. 1805-1814.

## **Abstract**

The diffusion-sorption drying model has been developed as a physics-based way to model the decreasing drying rate at low moisture contents. This new model is founded on the existence of different classes of water: free and bound water. The transition between these classes and the corresponding thermodynamics form distinct components of the drying model. This chapter shows that the characteristics of the different classes of water and of the transition between them can be deduced from the GAB sorption isotherm.

The parameters in the GAB sorption isotherm support the theory of localised sorption, establishing the existence of different classes of water. Moreover, the sorption mechanism retrieved from the GAB parameters is in accordance with the sorption mechanism, which is obtained from the moisture dependence of the net isosteric heat of sorption. This holds for experimental sorption data of corn and starch as well as for literature data on five vegetables and four fortified cassave products.

An extremum in the net isosteric heat of sorption coincides with the transition between bound and free water, and the partition moisture content corresponds with the monolayer value derived from the GAB equation. This confirms that the GAB monolayer value can be chosen as model boundary between bound and free water. Moreover, it reveals that this method can be developed into a technique to estimate the bound water content in foods.

## Nomenclature

$a_w$	water activity of material	[-]
$C_g$	Guggenheim constant in GAB sorption equation	[-]
$C_{g0}$	Arrhenius type constant to express temperature dependence of $C_g$	[-]
dm	dry matter	[kg]
$H_1$	molar enthalpy of sorption of molecules sorbed in the first layer	[J.mol <sup>-1</sup> ]
$H_\ell$	molar enthalpy for condensation of bulk liquid	[J.mol <sup>-1</sup> ]
$H_m$	molar enthalpy of sorption of molecules sorbed in the multilayer	[J.mol <sup>-1</sup> ]
$K$	constant in GAB sorption equation, factor correcting properties of the multilayer molecules relative to the bulk liquid	[-]
$K_0$	Arrhenius type constant to express temperature dependence of $K$	[-]
$Q_{st}$	total heat of sorption	[J.mol <sup>-1</sup> ]
$q_1$	partition function of molecule in monolayer	[-]
$q_\ell$	partition function of molecule in bulk liquid	[-]
$q_m$	partition function of molecule in multilayer	[-]
$\mathcal{R}$	gas constant	[J.mol <sup>-1</sup> .K <sup>-1</sup> ]
$T$	temperature	[K]
$X$	moisture content (dry basis)	[kg.kg <sup>-1</sup> <sub>dm</sub> ]
$X_m$	monolayer moisture content	[kg.kg <sup>-1</sup> <sub>dm</sub> ]
$X_{m0}$	constant to express temperature dependence of $X_m$	[kg.kg <sup>-1</sup> <sub>dm</sub> ]
$\Delta H_{Cg}$	difference in enthalpy between monolayer and multilayer $H_1 - H_m$	[J.mol <sup>-1</sup> ]
$\Delta H_{is}$	isosteric enthalpy of sorption	[J.mol <sup>-1</sup> ]
$\Delta H_K$	difference in enthalpy between bulk liquid and multilayer $H_\ell - H_m$	[J.mol <sup>-1</sup> ]
$\Delta H_v$	evaporation enthalpy of water	[J.mol <sup>-1</sup> ]
$\Delta H_X$	constant to express temperature dependence of $X_m$	[J.mol <sup>-1</sup> ]

## Introduction

Biological materials have a decreasing drying rate at low moisture contents. In most drying models this behaviour is captured by making the diffusion coefficient dependent on moisture content. During drying, the effective diffusion coefficient is constant with moisture down to a critical moisture content. Below this critical value, the diffusion coefficient shows a sharp decrease with decreasing water concentration (Xiong *et al.*, 1991; Balaban, 1989; Van den Berg, 1981). It can be assumed that the observed decrease of the drying rate is mainly caused by the decreasing availability of free water molecules (Xiong *et al.*, 1991; Kiranoudis *et al.*, 1995). This assumption is based on the existence of two classes of water: the bound and free water. The bound moisture corresponds to water molecules connected strongly to the material molecules. The free moisture corresponds to the water molecules connected loosely to the material molecules (Xiong *et al.*, 1991; Kiranoudis *et al.*, 1995). The portion of free moisture content is initially very large. As drying reaches its last stages, the bound moisture molecules form the majority of the water molecules, and then the conversion between the bound and free water controls the overall mass transfer phenomenon (Xiong *et al.*, 1991; Kiranoudis *et al.*, 1995). This forms the basis of the newly developed diffusion-sorption drying model, which is presented in *Chapter 4.1*. In this model, the moisture transfer during the drying process is described by three basic transfer phenomena: free water diffusion, conversion between bound and free water inside the material and external convection at the boundary of the material. The model for the conversion between bound and free water makes the diffusion-sorption model original. The conversion is physically described as a sorption process. The interaction between water and the material is then modelled through the adsorption of free water to become bound water and, in reverse, the desorption of bound water to become free water. The thermodynamic variables for sorption required in the model are derived from the sorption isotherm.

The sorption isotherm relates the *water activity* to the *water content* of the mixture of water and material at a certain temperature and pressure. The water activity is defined as the ratio of the partial vapour pressure in equilibrium with the water in the food material and the vapour pressure in equilibrium with pure water at the same temperature (Van den Berg, 1981). Therefore, it characterises the state of the water in foods. This means that the sorption isotherm gives an impression how strong and in which way water is bound by the material constituents (Van den Berg, 1981; McMinn and Magee, 1997; Acker, 1969). The diffusion-sorption drying model uses this information for three purposes. First, it describes the existence of two different classes of moisture in the material: bound and free moisture.

Second, it determines the boundary between bound and free water. Since the distinction between the different classes is not sharp (Van den Berg, 1981), the term boundary is mainly an operational term, required for the model (*Chapter 4.1*). Third, the thermodynamics corresponding to this boundary are derived from the sorption isotherm. Both the boundary and the corresponding thermodynamics are used to model the conversion between bound and free water.

In this chapter, we investigate whether this physico-chemical background is supported by experimental sorption isotherms at different temperatures. To this end, the experimental sorption isotherms need to:

- a. give an accurate prediction of sorption at low moisture contents, since the conversion between bound and free water takes place at low moisture contents.
- b. describe the localised sorption behaviour, in order to derive the characteristics of the different classes of water and the transition between them.

More specifically, it is the goal of the present study to investigate whether the characteristics of the different classes of water and of the transition between them can be deduced from the experimental GAB (Guggenheim, Anderson and de Boer) sorption isotherm. This endeavour is successful when:

- 1) the theoretical sorption behaviour is supported by the experimentally derived sorption behaviour from the GAB parameters and from the net isosteric heat of sorption.
- 2) from the experimental isosteric heat of sorption a model of the boundary between bound and free water is obtained and subsequently is related to the GAB parameters.

## Theory

### Theoretical background of the GAB sorption isotherm

The GAB sorption isotherm represents a refined extension of the Langmuir and BET theories. The theoretical basis for the GAB sorption isotherm is the assumption of localised physical adsorption in multilayers with no lateral interactions. The first shell of water evenly covers the sorbent surface and is very tightly bound in a monolayer. Subsequent layers of water have less interaction with the sorbent surface. The molecules in this so called multilayer (layer 2-9) have interactions with the sorbent which range in energy levels somewhere between those of

the monolayer molecules and the bulk liquid. Succeeding layers of water molecules exhibit more and more bulk liquid properties (Van den Berg, 1981; McMinn and Magee, 1997; Rizvi, 1986; Dural and Hines, 1993; Lomauro *et al.*, 1985a; Vertucci and Leopold, 1984).

The GAB model thus discriminates between multilayer and condensate properties of molecules sorbed on top of the first molecule at a site. For the derivation of the GAB equation three assumptions are made: the sorption system consists of identical active sites (distinguishable and independent), it is isothermal and it is open to the sorbing vapour. Statistical thermodynamics then lead to the GAB sorption isotherm, expressing  $X = f(a_w)$  (Van den Berg, 1981; Rizvi, 1986):

$$\frac{X}{X_m} = \frac{C_g \cdot K \cdot a_w}{(1 - K \cdot a_w) \cdot (1 - K \cdot a_w + C_g \cdot K \cdot a_w)} \quad (4.3.1)$$

where the three GAB parameters,  $C_g$ ,  $K$  and  $X_m$  have a physical meaning:

$C_g$  is defined as the ratio of the partition function of the first molecule sorbed on a site ( $q_l$ ) and the partition function of molecules sorbed beyond the first molecule in the multilayer ( $q_m$ ) (Van den Berg, 1981).  $C_g$  is almost enthalpic in nature (Van den Berg, 1981). It is a measure of the strength of binding of water to the primary binding sites. The larger  $C_g$ , the stronger water is bound in the monolayer and the larger the difference in enthalpy between the monolayer molecules and multilayer molecules. Since the water molecules are still localised in the multilayer, the entropic contributions to  $C_g$  are less compared to the enthalpic (Van den Berg, 1981).

$K$  is defined as the ratio of the partition function of molecules in bulk liquid ( $q_l$ ) and the partition function of molecules sorbed in the multilayer ( $q_m$ ) (Van den Berg, 1981). Next to an enthalpic part,  $K$  contains an important entropic part. The enthalpic contribution to  $K$  is less compared to  $C_g$ , due to the considerably lower interaction enthalpy of the multilayer molecules with the sorbent. The higher entropic content of  $K$  can be explained by the strongly increased number of configurations and mobility of molecules in the bulk liquid compared to the molecules in the multilayer (Van den Berg, 1981; Fasina *et al.*, 1997).  $K$  is called a correction factor, since it corrects the properties of the multilayer molecules relative to the bulk liquid (Labuza *et al.*, 1985; Andrieu *et al.*, 1985; Wolf *et al.*, 1984). When  $K$  approaches one, there is almost no distinction between multilayer molecules and liquid molecules. In that case the water molecules beyond the monolayer are not structured in a multilayer, but have the same characteristics as the molecules in the bulk liquid. The GAB equation is then

reduced to the BET equation for sorption. The more the sorbed molecules are structured in a multilayer, the lower the value for  $K$ .

The theoretical interpretation of the GAB parameters makes it possible to derive the sorption behaviour of moisture in materials from the combination of the values of  $C_g$  and  $K$ , as is elucidated in Table 4.3.1.

$X_m$  is called the monolayer value. It is a measure of the availability of active sites for water sorption by the material (Van den Berg, 1981; McMinn and Magee, 1997; Rizvi, 1986; Kiranoudis *et al.*, 1993).

**Table 4.3.1.** The combination of the magnitude of GAB parameters  $C_g$  and  $K$  and the corresponding mechanism of sorption, where mono stands for monolayer, multi for multilayer and liquid for the bulk liquid.

mono $\approx$ multi $\approx$ liquid	mono $\approx$ multi $\neq$ liquid	mono $\neq$ multi $\neq$ liquid	mono $\neq$ multi $\approx$ liquid
$C_g \approx 1$	$C_g \approx 1$	$C_g \gg 1$	$C_g \gg 1$
$K \approx 1$	$K \ll 1$	$K \ll 1$	$K \approx 1$

### The influence of temperature on sorption isotherms

Sorption isotherms are temperature dependent. A higher temperature will decrease the binding energy between molecules. Because of an increased state of excitation of the molecules, their mutual distances increase and the attractive forces between them decrease. They become less stable and break away from the water binding site of the food materials. Consequently, an increase in temperature induces a reduction in the equilibrium moisture content at a specific water activity. This is consistent with the thermodynamics of sorption (Hossain *et al.*, 2001; Sanni and Kuye, 2000; McLaughlin and Magee, 1998). It is also established in other fields of food research, for example in a study to dielectric properties of foods, where the increased mobility of the water molecules as well as the reduced amount of hydrated water with increasing temperature are demonstrated (Van Loon *et al.*, 1995).

The character of the sorption process will become less strongly localised, due to the increasingly shorter residence time for the sorbed molecules in the first layer (Van den Berg, 1981).

Owing to their thermodynamic character, the temperature dependence of sorption can be incorporated in the parameters  $C_g$  and  $K$  (Van den Berg, 1981):

$$C_g = \frac{q_1}{q_m} = C_{g0} \cdot \exp\left(\frac{\Delta H_{C_g}}{\mathfrak{R} \cdot T}\right) \quad (4.3.2)$$

$$K = \frac{q_\ell}{q_m} = K_0 \cdot \exp\left(\frac{\Delta H_K}{\mathfrak{R} \cdot T}\right) \quad (4.3.3)$$

in which:

$\Delta H_{C_g} = H_l - H_m$  = difference in enthalpy between monolayer and multilayer sorption. This value is expected to be positive, due to the exothermic interaction of water with primary sorption sites.

$\Delta H_K = H_\ell - H_m$  = difference between the heat of condensation of water and the heat of sorption of a multimolecular layer. This value will be negative and smaller, since the multilayer molecules are less firmly bound. Sometimes a positive value can be found due to the endothermic dissolution of fruit sugars, as in Maroulis *et al.* (1988) and Gabas *et al.* (2000).

$C_{g0}$  and  $K_0$  are entropic in nature. They are defined as the ratio of reduced partition functions or accommodation functions between the first and multilayer, and between the bulk liquid and the multilayer respectively (Van den Berg, 1981).  $C_{g0}$  is expected to be smaller than 1, since the molecules prefer to be in the multilayer above the monolayer from entropic point of view. Similarly,  $K_0$  will be larger than 1, due to the high entropy of the molecules in the bulk liquid.

In the majority of cases in literature,  $X_m$  is considered to be constant with temperature. Yet independent fits elucidate that the parameter decreases with temperature (McMinn and Magee, 1997; Maroulis *et al.*, 1988; Monterrey-Q and Sobral, 2000). The decrease in the monolayer with temperature may be due to a reduction in the total number of active sites for water binding as a result of physical or chemical changes induced by temperature (Fasina *et al.*, 1997; Labuza *et al.*, 1985; Iglesias and Chirife, 1984; Maskan and Karataş, 1997). Hence, a dependence of the  $X_m$  on temperature has to be considered, which can be expressed in an exponential relation:

$$X_m = X_{m0} \cdot \exp\left(\frac{\Delta H_X}{\mathfrak{R} \cdot T}\right) \quad (4.3.4)$$

### The heat of sorption derived from sorption isotherm

Thermodynamic parameters can be derived from sorption isotherms at different temperatures (Van den Berg, 1981; Vertucci and Leopold, 1984; Gabas *et al.*, 2000; Palou *et al.*, 1997; Kumagai *et al.*, 1994). An important thermodynamic parameter is the net isosteric heat of sorption, which measures the binding energy of the forces between the water vapour molecules and the solid. It yields information for the understanding of the sorption mechanism. Moreover, it can help to detect the type of water binding, that is occurring at a given moisture content (Hossain *et al.*, 2001; McLaughlin and Magee, 1998; Palou *et al.*, 1997; Iglesias and Chirife, 1976; Serris and Biliaderis, 2001).

The difference between the amount of energy required to remove water from the material ( $Q_{st}$ ) and the amount of energy required for normal water vaporisation ( $\Delta H_v$ ) is defined as the net isosteric heat of sorption ( $\Delta H_{is}$ ):  $\Delta H_{is} = Q_{st} - \Delta H_v$ .

The molar net isosteric heat of sorption, can be derived from sorption isotherms at several temperatures using the Clausius-Clapeyron equation (Van den Berg, 1981; Maskan and Karataş, 1997; Cadden, 1988; Tsami *et al.*, 1990):

$$\Delta H_{is} = -\mathfrak{R} \cdot \left( \frac{\partial \ln a_w}{\partial T^{-1}} \right)_x \quad (4.3.5)$$

The values obtained from this equation are adequate only for qualitative considerations of thermodynamic properties for two reasons. First, these values can include considerable error, arising from various graphical manipulations as well as the experimental error in the isotherm data (Bushuk and Winkler, 1957; Wang and Brennan, 1991). Second, the Clausius-Clapeyron equation is based on the assumption that  $\Delta H_{is}$  is invariant with temperature (Kiranoudis *et al.*, 1993; McLaughlin and Magee, 1998; Iglesias and Chirife, 1976; Tsami *et al.*, 1990). This assumption can be met for pure systems at low temperatures (Labuza *et al.*, 1985). However, irreversible changes in the binding properties at increased temperatures cause  $\Delta H_{is}$  to depend on temperature for almost all foods (Iglesias *et al.*, 1989). Nevertheless, temperature invariance of  $\Delta H_{is}$  is assumed, because it allows analysis of more sorption isotherms at different temperatures, resulting in more accurate fits of the Clausius-Clapeyron equation. Therefore, the resulting net isosteric heat of sorption is considered as the average value for the temperature range under consideration.

Hysteresis effects may complicate thermodynamic data derived from sorption isotherms (Vertucci and Leopold, 1984; Palou *et al.*, 1997; Schneider and Schneider, 1972). In this research hysteresis is avoided since only desorption characteristics are considered (*Chapter 4.2*). This is justified as drying is the practical application. An additional advantage is that equilibria during desorption give the best representation (Van den Berg, 1981).

## Material and methods

### *Materials*

Corn was purchased in cans (Dutch supermarket C1000). The average initial moisture content was 2.6 [kg.kg<sup>-1</sup><sub>dm</sub>].

Starch cylinders with immobilised catalase were prepared, by manually mixing native potato starch (Perfectamyl D6, AVEBE, Veendam, The Netherlands) with 0.05 M phosphate buffer (pH=7) containing catalase (EC 1.11.1.6, Sigma, Zwijndrecht, The Netherlands, C-40) in a mass ratio 1.5:1 to a homogeneous paste. The paste was extruded into cylinders of diameter 3 mm and length > 30 mm. During preparation the starch cylinders were kept on ice, and then stored in a sealed glass container in a refrigerator (4°C) until use. The average initial moisture content was 0.97 [kg.kg<sup>-1</sup><sub>dm</sub>].

### *Experimental GAB sorption isotherm*

The experimental sorption data for corn and starch cylinders at four different temperatures were taken from *Chapter 4.2*. The sorption isotherms were always related to desorption. The major difference of these experiments with respect to standard sorption isotherm determinations were the measurement at very low water activity ( $a_w < 0.11$ ) and the long equilibration time of several weeks. Moreover, an improved regression methodology, based on the weighed sum of squares, was applied. This yielded accurate, consistent and physically relevant GAB parameters. The corresponding GAB parameters are presented in Table 4.3.2 at each temperature. In Table 4.3.3 the temperature dependence of the parameters is given.

**Table 4.3.2:** GAB parameters and confidence intervals for desorption isotherms of corn at 30, 45, 60 and 70°C ( $0.11 \leq a_w \leq 0.9$ ) and starch cylinders at 4, 30, 45 and 60°C ( $0.05 \leq a_w \leq 0.9$ ) (regression method: weighed least squares).

Material	Temperature [°C]	GAB parameters		
		$C_g$	$K$	$X_m$ [kg.kg <sup>-1</sup> ]
Corn	30	$9 \times 10^3$ *	0.89 (±7%)	0.072 (±16%)
	45	$9 \times 10^3$ *	0.97 (±2%)	0.059 (±3%)
	60	16 (±59%)	0.97 (±3%)	0.048 (±10%)
	70	19 (±36%)	1.03 (±3%)	0.046 (±9%)
Starch cylinders	4	24 (±15%)	0.67 (±5%)	0.16 (±5%)
	30	11 (±9%)	0.54 (±7%)	0.16 (±6%)
	45	21 (±10%)	0.73 (±3%)	0.10 (±4%)
	60	18 (±17%)	0.72 (±3%)	0.088 (±5%)

ad \*: Confidence interval larger than 100%.

**Table 4.3.3.** Temperature dependence and confidence intervals of GAB parameters for sorption isotherms of corn ( $0.11 < a_w < 0.9$ ) and starch cylinders ( $0.02 < a_w < 0.9$ ) obtained after direct regression based on weighed least squares.

Material	GAB parameters					
	$C_{g0}$	$\Delta H_{C_g}$ [J.mol <sup>-1</sup> ]	$K_0$	$\Delta H_K$ [J.mol <sup>-1</sup> ]	$X_{m0}$ [kg.kg <sup>-1</sup> ]	$\Delta H_X$ [J.mol <sup>-1</sup> ]
Corn	$4 \cdot 10^{-5}$ *	$4 \cdot 10^4$ (±94%)	3.6 (±41%)	$-3.6 \cdot 10^3$ (±31%)	$8 \cdot 10^{-4}$ (±98%)	$1.2 \cdot 10^4$ (±23%)
Starch cylinders	$1 \cdot 10^3$ *	$-1.1 \cdot 10^4$ (±36%)	3.5 (±60%)	$-4.3 \cdot 10^3$ (±36%)	$9.5 \cdot 10^{-4}$ (±68%)	$1.3 \cdot 10^4$ (±14%)

ad \*: confidence interval larger than 100%.

### **Experimental determination of heat of sorption**

It follows from equation 4.3.5 that the isosteric heat can be obtained from the slope of the plot representing  $\ln(a_w)$  versus  $1/T$ , at constant value for  $X$ . In order to construct this plot,  $a_w$  values at different temperatures are required at constant moisture content. However, the sorption data were not determined at constant moisture content. Therefore, the following procedure was applied. The experimental sorption data were used as much as possible,

starting from the lowest experimental data point. Since at one moisture content data points were mostly available at only one or two temperatures, the data points at other temperatures were obtained by applying the GAB parameters of Table 4.3.2 in the transformed GAB equation form  $a_w=f(X)$  (Maroulis *et al.*, 1995):

$$a_w = \frac{\left[ 2 + \left( \frac{X_m}{X} - 1 \right) \cdot C_g - \left\{ \left( 2 + \left( \frac{X_m}{X} - 1 \right) \cdot C_g \right)^2 - 4 \cdot (1 - C_g) \right\}^{\frac{1}{2}} \right]}{[2 \cdot K \cdot (1 - C_g)]} \quad (4.3.6)$$

When the predicted sorption isotherms began to deviate considerably from the experimental ones, these predictions were not applied anymore ( $a_w > 0.85$ ). A least squares analysis was performed to acquire the slope of the plot of  $\ln(a_w)$  versus  $1/T$ .

#### **Literature data**

Experimental desorption data at 30, 45 and 60°C were taken from Kiranoudis *et al.* (1993) for several vegetables: potato, carrot, green pepper, onion and tomato. These data were obtained using the standard experimental setup ( $a_w > 0.11$ ). The GAB parameters presented by Kiranoudis *et al.* (1993) could not be used in present study, since  $X_m$  was considered to be constant with temperature, giving wrong values for  $C_g$  and  $K$ . To obtain the GAB parameters at each temperature, the data were analysed again according to the regression methodology presented in *Chapter 4.2*. Since the parameters are only used for comparison in sorption behaviour of the vegetables, the average of the resulting parameters is presented in Table 4.3.4. The isosteric heat of sorption was determined from the experimental sorption data with the presented method.

GAB parameters for fortified cassava products were taken from Sanni *et al.* (1997) for fufu and tapioca and from Sanni and Kuye (2000) for soylafun and soyfufu. These data were obtained applying standard experimental ( $a_w > 0.11$ ) and regression methodology. The average parameters are presented in Table 4.3.5 together with the isosteric heat of sorption.

**Table 4.3.4.** Average of GAB parameters for desorption isotherms of several vegetables (Kiranoudis *et al.*, 1993) at 30, 45 and 60°C ( $0.11 \leq a_w \leq 0.9$ ) and characteristics of the moisture dependence of the net isosteric heat of sorption:  $\Delta H_{is,max}$  and moisture content where  $\Delta H_{is} = 0$  [kJ.mol<sup>-1</sup>].

Parameter	Product				
	potato	carrot	green pepper	onion	tomato
$C_g$	18.70	6.38	10.86	9.38	18.48
$K$	0.820	0.764	0.790	0.750	0.777
$X_m$ [kg.kg <sup>-1</sup> ]	0.068	0.150	0.146	0.155	0.149
$\Delta H_{is,max}$ [kJ.mol <sup>-1</sup> ]	52	23	31	28	33
$X_{\Delta H_{is}=0}$	0.35	0.8	0.6	0.8	0.6

**Table 4.3.5.** Average GAB parameters for adsorption isotherms of fortified cassava products at 25, 32 and 45°C ( $0.11 \leq a_w \leq 0.9$ ) (Sanni *et al.*, 1997; Sanni and Kuye, 2000) and characteristics of the moisture dependence of the net isosteric heat of sorption:  $\Delta H_{is,max}$  and moisture content where  $\Delta H_{is} = 0$  [kJ.mol<sup>-1</sup>].

Parameter	Product			
	fufu	tapioca	soyfufu	soylafun
$C_g$	61.76	14.72	52.24	72.36
$K$	0.688	0.566	0.579	0.594
$X_m$ [kg.kg <sup>-1</sup> ]	0.046	0.057	0.059	0.060
$\Delta H_{is,max}$ [kJ.mol <sup>-1</sup> ]	78	52	72	82
$X_{\Delta H_{is}=0}$	0.10	>> 0.10	0.11	0.11

## Results and discussion

### Sorption behaviour derived from experimental GAB sorption isotherms

For corn a (very) high value for  $C_g$  is accompanied by a value for  $K$ , approaching 1 (Table 4.3.2). This means that the multilayer molecules have properties comparable with those of bulk liquid molecules. The sorption of water by corn is apparently characterised by a monolayer of molecules, which are strongly bound to the material (high  $C_g$ ). The subsequent molecules are not or slightly structured in a multilayer, but have characteristics comparable with the molecules in the bulk liquid.

In the case of the starch cylinders, a lower value of  $C_g$  is accompanied by a value of  $K$  smaller than 1. Those values of the GAB parameters indicate that the water molecules are organised in a monolayer with water molecules strongly bound with the material and a multilayer, in

which the water molecules do differ considerably from bulk liquid molecules. Since  $C_g$  is smaller for starch cylinders compared to corn, the water molecules are less strongly bound to the material.

These two combinations of  $C_g$  and  $K$  values demonstrate the way in which water molecules are organised in layers (localised sorption). The existence of different classes of water molecules in the materials is established.

In literature, the combination of GAB parameter values has never been related before to the sorption mechanism of water molecules to the material. Nevertheless, in the majority of the reported data and parameters, a mechanism of sorption can be deduced from the combination of  $C_g$  and  $K$  values. The GAB parameters for potato ( $C_g = 19$ ,  $K = 0.82$ ,  $X_m = 0.068$ ) in Table 4.3.4 illustrate the presence of a monolayer, with strongly bound water molecules and a multilayer, which has characteristics comparable with bulk liquid. Carrot, in contrast ( $C_g = 6.4$ ,  $K = 0.76$ ,  $X_m = 0.15$ ) has a less strong monolayer and a more structured multilayer, where the water molecules are different from bulk liquid molecules. The GAB parameters of the fortified cassava products (Table 4.3.5) illustrate that soyfafun has the strongest monolayer, followed by fufu, soyfufu and tapioca. The water sorbed by tapioca is the least tightly bound. The water in the multiplayer, however, has comparable properties for tapioca, soyfufu and soyfafun, while the multilayer is less structured for fufu. Much more examples can be found in comprehensive overviews of sorption data (Lomauro *et al.*, 1985a/b; Chen and Jayas, 1998; Lewicki, 1998; Timmermann *et al.*, 2001).

The GAB parameters reported in literature do not always support the theory of localised sorption. For example a low value for  $C_g$  accompanied with  $K$  approaching 1 would mean that the monolayer and multilayer molecules do not differ very much and that the multilayer molecules behave like liquid molecules at the same time. Consequently, all three classes behave similar. No localised sorption can be illustrated by the parameters. Examples are the resulted parameters for grapefruit ( $C_g = 0.54$ ,  $K = 0.83$ ,  $X_m = 0.275$ ) and pineapple ( $C_g = 0.87$ ,  $K = 0.82$ ,  $X_m = 0.21$ ) in Lomauro *et al.* (1985a), and for grapes ( $C_g = 0.701$ ,  $K = 0.929$ ,  $X_m = 0.119$ ) in Vazquez *et al.* (1999). It is possible that the experimental sorption data do illustrate a gradual increase of moisture content, indicating that the water is not sorbed in a localised way, which is in accordance with the GAB parameters (Tsami *et al.*, 1990; Velázquez de la Cruz *et al.*, 2001). However, it is also possible that those parameters are a consequence of limitations of the applied experimental or regression methodology as explained in *Chapter 4.2*.

### Sorption behaviour derived from isosteric heat of sorption

The isosteric heat of sorption of corn and the starch cylinders are presented in Figure 4.3.1 as function of the moisture content of the material. The isosteric heat is given as a positive quantity, illustrating the endothermic character of desorption. For both materials, the isosteric heat of sorption decreases with increasing moisture content after a maximum has been reached. This is indicative for the intermolecular attraction forces between sorptive sites and water vapour (Serris and Biliaderis, 2001; Wang and Brennan, 1991). At moisture contents in the monolayer region, the water is tightly bound to the material, corresponding with high interaction energy. At increasing moisture content, the most active sites become occupied and sorption occurs on the less active sites giving lower heats of sorption (Maskan and Karataş, 1997; Iglesias and Chirife, 1976). The net isosteric heat of sorption ultimately approaches zero, indicating that the total heat of sorption is equal to the heat of vaporisation. The water molecules behave as the molecules in the liquid state. From a drying point of view, the higher

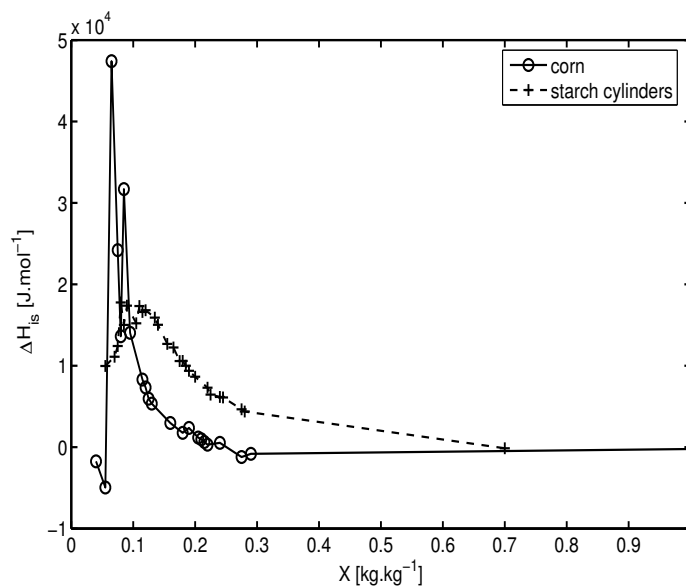


**Figure 4.3.1.** Average net isosteric heat of sorption as function of moisture content derived from experimental sorption data for corn and starch cylinders.

the moisture content, the less energy is required to remove water molecules from the material. Desorption will initially occur at the least active sites, requiring low interactive energies in addition to the latent heat of vaporisation of pure water. As drying continues sorption will occur at active sites requiring higher interactive energies (McLaughlin and Magee, 1998).

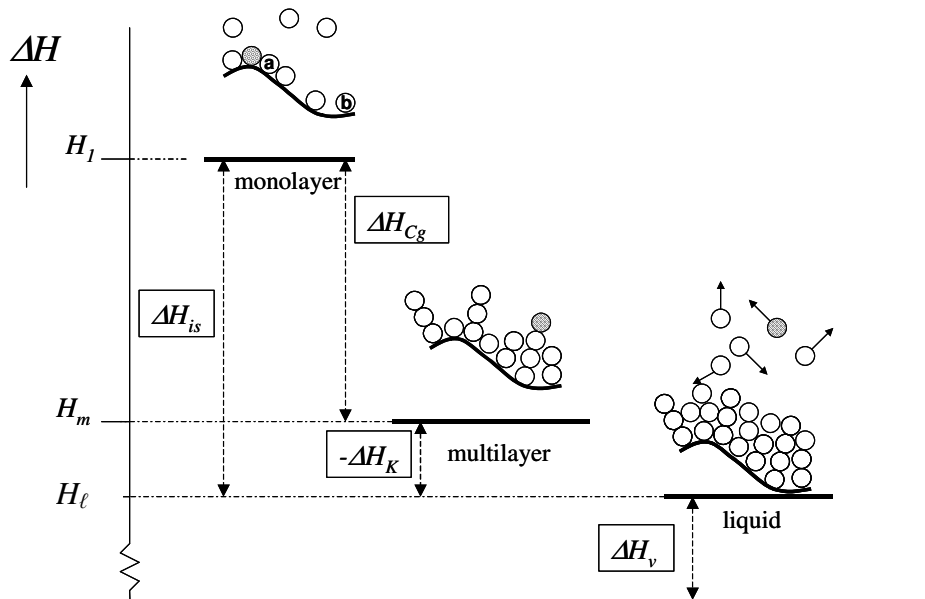


**Figure 4.3.2.** Illustration of localised sorption and the corresponding enthalpy levels of the shaded water molecules to derive the relation between the net isosteric heat of sorption,  $\Delta H_{is}$  and GAB parameters  $\Delta H_{Cg}$  and  $\Delta H_K$ .

Consequently, the existence of different classes of water is demonstrated by the isosteric heat of sorption: three classes with a continuous transition from the tightly bound water to the free water molecules. The classes correspond with the classification of Van den Berg (1981) and Vertucci and Leopold (1984).

The maximum net isosteric heat for corn ( $\Delta H_{is} \approx 47$  [kJ.mol<sup>-1</sup>]) is achieved at  $X = 0.065$  [kg.kg<sup>-1</sup>]. At  $X \approx 0.27$  [kg.kg<sup>-1</sup>],  $\Delta H_{is}$  becomes zero. For starch cylinders the maximum net isosteric heat is approximately 17 [kJ.mol<sup>-1</sup>] at  $X = 0.090$ - $0.110$  [kg.kg<sup>-1</sup>].  $\Delta H_{is}$  reaches zero at  $X \approx 0.60$  [kg.kg<sup>-1</sup>]. The net isosteric heat of both materials shows an increase at very low moisture contents (Figure 4.3.1). An initial increase of the net isosteric heat of sorption is found for adsorption (Fasina *et al.*, 1997; Palou *et al.*, 1997; Maskan and Göğüş, 1998). Only once, this increase is also found for desorption (Maskan and Göğüş, 1998). The increase at low moisture contents has been explained by considering that the sorption of water by the dry matrix leads to swelling of the material, resulting in the exposure of sorption sites of higher binding energies, which were previously not available (Fasina *et al.*, 1997; Palou *et al.*, 1997; Maskan and Göğüş, 1998). However, this explanation is not convincing in the case of

desorption. It is more likely, that during desorption at moisture contents near the monolayer value, the attraction between adjacent sorbed water molecules plays a cooperative role. The binding force of the water molecules on the material surface is strengthened by attractive forces between the water molecules. This means that the energy needed to remove water molecule **a** in Figure 4.3.2 from the material will be larger than for molecule **b**. When desorption proceeds, the attractive forces between water molecules will vanish, leading to the decrease in net isosteric heat of sorption at lower moisture contents.

### **Comparison of the experimentally derived sorption behaviours**

To be able to deduce the characteristics of the different classes of water and of the transition between them from the experimental GAB sorption isotherm, the sorption behaviour derived from the GAB parameters needs to match with the sorption behaviour derived from the isosteric heat of sorption. Figure 4.3.1 shows that the maximum net isosteric heat of sorption is much higher for corn than for starch cylinders. Moreover, after reaching the maximum the net isosteric heat reduces much faster to zero for corn, indicating that, after the monolayer, the molecules are less structured and behave like water in the liquid state at lower moisture content. This corresponds with the sorption behaviour for corn and starch cylinders derived from the physical interpretation of the GAB parameters  $C_g$  and  $K$ . For corn  $C_g$  was higher, illustrating the stronger binding of the monolayer compared to the multilayer molecules, which in turn corresponds with a higher net isosteric sorption heat. On the other hand,  $K$  was smaller for the starch cylinders. The water molecules in the multilayer deviate considerably in behaviour from the molecules in the liquid state. Therefore, the net isosteric heat of the starch cylinders will approach zero at higher moisture contents. It is clearly demonstrated that the mechanism of sorption derived from the independent knowledge of the heat of sorption is in accordance with the one deduced from the physical relevance of the GAB parameters.

This relation between the GAB parameters,  $C_g$  and  $K$ , and the moisture dependence of the isosteric heat of sorption is schematically illustrated by Figure 4.3.3. A stronger monolayer corresponds with a higher value of  $C_g$  and of the isosteric heat of sorption. When the water molecules are subsequently less structured in a multilayer,  $K$  increases and the isosteric heat of sorption reaches zero at lower moisture contents. The literature examples of both desorption and adsorption (Table 4.3.4 and 4.3.5) confirm the pattern in this figure. The maximum isosteric heat of sorption has the highest value for potato, followed by tomato, green pepper, onion and carrot. This corresponds with the sequence in magnitude of  $C_g$  (Table

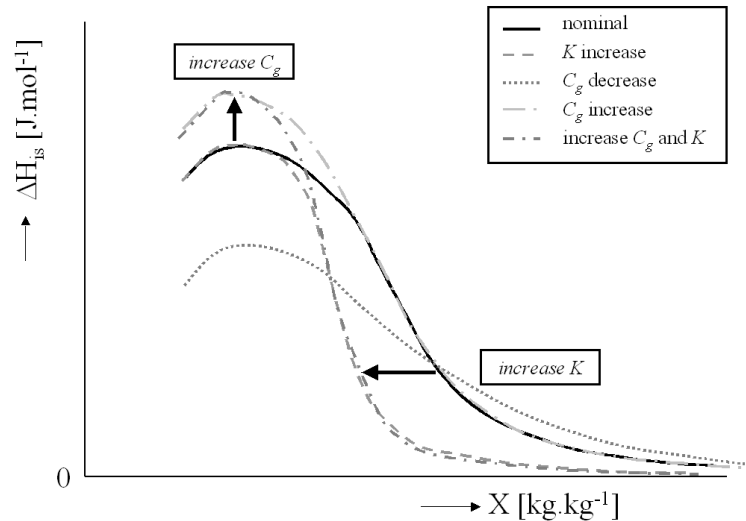


**Figure 4.3.3:** The relationship between the moisture dependence of the net isosteric heat of sorption and the ratio of the GAB parameters,  $C_g$  and  $K$ .

4.3.4). The isosteric heat of sorption reaches zero at the lowest moisture content for potato, that also has the highest value for  $K$ . Green pepper and tomato have comparable values for  $K$  and the net isosteric heat of sorption reaches zero at higher moisture content. The net isosteric heat of sorption reaches zero at the highest moisture content for onion and carrot, corresponding with the lowest value for  $K$ . The GAB parameters for adsorption of fortified cassava products describe a sorption behaviour that supports the moisture dependence of the heat of sorption presented in the corresponding papers (Sanni *et al.*, 1997; Sanni and Kuye, 2000): soylafun has the highest heat of sorption followed by fufu, soyfufu and tapioca. The heat of sorption of fufu reaches zero at the lowest moisture content (highest  $K$ ), while the other products reach zero at comparable higher moisture content.

Theoretically it is also possible to derive the maximum net isosteric heat of sorption from the parameters expressing the temperature dependence of the GAB equation,  $\Delta H_{C_g}$  and  $\Delta H_K$ . This is demonstrated in Figure 4.3.2, referring to the enthalpy levels of the shaded molecules:  $\Delta H_{is} = \Delta H_{C_g} + (-\Delta H_K)$ . Since these values have very large confidence intervals (Table 4.3.3), it is questionable to use  $\Delta H_{C_g}$  independently from  $C_{g0}$  or  $\Delta H_K$  independently from  $K_0$ . Moreover, this analysis is only allowed when the magnitude of the parameters is corresponding with the theoretical expectation. In *Chapter 4.2*, it was argued that the physical relevance of those

parameters ( $\Delta H_{Cg}$  and  $\Delta H_K$ ) could get lost during direct regression methods. With the discussion about the physical relevance of the parameters kept in mind, the analysis is only illustrated for corn. The parameters presented in Table 4.3.3 are applied in the analysis, leading to a value of 41 [kJ.mol<sup>-1</sup>], which is very close to the value of  $\Delta H_{is} \approx 47$  [kJ.mol<sup>-1</sup>]. Because of the high correlation between the parameters expressing the temperature dependence of the GAB parameters and their large confidence intervals, this is only a rough indication of the net isosteric heat of sorption. Tsami *et al.* (1990) and Vazquez *et al.* (1999) also try to derive  $\Delta H_{is}$  from the GAB parameters. However, they equate the value for  $\Delta H_{Cg}$  with  $\Delta H_{is}$ , which is not according to the theory outlined in Figure 4.3.2.

### Model boundary between bound and free water

The main reason for deriving the heat of sorption from experimental data is to obtain a model boundary between bound and free water. This model boundary plays a crucial role in the diffusion-sorption model (*Chapter 4.1*). The moisture content at which the heat of sorption approaches the heat of vaporisation of water (i.e.  $\Delta H_{is} \approx 0$  [J.mol<sup>-1</sup>]) is generally taken as indicative of the amount of bound water existing in the material (Kiranoudis *et al.*, 1993; McLaughlin and Magee, 1998; Palou *et al.*, 1997; Iglesias and Chirife, 1976; Wang and Brennan, 1991). In view of the localised sorption theory, this point corresponds with the level of moisture content where the multilayer molecules behave like liquid water molecules. Related studies on thermodynamic properties show that the maximum enthalpy is reached at the same moisture content as the extremum in entropy (Van den Berg, 1981; Vertucci and Leopold, 1984; Fasina *et al.*, 1997; Kumagai *et al.*, 1994; Schneider and Schneider, 1972). Since at this moisture content, the water behaves quite differently from free or bulk water, it is presumed to be the transition between bound and free water. For corn, this boundary corresponds with  $X_{part} = 0.065$  [kg.kg<sup>-1</sup>], for starch cylinders with  $X_{part} = 0.110$  [kg.kg<sup>-1</sup>]. From Table 4.3.2, it appears that this boundary is comparable with the average of the monolayer values  $X_m$ . This confirms the statement that, due to the assumed invariance of  $\Delta H_{is}$  with temperature, only average conditions can be considered. Moreover, it shows that the GAB monolayer value  $X_m$  can be considered as suitable model boundary between bound and free water.

The correspondence between the GAB parameter  $X_m$  and the maximum isosteric heat of sorption for corn and starch cylinders demonstrates that the presented method can be used as a technique to estimate the amount of tightly bound water in the material. The maximum in

isosteric heat of sorption clearly indicates a different behaviour between the tightly bound and the less bound water molecules. This method will also be useful to make a distinction between BET and GAB monolayer values, which always differ in magnitude (McLaughlin and Magee, 1998; Timmermann *et al.*, 2001). To establish the technique, the demonstrated correspondence needs to be illustrated for more materials. Moreover, to obtain the possibility to retrieve accurate values for the bound water as function of temperature, the sorption isotherms need to be determined for more temperatures, otherwise the sensitivity of Clausius-Clapeyron to experimental and graphical errors would cause unacceptable large inaccuracy of the results. The experimental and regression methodology (*Chapter 4.2*) is recommended for the determination of the sorption isotherm, in order to obtain data at low water activity as well as accurate, consistent and physically relevant GAB parameters. Although not the purpose of this study, it is illustrated that the comparison of the moisture dependence of the isosteric heat of sorption with the GAB parameters can be used as an estimation technique for the tightly bound water content in foods.

## Conclusions

The diffusion-sorption drying model uses a sorption process to describe the conversion between bound and free water at low moisture content. The drying model is founded on the existence of different classes of water, i.e. the bound and free water, caused by localised sorption. The transition between the bound and free water and the corresponding thermodynamics form distinct components of the drying model. In this chapter, we show that the characteristics of the different classes of water as well as the transition between them can be deduced from the GAB sorption isotherm.

The ratio of the estimated GAB parameters,  $C_g$  and  $K$  elucidate the mechanism of sorption in layers, establishing the existence of different classes of water. Not two, but three classes of water can be distinguished: the monolayer, the multilayer and the free water. The multilayer forms a continuous transition from the tightly bound water to the free water molecules. Knowledge of the net isosteric heat of sorption derived from experimental sorption data is confirming this mechanism of sorption. This correspondence in the mechanism of sorption is found for our own measurements as well as for results reported in literature.

The extremum in the net isosteric heat of sorption as function of the moisture content reveals the transition between tightly bound and free water, which corresponds with the monolayer value  $X_m$  obtained from the GAB sorption isotherm. Hence,  $X_m$  can be used as a suitable independent parameter in the diffusion-sorption model.

## **Acknowledgement**

We would like to thank AVEBE, Veendam The Netherlands for their free supply of native potato starch, perfectamyl D6.

## References

- Acker, L.W. Water activity and enzyme activity. *Food Technology*, vol. 23, 1969, p. 1257-1270.
- Andrieu, J., A. Stamatopoulos and M. Zafiropoulos. Equation for fitting desorption isotherms of durum wheat pasta. *Journal of Food Technology*, vol. 20, 1985, p. 651-657.
- Balaban, M. Effect of volume change in foods on the temperature and moisture content predictions of simultaneous heat and moisture transfer models. *Journal of Food Process Engineering*, vol. 12, 1989, p. 67-88.
- Bushuk, W. and C.A. Winkler. Sorption of water vapor on wheat flour, starch and gluten. *Cereal Chemistry*, vol. 34, 1957, no. 2, p. 73-86.
- Cadden, A. Moisture sorption characteristics of several food fibers. *Journal of Food Science*, vol. 53, 1988, no. 4, p. 1150-1155.
- Chen, C. and D.S. Jayas. Evaluation of the GAB equation for the isotherms of agricultural products. *Transactions of the ASAE (American Society of Agricultural Engineers)*, vol. 41, 1998, no. 6, p. 1755-1760.
- Dural, N.H. and A. L. Hines. A new theoretical isotherm equation for water vapor-food systems: multilayer adsorption on heterogeneous surfaces. *Journal of Food Engineering*, vol. 20, 1993, p. 75-96.
- Fasina, O, S. Sokhansanj and R. Tyler. Thermodynamics of moisture sorption in alfalfa pellets. *Drying Technology*, vol. 15, 1997, no. 5, p. 1553-1570.
- Gabas, A.L., F.C. Menegalli and J. Telis-Romero. Water sorption enthalpy-entropy compensation based on isotherms of plum skin and pulp. *Journal of Food Science*, vol. 65, 2000, no. 4, p. 680-684.
- Hossain, M.D., B.K. Bala, M.A. Hossain and M.R.A. Mondol. Sorption isotherms and heat of sorption of pineapple. *Journal of Food Engineering*, vol. 48, 2001, no. 2, p. 103-107.

Iglesias, H.A. and J. Chirife. Isothermic heats of water vapor sorption on dehydrated foods. Part I: Analysis of the differential heat curves. *Lebensmittel-Wissenschaft und -Technologie*, vol. 9, 1976, no. 2, p. 116-122.

Iglesias, H.A. and J. Chirife. Technical note: correlation of BET-monolayer moisture content in foods with temperature. *Journal of Food Technology*, vol. 19, 1984, p. 503-506.

Iglesias, H.A., J. Chirife and C.F. Fontan. On the temperature dependence of isothermic heats of water sorption in dehydrated foods. *Journal of Food Science*, vol. 54, 1989, no. 6, p. 1620-1624.

Kiranoudis, C.T., Z.B. Maroulis and D. Marinos-Kouris. Heat and mass transfer model building in drying with multiresponse data. *International Journal of Heat and Mass Transfer*, vol. 38, 1995, no. 3, p. 463-480.

Kiranoudis, C.T., Z.B. Maroulis, E. Tsami and D. Marinos-Kouris. Equilibrium moisture content and heat of desorption of some vegetables. *Journal of Food Engineering*, vol. 20, 1993, p. 55-74.

Kumagai, H., M. Iwase, H. Kumagai, A. Mizuno and T. Yano. Application of solution thermodynamics to the water sorption isotherms of food materials. *Bioscience, Biotechnology and Biochemistry*, vol. 58, 1994, no. 3, p. 475-481.

Labuza, T.P., A. Kaanane and J.Y. Chen. Effect of temperature on the moisture sorption isotherms and water activity shift of two dehydrated foods. *Journal of Food Science*, vol. 50, 1985, p. 385-391.

Lewicki, P.P. A three parameter equation for food moisture sorption isotherms. *Journal of Food Process Engineering*, vol. 21, 1998, no. 2, p. 127-144.

Lomauro, C.J., A.S. Bakshi and T.P. Labuza. Evaluation of food moisture sorption isotherm equations. Part I: fruit, vegetables and meat products. *Lebensmittel-Wissenschaft und -Technologie*, vol. 18, 1985a, no. 2, p. 111-117.

Lomauro, C.J., A.S. Bakshi and T.P. Labuza. Evaluation of food moisture sorption isotherm equations. Part II: milk, coffee, tea, nuts, oilseeds, spices and starchy products. *Lebensmittel-Wissenschaft und -Technologie*, vol. 18, 1985b, no. 2, p. 118-124.

Maroulis, Z.B., C.T. Kiranoudis and D. Marinos-Kouris. Heat and mass transfer modeling in air drying of foods. *Journal of Food Engineering*, vol. 26, 1995, p. 113-130.

Maroulis, Z.B., E. Tsami, D. Marinos-Kouris and G.D. Saravacos. Application of the GAB model to the moisture sorption isotherms of dried fruits. *Journal of Food Engineering*, vol. 7, 1988, p. 63-78.

Maskan, M. and F. Göğüş. Sorption isotherms and drying characteristics of Mulberry (*Morus alba*). *Journal of Food Engineering*, vol. 37, 1998, no. 4, p. 437-449.

Maskan, M. and Ş. Karataş. Sorption characteristics of whole pistachio nuts (*Pistacia vera L.*). *Drying Technology*, vol. 15, 1997, no. 3&4, p. 1119-1139.

McLaughlin, C.P. and T.R.A. Magee. The determination of sorption isotherm and the isosteric heats of sorption for potatoes. *Journal of Food Engineering*, vol. 35, 1998, no. 3, p. 267-280.

McMinn, W.A.M. and T.R.A. Magee. Moisture sorption characteristics of starch materials. *Drying Technology*, vol. 15, 1997, no. 5, p. 1527-1551.

Monterrey-Q, E.S. and P.J.A. Sobral. Sorption isotherms of edible films of tilapia myofibrillar proteins. Paper No.161. In: Kerkhof, P.J.A.M., W.J. Coumans and G.D. Mooiweer. *Proceedings of the 12th International Drying Symposium IDS2000*. Amsterdam: Elsevier Science, 2000.

Palou, E., A. López-Malo and A. Argai. Effect of temperature on the moisture sorption isotherms of some cookies and corn snacks. *Journal of Food Engineering*, vol. 31, 1997, no. 1, p. 85-93.

Rizvi, S.S.H. Thermodynamic properties of foods in dehydration. p. 133-214. In: Rao, M.A. and S.S.H. Rizvi (Eds.). *Engineering properties of foods*. New York: Marcel Dekker, Inc., 1986. 398 p.

Sanni, L.O., C. Atere and A. Kuye. Moisture sorption isotherms of fufu and tapioca at different temperatures. *Journal of Food Engineering*, vol. 34, 1997, p. 203-212.

Sanni, L.O. and A. Kuye. Effect of temperatures on water sorption isotherms of some fortified cassava products. Paper No.23. In: Kerkhof, P.J.A.M., W.J. Coumans and G.D. Mooiweer. *Proceedings of the 12th International Drying Symposium IDS2000*. Amsterdam: Elsevier Science, 2000.

Schneider, M.J.T. and A.S. Schneider. Water in biological membranes: adsorption isotherms and circular dichroism as a function of hydration. *Journal of Membrane Biology*, vol. 9, 1972, p. 127-140.

Serris, G.S. and C.G. Biliaderis. Degradation kinetics of beetroot pigment encapsulated in polymeric matrices. *Journal of the Science of Food and Agriculture*, vol. 81, 2001, p. 691-700.

Timmermann, E.O., J. Chirife and H.A. Iglesias. Water sorption isotherms of foods and foodstuffs: BET or GAB parameters? *Journal of Food Engineering*, vol. 48, 2001, no. 1, p. 19-31.

Tsami, E., D. Marinos-Kouris and Z.B. Maroulis. Water sorption isotherms of raisins, currants, figs, prunes and apricots. *Journal of Food Science*, vol. 55, 1990, no. 6, p. 1594-1597, 1625.

Tsami, E., Z.B. Maroulis, D. Marinos-Kouris and G.D. Saravacos. Heat of sorption of water in dried fruits. *International Journal of Food Science and Technology*, vol. 25, 1990, p. 350-359.

Van den Berg, C. *Vapour sorption equilibria and other water-starch interactions; a physico-chemical approach*. Wageningen: Wageningen Agricultural University, Section Process Engineering, Department of Food Science, 1981. 186 p. PhD thesis.

Van Loon, W.K.P., P.E.A. Smulders, C. van den Berg and I.A. van Haneghem. Time-domain reflectometry in carbohydrate solutions. *Journal of Food Engineering*, vol. 26, 1995, p. 319-328.

Vazquez, G., F. Chenlo, R. Moreira and L. Carballo. Desorption isotherms of *muscatel* and *aledo* grapes, and the influence of pretreatments on muscatel isotherms. *Journal of Food Engineering*, vol. 39, 1999, p. 409-414.

Velázquez de la Cruz, G., J.A. Torres and M.O. Martín-Polo. Temperature effect on the moisture sorption isotherms for methylcellulose and ethylcellulose films. *Journal of Food Engineering*, vol. 48, 2001, no. 1, p. 91-94.

Vertucci, C.W. and A.C. Leopold. Bound water in soybean seed and its relation to respiration and imbibitional damage. *Plant Physiology*, vol. 75, 1984, no. 1, p. 114-117.

Wang, N. and J.G. Brennan. Moisture sorption isotherm characteristics of potatoes at four temperatures. *Journal of Food Engineering*, vol. 14, 1991, p. 269-287.

Wolf, W., W.E.L. Spiess, G. Jung, H. Weisser, H. Bizot and R.B. Duckworth. The water-vapour sorption isotherms of microcrystalline cellulose (MCC) and of purified potato starch. Results of a collaborative study. *Journal of Food Engineering*, vol. 3, 1984, p. 51-73.

Xiong, X., G. Narsimhan and M.R. Okos. Effect of composition and pore structure on binding energy and effective diffusivity of moisture in porous food. *Journal of Food Engineering*, vol. 15, 1991, p. 187-208.

## **Chapter 4.4**

Mathematical description and parameter values of the diffusion-sorption drying model

## Nomenclature

$A$	constant in relation for saturated vapour pressure as function of temperature	
$A_{bed}$	cross area of dryer	[m <sup>2</sup> ]
$A_m$	exchange area of the material	[m <sup>2</sup> ]
$a_{Sh}$	parameter in relation for Sherwood number	
$a_w$	water activity of material	[-]
$a_{w,m}$	water activity at surface of material	[-]
$b_{Sh}$	parameter in relation for Sherwood number	
$C_g$	Guggenheim constant in GAB sorption equation	[-]
$C_{g0}$	Arrhenius type constant to express temperature dependence of $C_g$	[-]
$c_{p,a}$	heat capacity of air	[J.kg <sup>-1</sup> .K <sup>-1</sup> ]
$c_{p,dm}$	heat capacity of material	[J.kg <sup>-1</sup> .K <sup>-1</sup> ]
$c_{p,v}$	specific heat of vapour	[J.kg <sup>-1</sup> .K <sup>-1</sup> ]
$c_{p,w}$	specific heat of water	[J.kg <sup>-1</sup> .K <sup>-1</sup> ]
$D$	internal diffusion coefficient of moisture in material	[m <sup>2</sup> .s <sup>-1</sup> ]
$D_0$	parameter in Arrhenius-type relation for diffusion coefficient	[m <sup>2</sup> .s <sup>-1</sup> ]
$DM_{tot}$	total amount of dry matter	[kg]
$D_p$	characteristic diameter of particle	[m]
$D_{w,a}$	diffusion coefficient of moisture in air	[m <sup>2</sup> .s <sup>-1</sup> ]
$E_a$	activation energy for moisture diffusion	[J.mol <sup>-1</sup> ]
$G_a$	air flow rate	[m <sup>3</sup> .s <sup>-1</sup> ]
$h$	external convective heat transfer coefficient	[J.s <sup>-1</sup> .m <sup>-2</sup> .K <sup>-1</sup> ]
$h_m$	material specific enthalpy	[J.kg <sup>-1</sup> ]
$J_T$	heat flux, at surface of material	[J.s <sup>-1</sup> .m <sup>-2</sup> ]
$J_{Xs}$	mass flux, at surface of material	[kg.m <sup>-2</sup> .s <sup>-1</sup> ]
$K$	constant in GAB sorption equation	[-]
$K_0$	Arrhenius type constant to express temperature dependence of $K$	[-]
$K_{eq}$	equilibrium constant in sorption process	[-]
$k$	external convective mass transfer coefficient	[m.s <sup>-1</sup> ]
$k_a$	adsorption rate constant	[s <sup>-1</sup> ]
$k_d$	desorption rate constant	[s <sup>-1</sup> ]
$L_{cyl}$	length of the cylinder	[m]

$L_{bed}$	height of the bed	[m]
$M_a$	molecular mass of air	[kg.mol <sup>-1</sup> ]
$M_w$	molecular mass of water	[kg.mol <sup>-1</sup> ]
$m$	constant in relation for saturated vapour pressure as function of temperature	
$N_m$	number of material particles	[-]
$P_{sat}$	saturated vapour pressure	[Pa]
$P_{tot}$	total pressure	[Pa]
$\mathcal{R}$	gas constant, 8.314	[J.mol <sup>-1</sup> .K <sup>-1</sup> ]
$\mathcal{R}^*$	modified gas constant, 0.462	[kJ.kg <sup>-1</sup> .K <sup>-1</sup> ]
$\mathcal{R}_{air}$	gas constant	[kJ.kg <sup>-1</sup> <sub>air</sub> .K <sup>-1</sup> ]
$\mathcal{R}_{vapour}$	gas constant	[kJ.kg <sup>-1</sup> <sub>vapour</sub> .K <sup>-1</sup> ]
$R$	maximum radius of material	[m]
$R_{cyl}$	maximum radius of cylindrical material	[m]
Re	Reynolds number	
RH	relative air humidity	[%]
$r$	radius of material	[m]
$r_B$	conversion rate between bound and free water	[s <sup>-1</sup> ]
Sc	Schmidt number	
Sh	Sherwood number	
$T_a$	air temperature	[K]
$T_a^{\circ C}$	air temperature	[°C]
$T_a^{\circ C,i}$	ingoing air temperature	[°C]
$T_m$	immediate temperature of material	[K]
$T_m^{\circ C}$	immediate temperature of material	[°C]
$T_{m0^{\circ C}}$	initial temperature of material	[°C]
$T_n$	constant in relation for saturated vapour pressure as function of temperature	
$t$	time	[s]
$V_m$	volume of material	[m <sup>3</sup> ]
$v_a$	velocity of air	[m.s <sup>-1</sup> ]
$X$	total moisture content	[kg <sub>water</sub> .kg <sub>dm</sub> <sup>-1</sup> ]
$X_0$	initial moisture content of material	[kg <sub>water</sub> .kg <sub>dm</sub> <sup>-1</sup> ]
$X_B$	concentration of bound water	[kg <sub>water</sub> .kg <sub>dm</sub> <sup>-1</sup> ]
$X_{B0}$	initial concentration of bound water	[kg <sub>water</sub> .kg <sub>dm</sub> <sup>-1</sup> ]
$X_F$	concentration of free water	[kg <sub>water</sub> .kg <sub>dm</sub> <sup>-1</sup> ]

$X_{F0}$	initial concentration of free water	$[\text{kg}_{\text{water}} \cdot \text{kg}_{\text{dm}}^{-1}]$
$X_m$	monolayer moisture content or GAB monolayer value	$[\text{kg}_{\text{water}} \cdot \text{kg}_{\text{dm}}^{-1}]$
$X_{m0}$	constant to express temperature dependence of $X_m$	$[\text{kg}_{\text{water}} \cdot \text{kg}_{\text{dm}}^{-1}]$
$X_{part}$	partition moisture content: moisture content as boundary between bound and free water	$[\text{kg}_{\text{water}} \cdot \text{kg}_{\text{dm}}^{-1}]$
$Y_a$	absolute humidity of air	$[\text{kg}_{\text{water}} \cdot \text{kg}_{\text{da}}^{-1}]$
$Y_{a,i}$	absolute humidity of ingoing air	$[\text{kg}_{\text{water}} \cdot \text{kg}_{\text{da}}^{-1}]$
$\Delta G_a^s$	difference in Gibbs free energy between solid/solute in solution and of pure solid	$[\text{kJ} \cdot \text{kg}_{\text{dm}}^{-1}]$
$\Delta G_{X_{part}}^s$	Gibbs free energy of sorption at the transition between bound and free water, the partition moisture content	$[\text{J} \cdot \text{mol}^{-1}]$
$\Delta G_w^s$	difference in Gibbs free energy between water in solution and in pure water	$[\text{kJ} \cdot \text{kg}_{\text{water}}^{-1}]$
$\Delta H_{Cg}$	difference in enthalpy between monolayer and multilayer	$[\text{J} \cdot \text{mol}^{-1}]$
$\Delta H_K$	difference in enthalpy between bulk liquid and multilayer	$[\text{J} \cdot \text{mol}^{-1}]$
$\Delta H_X$	constant to express temperature dependence of $X_m$	$[\text{J} \cdot \text{mol}^{-1}]$
$\Delta h_{vo}$	evaporation enthalpy of water at 0 °C	$[\text{J} \cdot \text{kg}^{-1}]$
$\varepsilon$	bed porosity	$[\text{m}^3_{\text{air}} \cdot \text{m}^{-3}_{\text{bed}}]$
$\varepsilon_m$	volume fraction material	$[\text{m}^3_{\text{material}} \cdot \text{m}^{-3}_{\text{bed}}]$
$\phi$	sphericity particle	[-]
$\eta_a$	dynamic viscosity of air	$[\text{Pa} \cdot \text{s}]$
$\lambda_a$	thermal conductivity of air	$[\text{J} \cdot \text{s}^{-1} \cdot \text{m}^{-1} \cdot \text{K}^{-1}]$
$\lambda_m$	thermal conductivity of material	$[\text{J} \cdot \text{s}^{-1} \cdot \text{m}^{-1} \cdot \text{K}^{-1}]$
$\rho_a$	density of air	$[\text{kg} \cdot \text{m}^{-3}]$
$\rho_m$	density of material	$[\text{kg} \cdot \text{m}^{-3}]$
$\rho_{w,a}$	water concentration in the air stream	$[\text{kg} \cdot \text{m}^{-3}]$
$\rho_{w,s}$	water concentration at the surface of the material	$[\text{kg} \cdot \text{m}^{-3}]$
$\nu_a$	kinematic viscosity	$[\text{m}^2 \cdot \text{s}^{-1}]$

## Introduction

The mathematical description of the diffusion-sorption drying model together with the parameter values is presented in a concise way in this chapter. The purpose of this chapter is to list all (partial) differential equations, relations and parameters that are needed for the simulation of the diffusion-sorption model for the experimental set-up of this thesis. First the micro-scale models are presented that describe the mass and heat transfer on the material level. They are accompanied by their initial and boundary conditions. Then the models on the process level are described based on the macroscopic balances on mass and enthalpy. The used relations and parameter values for material, air and bed characteristics are finally given. The time and space dependency of the state variables and output variables are left out for brevity of notation.

## Model on micro-scale: material level

### Micro-scale model for mass transfer

$$\frac{\partial (\rho_m \cdot X_F)}{\partial t} = \nabla(\rho_m \cdot \mathcal{D}(T_m) \cdot \nabla X_F) + \rho_m \cdot r_B \quad (4.4.1)$$

$$-\frac{\partial X_B}{\partial t} = r_B \quad (4.4.2)$$

with

$$X = X_F + X_B \quad (4.4.3)$$

$$r_B = k_d \cdot X_B - k_a \cdot (X_{part} - X_B) \cdot X_F \quad (4.4.4)$$

for a cylindrical particle:

$$\frac{\partial (\rho_m \cdot X_F)}{\partial t} = \frac{1}{r} \frac{\partial}{\partial r} \left( \rho_m \cdot r \cdot D(T_m) \cdot \frac{\partial X_F}{\partial r} \right) + \rho_m \cdot r_B \quad (4.4.5)$$

### Micro-scale model for energy transfer

$$\frac{\partial (\rho_m \cdot h_m)}{\partial t} = \nabla (\lambda_m(T_m) \cdot \nabla T_{m^{\circ}C}) \quad (4.4.6)$$

$$h_m = c_{p,dm}(T_m) \cdot T_{m^{\circ}C} + X \cdot c_{p,w} \cdot T_{m^{\circ}C} \quad (4.4.7)$$

for a cylindrical particle:

$$\frac{\partial (\rho_m \cdot h_m)}{\partial t} = \frac{1}{r} \frac{\partial}{\partial r} \left( r \cdot \lambda_m(T_m) \cdot \frac{\partial T_{m^{\circ}C}}{\partial r} \right) \quad (4.4.8)$$

Incorporation of the relation for the material specific enthalpy  $h_m$  into the partial differential equation, results in the relation describing the temperature changes inside the material:

$$\frac{\partial T_{m^{\circ}C}}{\partial t} = \frac{\frac{1}{r} \cdot \frac{\partial}{\partial r} \left( r \cdot \lambda_m(T_m) \cdot \frac{\partial T_{m^{\circ}C}}{\partial r} \right) - \rho_m \cdot \frac{\partial X}{\partial t} \cdot c_{p,w} \cdot T_{m^{\circ}C}}{\rho_m \cdot \left( c_{p,dm} + X \cdot c_{p,w} + T_{m^{\circ}C} \cdot \frac{\partial c_{p,dm}}{\partial T_{m^{\circ}C}} \right)} \quad (4.4.9)$$

**Initial conditions**

In the beginning of the drying process, it is assumed that the moisture concentration and temperature profiles in the material are uniform:

$$\begin{aligned} t = 0 \quad 0 \leq r \leq R \quad X_F &= X_{F0} & (4.4.10) \\ t = 0 \quad 0 \leq r \leq R \quad X_B &= X_{B0} \\ t = 0 \quad 0 \leq r \leq R \quad T_{m^{\circ}C} &= T_{m0^{\circ}C} \end{aligned}$$

Moreover, it is assumed that at the beginning of the drying process, the material is at equilibrium. Therefore, the initial moisture contents,  $X_{F0}$  and  $X_{B0}$  have to fulfil the following conditions:

$$\frac{X_{B0}}{X_{part}} = \frac{K_{eq} \cdot X_{F0}}{1 + K_{eq} \cdot X_{F0}} \quad \text{and} \quad X_0 = X_{F0} + X_{B0} \quad (4.4.11)$$

**Boundary conditions*****Boundary conditions in centre of material***

During drying, the distribution of moisture and temperature are assumed to be symmetrical:

$$r = 0 \quad t > 0 \quad \left. \frac{\partial X_F}{\partial r} \right|_{r=0} = 0 \quad (4.4.12)$$

$$r = 0 \quad t > 0 \quad \left. \frac{\partial T_{m^{\circ}C}}{\partial r} \right|_{r=0} = 0 \quad (4.4.13)$$

### Boundary conditions at boundary of material

The mass flux of water from the surface to the air ( $J_{Xs}$ ) is proportional to the difference between the water concentration at the surface of the material ( $\rho_{w,s}$ ) and in the bulk air stream ( $\rho_{w,a}$ ):

$$J_{Xs} = k \cdot (\rho_{w,s} - \rho_{w,a}) \quad (4.4.14)$$

leading to:

$$r = R \quad t > 0 \quad J_{Xs} = -D(T_m) \cdot \rho_m \cdot \left. \frac{\partial X_F}{\partial r} \right|_{r=R} = k \cdot \frac{M_w}{\mathfrak{R}} \cdot \left( \frac{a_{w,m} \cdot P_{sat}(T_m|_{r=R})}{T_m|_{r=R}} - \frac{RH \cdot P_{sat}(T_a)}{T_a} \right) \quad (4.4.15)$$

The energy flux ( $J_T$ ) is determined by the residue of the convective heat transport, which is proportional to the difference between the temperature of the drying air ( $T_a$ ) and the surface temperature ( $T_m|_{r=R}$ ), and the heat transfer required for the evaporation of moisture, under the assumption that evaporation of moisture only takes place at the surface of the material:

$$r = R \quad t > 0 \quad J_T = \lambda_m(T_m) \cdot \left. \frac{\partial T_{m^{\circ}C}}{\partial r} \right|_{r=R} = h \cdot (T_{a^{\circ}C} - T_{m^{\circ}C}|_{r=R}) - J_{Xs} \cdot (\Delta h_{vo} - (c_{p,w} - c_{p,v}) \cdot T_{m^{\circ}C}|_{r=R}) \quad (4.4.16)$$

## Model on macro-scale: process level

### Macro-scale model for air humidity

The absolute humidity of the air changes as a consequence of the mass flux of moisture ( $J_{Xs}$ ) from the cylinders to the air, which is the same for all cylinders:

$$\frac{dY_a}{dt} = \frac{\rho_a \cdot G_a \cdot (Y_{a,i} - Y_a) + J_{Xs} \cdot A_m \cdot N_m}{\varepsilon \cdot \rho_a \cdot L_{bed} \cdot A_{bed}} \quad (4.4.17)$$

### Macro-scale model for air temperature

The enthalpy content of the mass flux of evaporated water causes an increase in the enthalpy of the air. Besides, the air enthalpy decreases due to the transfer of energy to all cylinders. The enthalpy residue determines the change in air enthalpy, which leads to a corresponding change in air temperature:

$$\frac{dT_{a^{\circ}C}}{dt} = \frac{\rho_a \cdot G_a \cdot (T_{a^{\circ}C,i} - T_{a^{\circ}C}) \cdot (c_{p,a} + Y_{a,i} \cdot c_{p,v}) - A_m \cdot N_m \cdot ((h + J_{Xs} \cdot c_{p,v}) \cdot (T_{a^{\circ}C} - T_{m^{\circ}C}|_{r=R}))}{\varepsilon \cdot \rho_a \cdot L_{bed} \cdot A_{bed} \cdot (c_{p,a} + c_{p,v} \cdot Y_a)} \quad (4.4.18)$$

## Relations and parameters for material, air and bed characteristics

### Material characteristics: mass transfer

#### *Sorption isotherm*

The GAB sorption isotherm is given by:

$$\frac{X|_{r=R}}{X_m} = \frac{C_g \cdot K \cdot a_{w,m}}{(1 - K \cdot a_{w,m}) \cdot (1 - K \cdot a_{w,m} + C_g \cdot K \cdot a_{w,m})} \quad (4.4.19)$$

and in its transformed form as:

$$a_{w,m} = \frac{\left[ 2 + \left( \frac{X_m}{X|_{r=R}} - 1 \right) \cdot C_g - \left\{ \left( 2 + \left( \frac{X_m}{X|_{r=R}} - 1 \right) \cdot C_g \right)^2 - 4 \cdot (1 - C_g) \right\}^{\frac{1}{2}} \right]}{[2 \cdot K \cdot (1 - C_g)]} \quad (4.4.20)$$

with additional condition:

$$a_{w,m} \leq 1$$

The GAB parameters are a function of temperature:

$$C_g = C_{g0} \cdot \exp\left(\frac{\Delta H_{Cg}}{\mathfrak{R} \cdot T_m}\right) \quad (4.4.21)$$

$$K = K_0 \cdot \exp\left(\frac{\Delta H_K}{\mathfrak{R} \cdot T_m}\right) \quad (4.4.22)$$

$$X_m = X_{m0} \cdot \exp\left(\frac{\Delta H_X}{\mathfrak{R} \cdot T_m}\right) \quad (4.4.23)$$

with for starch cylinders:

$$\begin{aligned} C_{g0} &= 1.2 \cdot 10^3 & [-] \\ \Delta H_{Cg} &= -1.1 \cdot 10^4 & [\text{J} \cdot \text{mol}^{-1}] \\ K_0 &= 3.52 & [-] \\ \Delta H_K &= -4.28 \cdot 10^3 & [\text{J} \cdot \text{mol}^{-1}] \\ X_{m0} &= 9.52 \cdot 10^{-4} & [\text{kg} \cdot \text{kg}^{-1}] \\ \Delta H_{Xm} &= 1.3 \cdot 10^4 & [\text{J} \cdot \text{mol}^{-1}] \end{aligned}$$

### **Density**

The density of the starch cylinders is experimentally determined:

$$\begin{aligned} \rho_{m,d=2mm} &= 411 & [\text{kg} \cdot \text{m}^{-3}] \\ \rho_{m,d=3mm} &= 458 & [\text{kg} \cdot \text{m}^{-3}] \\ \rho_{m,d=5mm} &= 526 & [\text{kg} \cdot \text{m}^{-3}] \end{aligned}$$

### **Diffusion coefficient**

The diffusion coefficient is given by an Arrhenius-type equation:

$$D = D_0 \cdot e^{\frac{-E_a}{\mathfrak{R} \cdot T_m}} \quad (4.4.24)$$

$D_0$  and  $E_a$  are fitted with drying experiments experiments:

$$\begin{aligned} D_0 &= 3.75 \cdot 10^{-8} & [\text{m}^2 \cdot \text{s}^{-1}] \\ E_a &= 1.06 \cdot 10^4 & [\text{J} \cdot \text{mol}^{-1}] \end{aligned}$$

**Parameters in the conversion between bound and free water**

The relations in this section are all related to the partition moisture content  $X_{part}$ , where the transition between free and bound water is located.

At each position in the material, equilibrium exists between bound and free water, indicated by  $K_{eq}$ . Therefore, at each position  $X_{part}$  between bound and free water is determined, since this transition is a function of temperature. Then the Gibbs free energy for sorption is determined, which yields the  $K_{eq}$  and the ratio between  $k_a$  and  $k_d$ :

$$X_{part} = X_m \quad (4.4.25)$$

$$K_{eq} = \frac{k_a}{k_d} \quad (4.4.26)$$

with

$$\ln K_{eq} = - \frac{\Delta G_{X_{part}}^s}{\mathfrak{R}' \cdot T_m \cdot X_{part}} \quad (4.4.27)$$

in which:

$$\Delta G_{X_{part}}^s = X_{part} \cdot \Delta G_w^s + \Delta G_a^s \quad (4.4.28)$$

$$\Delta G_a^s = -\mathfrak{R}' \cdot T_m \cdot X_m \cdot \ln \frac{1 + (C_g - 1) \cdot K \cdot a_w|_{X=X_{part}}}{1 - K \cdot a_w|_{X=X_{part}}} \quad (4.4.29)$$

$$\Delta G_w^s = \mathfrak{R}' \cdot T_m \cdot \ln(a_w|_{X=X_{part}}) \quad (4.4.30)$$

For the calculation of  $a_w|_{X=X_{part}}$ , the presented transformed GAB sorption isotherm can be applied.

**Material characteristics: energy transfer**

The material characteristics with respect to heat transfer are obtained from literature.

**Thermal conductivity**

$$\lambda_m = 0.19306 + 8.4997 \cdot 10^{-4} \cdot T_{m^\circ C} \quad (4.4.31)$$

(Bowser and Wilhelm, 1995)

**Heat capacity**

heat capacity of material

$$c_{p,dm} = 5.737 \cdot (T_{m^{\circ}C} + 273.15) - 239.1 \quad (4.4.32)$$

(Lieveense, 1991)

heat capacity of water

$$c_{p,w} = 4180 \quad [\text{J.kg}^{-1}\text{K}^{-1}]$$

heat capacity of vapour

$$c_{p,v} = 1870 \quad [\text{J.kg}^{-1}\text{.K}^{-1}]$$

**Evaporation enthalpy of water at 0°C**

$$\Delta h_{v0} = 2504 \cdot 10^3 \quad [\text{J.kg}^{-1}]$$

**External mass and heat transfer: surface material/air and air characteristics**

**External mass and heat transfer coefficient**

The external mass transfer coefficient is calculated with a semi-empirical relation of dimensionless numbers (e.g. Fyhr and Kemp, 1998):

$$Sh = a_{Sh} + b_{Sh} \cdot \text{Re}^{1/2} \cdot \text{Sc}^{1/3} \quad (4.4.33)$$

in which  $a_{Sh}$  and  $b_{Sh}$  are estimated for the experimental set-up:

$$a_{Sh} = -15 \quad [\pm 43\%]$$

$$b_{Sh} = 2.1 \quad [\pm 28\%].$$

The definition of the dimensionless numbers is taken from Bird *et al.* (2002):

$$Sh = \frac{k \cdot D_p}{D_{w,a} \cdot (1 - \varepsilon) \cdot \phi} \quad (4.4.34)$$

$$\text{Re} = \frac{v_a \cdot D_p}{v_a \cdot (1 - \varepsilon) \cdot \phi} \quad (4.4.35)$$

with  $D_p$  the characteristic dimension of the particle and  $\phi$  its sphericity:

$$D_p = \frac{6 \cdot V_m}{A_m} \quad (4.4.36)$$

$$\phi = 0.92 \text{ or } 1$$

and

$$\text{Sc} = \frac{\eta_a}{\rho_a \cdot \mathcal{D}_{w,a}} \quad (4.4.37)$$

The external mass and heat transfer coefficient are related by the Chilton-Colburn relation:

$$h = k \cdot (\rho_a \cdot c_{p,a})^{\frac{1}{3}} \cdot \left( \frac{\lambda_a}{\mathcal{D}_{w,a}} \right)^{\frac{2}{3}} \quad (4.4.38)$$

### ***Air properties***

*Density of air*

$$\rho_a = 10^{-3} \cdot \left( \frac{P_{tot}}{\mathfrak{R}_{air} \cdot T_a} - \left[ \frac{1}{\mathfrak{R}_{air}} - \frac{1}{\mathfrak{R}_{vapour}} \right] \cdot \frac{RH \cdot P_{sat}}{T_a} \right) \quad (4.4.39)$$

with:

$$\begin{aligned} P_{tot} &= 101325 && [\text{Pa}] \\ \mathfrak{R}_{air} &= 0.2871 && [\text{kJ} \cdot \text{kg}^{-1} \cdot \text{K}^{-1}] \\ \mathfrak{R}_{vapour} &= 0.4615 && [\text{kJ} \cdot \text{kg}^{-1} \cdot \text{K}^{-1}] \end{aligned}$$

*Saturated vapour pressure*

$$P_{sat} = A \cdot 10^{\frac{m \cdot T_a + c}{T_a + T_n}} \cdot \frac{10^5}{10^3} \quad (4.4.40)$$

where:

$$\begin{array}{llll}
 A & = & 6.1078 & \text{for } -40^{\circ}\text{C} < T < 50^{\circ}\text{C} \\
 & & 5.9987 & 50^{\circ}\text{C} < T < 100^{\circ}\text{C} \\
 m & = & 7.500 & \text{for } -40^{\circ}\text{C} < T < 50^{\circ}\text{C} \\
 & & 7.3313 & 50^{\circ}\text{C} < T < 100^{\circ}\text{C} \\
 T_n & = & 237.3 & \text{for } -40^{\circ}\text{C} < T < 50^{\circ}\text{C} \\
 & & 229.1 & 50^{\circ}\text{C} < T < 100^{\circ}\text{C}
 \end{array}$$

*Heat capacity of air*

$$c_{p,a} = 1000 \text{ [J.kg}^{-1}\text{.K}^{-1}\text{]}$$

*Thermal conductivity of air*

$$\lambda_a = 4.5 \cdot 10^{-3} + 7.26 \cdot 10^{-5} \cdot T_a \quad (4.4.41)$$

(Lievens, 1991)

*Diffusion coefficient of water in air*

$$D_{w,a} = 5.28 \cdot 10^{-9} \cdot (T_a)^{3/2} \quad (4.4.42)$$

(Liou, 1982).

*Viscosity of air*

Dynamic viscosity of air:

$$\eta_a = 1.719 \cdot 10^{-5} \cdot \left( \frac{T_a}{273.15} \right)^{0.76} \quad (4.4.43)$$

(Lievens, 1991)

Kinematic viscosity of air:

$$v_a = \frac{\eta_a}{\rho_a} \quad (4.4.44)$$

Relation between absolute and relative humidity of air

$$Y_a = \frac{M_w}{M_a} \cdot \frac{RH \cdot P_{sat}}{P_{tot} - RH \cdot P_{sat}} \quad (4.4.45)$$

$$RH = \frac{P_{tot} \cdot \frac{M_a}{M_w} \cdot Y_a}{P_{sat} \cdot \left( 1 + \frac{M_a}{M_w} \cdot Y_a \right)} \quad (4.4.46)$$

with

$$M_a = 28.94 \cdot 10^{-3} \quad [\text{kg} \cdot \text{mol}^{-1}]$$

$$M_w = 18 \cdot 10^{-3} \quad [\text{kg} \cdot \text{mol}^{-1}]$$

### Bed characteristics

$$L_{bed} = 2 \cdot R_{cyl} \quad \text{height of thin layer}$$

$$A_{bed} = 1.539 \cdot 10^{-2} \text{ [m}^2\text{]} \quad \text{packed bed}$$

$$= 1.963 \cdot 10^{-3} \text{ [m}^2\text{]} \quad \text{fluidised bed}$$

$$\varepsilon = 1 - \varepsilon_m \quad [m_{air}^3 \cdot m_{bed}^{-3}] \quad (4.4.47)$$

in which for a cylindrical particle:

$$\varepsilon_m = \frac{\pi \cdot R_{cyl}^2 \cdot L_{cyl} \cdot N_m}{A_{bed} \cdot L_{bed}} \quad [m_{material}^3 \cdot m_{bed}^{-3}] \quad (4.4.48)$$

$$\text{with } A_m \cdot N_m = 2 \cdot \frac{DM_{tot}}{\rho_m \cdot R_{cyl}} \quad (4.4.49)$$

$$\text{and } A_m = 2 \cdot \pi \cdot R_{cyl} \cdot L_{cyl} \quad (4.4.50)$$

The relation for  $\varepsilon_m$  then results in:

$$\varepsilon_m = \frac{DM_{tot}}{A_{bed} \cdot L_{bed} \cdot \rho_m} \quad [m_{material}^3 \cdot m_{bed}^{-3}] \quad (4.4.51)$$

## References

Bird, R.B., W.E. Stewart and E.N. Lightfoot. *Transport Phenomena*. 2<sup>nd</sup> edition. New York, etc.: John Wiley & Sons, Inc., 2002. 895 p.

Bowser, T.J. and L.R. Wilhelm. Modeling simultaneous shrinkage and heat and mass transfer of a thin, nonporous film during drying. *Journal of Food Science*, vol. 60, 1995, no. 4, p. 753-757.

Fyhr, C. and I.C. Kemp. Comparison of different drying kinetics models for single particles. *Drying Technology*, vol. 16, 1998, no. 7, p. 1339-1369.

Lievense, L.C. *The inactivation of Lactobacillus plantarum during drying*. Wageningen: Wageningen Agricultural University, Department of Food Processing, 1991. 118 p. PhD thesis.

Liou, J.K. *An approximate method for nonlinear diffusion applied to enzyme inactivation during drying*. Wageningen: Agricultural University, 1982. 137 p. PhD-thesis.



## **Chapter 5**

# **Development and validation of the quality model**

Quality indicator profiles inside food during drying

This chapter is submitted for publication as:

Quirijns, E.J., W.K.P. van Loon, M.A.J.S. van Boekel and G. van Straten. Quality indicator profiles inside food during drying.

## Abstract

Temperature and moisture content changes may degrade the quality of food and agricultural materials during drying. Because the minimum value of the quality is often more important than the average value, good quality control should be based on profiles of a quality indicator inside the material.

The existence of quality indicator profiles (QIPs) has been demonstrated experimentally in model food composed of starch cylinders incorporating the enzyme catalase. The residual enzyme activity is the quality indicator. Although the experimental results are sensitive to experimental error (8-21%), significant differences between different drying treatments (temperature and relative humidity) are found. Drying experiments show that air conditions are instrumental in influencing the QIPs.

A model of the quality indicator has been developed for the prediction of its profiles during drying, based on independent inactivation experiments. To describe the inactivation kinetics a fractional conversion model has been used, because always a non zero rest activity has been measured. The experimentally determined rest activity and reaction rate constant are both dependent on temperature and moisture content.

To predict the QIPs the independent quality model is combined with the diffusion-sorption drying model. The drying model agrees well with the moisture content measurements. Since this model provides moisture and temperature distribution profiles, QIPs can be calculated. The predicted QIPs are comparable with the experimental ones, though higher in enzyme activity. The predicted profiles can subsequently be applied in product and process design, improving critical quality aspects.

## Nomenclature

$a$	empirical parameter in model for residual enzyme activity	[-]
$b$	empirical parameter in model for residual enzyme activity	[-]
$c$	empirical parameter in model for residual enzyme activity	[K <sup>-1</sup> ]
$d$	empirical parameter in model for inactivation constant	[-]
$E$	enzyme activity	[-]
$E_{exp}$	experimental enzyme activity	[-]
$E_{in}$	inner enzyme activity	[-]
$E_{mod}$	predicted enzyme activity	[-]
$E_{out}$	outer enzyme activity	[-]
$E_0$	initial enzyme activity	[-]
$E_{\infty}$	enzyme rest activity	[-]
$e$	empirical parameter in model for inactivation constant	[-]
$f$	empirical parameter in model for inactivation constant	[K <sup>-1</sup> ]
$k_1$	first order inactivation constant of decomposition of H <sub>2</sub> O <sub>2</sub> by catalase	[s <sup>-1</sup> ]
$k_e$	first order inactivation constant, describing the inactivation of catalase	[s <sup>-1</sup> ]
QIP	Quality Indicator Profile	
$RH$	air humidity relative to saturated air humidity at considered temperature	[-]
$S$	substrate concentration	[M]
SSQ	sum of squares	[-]
$T$	temperature	[K]
$t$	time	[s]
$X$	starch moisture content	[kg.kg <sub>dm</sub> <sup>-1</sup> ]

## Introduction

Nowadays consumers and governmental legislation increasingly ask for high quality products (Uddin *et al.*, 2000). Drying processes may cause quality loss. During drying product quality degenerates as a consequence of the elimination of water from the product as well as the increase of the temperature during the course of drying (Adamiec *et al.*, 1995). Wanted or unwanted changes in foods or bio products, can be classified into biochemical or microbial changes, enzymatic reactions, chemical reactions and physical changes (McMinn and Magee, 1997). Examples of changes in quality are: formation of cracks or crusts, colouring, loss of natural pigments, loss of vitamins and minerals, flavour loss and lipid oxidation leading to rancidity (Langrish *et al.*, 1997; Jayaraman and Das Gupta, 1995; Villota and Karel, 1980). It is obvious that there is a need for product and process design in order to optimise quality (Madamba, 1997; Banga and Singh, 1994).

To optimise quality during the drying process, three aspects are required: a definition of quality, a quality model and a model of quality evolution during the drying process.

Quality can be defined as a measure of adequacy of a product for specific uses. Different situations require different quality criteria (Adamiec *et al.*, 1995). Actually, quality is more a property of the consumer, who gives a quality judgement to a food. The quality experience of a consumer is linked to product properties, which can be described to as quality attributes. A quality attribute is for example colour. Colour may be caused by many factors. Therefore, quality attributes are discerned into quality indicators, which are measurable. In the present research the quality indicator is a function of the characteristics of the drying process and of the material used. In the analysis of *Chapter 2*, it is shown that the quality indicator is determined by gradients of moisture content and temperature inside the material. Crack formation is a good example. In quality control or optimisation average values are generally used (Mishkin *et al.*, 1984; Banga and Singh, 1994; Villota and Karel, 1980; Van Boxtel and Knol, 1996). However, it is not so much the average value that is important in control, but the spatial distribution of the indicator inside the material: the quality indicator profile (QIP). Actually, the position with the worst quality indicator inside the material is the most important factor. This becomes clear when looking at examples as colouring or spoilage by deteriorative micro organisms or enzymes. Although in the case of spoilage the average quality indicator may fulfil the safety criteria, there may still exist a location inside the material where this criterion is not met and spoilage still occurs. So for the definition of quality, a quality indicator should be determined, which takes spatial distribution into account.

The quality indicator considered in this study is enzymatic activity. Two aspects are relevant here: the activity of certain enzymes during drying (for example in colouring and flavour loss, Pezzutti and Crapiste, 1997) and the residual activity of enzymes after drying. In food industry, the aim is often to inactivate those enzymes which catalyse undesired degradation reactions during storage, like enzymatic browning reactions in vegetables and fruits, starch degradation in grain products, reactions causing rancidity in pasta (Luyben *et al.*, 1982; Meerdink and van 't Riet, 1991). In biotechnology, immobilised enzymes in dried form are produced for use in detergents, beer and bread or in pharmaceutical industry (Luyben *et al.*, 1982). In that case, the enzyme activity should be as large as possible after the drying process.

The residual enzyme activity is taken as the focal point in the present study. Starch cylinders with an immobilised enzyme were used as model food. The residual enzyme activity during drying is the quality indicator. An enzyme is chosen which has both positive and negative properties for food industry: catalase. Catalase is applied in food industry e.g. to remove residues of H<sub>2</sub>O<sub>2</sub> from products (Aebi, 1983), in cold sterilisation of milk (Fox and Grufferty, 1991), and as antioxidant (Lee *et al.*, 1997). The major negative characteristic of catalase is its responsibility for colouring and loss of nutrients in vegetables and other food (Kmieciak and Lisiewska, 2000).

The second requirement is a model that describes quality loss with use of the quality indicator. In drying processes, temperature, moisture content and drying time influence the final product quality (Jayaraman and Das Gupta, 1995; Aguilera *et al.*, 1975). So, the behaviour of enzyme inactivation as function of temperature and moisture content needs to be established. In the field of enzymatic research, lots of information is present about thermal inactivation of enzymes in aqueous environments. Not much is known about the enzyme activity in non-aqueous environments. Only in the 80's some models of enzyme activity as function of moisture content and temperature in drying have been developed (Liou *et al.*, 1985; Luyben *et al.*, 1982; Daemen, 1984; Mishkin *et al.*, 1983). All these models are based on first order reaction kinetics. In recent years thermal inactivation of enzymes has also been described in other than first order reaction kinetics (Aymard and Belarbi, 2000; Polakovič and Vrábek, 1996). The role of water in these reactions has never been elucidated. Moreover, experimental literature data cannot be extrapolated to our situation. This means that for the current quality indicator an appropriate quality model needs to be derived from experiments.

The third prerequisite for control is a model for the evolution of the quality indicator inside the material during drying. For this purpose the quality model needs to be combined with a

drying model describing the moisture content and temperature as a function of location and time. In the past this has been done for micro organisms, enzymes, nutrients, and browning. In all these cases an average quality indicator is considered. The drying models vary from empirical and surface response models to diffusion models (Kamiński *et al.*, 1989; Madamba, 1997; Strumiłło *et al.*, 1994; Van Boxtel and Knol, 1996; Liou *et al.*, 1985; Villota and Karel, 1980; Uddin *et al.*, 2000; Mishkin *et al.*, 1984; Aguilera *et al.*, 1975; Langrish *et al.*, 1997). In *Chapter 4.1*, a new microscopic drying model has been developed: the diffusion-sorption drying model. This model resulted in better and more reliable predictions of drying curves than other drying models known from literature. Its superior features, such as the ability to obtain its parameters from independent experiments and the uniqueness and accuracy of the parameter estimates, is supposed to give the diffusion-sorption model the most reliable prediction of gradients inside the material.

Until now, the modelling and control of quality during drying has always been based on average conditions of the quality indicators. In *Chapter 2* and *3*, the need to consider spatial distribution is illustrated by simulation study. These simulations need to be founded on experimental evidence. The purpose of this chapter is threefold:

1. showing experimentally the existence of QIPs in the material during and after drying.
2. showing experimentally the influence of air conditions on QIPs.
3. predicting profiles of quality indicator during drying based on an independent quality model interacting with the diffusion-sorption drying model.

## **Modelling enzyme inactivation during drying**

### **Mechanisms involved in enzyme inactivation**

#### ***Influence of temperature on enzyme inactivation***

Enzymes are denaturated by heat. The three dimensional structure of the enzyme protein, which is responsible for its biological activity, alters with temperature, leading to loss of enzyme activity (Liou *et al.*, 1985). A large number of factors influence the effect of heat treatment on enzymes, like the level of temperature, rate of temperature rise, the duration of the heat treatment, the moisture content during the heat treatment and environmental conditions (Tumerman, 1974). In spite of the complexity, a two-reaction step model is often satisfactory to describe the kinetics of thermal inactivation (Polakovič and Vrábel, 1996).

### ***Influence of moisture content on enzyme inactivation***

Dehydrated enzymes are much more thermostable than the same enzymes in solution. This has been reported for instance for  $\alpha$ -amylase,  $\beta$ -lactoglobuline and peroxidase (Van Loey, 1996; Meerdink and van 't Riet, 1991; Yamamoto and Sano, 1992; Hendrickx *et al.*, 1992). It is clear that water has a fundamental role in the thermal inactivation of proteins, but its exact role in the inactivation mechanism of a dried enzyme is not known (Saraiva *et al.*, 1996). Its role in quality decay kinetics in foods has been an important subject of discussion and several hypothesis on how water content and molecular mobility affect the chemical/biochemical reactions involved have been proposed (Frías and Oliveira, 2001). The dual effect of water in enzymatic systems may explain the increase in thermo stability at lower moisture contents (Van Loey, 1996; Hendrickx *et al.*, 1992; Saraiva *et al.*, 1996; Tumerman, 1974):

- 1) Some water is essential for acquisition and maintenance of the enzymes' catalytically active conformation, since water participates in all noncovalent interactions.
- 2) Water is required for most enzyme inactivation processes, in particular those of thermal inactivation: water can be a reactant; water molecules provide competitive hydrogen binding possibilities; water acts as plasticiser of the protein conformation by providing alternative hydrogen bond donors and acceptor for peptide groups; and water acts as a lubricant during the partial unfolding of the protein molecule.

Whatever the mechanisms of enzyme thermo stabilisation at low water contents, it is obvious that the increase in thermal stability has to be considered during the experimental verification of the quality profiles.

### **Model of enzyme inactivation as function of moisture content and temperature**

During drying the increasing temperature inactivates the enzyme. However, the decreasing water content increases the thermostability. In literature, some models can be found which incorporate the influence of moisture content in the thermal inactivation models (Liou *et al.*, 1985; Yamamoto and Sano, 1992; Luyben *et al.*, 1982; Wijlhuizen *et al.*, 1979; Daemen, 1984). None of these relations are based on fundamental insight into enzyme inactivation mechanisms at different moisture contents (Meerdink and van 't Riet, 1991).

General descriptions of enzyme inactivation can be found in several papers: first order in for example Van Loey (1996), biphasic in Hendrickx *et al.* (1992) and fractional conversion in Van den Broeck *et al.* (1999). Analysis of literature data on catalase inactivation by

temperature or by drying (Luyben *et al.*, 1982; Sapers and Nickerson, 1962; Lee *et al.*, 1997) suggests that its inactivation can be first order, biphasic or first order with a rest activity (which is the same as fractional conversion).

In the present work catalase was immobilised in starch cylinders. Due to the immobilisation, it might be possible that a part of the enzymes retains its activity. Our experiments with catalase always show a time invariant rest activity  $E_\infty$ . This means that both the first order model and the biphasic model are not applicable, since in both models the activity  $E_\infty$  has to be zero. Therefore, the fractional conversion model for enzyme inactivation is most appropriate:

$$\frac{dE}{dt} = -k_e \cdot (E - E_\infty) \quad (5.1)$$

with  $k_e$  the inactivation constant. Furthermore it is assumed that no partial inactivation can take place: an enzyme either becomes inactive or stays active. Moreover, no renaturation is assumed, since our experiments gave no evidence to incorporate it.

The fractional conversion model has never been used for drying, only for thermal inactivation (e.g. Martins and Silva, 2003) and thermal inactivation in combination with pressure-induced inactivation (e.g., Van den Broeck *et al.* (1999)). Therefore relations for  $k_e$  and  $E_\infty$  are to be determined experimentally. Since the role of water in the mechanisms of catalase inactivation is not clear, we decided to use simple models. Nevertheless, it should be stressed that more reliable information can be obtained when an understanding of the reaction pathways is achieved.

Based on the described mechanisms involved in enzyme inactivation (former section), it may be expected that  $E_\infty$  is a function of both temperature and moisture content. A higher temperature as well as a higher moisture content will result in lower final enzyme concentration. For  $E_\infty$  no relations are available in literature. The simplest linear model to incorporate both effects is:

$$\frac{E_\infty}{E_0} = a + b \cdot X + c \cdot T \quad (5.2)$$

with  $E_0$  the initial activity,  $X$  the starch moisture content and  $T$  the starch temperature;  $a$ ,  $b$  and  $c$  empirical parameters.

How inactivation constant  $k_e$  depends on  $X$  and  $T$  has only been documented for the first order model. Since similar influences are expected for the fractional conversion model, similar relations can be used. The simplest relation found in literature is used here (Adamiec *et al.*, 1995):

$$k_e = \exp\left(d + \frac{e}{X} + f \cdot T\right) \quad (5.3)$$

This empirical relation adds three more parameters to the model:  $d$ ,  $e$  and  $f$ .

### **Drying model**

In drying processes, two mass transfer resistances control the removal of moisture from the material: diffusion, controlling the transfer of moisture inside the material and convection, controlling the transfer of moisture from the surface of the material to the air.

Many researchers have tried to explain the reason for the reduced diffusion at low moisture contents. They assume that the diffusion coefficient decreases with reducing moisture content, due to the increase of energy requirement as drying progresses. As moisture content reduces the water molecules are more firmly bound to the material and more energy is required to remove the sorbed water molecules (Xiong *et al.*, 1991; Van den Berg, 1981; Wang and Brennan, 1992). In the diffusion-sorption model three postulations are used for the development of this new microscopic drying model. The first postulation is that different classes of water exist in biological material: bound and free water. Secondly, it is assumed that only free water molecules are diffusing. So the driving force for diffusion is the gradient in free moisture content. Finally, the decrease of the drying rate at low moisture content is caused by the decreasing availability of free water molecules (*Chapter 4.1*).

The diffusion-sorption model has been calibrated using experiments in such a way that the various effects have been determined independently. Experiments with external limitations (constant rate period) were used for the estimation of the external mass transfer coefficient  $k$ . Experiments with diffusion limitation were used for the estimation of parameters characterising the transfer of moisture inside the material. The unknown parameters in the

model for the conversion between bound and free have been obtained from the GAB sorption isotherm, which was determined in independent experiments (*Chapter 4.2 and 4.3*).

After the calibration of the model with 7 drying experiments, 11 other experiments were used to validate the model. The parameters obtained from the calibration have been used with high accuracy in the validation. The diffusion-sorption model exhibits an improvement of about 15% with respect to constant diffusion coefficient model. It even predicts the measured drying curve better than models with more parameters. Clearly, additional physical knowledge, in the form of the sorption isotherm, not only contributes to a better understanding, but also to a better agreement with the measurements.

## **Location dependent catalase activity analysis in starch cylinders during drying: material and methods**

### ***Material***

The starch cylinders with immobilised catalase were prepared, by manually mixing native potato starch (Perfectamyl D6, AVEBE) with 0.05 M phosphate buffer (pH=7) containing catalase (EC 1.11.1.6, Sigma C-40) in a mass ratio 1.5:1 to a homogeneous paste. The paste was extruded to cylinders with the desired diameter (3 or 5 mm) and length (>10 times diameter). During preparation the starch cylinders were kept on ice. Until use they were stored in a sealed glass in a refrigerator (4°C). The average initial moisture content was 0.97 kg per kg dry basis.

### ***Moisture content***

The moisture content of equilibrated samples was determined gravimetrically, by drying in a conventional oven at 103°C and atmospheric pressure, until equilibrium was reached ( $\pm 1$  mg/successive weighing). The moisture content of all samples was measured in triplicate.

### ***Catalase activity measurement, sample preparation and enzyme activity analysis***

The enzymatic decomposition of hydrogen peroxide by catalase was used to determine the catalase concentration. The decomposition of  $H_2O_2$  can be followed directly with a spectrophotometer by the decrease of absorbance at 240 nm:  $A_{240}$ . The assay was carried out

in 1 ml quartz cuvettes with magnetic stirrer, at 20°C and pH=7. The  $A_{240}$  was measured every 0.2 [s]. The used concentration  $H_2O_2$  was relatively low (0.01 M), due to the rapid inactivation of catalase at high  $H_2O_2$  concentration. Moreover, to avoid a rapid decrease in the initial rate of the reaction and the formation of oxygen bubbles, the assay should be carried out at this relatively low concentration (Aebi, 1983). The substrate solution was always freshly prepared. Only the  $A_{240}$  values during the first 60 [s] were used in the analysis, since after one minute or less the rate began to decrease considerably (Maehly and Chance, 1954). Moreover, for a proper analysis of catalase activity, the values of  $\Delta A_{240}$  in 15 [s] should be between 0.02 and 0.1 (Aebi, 1983). Since the assay is very sensitive to inaccuracies, the catalase activity in each sample was determined in triplicate.

The starch cylinders with immobilised catalase were resuspended in phosphate buffer (pH=7). After cold centrifuging the suspensions for 20 minutes at 2500 rpm and 4°C, the supernatant was used for the enzymatic analysis. The supernatants were diluted when necessary with phosphate buffer, so that  $0.02 < \Delta A_{240} < 0.1$  during the first 15 [s].

In contrast to reactions proceeding at substrate saturation (0 order), the enzymatic decomposition of  $H_2O_2$  by catalase is a first order reaction, the rate of which is always proportional to the peroxide concentration (Aebi, 1983):

$$\frac{d[S]}{dt} = -k_1 \cdot [S] \quad (5.4)$$

where  $S$  is substrate ( $H_2O_2$ ) concentration,  $k_1$  is the first order inactivation constant [ $s^{-1}$ ]. The absorbance is proportional to the substrate concentration according to Lambert Beer 's law (Maehly and Chance, 1954). Linear regression was applied to estimate  $k_1$  from the slope of  $\ln[S]$  against time (for  $t < 60$  s and  $0.02 < \Delta A_{240} < 0.1$ ). The inactivation constant was then corrected for the reaction volume, dilution factor, the sample weight and dry matter content.

This first order reaction constant  $k_1$  was used as a direct measure of catalase concentration, since it shows an accurate proportionality to the catalase concentration:  $k_1 = k_0 \cdot [E]$ , where  $k_0$  is a characteristic of the applied catalase (Aebi, 1983). The same catalase was used in all experiments.

### *Catalase inactivation experiments*

The enzyme activity was determined at different moisture contents and different temperatures as function of time. In order to obtain material with different moisture content, the starch cylinders with immobilised enzyme were placed in sorbostats with saturated salt solutions at 4°C (Table 5.1), assuming that no inactivation of the enzyme took place at this low temperature. In each sorbostat a small amount of crystal thymol to prevent the growth of micro organisms was present (Wolf *et al.*, 1985). The samples were equilibrated for a few weeks at the specified relative humidity. When equilibrium was reached ( $\pm 2$  mg/day), one vial was removed from the sorbostat for the determination of the corresponding moisture content (see Table 5.1).

The vials with the samples with defined moisture content were tightly crimped. This step was performed within 5 [s], to avoid changes in moisture content.

**Table 5.1.** Experiments with catalase for establishing (x) and validating (o) the enzyme inactivation model at different temperatures and moisture contents ( $X$ ), obtained in sorbostats with oversaturated salt solutions (Greenspan, 1977).

	Solution (with corr. $RH$ at 4°C)	Moisture content [kg.kg <sub>dm</sub> <sup>-1</sup> ]	Temperature [°C]			
			40	50	60	70
LiCl	( $RH=11.2\%$ )	0.110	x	x	x	x
MgCl <sub>2</sub>	( $RH=33.6\%$ )	0.173	x	o	o	x
Mg(NO <sub>3</sub> ) <sub>2</sub>	( $RH=58.9\%$ )	0.242	x	o	o	x
NaCl	( $RH=75.7\%$ )	0.301	x	o	o	o
KNO <sub>3</sub>	( $RH=96.3\%$ )	0.814	x	o	gel	gel

Thermal degradation experiments were performed at different temperatures in thermostatic baths at 40, 50, 60 and 70°C. The closed vials with defined moisture content were placed in the bath. At ten different pre-defined sampling times, one vial was removed from the bath and put on ice to stop the enzyme inactivation. Zero time samples were taken 2 minutes after immersion. The samples turned into a gel at 60 en 70°C and 0.814 [kg.kg<sub>dm</sub><sup>-1</sup>] moisture content (see Table 5.1). Those samples were not useful anymore. The catalase activity was determined in each sample in threefold. The experiments were divided into two groups: ten were used to establish the required relations and the other eight for validation of the inactivation model (see Table 5.1).

### ***Location dependent catalase activity during drying***

After the independent inactivation experiments, the inactivation during drying had to be measured. Experiments at four different drying conditions were performed: one on 5 mm starch cylinders (at air temperature of  $T=60^{\circ}\text{C}$  and relative humidity of  $RH=5\%$ ) and three on 3 mm cylinders at air conditions of ( $T=45^{\circ}\text{C}$ ;  $RH=5\%$ ), ( $T=60^{\circ}\text{C}$ ;  $RH=5\%$ ) and ( $T=60^{\circ}\text{C}$ ;  $RH=40\%$ ). In each drying curve, apart from the start  $t_0$ , four sampling times were selected (see e.g. Figure 5.5). At all temperatures and relative humidities four drying experiments were performed. In order to obtain a picture of the inactivation as function of drying duration, the first experiment was stopped at  $t_1$ , the second experiment was stopped at  $t_2$ , etc. At the specified time the material was divided into several portions: 6 portions to determine the moisture content; two or four portions to measure average enzyme activity. The remaining material was used to investigate the spatial distribution of enzyme activity in the cylinders.

To investigate the location dependency of the catalase inactivation a microtome was designed. The microtome consists of a couple of sharp knives inside a hollow cylinder. The starch cylinders were forced through the microtome and hence sliced laterally. This resulted into a division of the starch cylinder into an inner and an outer section. Only a coarse division between the inner and outer material was obtained, in which the mass ratio is about inner:outer = 1:1. For the cylinders with 3 mm diameter, this procedure was only possible at rather moist conditions, where the material did not crumble too much.

## **Results and discussion**

### **Quality profiles during drying**

The first question to be answered was: can the expected QIPs be confirmed experimentally? The results obtained with the 5 mm sample clearly demonstrate the spatial distribution of enzyme activity during drying: the measured activities in the outer part are usually larger than the average, which is in turn higher than the inner part (Figure 5.1). In the outer area the water content is low, causing retention of enzyme activity. The average activity is not always between the inner and outer activity, since it is measured separately. This is an indication for the low experimental accuracy. The measurements of the 3 mm samples, presented in Table 5.2, also show a higher enzyme activity in the outer than in the inner part. The largest differences in activity are found in the 5 mm samples. This is not surprising. If a similar

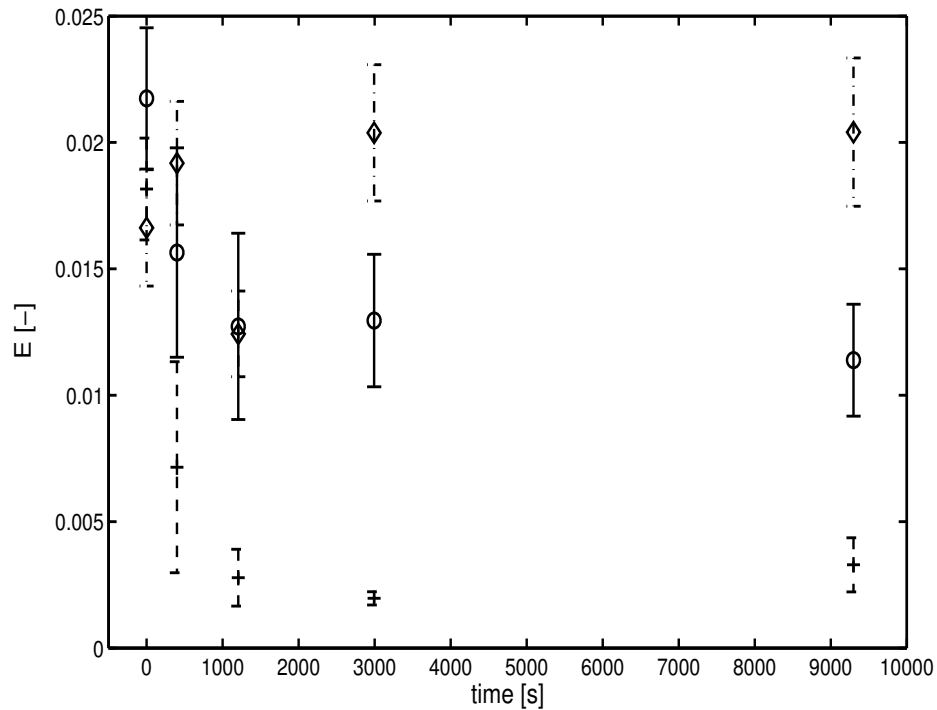


**Figure 5.1.** Enzyme activity  $E$  [-] as function of time during drying of 5 mm starch cylinders at  $T= 60^{\circ}\text{C}$  and  $RH= 5\%$ : average (o and continuous errorbar), inner (+ and --- errorbar) and outer ( $\diamond$  and -.-. errorbar) enzyme activity.

moisture profile in both samples is assumed, a larger distance from which the drying profile penetrates, will result in a larger enzyme concentration difference.

The second question was about the influence of air conditions on QIPs. All presented experiments are performed at  $60^{\circ}\text{C}$  in order to show only the influence of air humidity on inactivation.

Looking at the 5% air humidity data of Table 5.2, a clear difference in activity between inner and outer area can be seen: the enzyme activity of the outer part is hardly changing, while in the inner part it decreases considerably. Under the dry conditions at the surface, inactivation of catalase hardly takes place. Unfortunately the location dependent sampling for longer

**Table 5.2.** Inner and outer enzyme activity  $E$  [-] in 3 mm samples as a function of time during drying experiment at  $T= 60^{\circ}\text{C}$  and  $RH= 5$  and 40%, respectively.

Time [s]	$RH = 5\%$		Time [s]	$RH = 40\%$	
	$E_{in}$ [-]	$E_{out}$ [-]		$E_{in}$ [-]	$E_{out}$ [-]
0	0.0085 ( $\pm 12\%$ )	0.0112 ( $\pm 18\%$ )	0	0.0186 ( $\pm 21\%$ )	0.0196 ( $\pm 13\%$ )
300	0.0059 ( $\pm 20\%$ )	0.0068 ( $\pm 51\%$ )	200	0.0190 ( $\pm 16\%$ )	0.0219 ( $\pm 21\%$ )
800	0.0045 ( $\pm 11\%$ )	0.0106 ( $\pm 15\%$ )	1000	0.0080 ( $\pm 49\%$ )	0.0152 ( $\pm 31\%$ )
			2000	0.0024 ( $\pm 8\%$ )	0.0022 ( $\pm 21\%$ )

drying duration was impossible due to the crumbling of the starch in the microtome. At an air humidity of 40%, Table 5.2 shows not only a decrease in enzyme activity in the centre, but also near the surface. Higher relative air humidity causes a smaller moisture gradient in the cylinder, resulting in a more flat quality indicator profile.

So the experiments (Table 5.2) clearly illustrate the influence of air humidity on the remaining enzyme activity profiles as an indicator for quality. This supports the simulated results presented in *Chapter 2* and *3*.

The influence of air conditions on the average value of the quality indicator is experimentally demonstrated several times (Yamamoto and Sano, 1992; Meerdink and van 't Riet, 1991; Frías and Oliveira, 2001). However, the experimental demonstration of QIPs in the material as well as the influence of air conditions on the course of the gradients have not been presented before.

### **Enzyme inactivation as function of moisture content and temperature**

With the experimental proof that enzyme activity during drying is depending on its location in the starch cylinder, a location dependent model for water content, temperature and enzyme inactivation needs to be developed. The first step is to establish an independent model that relates the enzyme activity with temperature and moisture content. Therefore ten inactivation experiments were performed to establish the required relations. An example is shown in Figure 5.2. The figure shows that the experimental error is high. The average deviation is 8-21%. These high variations are mainly caused by the sensitivity of the catalase assay to experimental error. The liberation of oxygen can disturb the analysis of catalase activity. Moreover, catalase is inactivated in dilute solutions. The region in which the absorbance is measured, 240 nm, is also very sensitive for turbidity of the samples. Comparable variations in experimental catalase activity are found in blood (Aebi, 1983), pork (Lee *et al.*, 1997) and milk (Griffiths, 1986).

The experimental data clearly demonstrate the existence of a time invariant final activity  $E_{\infty}$ . For each inactivation experiment an individual set of initial activity  $E_0$ , final activity  $E_{\infty}$  and reaction constant  $k_e$  has been determined. The measured activity is fitted with the fractional conversion model:

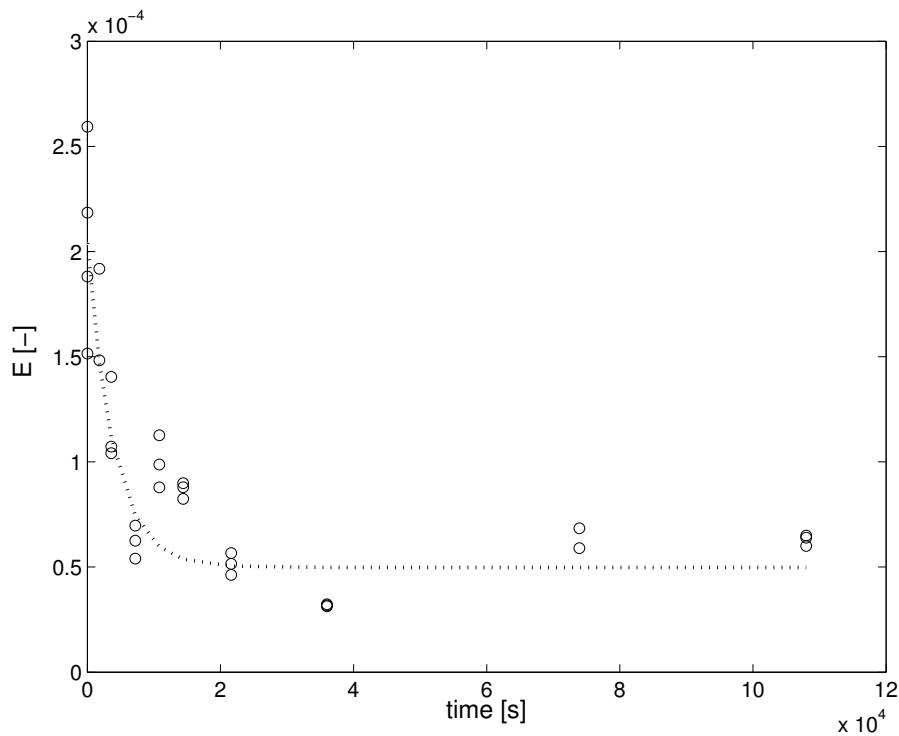


**Figure 5.2.** Experimental (o) catalase activity at 40°C and  $X = 0.814 \text{ [kg.kg}^{-1}\text{]}$  and predicted (--) catalase activity with fractional conversion model.

$$E = E_{\infty} + (E_0 - E_{\infty}) \exp(-k_e \cdot t) \quad (5.5)$$

by searching for the parameters minimising the following sum of squares  $SSQ$ :

$$SSQ = \sum_i (E_{\text{exp},i} - E_{\text{mod},i})^2 \quad (5.6)$$

Provided the model describes the data sufficiently, the estimated values for  $E_0$  are more reliable than the average of measured replications of initial concentration, because observed concentrations at different time intervals have some information about the initial concentration. Also, in this way, the experimental error in  $E_0$  is taken into account in the same way as in the other data points (Arabshahi and Lund, 1985; Van Boekel, 1996).

The confidence intervals of the estimated  $k_e$  of the individual experiments are large (>100% in some cases). These must be due to the high experimental error in the catalase assay. The  $E_{\infty}$  is estimated with higher accuracy (around 30%). The possible inhomogeneity of the samples,

due to the manual mixing, can also contribute to the experimental error. Large confidence intervals of the inactivation constant  $k_e$  are not uncommon in enzyme research (Van Boekel, 1996; Serris and Biliaderis, 2001; Soliva-Fortuny *et al.*, 2001).

The established values for  $k_e$  and  $E_\infty$  were used to estimate the parameters in the corresponding relations 5.2 and 5.3 by minimising the corresponding  $SSQ$ 's. Because the same catalase and the same starch has been used in all experiments one set of relations with temperature and moisture content can be established. Relative rest activity  $E/E_0$  is described by the simple linear model (equation 5.2). The fitting procedure for the ten experiments shown in Table 5.1 results in significant but not very accurate parameters:  $a = 3.74 \pm 1.5$ ;  $b = -0.57 \pm 0.33$ ; and  $c = -0.0097 \pm 0.0046$  (95% confidence intervals). The negative  $b$ -value indicates a decrease in rest activity at higher moisture contents. The negative  $c$ -value corresponds with a decrease in rest activity at higher temperatures. Both trends are in agreement with the theory in the modelling section: inactivation of enzymes is faster at higher temperature and moisture content.

Also for the inactivation constant  $k_e$  a dependency on moisture content and temperature is expected. The individual experimental values were therefore compared with the simplest model found in literature (equation 5.3), resulting in significant, but not very accurate parameters:  $d = -33 \pm 13$ ;  $e = -0.20 \pm 0.11$ ; and  $f = 0.08 \pm 0.04$  (95% confidence intervals). The negative  $e$ -value corresponds with faster deactivation at higher moisture contents. The positive  $f$ -value also shows a faster deactivation at higher temperatures. This trend is in agreement with the one found for first order kinetics in literature (Meerdink and van 't Riet, 1991; Villota and Karel, 1980; Yamamoto and Sano, 1992).

In Figure 5.2 the model prediction of the catalase activity is shown, calculated with the parameter estimates of  $a$ - $f$ . To our knowledge, this is the first time that a fractional conversion model is applied for enzyme inactivation during drying. The activation after very long time  $E_\infty$  simply appears from the experiments and hence gives a better description than first order. The figure shows that the fractional conversion model with the simplest relations for  $E_\infty$  and  $k_e$  gives satisfactory model results. It makes no sense to apply a more sophisticated model, due to the poor experimental accuracy.

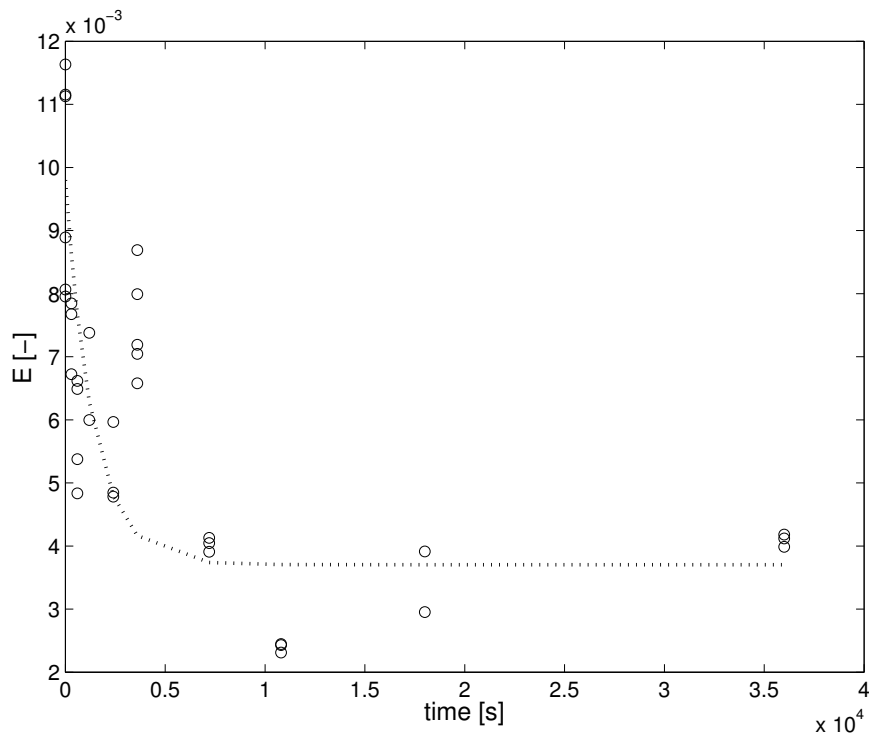


**Figure 5.3.** Validation of enzyme inactivation model at  $T=60^{\circ}\text{C}$  and  $X=0.242$  [ $\text{kg}\cdot\text{kg}^{-1}$ ] (o experimental and -- predicted enzyme activity).

The other 8 experiments have been used to validate the inactivation model. Figure 5.3 shows a representative result. The predicted enzyme activity follows the general trend of the measured activities. In general the deviation between prediction and experiment is within the experimental accuracy of 20%. However, at some points the prediction deviates more than 50%. This is true for all 8 validation experiments. The relative high deviations can also be found in literature (Meerdink and van 't Riet, 1991; Martins and Silva, 2003; Soliva-Fortuny *et al.*, 2001).

### Enzyme inactivation during drying

The third prerequisite for the control of quality is experimental support for the quality indicator model inside the material during drying. The quality indicator model itself has been developed in the previous section. This model is incorporated in the diffusion-sorption model as described in *Chapter 4.1*. Since the experimental and analysing procedure are very elaborate, only four drying conditions have been performed. As an example Figure 5.4 compares the experimental points of the drying curve of the 5 mm starch cylinders at  $T =$

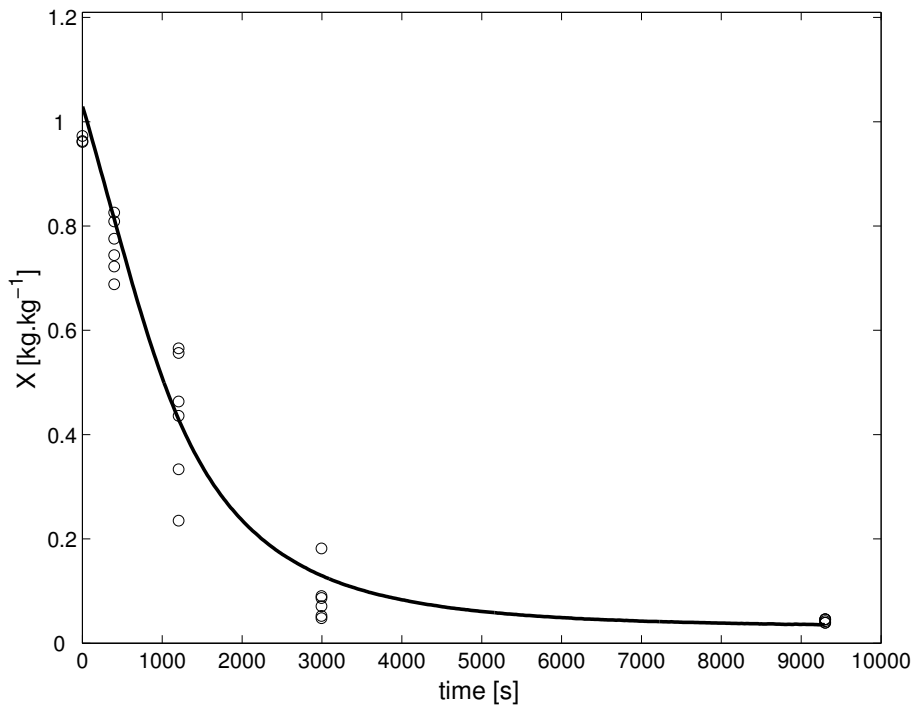


**Figure 5.4.** Comparison of experimental (o) with predicted (-) moisture content of 5 mm starch cylinders as a function of time at  $T=60^{\circ}\text{C}$  and  $RH=5\%$ .

$60^{\circ}\text{C}$  and  $RH=5\%$  with the diffusion-sorption model. As can be seen excellent agreement exists. The three experiments with the 3 mm starch cylinders act qualitatively similar to the experiment with the 5 mm cylinders.

In spite of a very good prediction of the drying curve, the enzyme activity or quality model does not predict the measurements so well (see Figure 5.5). Rather, the individual measurements do not follow the detailed prediction of the model, which is based on dozens of measurements. The reasons for this deviation are:

1. the inaccuracy of the measured enzyme activity
2. the lack of enzyme inactivation data at high moisture content and high temperature, where the samples turned into a gel
3. the inaccuracy of the parameters of enzyme inactivation (quality model)
4. the lack of drying data in the 3 mm samples at more dry conditions (later in time), due to crumbling of the starch cylinders.

Yet, the quality model does describe comparable QIPs as experimentally demonstrated: the enzyme is barely inactivated at the surface and more inactivated in the centre of the cylinder.

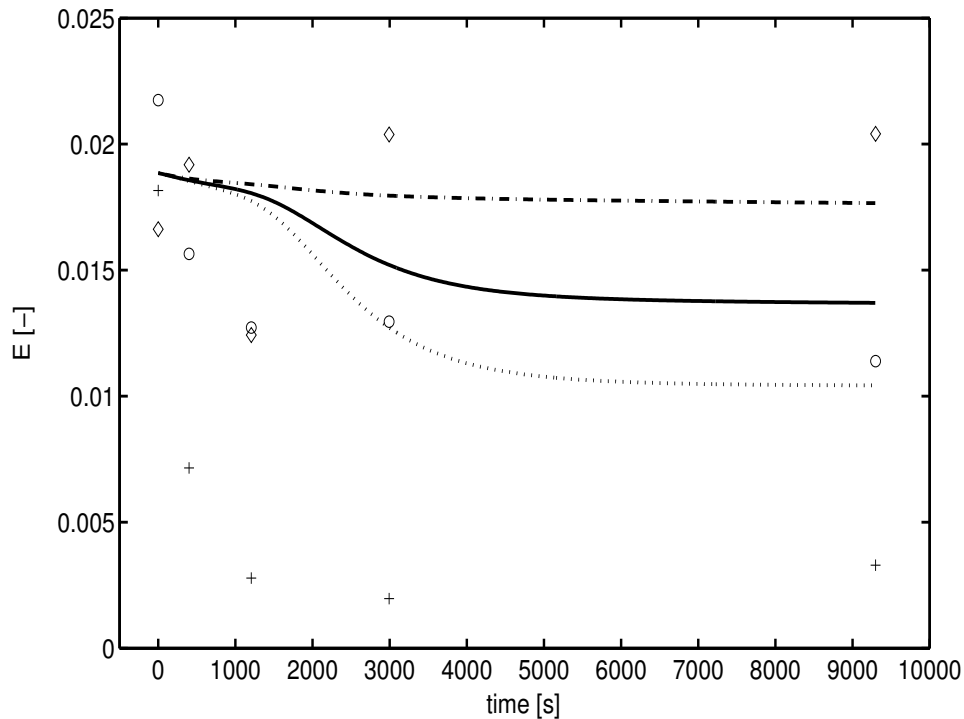


**Figure 5.5.** Comparison of experimental enzyme activity with model prediction as function of time during drying of 5 mm starch cylinders at  $T= 60^{\circ}\text{C}$  and  $RH =5\%$ : average (o and continuous line), inner (+ and ---) and outer ( $\diamond$  and -.-) enzyme activity.

Predicted QIPs are never validated with experiments before. The average quality indicator during drying, on the other hand, is validated in some cases. Similar results are found: good or moderate prediction of the drying curve, but an overestimation or underestimation of the average enzyme activity (Liou *et al.*, 1985; Villota and Karel, 1980; Uddin *et al.*, 2000; Meerdink and van 't Riet, 1991). In Liou *et al.* (1985) and Villota and Karel (1980), it is illustrated that a wrong prediction of the temperature during the drying process caused the deviation in product quality. Meerdink and van 't Riet (1991) demonstrated the sensitivity to variations in temperature. This might also be a possible reason for the underestimation of catalase activity in this study, since the influence of temperature on catalase inactivation is larger than the influence of moisture content. However, the product temperature has not been measured.

Nevertheless, quality profiles during drying can be predicted. The quality model was established independently and was combined with the diffusion-sorption model. The

predicted quality profiles can now be used to control the drying process in order to obtain the required quality at each location in the food.

## **Conclusions**

Quality of food and agricultural materials may degrade during drying, due to temperature and moisture content changes. The control or optimisation of quality is therefore desired. Good quality control is based on the quality indicator profiles (QIPs) inside the material during the drying process. A model food composed of starch cylinders incorporating the enzyme catalase has been developed. The residual enzyme activity has been taken as the quality indicator, to verify experimentally its evolution. Although the experimental results were sensitive to experimental error (8-21%), significant differences between different treatments have been found. With this model food it has been shown that the three requirements to predict QIPs during drying can be met: they were confirmed in experiments, they appeared to be influenced by the air conditions and they could be modelled.

The existence of QIPs has been demonstrated experimentally during drying. The measured activities in the outer part were usually larger than the average, which was in turn higher than the inner part. During drying water is transferred from the surface of the sample to the ambient air, so the outer part is expected to be dryer than the inner part, preventing the enzyme to be inactivated.

Next, it has been demonstrated experimentally that air conditions influence the profiles of the quality indicator. At a relative humidity of 5%, only the enzyme activity in the inner part decreased, while at a relative humidity of 40% also the outer part inactivated. Unfortunately the location dependent sampling later on in the drying curve was impossible due to the crumbling of the starch in the microtome.

In order to predict QIPs during drying, a model of the quality indicator has been developed, based on independent inactivation experiments. During the inactivation experiments always a time invariant rest activity  $E_{\infty}$  has been observed. Therefore inactivation of catalase in starch was modelled with a fractional conversion model. The experimentally determined rest activity and the reaction constant were both dependent on temperature and moisture content. These

relations make catalase suitable as a measure for the quality indicator inside the material during drying.

The independent quality model is combined with the diffusion-sorption drying model, to predict the QIPs during drying. The diffusion-sorption model described the drying curve very well. Since this model provides moisture and temperature distribution profiles, QIPs can be calculated with the moisture and temperature dependency. However, the resolution of the measurements was insufficient to follow the detailed prediction of the model. The major reasons for this deviation are the inaccuracy of the measured enzyme activity, the absence of enzyme inactivation data at high moisture content and high temperature and the lack of data at more dry conditions (later in time) during drying, due to crumbling of the starch cylinders. Despite these deviations between model and experimental enzyme activity, the QIPs are comparable.

So, profiles of quality indicators in food during drying can be predicted. The predicted profiles can subsequently be applied in product and process design, improving critical quality aspects. It is therefore recommended to implement a spatial distribution not only for the control of quality of drying, but for all processes in biotechnology, agricultural and food engineering, where gradients in moisture or temperature are to be expected.

## **Acknowledgements**

We would like to thank Hennie Boshoven for the development of the microtome. We would also like to thank AVEBE, Veendam The Netherlands for their free supply of native potato starch, perfectamyl D6.

## References

- Adamiec, J., W. Kamiński, A.S. Markowski and C. Strumiłło. Drying of biotechnological products. p. 775-808. In: Mujumdar, A.S. (Ed.). *Handbook of industrial drying. Volume II*. New York, etc.: Marcel Dekker, Inc., 1995. 743-1423 p.
- Aebi, H.E. Catalase. Hydrogen-peroxide: hydrogen-peroxide oxidoreductase E.C. 1.11.1.6. p. 273-286. In: Bergmeijer, H.U., J. Bergmeijer and M. Grassl. *Methods of enzymatic analysis. 3<sup>rd</sup> Edition. Vol. 3: Enzymes 1: oxidoreductases, transferases*. Weinheim, etc: Chemie, 1983. vol 1-12.
- Aguilera, J.M., J. Chirife, J.M. Flink and M. Karel. Computer simulation of non-enzymatic browning during potato dehydration. *Lebensmittel-Wissenschaft und –Technologie*, vol. 8, 1975, no. 3, p. 128-133.
- Arabshahi, A. and D.B. Lund. Considerations in calculating kinetic parameters from experimental data. *Journal of Food Process Engineering*, vol. 7, 1985, p. 239-251.
- Aymard, C. and A. Belarbi. Kinetics of thermal deactivation of enzymes: a simple three parameters phenomenological model can describe the decay of enzyme activity, irrespectively of the mechanism. *Enzyme and Microbial Technology*, vol. 27, 2000, no. 8, p. 612-618.
- Banga, J.R. and R.P. Singh. Optimization of air drying of foods. *Journal of Food Engineering*, vol. 23, 1994, p. 189-211.
- Daemen, A.L.H. The destruction of enzymes and bacteria during the spray-drying of milk and whey. 4. A comparison of theoretical computed results concerning the destruction of phosphatase with those obtained experimentally. *Netherlands Milk and Dairy Journal*, vol. 38, 1984, p. 55-70.
- Fox, P.F. and M.B. Grufferty. Exogenous enzymes in dairy technology. p. 219-270. In: Fox, P.F. (Ed.). *Food enzymology. Vol. 1*. London and New York: Elsevier Applied Science, 1991. 636 p.

Frías, J.M. and J.C. Oliveira. Kinetic models of ascorbic acid thermal degradation during hot air drying of maltodextrin solutions. *Journal of Food Engineering*, vol. 47, 2001, no. 4, p. 255-262.

Greenspan, L. Humidity fixed points of binary saturated aqueous solutions. *Journal of Research of the National Bureau of Standards – A. Physics and Chemistry*, vol. 81A, 1977, no. 1, p. 89-96.

Griffiths, M.W. Use of milk enzymes as indices of heat treatment. *Journal of Food Protection*, vol. 49, 1986, no. 9, p. 696-705.

Hendrickx, M., J. Saraiva, J. Lyssens, J. Oliveira and P. Tobback. The influence of water activity on thermal stability of horseradish peroxidase. *International Journal of Food Science and Technology*, vol. 27, 1992, p. 33-40.

Jayaraman, K.S. and D.K. Das Gupta. Drying of fruits and vegetables. p. 643-691. In: Mujumdar, A.S. (Ed.). *Handbook of industrial drying. Volume 1*. New York, etc.: Marcel Dekker, Inc., 1995. 742 p.

Kamiński, W., I. Zbiciński, S. Grabowski and C. Strumiłło. Multiobjective optimization of drying process. *Drying Technology*, vol. 7, 1989, no. 1, p. 1-16.

Kmiecik, W. and Z. Lisiewska. Studies on the morphological traits and chemical composition of the fruit of six tomato cultivars recommended as raw material for freezing. *Nahrung Food*, vol. 44, 2000, no. 5, p. 349-353.

Langrish, T.A.G., A.S. Brooke, C.L. Davis, H.E. Musch and G.W. Barton. An improved drying schedule for Australian ironbark timber: optimisation and experimental validation. *Drying Technology*, vol. 15, 1997, no. 1, p. 47-70.

Lee, S.K., L. Mei and E.A. Decker. Influence of sodium chloride on antioxidant enzyme activity and lipid oxidation in frozen ground pork. *Meat Science*, vol. 46, 1997, no. 4, p. 349-355.

- Liou, J.K., K.Ch.A.M. Luyben and S. Bruin. A simplified calculation method applied to enzyme inactivation during drying. *Biotechnology and Bioengineering*, vol. 27, 1985, p. 109-116.
- Luyben, K.Ch.A.M, J.K. Liou and S. Bruin. Enzyme degradation during drying. *Biotechnology and Bioengineering*, vol. 24, 1982, p. 533-552.
- Madamba, P.S. Optimization of the drying process: an application to the drying of garlic. *Drying Technology*, vol. 15, 1997, no. 1, p. 117-136.
- Maehly, A.C. and B. Chance. The assay of catalases and peroxidases. p. 357-424. In: Glick, D. (Ed.). *Methods of Biochemical Analysis. Vol. I*. New York, Interscience Publishers, 1954.
- Martins, R.C. and C.L.M. Silva. Kinetics of frozen stored green bean (*Phaseolus vulgaris* L.) quality changes: texture, vitamin C, reducing sugars, and starch. *Journal of Food Science*, vol. 68, 2003, no. 7, p. 2232-2237.
- McMinn, W.A.M. and T.R.A. Magee. Quality and physical structure of a dehydrated starch-based system. *Drying Technology*, vol. 15, 1997, no. 6-8, p. 1961-1971.
- Meerdink, G. and K. van 't Riet. Inactivation of a thermostable  $\alpha$ -amylase during drying. *Journal of Food Engineering*, vol. 14, 1991, p. 83-102.
- Mishkin, M., I. Saguy and M. Karel. Minimizing ascorbic acid loss during air drying with a constraint on enzyme inactivation for a hypothetical foodstuff. *Journal of Food Processing and Preservation*, vol. 7, 1983, p. 193-210.
- Mishkin, M., I. Saguy and M. Karel. Optimization of nutrient retention during processing: ascorbic acid in potato dehydration. *Journal of Food Science*, vol. 49, 1984, p. 1262-1266.
- Pezzutti, A. and G.H. Crapiste. Sorption equilibrium and drying characteristics of garlic. *Journal of Food Engineering*, vol. 31, 1997, p. 113-123.
- Polakovič, M. and P. Vrábel. Analysis of the mechanism and kinetics of thermal inactivation of enzymes: critical assessment of isothermal inactivation experiments. *Process Biochemistry*, vol. 31, 1996, no. 8, p. 787-800.

Sapers, G.M. and J.T.R. Nickerson. Stability of spinach catalase. II. Inactivation by heat. *Journal of Food Science*, vol. 27, 1962, p. 282-286.

Saraiva, J., J.C. Oliveira, M. Hendrickx, F.A.R. Oliveira and P. Tobback. Analysis of the inactivation kinetics of freeze-dried  $\alpha$ -amylase from *Bacillus amyloliquefaciens* at different moisture contents. *Lebensmittel-Wissenschaft und -Technologie*, vol. 29, 1996, no. 3, p. 260-266.

Serris, G.S. and C.G. Biliaderis. Degradation kinetics of beetroot pigment encapsulated in polymeric matrices. *Journal of the Science of Food and Agriculture*, vol. 81, 2001, p. 691-700.

Soliva-Fortuny, R.C., N. Grigelmo-Miguel, I. Odriozola-Serrano, S. Gorinstein and O. Martín-Belloso. Browning evaluation of ready-to-eat apples as affected by modified atmosphere packaging. *Journal of Agricultural and Food Chemistry*, vol. 49, 2001, no. 8, p. 3685-3690.

Strumiłło, Cz. I. Zbiciński and X.D. Liu. Thermal drying of biomaterials with porous carriers. p. 1113-1120. In: Rudolph, V., R.B. Keey and A.S. Mujumdar (Eds.). *Drying '94*. Gold Coast, Australia: Proceedings of the 9th International Drying Symposium (IDS '94), 1994. 1402 p.

Tumerman, L. Denaturation of proteins. p. 292-306. In: Johnson, A.H. and M.S. Peterson (Eds.). *Encyclopaedia of food technology*. Westport : [s.n.], 1974. 993 p.

Uddin, M.S., M.N.A. Hawlader and L.W. Zhou. An accelerated test model for ascorbic acid degradation in kiwifruits during drying. Paper No.20. In: Kerkhof, P.J.A.M., W.J. Coumans and G.D. Mooiweer. *Proceedings of the 12th International Drying Symposium IDS2000*. Amsterdam: Elsevier Science, 2000.

Van Boekel, M.A.J.S. Statistical aspects of kinetic modeling for food science problems. *Journal of Food Science*, vol. 61, 1996, no. 3, p. 477-485, 489.

Van Boxtel, A.J.B. and L. Knol. A preliminary study on strategies for optimal fluid-bed drying. *Drying Technology*, vol. 14, 1996, no. 3&4, p. 481-500.

Van den Berg, C. *Vapour sorption equilibria and other water-starch interactions; a physico-chemical approach*. Wageningen: Wageningen Agricultural University, Section Process Engineering, Department of Food Science, 1981. 186 p. PhD thesis.

Van den Broeck, I., L.R. Ludikhuyze, A.M. Van Loey, C.A. Weemaes and M.E. Hendrickx. Thermal and combined pressure-temperature inactivation of orange pectinesterase: influence of pH and additives. *Journal of Agricultural and Food Chemistry*, vol. 47, 1999, no. 7, p. 2950-2958.

Van Loey, A. *Enzymic time temperature integrators for the quantification of thermal processes in terms of food safety*. Leuven: Katholieke Universiteit Leuven, Faculteit Landbouwkundige en Toegepaste Biologische Wetenschappen, 1996. 159 p. PhD thesis.

Villota, R. and M. Karel. Prediction of ascorbic acid retention during drying. II. Simulation of retention in a model system. *Journal of Food Processing and Preservation*, vol. 4, 1980, p. 139-159.

Wang, N. and J.G. Brennan. Effect of water binding on the drying behaviour of potato. p. 1350-1359. In: Mujumdar, A.S. (ed.). *Drying '92. Vol. I*. Amsterdam, etc.: Elsevier Science Publishers B.V., 1992. 1953 p.

Wijlhuizen, A.E., P.J.A.M. Kerkhof and S. Bruin. Theoretical study of the inactivation of phosphatase during spray drying of skim-milk. *Chemical Engineering Science*, vol. 34, 1979, p. 651-660.

Wolf, W., W.E.L. Spiess and G. Jung. Standardisation of isotherm measurements (cost-project 90 and 90 bis). p. 661-679. In: Simatos, D. and J.L. Multon (Eds.). *Properties of water in foods*. Dordrecht, The Netherlands: Martinus Nijhoff Publishers, 1985. 693 p.

Xiong, X., G. Narsimhan and M.R. Okos. Effect of composition and pore structure on binding energy and effective diffusivity of moisture in porous food. *Journal of Food Engineering*, vol. 15, 1991, p. 187-208.

Yamamoto, S. and Y. Sano. Drying of enzymes: enzyme retention during drying of a single droplet. *Chemical Engineering Science*, vol. 47, 1992, no. 1, p. 177-183.



## Chapter 6

# Optimisation of quality during drying with the diffusion-sorption drying model

New perspectives for optimal control of drying processes

This chapter has been published with minor modifications as:

Quirijns, E.J., L.G. van Willigenburg and A.J.B. van Boxtel. New perspectives for optimal control of drying processes. p. 431-437. In: Biegler, L.T., A. Brambilla and C. Scali (Eds.). *Adchem2000: International Symposium on Advanced Control of Chemical Processes*. Pisa, Italy: IFAC Publications Elsevier Science Ltd, 2001. 1088 p.

## **Abstract**

A new distributed model that describes the drying of individual particles is presented. It considers internal resistances towards mass transfer, controlled by diffusion and sorption, as well as external resistances. The parameters in this model all have a clear physical meaning and interpretation. Using a measure of the product quality, which deteriorates during drying, and a measure for the energy costs of drying, optimal control trajectories are computed for different drying times. The computations are based on a finite-difference approximation of the infinite-dimensional model. The results indicate the feasibility of the model to optimise drying processes of different type as well as the significance of optimising the drying time.

## Nomenclature

$a_w$	water activity	[-]
$C_g$	Guggenheim constant in GAB sorption equation	[-]
$c_{pa}$	heat capacity of air	[J.kg <sup>-1</sup> .K <sup>-1</sup> ]
$c_{p,dm}$	heat capacity of dry material	[J.kg <sup>-1</sup> .K <sup>-1</sup> ]
$c_{pv}$	heat capacity of vapour	[J.kg <sup>-1</sup> .K <sup>-1</sup> ]
$c_{pw}$	heat capacity of water	[J.kg <sup>-1</sup> .K <sup>-1</sup> ]
$c_1$	constant in penalty function (equation 6.42)	[-]
$D$	internal diffusion coefficient of moisture in material	[m <sup>2</sup> .s <sup>-1</sup> ]
$D_0$	parameter in Arrhenius-type relation for diffusion coefficient	[m <sup>2</sup> .s <sup>-1</sup> ]
$E_a$	activation energy for moisture diffusion	[J.mol <sup>-1</sup> ]
$G_a$	air flow into the dryer	[m <sup>3</sup> .s <sup>-1</sup> ]
$h$	external convective heat transfer coefficient	[J.s <sup>-1</sup> .m <sup>-2</sup> .K <sup>-1</sup> ]
$h_m$	specific enthalpy of material	[J.kg <sup>-1</sup> ]
$J$	total value of performance index	[fl.kg <sup>-1</sup> .s <sup>-1</sup> ]
$J_D$	cash flow	[fl.kg <sup>-1</sup> .s <sup>-1</sup> ]
$J_{energy}$	energy costs per unit product	[fl.kg <sup>-1</sup> ]
$J_T$	heat flux on surface of material	[J.s <sup>-1</sup> .m <sup>-2</sup> ]
$J_X$	value of penalty function	[fl.kg <sup>-1</sup> .s <sup>-1</sup> ]
$J_{Xs}$	mass flux, on surface of material	[kg.m <sup>-2</sup> .s <sup>-1</sup> ]
$K$	constant in GAB sorption equation	[-]
$K_{eq}$	equilibrium constant in sorption process	[-]
$k$	external convective mass transfer coefficient	[m.s <sup>-1</sup> ]
$k_a$	adsorption rate constant	[s <sup>-1</sup> ]
$k_d$	desorption rate constant	[s <sup>-1</sup> ]
$k_i$	inactivation rate constant of the micro organism	[s <sup>-1</sup> ]
$M_a$	molecular mass of air	[kg.mol <sup>-1</sup> ]
$M_w$	molecular mass of water	[kg.mol <sup>-1</sup> ]
$N$	number of discretisation points	
$N_u$	number of control intervals	
$P_{tot}$	air pressure	[Pa]
$P_{sat}$	saturation vapour pressure	[Pa]
$Q$	residual activity	[-]
$\mathcal{R}$	gas constant	[J.mol <sup>-1</sup> .K <sup>-1</sup> ]

$R$	maximum radius of material	[m]
$r$	radius of material	[m]
$r_B$	conversion rate between bound and free water	[s <sup>-1</sup> ]
$T_a$	air temperature	[°C]
$T_{env}$	temperature environment	[°C]
$T_m$	material temperature	[°C]
$T_{,K}$	absolute temperature	[K]
$t$	time	[s]
$t_f$	final drying time	[s]
$t_r$	reloading time	[s]
$X$	moisture content	[kg <sub>H2O</sub> .kg <sup>-1</sup> <sub>dm</sub> ]
$X_B$	concentration of bound water	[kg <sub>H2O</sub> .kg <sup>-1</sup> <sub>dm</sub> ]
$X_d$	desired final moisture content	[kg <sub>H2O</sub> .kg <sup>-1</sup> <sub>dm</sub> ]
$X_F$	concentration of free water	[kg <sub>H2O</sub> .kg <sup>-1</sup> <sub>dm</sub> ]
$X_m$	monolayer moisture content	[kg <sub>H2O</sub> .kg <sup>-1</sup> <sub>dm</sub> ]
$Y_a$	absolute humidity of air	[kg <sub>H2O</sub> .kg <sup>-1</sup> <sub>da</sub> ]
$Y_{a,i}$	ingoing absolute humidity of air	[kg <sub>H2O</sub> .kg <sup>-1</sup> <sub>da</sub> ]
$Y_{as}$	air humidity at surface of material	[kg <sub>H2O</sub> .kg <sup>-1</sup> <sub>da</sub> ]
$\Delta h_{vo}$	heat of evaporation at 0 °C	[J.kg <sup>-1</sup> ]
$\gamma$	constant in performance index related to energy costs	[fl.J <sup>-1</sup> .kg <sup>-1</sup> ]
$\eta$	constant in performance related to quality profit	[fl.kg <sup>-1</sup> ]
$\lambda_m$	thermal conductivity of material	[J.s <sup>-1</sup> .m <sup>-1</sup> .K <sup>-1</sup> ]
$\rho_a$	air density	[kg.m <sup>-3</sup> ]
$\rho_m$	material density	[kg.m <sup>-3</sup> ]

*parameter values quality model*

$a_1$	101.31	$a'_1$	5.01
$a_2$	253129.9	$a'_2$	20580.3
$b_1$	34.06	$b'_1$	-8.68
$b_2$	119744.9	$b'_2$	-22745.2
$p$	-906.58	$q$	6.09

## Introduction

The most important aspects of optimisation of drying processes are energy consumption and the product quality, which deteriorates during drying (Banga and Singh, 1994). Since the quality indicator is characterised by the spatial distribution of moisture content and temperature inside the product, it requires accurate modelling of the heat and mass transfer at the level of individual particles (material level) during drying. The moisture content, temperature and quality indicator differ significantly inside each particle (*Chapter 2*), requiring a model of distributed nature. Many models of drying processes have been presented in the literature ranging from empirical and semi-empirical to almost purely physical models (Fasina and Sokhansanj, 1996; Kerkhof, 1994; McMinn and Magee, 1996; Kiranoudis *et al.*, 1993). The drawback of the first two types of models is that it is difficult to extend them to different products and process conditions because their parameters depend on both in an unknown manner. The drawback of models of the latter type is that they are often too complicated for computation. Based on a number of assumptions that usually hold in practice, a distributed model is presented which describes the main transport properties inside and outside each particle during drying.

In biological material, the controlling resistance for drying is the internal mass transfer resistance, governed by moisture diffusion. Therefore the diffusion coefficient is a major parameter in drying models, which is a “lumped” parameter, involving all internal physical phenomena, known as well as unknown mechanisms. Since it is not possible to theoretically predict this parameter based on composition or structure of the material, generally *empirical* relations are chosen and fitted to obtain the so called effective diffusion coefficient (Zogzas *et al.*, 1996; McMinn and Magee, 1996; Waananen *et al.*, 1993). Often these relations state that the effective diffusion coefficient depends on moisture content, representing the decreasing drying rate as moisture content decreases. The effective diffusion coefficient has no clear physical meaning and furthermore it is not likely that such empirical relations cover the whole range of experimental conditions.

To maximally benefit from optimal control computations an accurate model and cost function must be selected for the whole range of drying conditions. To this end a new distributed model is developed, in which it is assumed that the decrease of drying rate with respect to moisture content is a result of the conversion from bound to free water inside the particle. Kiranoudis *et al.* (1995) modelled this conversion by a reversible reaction. In fact however, this conversion should be physically described by a sorption process, which takes place at low

moisture contents. This description allows the use of the “true” diffusion coefficient in the model, which now only depends on temperature. Moreover, the parameters describing the sorption process can be derived from the sorption isotherm. Hence, in the model obtained in this manner, the parameters have a physical meaning and are known or can be estimated in a known manner. The choice of this model is further motivated and explained in *Chapter 4.1*.

Based on a finite-difference approximation of the distributed model and a measure of product quality and energy consumption, optimal control trajectories are computed, using control parameterisation (Van Willigenburg and Loop, 1991) for different drying times. The results indicate the feasibility of the model to optimise drying processes of different type by increasing the value of the quality indicator and saving the energy costs. In addition the results indicate the significance of optimising the drying time.

## The model

The moisture transfer in each particle is modelled by three basic transfer phenomena: free water diffusion, conversion between bound and free water inside the particle and external convection at the boundary of the particle. The state variables of the infinite-dimensional model are bound and free moisture content,  $X_B$  and  $X_F$  respectively, and temperature  $T_m$ . The state variables are a function of both time and space, which is left out of notations for brevity.

### Conversion between bound and free water

The interaction between water and the solid is modelled through the adsorption of free water to become bound water and the desorption of bound water to become free water. The model, which describes these sorption processes is analogous to the model of heterogeneous catalysis and relies on the following assumptions (Aris, 1975):

- a) the solid surface is covered with a number of sites at which water molecules may be held.
- b) the number of active sites per unit area,  $X_m$  is constant
- c) all sites are equivalent
- d) each sorbed molecule occupies only one site
- e) there is no interaction between adsorbed molecules

- f) the thermodynamic variables for sorption are derived from a desorption isotherm. The phenomenon of hysteresis between ad- and desorption isotherms will not induce problems, since only desorption (equivalent to drying) plays a role.
- g) during drying, moisture content, vapour pressure and temperature are in thermodynamic equilibrium within the drying material and with the drying environment.

The rate of adsorption of free water is proportional to the product of the concentration of those sites not yet occupied and the concentration of free water above the surface,

$$r_a = k_a \cdot X_F \cdot X_m \cdot (1 - \theta) \quad (6.1)$$

where

$$\theta = \frac{X_B}{X_m} \quad (6.2)$$

From equation 6.1 and 6.2,

$$r_a = k_a \cdot X_F \cdot (X_m - X_B) \quad (6.3)$$

On the other hand the rate of desorption is proportional to the concentration of sites already occupied,

$$r_d = k_d \cdot X_m \cdot \theta \quad (6.4)$$

From equation 6.4 and 6.2,

$$r_d = k_d \cdot X_B \quad (6.5)$$

The desorption rate (equation 6.5) minus the adsorption rate (equation 6.3) equals the decrease of bound water and the increase of free water inside the particle,

$$-\frac{dX_B}{dt} = \frac{dX_F}{dt} = k_d \cdot X_B - k_a \cdot X_F \cdot (X_m - X_B) \quad (6.6)$$

At *equilibrium* the adsorption rate (equation 6.3) and the desorption rate (equation 6.5) balance resulting in:

$$k_d \cdot X_B = k_a \cdot X_F \cdot (X_m - X_B) \quad (6.7)$$

From equation 6.7 at equilibrium the ratio  $k_a/k_d$ , which is called an equilibrium constant  $K_{eq}$ , satisfies:

$$K_{eq} = \frac{k_a}{k_d} = \frac{X_{B,e}}{X_{F,e} \cdot (X_m - X_{B,e})} \quad (6.8)$$

where the index  $e$  refers to equilibrium.

### Partial differential equations, boundary and initial conditions of the drying model

The following partial differential equations describe moisture diffusion, conversion from bound and free water and the thermodynamics inside the particle:

$$\frac{\partial (\rho_m \cdot X_F)}{\partial t} = \nabla(\rho_m \cdot D \cdot \nabla X_F) + \rho_m \cdot r_B \quad (6.9)$$

$$-\frac{\partial X_B}{\partial t} = r_B \quad (6.10)$$

$$\frac{\partial (\rho_m \cdot h_m)}{\partial t} = \nabla(\lambda_m \cdot \nabla T_m) \quad (6.11)$$

with

$$r_B = k_d \cdot X_B - k_a \cdot (X_m - X_B) \cdot X_F \quad (6.12)$$

$$h_m = c_{p,dm} \cdot T_m + X \cdot c_{p,w} \cdot T_m \quad (6.13)$$

$$X = X_F + X_B \quad (6.14)$$

The first term after the equality sign in equation 6.9 represents free water diffusion inside the particle governed by the diffusion coefficient  $D$ . The second term together with equations 6.10 and 6.12 describes the conversion between bound and free water inside the particle governed by the bound to free water conversion rate  $r_B$ . Finally equation 6.11 describes the enthalpy dynamics inside the particle governed by the thermal conductivity  $\lambda_m$ . From now on the particle will be considered cylindrical with a length far greater than its radius  $R$ . Then equations 6.9 – 6.11 turn into:

$$\frac{\partial X_F}{\partial t} = \frac{1}{r} \cdot \left[ D \cdot \frac{\partial X_F}{\partial r} + r \cdot \frac{\partial D}{\partial r} \cdot \frac{\partial X_F}{\partial r} + r \cdot D \cdot \frac{\partial^2 X_F}{\partial r^2} \right] + r_B \quad (6.15)$$

$$-\frac{\partial X_B}{\partial t} = r_B \quad (6.16)$$

$$\frac{\partial T_m}{\partial t} = \frac{1}{r} \cdot \left( \lambda_X \cdot \frac{\partial T_m}{\partial r} + r \cdot \frac{\partial \lambda_X}{\partial r} \cdot \frac{\partial T_m}{\partial r} + r \cdot \lambda_X \cdot \frac{\partial^2 T_m}{\partial r^2} \right) \quad (6.17)$$

where

$$\lambda_X = \frac{\lambda_m}{(c_{p,dm} + c_{pw} \cdot X) \cdot \rho_m} \quad (6.18)$$

and where  $r$  denotes the distance measured from the centre line of the cylinder which varies from 0 to  $R$ . Because of the symmetry at the centre line of the cylindrical particle the following boundary conditions apply:

$$\left. \frac{\partial X_F}{\partial r} \right|_{r=0} = 0 \quad t > 0 \quad \left. \frac{\partial T_m}{\partial r} \right|_{r=0} = 0 \quad t > 0 \quad (6.19)$$

At the boundary of the cylinder where  $r=R$ , external convection and heat transfer determine the following boundary conditions:

$$J_{Xs} = -D \cdot \rho_m \cdot \left. \frac{\partial X_F}{\partial r} \right|_{r=R} = k \cdot (Y_{as} - Y_a) \cdot \rho_a \quad (6.20)$$

$$J_T = \lambda_m \cdot \frac{\partial T_m}{\partial r} \Big|_{r=R} = h \cdot (T_a - T_m|_{r=R}) - J_{Xs} \cdot (\Delta h_{vo} - (c_{pw} - c_{pv}) \cdot T_m|_{r=R}) \quad (6.21)$$

$Y_{as}$  is the absolute air humidity, which is in equilibrium with the moisture content at the surface of the material (assumption (g)).  $Y_{as}$  is determined by the water activity at the surface of the material and the saturated vapour pressure:

$$Y_{as} = \frac{M_w}{M_a} \cdot \frac{a_w \cdot P_{sat}}{P_{tot} - P_{sat}} \quad (6.22)$$

where  $a_w$  is given by the GAB sorption isotherm (Lievens, 1991):

$$\frac{X}{X_m} = \frac{C_g \cdot K \cdot a_w}{(1 - K \cdot a_w) \cdot (1 - K \cdot a_w + C_g \cdot K \cdot a_w)} \quad (6.23)$$

and  $P_{sat}$  by the psychrometric relation:

$$P_{sat} = 1000 \cdot 10^{7.06262 - (1650.27 / (T + 226.346))} \quad (6.24)$$

At the start of drying, it is assumed that the moisture content is

$$X(r)|_{t=0} = 1 \text{ [kg}_{H_2O} \cdot \text{kg}^{-1}_{dm}] \quad (6.25)$$

and the material is assumed to be in equilibrium, so equation 6.8 must be satisfied. Solving equation 6.8 and equation 6.25 gives for  $r \in [0, R]$ :

$$X_F(r)|_{t=0} = 0.9337 \text{ [kg}_{H_2O} \cdot \text{kg}^{-1}_{dm}] \quad (6.26)$$

$$X_B(r)|_{t=0} = 0.0663 \text{ [kg}_{H_2O} \cdot \text{kg}^{-1}_{dm}] \quad (6.27)$$

Furthermore,

$$T_{m,K}(r)|_{t=0} = 298 \text{ [K]} \quad (6.28)$$

while the remaining initial conditions are given by equation 6.31.

The sorption parameters  $X_m$  and  $K_{eq}$  can be obtained from the sorption isotherm (equation 6.23).  $X_m$  follows directly from the GAB equation, while  $K_{eq}$  is related to the Gibbs free energy, which can easily be derived from the sorption isotherm. Since  $K_{eq}$  is the ratio of  $k_a$  and  $k_d$  only one of these two parameters remains to be estimated. Since the other parameters in the model (6.15 - 6.21) all have a clear physical meaning and interpretation they are known in principal or can be estimated in a known manner (*Chapter 4.1*).

## Product quality, energy consumption and the performance index

In this section a description of product quality and energy consumption is presented in terms of the model in order to investigate the feasibility of the model to optimise drying processes. A performance index is obtained which represents the cash flow per unit of product per time unit obtained from drying. Let  $Q$ , the quality indicator, represent the residual activity of the biological material which is a measure of quality of for instance micro organisms and enzymes. The inactivation of micro organisms, among which *Lactobacillus plantarum* which is considered here, and enzymes can usually be described by first-order reaction kinetics. Then  $Q(r)$  at each location  $r$  in the particle can be determined with the following differential equation (Lievens, 1991):

$$\frac{dQ}{dt} = -k_i \cdot Q \quad (6.29)$$

with

$$\ln(k_i) = \left[ \left( a_1 - \frac{a_2}{\Re \cdot T_{m,K}} \right) \cdot X + \left( b_1 - \frac{b_2}{\Re \cdot T_{m,K}} \right) \right] + [1 - \exp(p \cdot X^q)] \cdot \left[ \left( a'_1 - \frac{a'_2}{\Re \cdot T_{m,K}} \right) \cdot X + \left( b'_1 - \frac{b'_2}{\Re \cdot T_{m,K}} \right) \right] \quad (6.30)$$

and initial condition,

$$Q(r)|_{t=0} = 1, \quad r \in [0, R] \quad (6.31)$$

Furthermore the energy costs to realise and maintain the trajectory of air conditions per unit product can be expressed as follows (Van Boxtel and Knol, 1996):

$$J_{energy} = \int_0^{t_f} \gamma \cdot \rho_a \cdot G_a \cdot (c_{p,a} + c_{p,v} \cdot Y_{a,i}) \cdot (T_{a,i} - T_{env}) dt \quad (6.32)$$

where 0 and  $t_f$  are the initial and final time of the drying process respectively,  $\gamma$  is the price of energy per unit product,  $G_a$  is the air flow and  $T_{a,i}$  and  $Y_{a,i}$  are the temperature and humidity of the ingoing air in the dryer respectively. The latter three can be applied as control variables to improve the performance of the drying process. In the optimal control computations in this chapter  $G_a$  and  $Y_{a,i}$  will be fixed and  $T_{a,i}$  will be the only control variable. Let  $t_r$  denote the time necessary to prepare for the next drying run. Then from equation 6.29 – 6.32 the following performance index is obtained which equals the cash flow per unit of time and material obtained after the drying process:

$$J_D(T_a(t)) = \frac{1}{t_f + t_r} \cdot \left( \frac{\eta}{\pi \cdot (R)^2} \cdot \int_0^R 2 \cdot \pi \cdot r \cdot Q(r) \Big|_{t=t_f} dr - \int_0^{t_f} \gamma \cdot \rho_a \cdot G_a \cdot (c_{p,a} + c_{p,v} \cdot Y_{a,i}) \cdot (T_{a,i} - T_{env}) dt \right) \quad (6.33)$$

In equation 6.33,  $\eta$  represents the price obtained for a unit of dried material. The first spatial integral on the right in equation 6.33 is a function of the value of the quality indicator at the final time. To compute the performance index the quality indicator, which is governed by the differential equation 6.29, must be added as a state variable to the model. Then the spatial integral becomes a function of the final state while the second time integral in equation 6.33 represents the running costs.

## Optimal control computations and results

A finite-difference approximation of the infinite dimensional model (equation 6.15 – 6.31) is used to compute the state evolution and performance, given the initial state and control. On the radius  $R$  of the cylinder  $N$  points are distinguished at equal distances,

$$r_i = (i-1) \cdot \Delta r, \quad i = 1, 2, \dots, N, \quad \Delta r = \frac{R}{N-1} \quad (6.34)$$

The first and second derivatives of  $X_F$  with respect to  $r$  are approximated for  $i = 2, 3, \dots, N-1$  with,

$$\frac{\partial X_F}{\partial r} = \frac{X_F(r_{i+1}) - X_F(r_{i-1}))}{2 \cdot \Delta r} \quad (6.35)$$

$$\frac{\partial^2 X_F}{\partial r^2} = \frac{X_F(r_{i+1}) - 2 \cdot X_F(r_i) + X_F(r_{i-1}))}{\Delta r^2} \quad (6.36)$$

and similarly for  $T_m$  and  $\lambda_X$ . Furthermore

$$\frac{\partial ID}{\partial r} = \frac{\partial ID}{\partial T_m} \cdot \frac{\partial T_m}{\partial r} \quad (6.37)$$

and

$$ID = ID_0 \cdot e^{\frac{-E_a}{R \cdot T_m, K}} \quad (6.38)$$

where the first term in equation 6.37 is obtained in analytic form from equation 6.38 while the second is approximated by 6.35 with  $X_F$  replaced by  $T_m$ . From equation 6.19 – 6.21, at the boundaries the first derivatives of  $X_F$  with respect to  $r$  are fixed and similarly for  $T_m$ . Then for the second derivative the following approximation was used for  $X_F$  at  $r = R$ :

$$\left. \frac{\partial^2 X_F}{\partial r^2} \right|_{r=R} = \frac{\left( \left. \frac{\partial X_F}{\partial r} \right|_{r=R} \cdot \Delta r - (X_F(r_N) - X_F(r_{N-1})) \right)}{\Delta r^2 / 2} \quad (6.39)$$

and similarly for  $T_m$ . Finally for  $\lambda_X$  at  $r = R$  the approximation

$$\left. \frac{\partial \lambda_X}{\partial r} \right|_{r=R} = \frac{\lambda_X(r_N) - \lambda_X(r_{N-1}))}{\Delta r} \quad (6.40)$$

was used. Given the spatial discretisation scheme (equation 6.34) the spatial integral in equation 6.35 and 6.36 was computed using the trapezoidal numerical integration rule. The time integration was performed with the Matlab/Simulink integrator ode15s for stiff systems. The number  $N$  was taken equal to 15 because larger values of  $N$  did not result in significant changes.

Although the performance index represents the cash flow obtained after drying it does not take into account the goal, which is to dry the product up to a certain level. Therefore the performance index is modified by a penalty function  $J_X$ , resulting in the performance index  $J$  to be minimised:

$$J = J_X - J_D \quad (6.41)$$

where

$$J_X = c_1 \cdot (\overline{X(t_f)} - X_d) \quad \overline{X(t_f)} > X_d, \quad J_X = 0 \quad \overline{X(t_f)} \leq X_d \quad (6.42)$$

in which  $X_d$  represents the desired moisture concentration at the end of drying. The coefficient  $c_1$  is used to weigh the goal to reach  $X_d$  against the cash flow during optimisation.

For different fixed final times  $t_f$  the control interval  $[0, t_f]$  was divided into  $N_u$  equidistant time-intervals over which the control variable remains constant. Then the piecewise constant control  $T_{a,i}(t)$ ,  $t \in [0, t_f]$  is uniquely determined by  $N_u$  values of the control variable. Then, given the initial state, the determination of the optimal control that minimises  $J$  (equation 6.41) constitutes a function minimisation where the variables are the  $N_u$  values of the control variable which is bounded from above and below:

$$313 \leq T_{a,iK} \leq 360 \text{ [K]} \quad (6.43)$$

$N_u$  equal to 1 corresponds with static control, where  $J$  is minimised while the control variable is kept constant during the operation. Figure 6.1 shows the results obtained from function minimisation using different values of  $N_u$  and  $t_f$  and a final desired moisture content  $X_d = 0.05$  (upper three) and  $X_d = 0.075$  (lower three) [ $\text{kg}_{\text{H}_2\text{O}} \cdot \text{kg}^{-1}_{\text{ds}}$ ]. As expected, increasing  $N_u$  results in better performance, except at some points, which is probably due to the existence of local minima. Furthermore Figure 6.1 shows that the optimal final time is about 12000 [s] for  $X_d = 0.05$  [ $\text{kg}_{\text{H}_2\text{O}} \cdot \text{kg}^{-1}_{\text{ds}}$ ] and that the quality indicator after drying is sensitive to the final desired

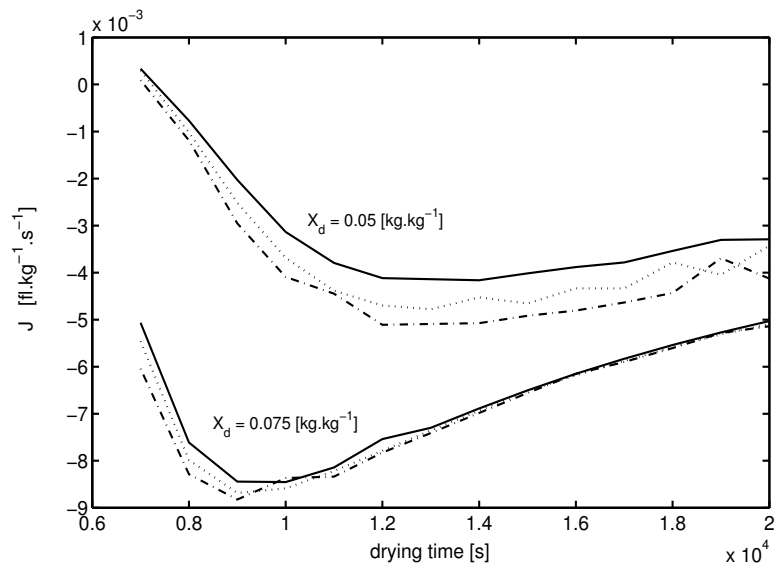


**Figure 6.1:** Optimal performance as function of final drying time for  $N_u = 1$ :-,  $N_u = 3$ :-,  $N_u = 6$ :-.- and  $X_d = 0.05$  and  $0.075$  [ $\text{kg}_{\text{H}_2\text{O}} \cdot \text{kg}_{\text{ds}}^{-1}$ ]

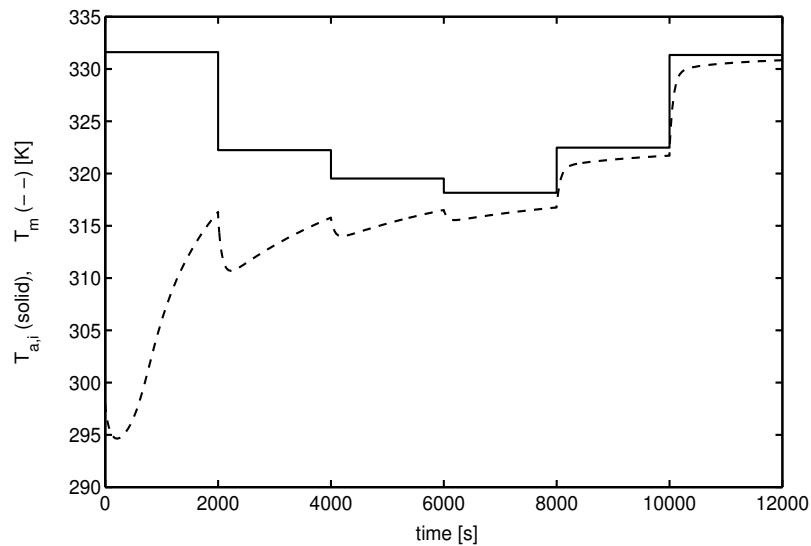


**Figure 6.2:** Optimal control trajectory for  $t_f = 12000$  [s],  $X_d = 0.05$  [ $\text{kg}_{\text{H}_2\text{O}} \cdot \text{kg}_{\text{ds}}^{-1}$ ] and  $N_u = 6$ ,  $J = -J_D = -5.1 \cdot 10^{-3}$  [ $\text{fl.kg}^{-1} \cdot \text{s}^{-1}$ ]

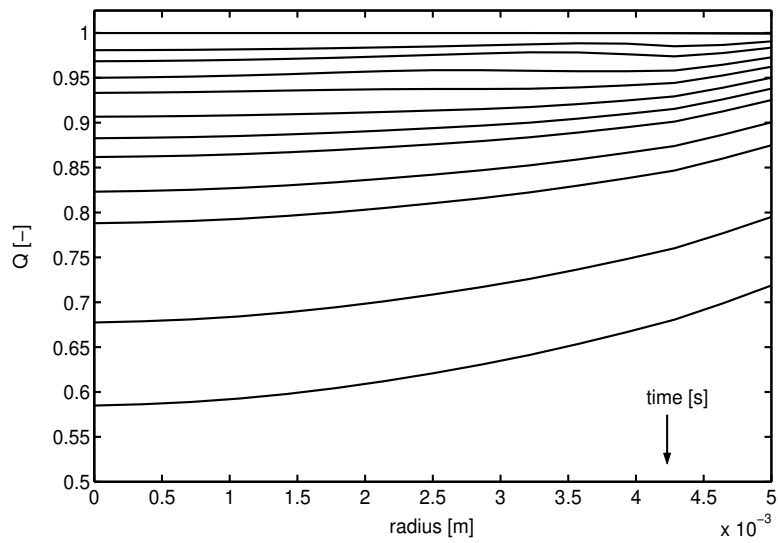


**Figure 6.3:** Optimal quality indicator profiles for  $t_f = 12000$  [s],  $X_d = 0.05$  [kg<sub>H2O</sub>.kg<sup>-1</sup><sub>ds</sub>] and  $N_u = 6$  (every 1000 [s])

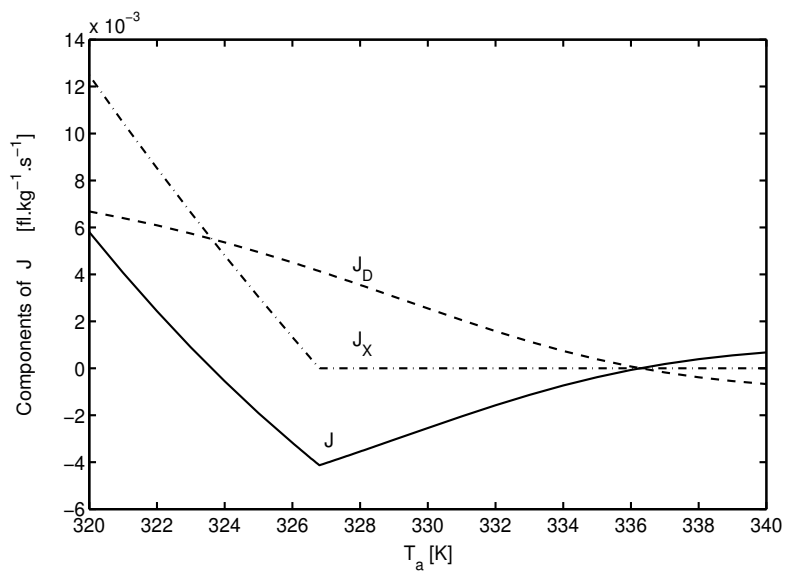


**Figure 6.4:** Sensitivity to the control for  $N_u = 1$ ,  $t_f = 12000$  [s],  $X_d = 0.05$  [kg<sub>H2O</sub>.kg<sup>-1</sup><sub>ds</sub>]

moisture content. A higher value for  $X_d$  at the same  $t_f$  allows drying at more moderate temperatures, causing less inactivation of the thermal sensitive biological material and a decrease in energy costs. Figures 6.2 and 6.3 show the optimal control trajectory, the average material temperature and quality indicator profiles of the solution with  $N_u = 6$  and  $t_f = 12000$  [s]. The considered micro organism is less sensitive to temperature at lower moisture contents, which explains the trajectory of  $T_{a,i}$ . The initial high temperature does not damage the quality, since the corresponding wet bulb temperature of the material in this period of the drying process is low. After this period the temperature of the material rises and  $T_{a,i}$  is decreased to protect the material during the temperature-sensitive phases. When during drying the moisture content is reduced the material is less sensitive to inactivation and  $T_{a,i}$  can increase to reach  $X_d$ . Compared to the static control with a constant  $T_{a,i}$  of 327 [K], this leads to a higher value of product quality indicator and less energy costs and therefore to an improved value of the performance index (24%). Figure 6.4 illustrates the sensitivity of the two components of the performance index (equation 6.41) to the value of the control variable if it remains constant during drying ( $N_u = 1$ ).

## Conclusions

Based on a physical description of the conversion of bound and free water inside particles during drying, a new distributed model with parameters which all have a physical meaning and interpretation is presented, that describes the drying of materials. Due to their physical meaning and interpretation the parameters are known or can be estimated from experiments while the model can be adjusted relatively easy to other materials and dryers.

Optimal control computations illustrate the significance and feasibility of this model to optimise drying processes. The improved operation appears from an increased value of the performance index in [ $\text{fl.kg}^{-1}.\text{s}^{-1}$ ] by protecting quality and saving energy costs. Moreover the results indicate the importance to optimise the drying time. Actually, spatial quality indicator distribution aspects should be considered in the optimisation procedure, since product quality is characterised by internal profiles (*Chapter 3, 4 and 5*). However, in order to judge the feasibility of the model, here commonly applied average quality aspects have been considered.

In this study the physical model parameters that need to be estimated have been obtained from literature describing, as much as possible, comparable drying circumstances and materials. Despite the physical meaning and interpretation of the model parameters, the model needs validation against experiments. These experiments will also be used to estimate those model parameters which could not reliably be obtained from the literature.

## References

- Aris, R. *The mathematical theory of diffusion and reaction in permeable catalysts. Volume 1. The theory of steady state.* Oxford: Clarendon press, 1975. 444 p.
- Banga, J.R. and R.P. Singh. Optimization of air drying of foods. *Journal of Food Engineering*, vol. 23, 1994, p. 189-211.
- Fasina, O. and S. Sokhansanj. Estimation of moisture diffusivity coefficient and thermal properties of alfalfa pellets. *Journal of Agricultural Engineering Research*, vol. 63, 1996, no. 4, p. 333-344.
- Kerkhof, P.J.A.M. A test of lumped-parameter methods for the drying rate in fluidized bed driers for bioproducts. p. 131-140. In: Rudolph, V., R.B. Keey and A.S. Mujumdar (Eds.). *Drying '94.* Gold Coast, Australia: Proceedings of the 9<sup>th</sup> International Drying Symposium (IDS '94), 1994. 1402 p.
- Kiranoudis, C.T., Z.B. Maroulis and D. Marinos-Kouris. Heat and mass transfer model building in drying with multiresponse data. *International Journal of Heat and Mass Transfer*, vol. 38, 1995, no. 3, p. 463-480.
- Kiranoudis, C.T., Z.B. Maroulis and D. Marinos-Kouris. Mass transfer model building in drying. *Drying Technology*, vol. 11, 1993, no. 6, p. 1251-1270.
- Lievense, L.C. *The inactivation of Lactobacillus plantarum during drying.* Wageningen: Wageningen Agricultural University, Department of Food Processing, 1991. 118 p. PhD thesis.
- McMinn, W.A.M. and T.R.A. Magee. Air drying of potato cylinders. *Drying Technology*, vol. 14, 1996, no. 9, p. 2025-2040.
- Van Boxtel, A.J.B. van and L. Knol. A preliminary study on strategies for optimal fluid-bed drying. *Drying Technology*, vol. 14, 1996, no. 3&4, p. 481-500.
- Van Willigenburg, L.G. and R.P.H. Loop. Computation of time-optimal controls applied to rigid manipulators with friction. *International Journal of Control*, vol. 54, p. 1097-1117.

Waananen, K.M., J.B. Litchfield and M.R. Okos. Classification of drying models for porous solids. *Drying Technology*, vol. 11, 1993, no. 1, p. 1-40.

Zogzas, N.P., Z.B. Maroulis and D. Marinos-Kouris. Moisture diffusivity data compilation in foodstuffs. *Drying Technology*, vol. 14, 1996, no. 10, p. 2225-2253.

## **Chapter 7**

### **General discussion**

Food quality is affected by processing. It is generally a consequence of subjective evaluation of quality attributes. To allow quantitative description, quality attributes are coupled to quality indicators that can be measured by objective instrumentation. In many processes a spatial distribution of the quality indicator arises inside the material. Therefore, it is expected that quality indicator profiles (QIPs) need to be considered in the optimisation of quality (*Chapter 1*). This formed the core hypothesis of this thesis.

This general discussion deals with the description, prediction and optimisation of quality, all applied to the case study. The case study concerns drying of the enzyme catalase, immobilised in starch cylinders, with its residual activity as quality indicator. The general discussion finishes with some recommendations and future perspectives, not only for drying but also for other processes.

## **Description of quality**

The major side effect of drying is the loss of quality of the material. It is caused by several irreversible modifications in the material (biological, chemical, physical) as a consequence of the removal of water and the increase of temperature during the drying process. In drying processes it is well established that the most important variables are time, temperature and moisture content. Due to differences between the inner and outer part of the material in resistance towards mass and heat transfer, profiles of moisture and or temperature arise. Consequently, quality indicator profiles (QIPs) will arise during and after drying (*Chapter 1, 2 and 4*). Whereas profiles in moisture content and temperature equate after drying, QIPs remain as is also demonstrated experimentally, due to the irreversibility of the inactivation (*Chapter 5*).

Simulations of catalase activity in starch cylinders during drying established the theoretical considerations for the description of quality (*Chapter 2*). The simulation results show firstly that the internal distribution of moisture content and temperature determine the quality indicator, i.e. the residual enzyme activity (Figure 2.2). They also demonstrate that the average value for the quality indicator does not give a unique description of product quality. The same value for the average quality indicator corresponds with different QIPs (Figure 2.2 and 2.3). Inside the material the residual enzyme activity can be much lower (0.25 [-]) as well as much higher (0.99 [-]) than the average value of 0.61 [-]. Such differences may be totally

unacceptable for quality attributes that are related to food safety, such as deteriorative enzymes or hazardous micro organisms.

The simulation studies clearly support the view that the quality of food material can only be adequately described by considering the spatial profiles. They also illustrate that the QIPs can be altered by dynamically changing the air conditions.

Although theory and simulation models demonstrate the central role of QIPs in quality description, the experimental verification is crucial. From the experiments two major conclusions can be drawn: 1) QIPs exist in material during and after drying and 2) QIPs can be influenced by varying the drying air conditions (*Chapter 5*). The influence of drying conditions on QIPs can be explained by their influence on the profiles of moisture content and temperature. When a drying experiment is diffusion limited, the moisture content near the surface will drop to the moisture content that is in equilibrium with the air conditions, while in the centre the moisture content remains high. Under this low moisture content, the enzyme is less sensitive to inactivation and therefore it remains active near the surface (94% of initial activity). Changing the drying air conditions, so that the process is limited by convection, alters the QIP. The moisture content profile inside the material will be more uniform: the moisture content at the surface remains high. Hence the enzyme is also inactivated near the surface (11% of initial activity) and the QIP is more flat. This experimental demonstration of QIPs and the influence of drying air conditions on them are unique.

In almost all papers describing quality indicators during drying average conditions are applied (Villota and Karel, 1980b; Mishkin et al., 1984). The influence of spatial distributions of moisture content and temperature in the description of quality indicator is recognised (Wang and Brennan, 1995; Mishkin et al., 1984; Villota and Karel, 1980a). However, this knowledge is not used to investigate the distribution of quality indicator inside the material. Even in cases with a quality attribute as colour, where differences between surface and centre appear visually, no attention is paid to the distribution of the indicator (Ávila and Silva, 1999; Maskan, 2001; Smout et al., 2003). The spatial distribution is only taken into account in cases where stress arises inside the material causing the formation of cracks (Andrieu et al., 1988; Kim et al., 2002; Masaaki and Hayakawa, 1995). In other cases, no distinction is made between the quality indicator at different locations inside the material. Theory, simulation and experiments have clearly shown, that a significant difference exists between the values of the quality indicator at various locations. QIPs are evidently essential for the description of quality. This means that in control, it is not so much the average values but the profiles of the quality indicators that are necessary to optimise quality.

## Prediction of quality

In drying, the most important variables affecting the quality indicator are time, moisture content and temperature. Hence, to predict the QIPs during drying, the dynamic evolution of moisture content and temperature profiles inside the food need to be predicted by a drying model. Since the microscopic drying model describes what actually happens inside the food material, it forms the core of the optimal quality control. The model needs to possess the ability to describe the gradients of moisture content and temperature in the material for a large range of experimental conditions and has to be independent of the dryer type. From the existing microscopic drying models, the distributed diffusion model is the simplest model that satisfies these requirements. In this model, an effective diffusion coefficient is defined that reduces with decreasing moisture content. An empirical relation expresses the moisture dependency. The problem is that various relations for the diffusion coefficient might lead to comparable drying curves. At the same time the various relations lead to different moisture profiles and hence to potentially different predictions of QIPs. Therefore a new model is required.

In the new model physical phenomena are incorporated that explain the reduced drying rate in terms of sorption (*Chapter 4.1*). Compared to existing diffusion models, the model structure is extended with a sorption process. It is therefore called the diffusion-sorption model.

A major advantage of the model is that all parameters have a physical meaning. The independently measured sorption isotherms (*Chapter 4.3*) provide the parameters essential in the description of the sorption process between bound and free water. After all, the sorption isotherm is always required, independent of the model type, for the determination of the externally controlled moisture transfer and the prediction of the final moisture content (*Chapter 4.2*). The fixed model structure, with its physical and known parameters, is in contrast with the existing diffusion models, where the relations for the moisture dependence of the diffusion coefficient are empirical.

Other advantages of the diffusion-sorption model appear during calibration and validation. The model has the least amount of parameters to be estimated from the drying curve. It is the best identifiable model, leading to unique parameter values. Moreover, the accuracy of the parameters is much higher: 8-19% against more than 25% for the other models. And finally, on average the model yields the most reliable and best prediction of drying curves over a wide

range of experimental conditions. These features enhance the confidence in the diffusion-sorption model for the prediction of QIPs.

Apart from the microscopic drying model, a quality model is essential for the prediction of QIPs during drying. The quality indicator, i.e. the residual activity of catalase is modelled as function of moisture content, temperature and time, based on independent inactivation experiments. The exact role of water in enzyme inactivation reactions is not clear (Frías and Oliveira, 2001; Saraiva et al., 1996). Therefore, the most simple model can be used. Since a time invariant nonzero rest activity remains after inactivation experiments, a fractional conversion model is satisfying. It predicts the residual enzyme activity in various inactivation experiments (at constant temperature and moisture content) within the experimental accuracy of 20% (*Chapter 5*).

Both the diffusion-sorption model and the quality model lead to reliable predictions. The diffusion-sorption model predicts the drying curve well and the quality model the catalase activity during inactivation. However, when the quality model is combined with the diffusion-sorption model to predict the experimentally demonstrated QIPs a problem arises. The combination results in an excellent agreement of the predicted average moisture content with the drying curve. Also the QIPs are qualitatively comparable with the experimental ones. Nevertheless the predicted residual enzyme activity is structurally higher than the experimental one.

The reason for this deviation is not clear. Several causes can be considered, but none of them gives a complete explanation for the observed differences.

- 1) Catalase is chosen as quality indicator, due to its theoretical relevance for food industry, in both positive and negative sense. Its practical evaluation, on the other hand, appears to be highly sensitive to experimental error (*Chapter 5*). It results in inaccuracy in measured enzyme activity and therefore also in the parameters in the quality model. However, this cannot be the only reason, since the prediction of the inactivation of catalase at other temperatures and moisture contents is satisfactory.
- 2) The inactivation kinetics of catalase are not accurate enough in the region of high temperature and high moisture content. After all, from the inactivation experiments no data are available at high moisture content and high temperature, due to gel formation in the samples. During the drying experiments, the samples come in this region without causing gel formation, due to the short residence time. It might be possible that the influence of high moisture content at high temperatures is larger than expected from the

present inactivation data. This will lead to the prediction of higher inactivation as is also shown experimentally.

- 3) The prediction of quality appears to be highly sensitive to temperature (Meerdink and van 't Riet, 1991). This indicates that it is possible that the temperature during drying is not predicted well enough, as is also found by other researchers (Liou et al., 1985; Villota and Karel, 1980b). In this case, the calibration on drying curves solely would be insufficient, although the drying curves are measured at several temperatures (*Chapter 4.1*). Parameters describing the temperature inside the material are derived from literature (thermal conductivity, heat capacity) or linked to the external mass transfer coefficient. Probably, wrong parameters are compensated for in the calibration. However, this can only play a minor role, since the diffusion-sorption model is calibrated on drying experiments at different air temperature. Moreover, the model prediction of drying curves at different temperatures is adequate as turns out during validation.

Within the limitations of experimental error, it can be maintained that the diffusion-sorption drying model adequately describes and predicts the experimental QIPs.

## Optimising quality

With the *model* describing QIPs in the material at various drying conditions, optimisation studies can be accomplished. The conflicting criteria of an efficient process and the highest possible quality are explicitly formulated in an economic multi-*objective function* (*Chapter 1, 3, 6*). The safe moisture content that is desired after drying is defined as a *constraint*. With *control parameterisation*, optimal time trajectories of the *control variables*, temperature and relative humidity, are computed. As microscopic drying model, both a standard diffusion model (*Chapter 3*) and the new diffusion-sorption model (*Chapter 6*) appear to be suitable for the optimisation procedure. The outcome of several optimisation studies with the case study has very promising features for food industry, as described below.

First, an optimal drying time exists. This optimal drying time is the most advantageous compromise between quality and energy consumption. Longer drying times do not save quality anymore, while energy consumption increases (*Chapter 3, 6*). This indicates the importance of optimising the drying time.

Secondly, product quality can be controlled. Due to the variation of temperature in time, the temperature-sensitive phases of the enzyme are passed more moderately, i.e. at lower temperatures, to maintain quality.

Thirdly, the moisture content is better controlled. This prevents the product from under- or overdrying, as can occur in conventional drying processes with constant control variables. Moreover, higher profit is achieved, by saving energy or improving quality, due to the variation of the control variables in time (*Chapter 3*; Figure 3.5 and *Chapter 6*; Figure 6.2). Finally and most important, the consideration of QIPs appears to be essential in the optimisations. The QIPs are necessary to guarantee safety of the whole product after drying. When only average values of the quality indicator are considered in the optimisation, control trajectories are obtained that lead to the situation where deteriorative enzymes retain their activity near the surface of the material, causing spoilage during storage (Figure 3.7). Consideration of QIPs, on the other hand, leads to the achievement of safety in the whole product (Figure 3.9). Also improved control of product quality can be achieved. The trajectory of control variables, resulting from the optimisation, can influence and change the QIPs inside the material. This enhances the possibilities to control product quality. In this way, phenomena as cracking and crust formation for example can be controlled.

The off-line optimisations are not verified experimentally. However, we are very confident in the practical applicability of this method. The experiments show that the QIPs can really be influenced by the air conditions (*Chapter 5*). Secondly, the optimal trajectories of control variables aiming to destruct the deteriorative enzyme, i.e. initially high temperature and high relative humidity (Figure 3.8), correspond with the ancient custom of blanching. Blanching is a relatively short heat treatment in aqueous environment of vegetables to inactivate undesirable enzymes responsible for quality deterioration. It is often applied to material prior to for example drying (Jayaraman and Das Gupta, 1995; Lund, 1977). Clearly, model based calculations agree with old practices.

The fact that the enzyme catalase is less sensitive to thermal inactivation at low moisture contents (*Chapter 5*), explains the optimal trajectories. The trajectories protect the material during temperature sensitive phases and lead to increased efficiency in other phases (*Chapter 3* and *6*). This will yield better product quality and process efficiency than other time-dependent drying schemes, based on practical consideration with predefined trajectories of the control variables, as for example the well known stepdown or stepup temperature profiles in Chua et al. (2001) or intermittent drying in Chou and Chua (2001).

Evidently, our results support the core hypothesis: consideration of quality indicator profiles (QIPs) inside the material is necessary to optimise quality.

## **Recommendations and future perspectives**

### ***Recommendations***

Optimisation studies are usually based on average conditions for the quality indicator. The major contribution of this thesis is that it has been demonstrated in theory, simulation and experiments that quality indicator *profiles* are required for optimisation of quality. In theory, QIPs exist in foods during drying irrespective of the concerned quality indicator (*Chapter 1*). Due to the irreversibility of the inactivation, QIPs remain after drying, while profiles in moisture content and temperature equate (*Chapter 5*).

Although the power of optimisation has been clearly established (*Chapter 3 and 6*), it would be desirable to perform experiments for verification of the practical utilisation of the method. The experimental demonstration of the influence of the air conditions on the QIPs (*Chapter 5*) give confidence in the practical applicability of the optimisation method.

The overestimation of the residual enzyme activity during drying (*Chapter 5*), can be overcome if it would be possible to measure the material temperature during drying. Development of methods to do so is advisable. Simultaneous fit on moisture content and temperature may improve the predictions and the correctness of the parameters.

The clarification of the mechanisms of water in enzyme inactivation will lead to valuable essential information that can improve the quality model. Moreover, the model of the quality indicator can be refined by calibration with dynamic experiments. This will render information about the inactivation at high moisture content and high temperature, where in the current experimental setup no data came available due to gel formation in the samples.

Based on a quick scan of 25 enzymes, catalase was chosen for its positive and negative features in food industry, its inactivation in the experimental range of the dryer equipment and the sample preparation before measurement of enzyme activity. On retrospect, the quality indicator residual activity of catalase, was not very sensitive. It is recommended to chose another enzyme for these experiments.

### ***Perspectives of the diffusion-sorption drying model***

The highly promising diffusion-sorption drying model needs to be supported by experimental validation for other materials. Due to the physical meaning and interpretation of all

parameters, the model can be adjusted relatively easily to other materials. When necessary the model can be extended to three classes of water, instead of two (*Chapter 4.1*). The generic model on micro-scale can be used not only for QIPs predictions and optimisation, but also in design and scale-up of drying processes.

### ***Perspectives of optimisation for drying processes***

The optimisation of drying of starch cylinders with enzyme, led to improved control of product properties as final moisture content and quality. The quality indicator could be controlled as defined in the objective function or in the constraint. It illustrates that an arbitrary quality attribute can be controlled when an adequate model is available, describing the indicator and the QIPs during drying. Not only chemical or biological attributes can be controlled as nutritional value, colour and safety, but also physical as shrinkage, cracks and crust formation, provided that suitable models are available or can be developed for the corresponding indicators.

In practice, more than one quality attribute of a product can be crucial and need to be controlled. It is very interesting to investigate whether it is possible to control two or more (conflicting) quality attributes. For example, the retention of nutrient while a deteriorative enzyme or micro organism is inactivated. Some research on this has been done by Lund (1977) and Banga and Singh (1994). However, they did not consider spatial quality distributions. Therefore, in the light of the findings in this thesis that QIPs are really essential, it would be very promising to investigate this. Other examples are the prevention of shrinkage and the retention of colour or the prevention of cracks and the control of organoleptic properties. Clearly, the presented method has a high potential in control of food properties in an optimal way.

### ***Perspectives for other processes***

Although the quality indicator is different for each individual product and process, methods to control and optimise are similar. The core hypothesis, that the consideration of quality indicator profiles (QIPs) inside the material is necessary to optimise quality, is therefore not only valid for drying processes, but for all processes, where gradients in quality indicators may arise. The implementation of spatial distributions of the quality indicator will lead to better prediction of product quality, and more importantly to an improved quality control. Product safety can only then be guaranteed if QIPs are considered. Moreover, quality attributes can be efficiently controlled in a desired manner. The optimal trajectory of control

variables saves quality in critical phases and is efficient in other phases. Optimal process control based on QIPs therefore is potentially of great economic value in biotechnology, agricultural and food engineering.

## References

- Andrieu, J., M. Bouvin and A. Stamatopoulos. Heat and mass transfer modelling during pasta drying. Application to crack formation risk reduction. p. 183-192. In: Bruin, S. (ed.). *Preconcentration and drying of food materials*. Amsterdam, etc.: Elsevier Science Publishers B.V., 1988. 353 p.
- Ávila, I.M.L.B. and C.L.M. Silva. Modelling kinetics of thermal degradation of colour in peach puree. *Journal of Food Engineering*, vol. 39, 1999, no. 2, p. 161-166.
- Banga, J.R. and R.P. Singh. Optimization of air drying of foods. *Journal of Food Engineering*, vol. 23, 1994, p. 189-211.
- Chou, S.K. and K.J. Chua. New hybrid drying technologies for heat sensitive foodstuffs. *Trends in Food Science and Technology*, vol. 12, 2001, no. 10, p. 359-369.
- Chua, K.J., A.S. Mujumdar, M.N.A. Hawlader, S.K. Chou and J.C. Ho. Batch drying of banana pieces - effect of stepwise change in drying air temperature on drying kinetics and product colour. *Food Research International*, vol. 34, 2001, no. 8, p. 721-731.
- Frías, J.M. and J.C. Oliveira. Kinetic models of ascorbic acid thermal degradation during hot air drying of maltodextrin solutions. *Journal of Food Engineering*, vol. 47, 2001, no. 4, p. 255-262.
- Jayaraman, K.S. and D.K. Das Gupta. Drying of fruits and vegetables. p. 643-691. In: Mujumdar, A.S. (Ed.). *Handbook of industrial drying. Volume 1*. New York, etc.: Marcel Dekker, Inc., 1995. 742 p.
- Kim, T.H., J.G. Hampton, L.U. Opara, A.K. Hardacre and B.R. Mackay. Effects of maize grain size, shape and hardness on drying rate and the occurrence of stress cracks. *Journal of the Science of Food and Agriculture*, vol. 82, 2002, no. 10, p. 1232-1239.
- Liou, J.K., K.Ch.A.M. Luyben and S. Bruin. A simplified calculation method applied to enzyme inactivation during drying. *Biotechnology and Bioengineering*, vol. 27, 1985, p. 109-116.

Lund, D.B. Design of thermal processes for ... maximizing nutrient retention. *Food Technology*, vol. 31, 1977, no. 2, p. 71-78.

Masaaki, I. and K.-I. Hayakawa. Heat and moisture transfer and hygrostress crack formation and propagation in cylindrical, elastoplastic food. *International Journal of Heat and Mass Transfer*, vol. 38, 1995, no. 6, p. 1033-1041.

Maskan, M. Kinetics of colour change of kiwifruits during hot air and microwave drying. *Journal of Food Engineering*, vol. 48, 2001, no. 2, p. 169-175.

Meerdink, G. and K. van 't Riet. Inactivation of a thermostable  $\alpha$ -amylase during drying. *Journal of Food Engineering*, vol. 14, 1991, p. 83-102.

Mishkin, M., I. Saguy and M. Karel. Optimization of nutrient retention during processing: ascorbic acid in potato dehydration. *Journal of Food Science*, vol. 49, 1984, p. 1262-1266.

Saraiva, J., J.C. Oliveira, M. Hendrickx, F.A.R. Oliveira and P. Tobback. Analysis of the inactivation kinetics of freeze-dried  $\alpha$ -amylase from *Bacillus amyloliquefaciens* at different moisture contents. *Lebensmittel-Wissenschaft und -Technologie*, vol. 29, 1996, no. 3, p. 260-266.

Smout, C., N.E. Banadda, A.M.L. Van Loey and M.E.G. Hendrickx. Nonuniformity in lethality and quality in thermal process optimization: A case study on color degradation of green peas. *Journal of Food Science*, vol. 68, 2003, no. 2, p. 545-550.

Villota, R. and M. Karel. Prediction of ascorbic acid retention during drying. I. Moisture and temperature distribution in a model system. *Journal of Food Processing and Preservation*, vol. 4, 1980a, p. 111-134.

Villota, R. and M. Karel. Prediction of ascorbic acid retention during drying. II. Simulation of retention in a model system. *Journal of Food Processing and Preservation*, vol. 4, 1980b, p. 139-159.

Wang, N. and J.G. Brennan. A mathematical model of simultaneous heat and moisture transfer during drying of potato. *Journal of Food Engineering*, vol. 24, 1995, no.1, p. 47-60.

## Summary

During processing of food materials, product properties alter, causing a change in the quality perception of the consumer. Quality is a complex topic. It is a measure of how the food product meets the wishes of the consumer, including sensory properties as well as psychological, sociological and cultural factors. The quality of a product can therefore differ for various situations. In order to make quality an objective quantity, the quality experience is linked to product properties, i.e. quality attributes, which can be expressed by a measurable quality indicator.

The changing product quality during processing asks for adequate process control that maximises both the product quality and keeps the process efficiency in mind. Optimisation procedures are a promising manner to achieve this, since they allow the explicit formulation of the conflicting objectives of quality and efficiency. They calculate a trajectory of process control variables in order to reach the formulated goal.

In order to perform the optimisation, a proper description of quality is essential. In many processes a spatial distribution of the quality indicator arises inside the material. This means that it is not so much the average values, but the profiles of the quality indicator that are important to optimise quality. Therefore, it is expected that quality indicator profiles (QIPs) need to be considered in the optimisation of quality. This formed the core hypothesis of this thesis. The hypothesis is studied with the residual enzyme activity as quality indicator and drying of starch cylinders containing catalase as case study, by answering the subsequent research questions:

- 1) do QIPs in simulation positively contribute to the prediction of quality?
- 2) do QIPs in simulation really make a difference in optimisation of quality?
- 3) can existing drying models describe QIPs adequately or does a new model need to be developed?
- 4) can it be demonstrated experimentally that QIPs make a difference in prediction and optimisation of quality?
- 5) can an adequate drying model predict the experimental QIPs?
- 6) can this adequate model be used in the optimisation routine?

*QIPs in the prediction of quality (Chapter 2)*

In a simulation study, different possibilities to express quality are compared in their prediction of the quality indicator during drying. The first possibility is the spatial distribution of the quality indicator. The second possibility is the averaged spatial quality indicator. The third way is to determine the average quality indicator based on average moisture content and temperature. The simulation results show that the consideration of QIPs does make a difference in the prediction of quality after drying. Averaged spatial quality indicators do not give an unambiguous description of the QIPs inside the material. Different QIPs correspond with the same averaged value. Moreover, inside the material the quality indicator at different positions deviate strongly from the average value. Both higher and lower enzyme activity are observed.

*QIPs in optimisation of quality (Chapter 3)*

Optimisation studies have been performed with a standard diffusion model. Based on a finite-difference approximation of the model, a measure of product quality and energy consumption, optimal control trajectories are calculated, using control parameterisation. Two quality objectives have been investigated: the retention of enzyme activity during drying and the inactivation of the enzyme in case of a hazardous feature. Next to very advantageous optimisation results, like the existence of an optimal drying time, higher profits and better controlled product properties as moisture content, the optimisations show that the consideration of QIPs in the optimisation routine does make a difference. Only by considering QIPs safety of the product can be guaranteed. Trajectories obtained with average quality indicator, lead to products where a deteriorative enzyme retains its activity at the surface of the product. Additionally, optimal trajectories can influence the spatial distribution of the quality indicator creating advanced possibilities to control product quality.

*A new drying model to describe QIPs adequately (Chapter 4)*

To describe QIPs during drying, a microscopic drying model is required that can predict gradients of moisture content and temperature in the material. Additional requirements for optimisation studies are the applicability of the model for a large range of experimental conditions and functioning independent of the dryer type. Traditionally, the distributed diffusion model is used to describe spatial distributions. The effective diffusion coefficient in this model is represented by an empirical relation, expressing the reduced diffusion at lower moisture contents. It appears that various relations for the diffusion coefficient can yield

comparable drying curves, while the predicted moisture content distribution differs, resulting in different predictions of QIPs. This means that it is impossible to judge the various submodels proposed for the diffusion coefficient based on the drying curves solely. Therefore a new microscopic model is developed, in which the dependence on moisture content does not need to be derived from the drying curve. In this model a distinction is made between different classes of water present in the material. The conversion between them is described by a sorption process. Since both diffusion and sorption are part of the description of moisture transfer, the model is called the diffusion-sorption drying model. In this model all parameters have a physical meaning. The assumptions made in the model are supported by independent sorption experiments. Improved experimental and regression methodologies are developed for these experiments. The diffusion-sorption model is compared with four diffusion models known from literature. Drying experiments are performed with a continuous weighing procedure: the airflow is not diverted from the dryer during weighing, resulting in a higher sampling frequency (800 times). Seven drying experiments are selected to calibrate the various microscopic drying models. Four drying experiments with a constant flux period (CFP) are used for the calibration of the parameters describing the external limited mass transfer. Three drying experiments without a CFP are applied for the calibration of the parameters describing the diffusion limited mass transfer. The models are put to validation by testing them on eleven other drying experiments. The new model is the best model in both calibration and validation.

*Experimental demonstration of QIPs and their relevance in prediction and optimisation of quality (Chapter 5)*

Drying experiments are performed under different conditions of temperature and relative humidity of the drying air. During the course of the drying process the quality indicator is measured at different positions in the material with the aid of a specially designed microtome. The experiments illustrate that QIPs exist during and after drying. In addition, the QIPs are significantly different when the material is dried under different air conditions. So, air conditions are instrumental in influencing the QIPs, which means that optimisation of quality is feasible in practice.

*The diffusion-sorption drying model to predict the experimental QIPs (Chapter 5)*

To predict the experimentally measured QIPs, the diffusion-sorption drying model is combined with a quality model. The quality model is determined with independent

inactivation experiments. Since a time invariant nonzero rest activity remains after prolonged inactivation, a fractional conversion model is applied. The model predicts the enzyme activity in various inactivation experiments within the experimental accuracy. Despite the fact that both the diffusion-sorption drying model and the quality model individually lead to reliable predictions, a problem arises when they are combined to describe the experimental QIPs. Their combination results in an excellent agreement of the predicted average moisture content with the experimental drying curve. Also the QIPs are qualitatively comparable with the experimental ones. Nevertheless the predicted residual enzyme activity is structurally higher than the experimental one. The reason for this overestimation is not clear. It is expected that the main reason can be found in experimental inaccuracies. Therefore, it can be stated that within the limitations of experimental error, the diffusion-sorption drying model adequately describes and predicts the experimental QIPs.

*The diffusion-sorption model in the optimisation routine (Chapter 6)*

The new diffusion-sorption model is successfully applied in optimal control computations. Some general properties of optimisations with the diffusion-sorption model are investigated and the results are as can be expected from practical considerations. Increasing the number of control intervals results in better performance. An optimal drying time exists. The quality indicator after drying is sensitive to the final desired moisture content. A higher value of the final moisture content at the same final time allows drying at more moderate temperatures, causing less inactivation of the thermal sensitive biological material and a decrease in energy costs. The calculated trajectories protect the material during temperature sensitive-phases and lead to increased efficiency in other phases.

The major contribution of this thesis is that it has been demonstrated in theory, simulation and experiments that quality indicator *profiles* are required for optimisation of quality.

The research presented in this thesis demonstrates the perspectives of optimal control based on QIPs (*Chapter 7*). The implementation of QIPs appears to be essential for a better prediction of product quality and leads to improved control of food properties and to a guarantee of product safety. Moreover, advanced possibilities to control quality arise, since the trajectories of control variables can influence the QIPs. These perspectives are potentially highly beneficial for drying processes and other processes in food, biotechnological and agro technological industries.

## Samenvatting

Tijdens het verwerken van grondstoffen en levensmiddelen veranderen de eigenschappen van een product. Dit kan leiden tot een andere kwaliteitsbeleving door de consument. Kwaliteit is een complex begrip. Het kan gedefinieerd worden als de mate waarin een product voldoet aan de wensen van de consument. Hierdoor omvat het vele verschillende factoren waaronder sensorische, psychologische, sociologische en culturele. De kwaliteitsperceptie kan dus afhankelijk zijn van de situatie. Ten einde het begrip kwaliteit te objectiveren, wordt de kwaliteitsbeleving gerelateerd aan specifieke product eigenschappen, de kwaliteitskenmerken. Deze worden op hun beurt gekoppeld aan een kwaliteitsindicator die met behulp van objectieve meetapparatuur gemeten kunnen worden. Een voorbeeld is het kwaliteitskenmerk kleur. De kleur in een product kan veroorzaakt worden door het pigment  $\beta$ -caroteen, dat dus kan fungeren als kwaliteitsindicator. Door het gehalte aan  $\beta$ -caroteen, de kwaliteitsindicator te meten is een objectieve maat verkregen voor de kleurwaarneming.

De kwaliteitsveranderingen tijdens de bewerking van producten vragen om een procesbeheersing die gericht is op het maximaliseren van zowel de productkwaliteit als de efficiëntie van het bewerkingsproces. Optimalisatieprocedures kunnen hierbij een essentiële rol spelen: ze bieden de mogelijkheid om kwaliteit enerzijds en efficiëntie anderzijds expliciet als doel te formuleren. Ze berekenen trajecten van de stuurvariabelen van het proces, zodat het geformuleerde doel bereikt wordt.

Voor het uitvoeren van de optimalisatie is het essentieel om een geschikte definitie te hebben van de kwaliteit. Gedurende veel processen is er sprake van plaatsafhankelijke verschillen van de kwaliteitsindicator binnen het materiaal. Dit betekent dat niet zozeer de gemiddelde waarde, maar juist de kwaliteitsindicatorprofielen (Engels: quality indicator profiles, QIPs) belangrijk zijn voor de optimalisatie van kwaliteit. Het is om die reden waarschijnlijk dat deze plaatsafhankelijkheid, zoals uitgedrukt in de QIPs moet worden meegenomen in de kwaliteitsoptimalisatie. Deze hypothese staat centraal in dit proefschrift en wordt getoetst aan de hand van de residuele enzymactiviteit van catalase als kwaliteitsindicator bij het drogen van zetmeel cilinders. Hiervoor worden de volgende onderzoeksvragen beantwoord:

- 1) leveren QIPs in simulaties een essentiële bijdrage aan de voorspelling van kwaliteit?
- 2) leiden QIPs in simulaties werkelijk tot verschil in de optimalisatie van kwaliteit?
- 3) kunnen bestaande droogmodellen QIPs adequaat beschrijven of is het nodig om een nieuw model te ontwikkelen?

- 4) kan het experimenteel aangetoond worden dat QIPs leiden tot een verschil in voorspelling en optimalisatie van kwaliteit?
- 5) kan een adequaat droogmodel de experimentele QIPs voorspellen?
- 6) kan dit adequate droogmodel toegepast worden in de optimalisatie routine?

#### *QIPs in de voorspelling van kwaliteit (Hoofdstuk 2)*

Verschillende beschrijvingen van kwaliteit zijn in simulaties met elkaar vergeleken in hun voorspelling van de kwaliteitsindicator tijdens het drogen: 1) de ruimtelijke verdeling van de kwaliteitsindicator; 2) het gemiddelde van de ruimtelijke verdeling van de kwaliteitsindicator en 3) de gemiddelde waarde voor de kwaliteitsindicator op basis van gemiddeld vochtgehalte en gemiddelde temperatuur. De resultaten tonen aan dat QIPs leiden tot een verschil in de gesimuleerde kwaliteitsvoorspelling na het drogen. De gemiddelde waarden voor de kwaliteitsindicator geven geen eenduidige beschrijving van de QIPs in het materiaal. Verschillende QIPs leiden tot eenzelfde gemiddelde waarde. Bovendien wijkt de kwaliteitsindicator op verschillende plaatsen in het materiaal sterk af van de gemiddelde waarde. Zowel een hogere als lagere enzymactiviteit is aanwezig.

#### *QIPs in de optimalisatie van kwaliteit (Hoofdstuk 3)*

Optimalisatie studies zijn uitgevoerd met een bestaand standaard diffusiemodel. Uitgaande van een eindige-differentie benadering van het model, de productkwaliteit en het energieverbruik, zijn optimale trajecten van stuurvariabelen berekend door middel van stuurparameterisatie. Hierbij zijn twee kwaliteitsdoelen bestudeerd: het behoud van enzymactiviteit gedurende een droogproces en het inactiveren van een schadelijk enzym. Dit resulteerde in een optimale droogtijd, een hogere opbrengst en toegenomen controle over producteigenschappen zoals het eindvochtgehalte. Daarnaast laten de optimalisatie resultaten zien dat het incorporeren van QIPs in de optimalisatie routine een belangrijk verschil uitmaakt. Alleen door het incorporeren van QIPs kan namelijk de veiligheid van het product worden gegarandeerd. Trajecten verkregen met de gemiddelde waarde van de kwaliteitsindicator resulteren in producten waarbij het bederfveroorzakende enzym zijn activiteit behouden heeft aan het oppervlakte van het product. Daarnaast kunnen de optimale trajecten van de stuurvariabelen de ruimtelijke verdeling van de kwaliteitsindicator beïnvloeden, waardoor betere mogelijkheden ontstaan om de productkwaliteit te sturen.

*Een nieuw model voor de beschrijving van QIPs (Hoofdstuk 4)*

Voor het beschrijven van QIPs gedurende een droogproces is een microscopisch droogmodel nodig dat vocht- en temperatuursgradiënten binnen het materiaal kan voorspellen. Extra vereisten voor de optimalisatiestudies zijn de toepasbaarheid van het model voor een breed scala aan experimentele condities en het functioneren van het model onafhankelijk van het type droger. Gewoonlijk wordt het diffusie model gebruikt voor de beschrijving van de gradiënten. In dit model komt een effectieve diffusiecoëfficiënt voor, die afneemt bij lagere vochtgehaltes. Deze afname wordt beschreven door een empirische relatie. Het blijkt dat verschillende relaties voor de diffusiecoëfficiënt leiden tot vergelijkbare tijdafhankelijke droogcurves. Dit betekent dat het onmogelijk is om alleen op basis van de droogcurves de submodellen voor de diffusiecoëfficiënt te beoordelen. Om die reden is een nieuw microscopisch model ontwikkeld waarin de afhankelijkheid van het vochtgehalte niet van de droogcurve hoeft worden afgeleid. In dit model wordt de mate van gebondenheid van water aan het materiaal onderscheiden in verschillende klassen. De overgang tussen deze klassen wordt beschreven door een sorptieproces. Aangezien zowel diffusie als sorptie onderdeel uitmaken van de beschrijving van de vochttransport, wordt dit model het diffusie-sorptie droogmodel genoemd. In dit model hebben alle parameters een fysische betekenis. De aannames die voor dit model werden gemaakt, worden ondersteund door onafhankelijke sorptie experimenten. Er zijn voor deze experimenten verbeterde experimentele en regressie methoden ontwikkeld. Het diffusie-sorptie model is vergeleken met vier andere, reeds beschreven, diffusie modellen. De droogexperimenten zijn uitgevoerd met een continue weegprocedure: de luchtstroom is voor de weegprocedure niet omgeleid van de droger, wat resulteerde in een 800 maal hogere bemonsteringsfrequentie. Voor de calibratie van de verschillende microscopische droogmodellen zijn zeven droogexperimenten geselecteerd. Vier droogexperimenten met een constante flux periode zijn gebruikt voor de calibratie van de parameters die de externe limitatie van massaoverdracht beschrijven. Drie droogexperimenten zonder deze constante flux periode zijn gebruikt voor de calibratie van de parameters die het diffusie gelimiteerde stoftransport beschrijven. Alle modellen zijn gevalideerd met elf andere droogexperimenten. Het nieuwe diffusie-sorptie model kwam als beste model naar voren zowel tijdens calibratie als validatie.

*Experimentele demonstratie van QIPs en hun belang in het voorspellen en optimaliseren van kwaliteit (Hoofdstuk 5)*

Droogexperimenten zijn uitgevoerd met verschillende condities van temperatuur en relatieve vochtigheid van de ingaande drooglucht. Gedurende het droogproces is de kwaliteitsindicator

op verschillende posities in het materiaal gemeten met behulp van een speciaal ontworpen microtoom. De experimenten illustreren dat QIPs ontstaan in het materiaal tijdens en na het drogen. Tevens blijkt dat de QIPs significant anders zijn als het materiaal met andere droogcondities is gedroogd. Dit betekent dat de drooglucht condities kunnen worden gebruikt om de QIPs te beïnvloeden, waardoor dynamische optimalisatie van kwaliteit ook praktisch uitgevoerd kan worden.

#### *Het voorspellen van de experimentele QIPs door het diffusie-sorptie model (Hoofdstuk 5)*

Het diffusie-sorptie model is gekoppeld aan een kwaliteitsmodel dat de residuele enzymactiviteit beschrijft, om de experimentele QIPs te voorspellen. Het kwaliteitsmodel is vastgesteld met behulp van onafhankelijke inactivatie experimenten. Omdat na langdurige inactivatie steeds een constante enzymactiviteit overbleef, is een eerste orde model met restactiviteit toegepast. Het model voorspelt voor verschillende inactivatie-experimenten de enzymactiviteit binnen de experimentele fout. Ondanks het feit dat zowel het diffusie-sorptie model als het kwaliteitsmodel afzonderlijk leiden tot betrouwbare voorspellingen, ontstaat er een probleem als ze gecombineerd worden om de experimentele QIPs tijdens het drogen te beschrijven. De combinatie van de modellen resulteert in een uitstekende voorspelling van het vochtgehalte in de droogcurve. Daarnaast zijn de voorspelde QIPs in vorm vergelijkbaar met de experimentele. De voorspelde enzym activiteit is echter structureel hoger dan de experimentele waarde, waarschijnlijk door experimentele onnauwkeurigheden. Daarom kan het diffusie-sorptie model binnen de grenzen van de experimentele nauwkeurigheid, de experimentele QIPs adequaat beschrijven en voorspellen.

#### *Het diffusie-sorptie model in de optimalisatie routine (Hoofdstuk 6)*

Het nieuwe diffusie-sorptie model is met succes toegepast in de berekeningen van de optimalisatie routine. De uitkomsten van de optimalisatie zijn zoals verwacht vanuit praktische overwegingen. Door het aantal stuurintervallen te vergroten wordt de prestatie verbeterd. Er bestaat tevens een optimale droogtijd. Daarnaast is de verkregen kwaliteitsindicator na het drogen gevoelig voor het gewenste eindvochtgehalte. Bij een hogere waarde van het gewenste eindvochtgehalte en dezelfde droogtijd, kan onder mildere omstandigheden worden gedroogd. Dit leidt tot minder inactivatie van het temperatuurgevoelige biologisch materiaal en een afname van energiekosten. Tenslotte beschermen de berekende trajecten van de stuurvariabele het materiaal tegen inactivatie

tijdens temperatuurgevoelige fasen en leiden ze tot toename van de efficiëntie in de overige fasen van het droogproces.

In dit proefschrift is zowel in theorie als met simulaties en experimenten aangetoond dat *profielen* in de kwaliteitsindicator essentieel zijn voor de optimalisatie van kwaliteit. Dit vormt de belangrijkste bijdrage van dit proefschrift.

Dit proefschrift beschrijft tenslotte de toekomstperspectieven van dynamische optimalisatie, als deze gebaseerd is op QIPs (*Hoofdstuk 7*). De implementatie van QIPs is essentieel voor een verbetering van de voorspelling van productkwaliteit. Het leidt tevens tot een verbeterde regeling van product eigenschappen en tot het waarborgen van de voedselveiligheid. Daarnaast zijn nieuwe mogelijkheden gevormd voor het sturen van productkwaliteit, omdat de QIPs beïnvloed kunnen worden door de trajecten van stuurvariabelen. Deze perspectieven hebben een grote potentie voor droogprocessen en andere processen in de levensmiddelenindustrie, biotechnologie en agrotechnologie.



## Dankwoord

Eindelijk, eindelijk is mijn proefschrift over drogen klaar. Zoals het woord droog qua betekenis kan variëren van uitermate saai tot leuke humor, zo kende ook dit proefschrift zijn uitersten. Gelukkig heb ik gedurende de hele periode mensen om me heen gehad, die me steunden, me afleiding bezorgden, mijn leven kleur gaven, met me mee dachten en interesse toonden.

Toen ik net op de vakgroep aan het onderzoek begon, waren Tien, Frank, Leo, Dirk en Jan-Paul de al-bijna-klare AIOs. Jullie hielpen me erg met compu-foefjes, relativering en een snufje Taiwanese cultuur. In de loop van de tijd kwamen er steeds meer AIOs en tijdelijke onderzoekers bij, die het werk op de vakgroep aangenaam maakten. Irineo, you were a very nice colleague. Before your family came to Holland, we spend a lot of time in Unitas, to have dinner. I was very happy when your family arrived in Holland, not only for you, but also for me, since you introduced me in a warm Mexican culture and family life. Dit geldt ook voor Abdallah. We kwamen zelfs in dezelfde straat te wonen, waardoor we elkaar ook toen we allebei al van de vakgroep waren verdwenen, nog regelmatig zagen. Olli en Ann, jullie begonnen tegelijkertijd beneden. We zagen elkaar regelmatig buiten het werk, hadden het over veel zaken (vooral niet over het werk) en genoten volop van de geweldige kookkunst van Olli. Na veel verhuizingen binnen het Argotechnion, kreeg ik eindelijk een kamergenoot, Camille. Supergezellig en ook functioneel (je wist echt enorm veel) was het met jou op de kamer. Vooral de vrijdagmiddagen met de wedstrijd ‘wie kan het langst een liedje van DoeMaar meeschreeuwen’ en de vele spelletjes zal ik niet gauw vergeten. Met de buurman Stefan verhuisde ik vervolgens naar het IMAG, waar we samen met Brenda de vaste bezetting van de grote kamer vormden. We hebben heel wat afgepraat en gediscussieerd. Stefan, jij zorgde er altijd voor om ook samen te eten, ook nadat Brenda en ik al waren verdwenen. Ik hoop dat je het erg goed gaat hebben samen met Jasper in Noorwegen. Brenda, je bent een goede vriendin geworden en we zijn erg blij met alle nieuwe ontwikkelingen. Evert en Josep (amazing trips), jullie hebben op geweldige wijze de vierde plek opgevuld. Bas, jij kwam in de plaats van Brenda. Je was een gezellige kamergenoot en altijd bereid om te helpen. Ronald, Roel, Gert, Martijn, Timo, Dirk, Tijmen en Klaas jullie versterkten de club, met gezellige koffie en lunch breaks. Hady, you were my last roommate, after moving to the Technotron. Thanks for your shown interest and concern. You were always very worried about the fact that I was still cycling until the end of the pregnancy. The bumps in the road could not be good for the baby. Happily you can sometimes see the result! En als laatste de AIO van de overkant, Jaap. We leerden elkaar kennen tijdens een cursus, waarin we veel opdrachten

samen moesten doen. Het bleek dat we veel raakvlakken hadden, waardoor deze samenwerking is uitgegroeid tot een waardevolle vriendschap. Bedankt voor alles!

I would like to thank my students, Raymi, Laszo, Chaba, Long, Patrick en Rinze. You were all very valuable for mainly the experimental part of the project. But more important, it was very enjoyable to work together with you.

Voor de inhoudelijke input voor mijn proefschrift wil ik mijn dank en waardering uitspreken voor Gerrit. Ik heb er enorme bewondering voor, dat je het steeds weer klaar speelde om tot in detail de stukken op tijd te lezen en van commentaar te voorzien. Dat gaf me veel vertrouwen. Je hebt een enorm breed kennisgebied. Daarnaast heb je, net als ik, veel oog voor detail; dit soms tot frustratie van de derde partij. Je hebt me veel mogelijkheden geboden, veel vrijheid gegeven en altijd vertrouwen in me getoond. De initiator van dit project was Ton. Ton, bedankt voor je begeleiding. Jij hield de grote lijn altijd in de gaten. Wilko, jij hebt me door de laatste fasen heen begeleid (= soms geslept). Bedankt voor je verhelderende inbreng en je volharding.

De overige inhoudelijke hulp kreeg ik van de andere (ex-)collega's: Jan, Gerard, Karel en Wil (Bedankt voor alles!), Hans, Kees en Rachel. Daarnaast leverden het veel gezellige lunches en pittige discussies. Marja, jij zorgde voor de goede afwisseling en de persoonlijke noot! Corrie en Miranda, jullie hebben me vooral in het begin erg geholpen, met een praatje, snoep en met materiaal. Paul, je zorgde voor de nodige, zeer gevarieerde afleiding. Jammer dat je dit moment niet meer mee mag maken. Een bijzonder woord van dank aan de mensen die me enorm hebben geholpen met de experimentele opstelling: Aart, Kees, Michel en Hennie. Hennie, je knutselacties hebben de mooiste resultaten van mijn proefschrift opgeleverd.

Op de vakgroep Productontwerpen en kwaliteitskunde heb ik een groot aantal experimenten kunnen uitvoeren. Tiny van Boekel wil ik heel hartelijk bedanken voor zijn enthousiasme en voor de mogelijkheid om op zijn lab te werken. Charlotte, bedankt voor je hulp tijdens de voorbereidingen van de analyse methode en voor het beschikbaar stellen van je tafel en je tijd, maar vooral voor je gezelligheid en je advies.

Met al de beschreven hulp was ik er echter niet gekomen. Vrienden, huisgenootjes en familie blijven het allerbelangrijkst. Jullie voelden precies aan wanneer je wel en vooral wanneer je niet over de promotie moest beginnen. Maar bovenal waren jullie erg trouw in het 'er zijn'. Jullie hebben enorm veel voor me betekend tijdens het AIO-gebeuren en gelukkig nog steeds. Ik kan niet iedereen noemen, maar toch wil ik graag een paar mensen eruit lichten: Gerard en

Mirjam, Johanna en Martijn, Margreet en Arjan (zelfs in Bangkok zien we elkaar nog!), Rense en Annemien, Henk en Eline, Kees en Joke, Roel en Mincke en de bijbehorende kids. Heel heel hartelijk bedankt voor alles!

En natuurlijk mijn paranimfen: Rob en Ellen. Vanaf het allereerste begin van mijn leven in Wageningen waren jullie erbij. We hebben heel wat met elkaar meegemaakt: avondjes doorzakken, nachtje doortrekken of in quarantaine voor de afronding van een vak, supervakanties, eindeloos geboom, gepraat en geouwehoer, maar vooral er voor elkaar zijn hoe het allemaal ook loopt. Ik vind het super dat jullie naast me op het podium willen staan. Ik hoop dat we nog heel veel samen mee mogen maken samen met Henriëtte en Gerard, Myrthe en Therese. Het wordt nu wellicht tijd voor onze zorgboerderij in India.

Tot slot, mijn familie en schoonfamilie. Pa en ma Pieterse, Linda en Marciano, jullie hebben ons gigantisch geholpen als oppas- en verhuisservice, waardoor we steeds verder konden met de proefschriften. Rianne, Pieter, Koen, Tom, Bart en Sanne en Dia, Herwald, Sifra, Linde en Nienke, jullie waren er steeds voor mij. Dank dank dank! Ik heb enorm genoten van de logeerpartijen en gelukkig hebben we er nog een paar voor de boeg.

Lieve pa en ma, dit proefschrift draag ik op aan jullie en jullie weten wel waarom. Ik kan geen woorden vinden om aan te geven wat jullie voor mij betekenen en om jullie te bedanken voor jullie bijdrage door dik en vooral dun aan dit boekje.

Lieve Merijn en xxxxx of yyyyyy, zonder dat jullie er erg in hadden zijn jullie de grote drijfveren geweest achter het afronden van dit proefschrift. De eerste dikke buik met Merijn zorgde voor het schrijven van alle artikelen, de huidige dikke buik voor de allerlaatste loodjes. Merijn, je maakt me nog gelukkiger dan ik me ooit had kunnen voorstellen. Met je krullen, je lach, je grapjes, je zingen en je gelukkig-zijn, zorgde jij voor precies de goede afleiding.

Lieve Bart, ik overdrijf niet als ik zeg dat zonder jou dit proefschrift nooit af was gekomen. Je hebt me geholpen met raad en daad, met het inzetten van grote proeven (vlak voor onze vakantie), met knopen doorhakken, met volhouden, met aanhoren..., maar vooral met te zijn wie je bent en met mij te laten zijn wie ik ben. Je vult me volledig aan, waardoor we één worden, maar toch twee blijven.

Het laatste woord van dank is aan de Laatste Die ook de Eerste is. Zonder Hem was dit alles nooit mogelijk geweest.





## List of publications

Quirijns, E.J., A.J.B. van Boxtel and G. van Straten. The use of moisture and temperature profiles in predicting product quality for optimal control of drying processes. p. 485-490. In: Skjöldebrand, C. and G. Trystam (Eds.). *Proceedings on Automatic Control of Food and Biological Processes IV*. Göteborg, Sweden, 1998.

Quirijns, E.J., L.G. van Willigenburg and A.J.B. van Boxtel. New perspectives for optimal control of drying processes. p. 431-437. In: Biegler, L.T., A. Brambilla and C. Scali (Eds.). *Adchem2000: International Symposium on Advanced Control of Chemical Processes*. Pisa, Italy: IFAC Publications Elsevier Science Ltd, 2001. 1088 p.

Quirijns, E.J., L.G. van Willigenburg, A.J.B. van Boxtel and G. van Straten. The significance of modelling spatial distributions of quality in optimal control of drying processes. *Journal A. Benelux Quarterly Journal on Automatic Control*, vol. 41, 2000, no. 3, p. 56-64.

Quirijns, E.J. De kunst van drogen. *Landbouwmecanisatie*, vol. 53, 2002, no. 5, p. 17.

Svantesson, T., E.J. Quirijns and G. Olsson. *Wood ash agglomerate moisture control- Hardware, sensors and control algorithms*. Lund: Industrial Engineering Department of Industrial Electrical Engineering and Automation Lund University, 2002. 72 p.

Quirijns, E.J., A.J.B. van Boxtel, W.K.P. van Loon and G. van Straten. An improved experimental and regression methodology for sorption isotherms. *Journal of the Science of Food and Agriculture*, vol. 85, 2005, no. 2, p. 175-185.

Quirijns, E.J., A.J.B. van Boxtel, W.K.P. van Loon and G. van Straten. Sorption isotherms, GAB parameters and isosteric heat of sorption. *Journal of the Science of Food and Agriculture*, vol. 85, 2005, no. 11, p. 1805-1814.

Pieterse, B., E.J. Quirijns, F.H.J. Schuren and M.J. van der Werf. Mathematical design of prokaryotic clone-based microarrays. *BMC Bioinformatics*, vol. 6, 2005, p. 238.

Quirijns, E.J., A.J.B. van Boxtel, W.K.P. van Loon, and G. van Straten. Diffusion-sorption drying model for optimal quality control. *Submitted for publication*.

Quirijns, E.J., W.K.P. van Loon, M.A.J.S. van Boekel and G. van Straten. Quality indicator profiles inside food during drying. *Submitted for publication.*

## **Curriculum Vitae**

Elisabeth Johanna (Ilse) Quirijns werd geboren op 30 mei 1972 in Sprang-Capelle. Na het behalen van haar VWO diploma aan het Willem van Oranje College in Waalwijk, begon ze in 1990 aan de studie Levensmiddelentechnologie aan de toenmalige Landbouw Universiteit in Wageningen. Ze koos voor de oriëntatie levensmiddelenbioprocestechnologie, waarbinnen ze verschillende afstudeerprojecten en een stage uitvoerde. Haar eerste project deed ze bij de vakgroep Levensmiddelenmicrobiologie, onder begeleiding van Géke Stoffels en Tjakko Abee. Het onderzoek betrof de karakterisering van een bacteriocine geproduceerd door de darmbacterie stam WAU-611. Haar tweede project was een samenwerkingsproject tussen het ATO-DLO en de vakgroep Meet-, Regel- en Systeemtechniek. Onder begeleiding van Jan Bontsema, Gerrit Eggink en Ruud Weusthuis, ontwierp ze een waarnemer voor de substraatconcentratie in een bioreactor. Haar laatste project vond plaats in India voor de vakgroep Levensmiddelenproceskunde. Aan de Indian Institute of Technology in Kharagpur ontwierp ze onder begeleiding van Prof. H. Das een vented single screw extruder voor de productie van een fruitreep. In 1996 studeerde zij cum laude af, waarna ze begon als AIO aan de vakgroep Meet-, Regel- en Systeemtechniek. De resultaten van dit promotieonderzoek staan in dit proefschrift beschreven. In 2002 werkte zij als toegevoegd docent aan dezelfde vakgroep. Hierna werd ze docent meet- en regeltechniek aan de Hogeschool/MBO-college Rens en Rens in Hilversum. Sinds 2005 werkt ze als docent voedingsmiddelentechnologie aan de HAS in Den Bosch.

cover: Drying of cow dung in Kharagpur, India

printed by: Ponsen & Looijen B.V., Wageningen